Photoelectron Spectroscopy of Organotransition metal complexes

J. E. van Tilborg

A thesis
presented to the Faculty of Science
of the University of London
in candidature for the degree of
Doctor of Philosophy

The Bourne Laboratory
Royal Holloway College
(University of London)
Egham Hill
Egham
Surrey

January 1979

ACKNOWLEDGEMENTS

The author wishes to acknowledge the help and guidance of her supervisor Dr. P. Powell, and of Dr. J. C. Green of the Inorganic Chemistry Laboratory, Oxford. She would also like to thank Dr. D. Peters for many helpful discussions.

The work described in this thesis was supported by a research studentship from the Science Research Council.

All photoelectron spectra were obtained using the spectrometer at the Inorganic Chemistry Laboratory, Oxford, and the author wishes to thank Dr. R. Egdell and Elaine Seddon for their help. Thanks also to Dr. L. J. Russell and J. W. Tindle of the Bourne Laboratory for aid with experimental synthetic work.

The rhodium, iridium and ruthenium complexes described in this thesis were synthesised from salts generously loaned by Johnson, Matthey and Co. Ltd.

Finally the author would also like to thank Mrs Margaret Peel for the typing of this thesis.

Photoelectron Spectroscopy of Organotransition metal complexes

J. E. van Tilborg

A brief introduction to photoelectron spectroscopy (PES) and its use in connection with molecular orbital (MO) calculations is given.

A series of diene-tricarbonyliron and -tricarbonylruthenium, and related complexes, has been synthesised. Previous studies of their molecular and electronic structure are reviewed. The UV photoelectron spectra of these complexes, together with those of the diene ligands are presented and assigned with the aid of qualitative MO diagrams and existing MO calculations. Bonding of the diene to the tricarbonylmetal unit is discussed and an attempt is made to correlate the diene conformation within the complex to UV photoelectron spectroscopic data.

HeI and HeII UV photoelectron spectra are presented for the metallocenes of the first row transition elements (V to Ni). Molecular and electronic structures and electronic ground states implied from spectroscopic data are reviewed. The PE spectra of open shell molecules are discussed, and the spectra of the metallocenes are assigned with the aid of previous assignments, MO, and crystal field theories. Use is made of the knowledge that ionisation cross sections for an orbital of particular atomic character change relative to each other for ionisation by photons of different energy. Relative ionisation cross sections are calculated from experimental data.

HeI and HeII PE spectra are obtained for a series of diene-cyclopentadienylM (M = Co, Rh, Ir) complexes. The expected similarity of spectra of the rhodium and iridium analogues is noted, and an unexpected marked difference in the PE spectra of rhodium and cobalt analogues is observed. This is discussed in relation to bonding and with reference to noted differences in chemical reactivity of some other similar rhodium/cobalt analogues. Assignments of the PE spectra are made with the help of qualitative MO diagrams.

The PE spectra of two cyclopentadienyldicarbonylM (M = Co, Rh) complexes are compared.

The instrumentation used for obtaining the photoelectron spectra is discussed in detail in Appendix 1.

CONTENTS

TABLES, FIGURES and PHOTOELECTRON SPECTRA

Page

Chapter 3

Chapter 5 cont.

Appendix 1

Chapter 1

Introduction to Photoelectron Spectroscopy

1.1 THE PHOTOELECTRIC EFFECT

In an atomic or molecular absorption process, an electron is excited from a lower to a higher energy level by absorption of electromagnetic radiation. If the electromagnetic radiation is of high enough energy, the electron will leave the atom or molecule and travel in free space. Since the free electron wave function may have any symmetry, there are effectively no selection rules and thus, provided the incident electromagnetic radiation is energetic enough, all electrons in atoms or molecules may be considered.

The ejection of electrons by electromagnetic radiation in such a process is known as the photoelectric effect and is summarised in equation (1)1, where M represents an atom or molecule, $h\nu$, the energy of incident radiation, and e_n an electron ejected from orbital n. This is the basic process with which photoelectron spectroscopy (PES)

$$M + h\nu \longrightarrow M^+ + e_n \qquad (1)1$$

is involved; the technique has been developed for the study of electronic structure in atoms and molecules.

1.2 HISTORICAL DEVELOPMENT

The photoelectric effect was first noted by Hertz in 1887 on observation that a spark gap illuminated with ultra-violet (UV) light could discharge more readily. In 1889, apparatus was assembled by Lenard to measure the velocity of electrons ejected from a metal surface by UV light, and in 1905, Einstein explained Lenard's observations in terms of quantum theory, deriving expression (1)2, where K.E. is the kinetic energy of the ejected electron, $h\nu$, the energy of

$$K.E. = h\nu - B.E. \qquad (1)2$$

incident radiation, and B.E. the energy of the electronic energy level from which the electron is ejected - the binding energy.

The Einstein relationship (1)2 was verified by Millikan, using UV radiation, and by Robinson [1] and de Broglie [2], using X-rays,

in the early twentieth century.

Early experiments were concerned with atomic binding energies since information was limited by the large source line width and low resolution analysers. With the advent of higher resolution the technique became interesting to chemical spectroscopists, but this development is recent, occurring over the past fifteen years. The valence bands of metals and semiconductors were studied for many years before this using an ultra-violet photoelectron spectroscopic (UVPES) technique and high vacuum conditions, by physicists and metallurgists. Radiation entered the system through a lithium fluoride window, thus limiting photon energies to less than 11.6 electron volts (eV), the cut-off point of the window. These studies were known as UV photoemission studies.

More recently the principle has been applied to complex molecular systems, and modern photoelectron spectroscopy (PES) using monochromatic photon sources has divided into two distinct fields, depending on the energy of the source.

1.3 PHOTON SOURCES

Binding energies of electrons in molecules range from several thousands of electron volts (eV) for inner core electrons, to a few eV for valence electrons. Both UV and X-ray photon sources are used in PES, giving the division into two regions:

(i) X-ray photoelectron spectroscopy (XPS)

X-ray photoelectron spectroscopy (XPS) or electron spectroscopy for chemical analysis (ESCA) makes use of a conventional X-ray tube as a source of monochromatic photons. In 1957, Siegbahn produced the first high quality spectrum, using Mo $K_{\alpha_1\alpha_2}$ radiation (17,479 eV; 17,374 eV). [3] The core level binding energies of copper were examined. In 1964 Siegbahn and co-workers published a study of atomic binding energies for 76 elements [4], showing that chemical shifts between the spectrum of an element and its compound could be related to the valence state of that element within the compound, and also that elements could be identified by their binding energies.

The resolution of this technique, using current commercially available instrumentation, is approximately 0.6 eV. XPS was originally applied to solid phase surface studies, but recently has been applied to the study of liquids [5].

(ii) UV photoelectron spectroscopy (UVPES, UPS)

The most commonly used photon source in UVPES is that provided by a direct current discharge through helium gas producing a very intense line at 584 Å (21.22 eV), the HeI source, with a natural linewidth of only 0.005 eV. The development of UVPES using this, and other sources, owes much to Turner [6] and has so far been mainly concerned with the study of gases and solid surfaces.

The technique is limited to the study of valence electrons since the energy of the source photons is too low for inner core ionisation to occur.

More recently, by use of lower helium pressures and higher discharge voltages, nearly 100% of the HeII line at 303.8 Å (40.81 eV) has been obtained and used as a photon source for this technique.

As well as Turner and co-workers, the groups of Price [7] in London, and McDowell [8] in Vancouver, have contributed a great deal to the development of UVPES.

For both practical and theoretical reasons, gas-phase UVPES is capable of higher resolution than XPS (about 15 meV for HeI spectra) and is therefore more commonly used than XPS in the study of valence electrons. However the resolution for solid phase UPS studies is approximately the same as for XPS (0.6 eV).

Recently, HeII photon sources have been used in conjunction with HeI to compare spectra of several compounds and to deduce partial ionisation cross sections for the two different photon energies. [9] This is, in part, the aim of this thesis.

1.4 RECENT DEVELOPMENTS

During the past few years, continuous monochromatic photon sources have become available with the use of synchrotron radiation, [10] and the distinction between the UV and X-ray techniques has become blurred, since the synchrotron sources span both regions. This development has two main advantages for chemical spectroscopists; firstly, after monochromatisation, it is possible to obtain considerably better resolution than for currently marketed XPS instruments, and secondly, the variable photon energy enables an optimum photon energy to be chosen for study of a given effect and allows ionisation cross sections to be studied as a function of photon energy.

Although early work in the field of PES was mainly concerned with measurement of energy levels seen in the PE spectrum, it was found possible to measure the angular distribution of the photoelectron flux, and it was hoped to be possible to relate these measurements to the symmetry of the molecules undergoing study. The theory is complex, and quantitative predictions depend on the use of good molecular wave functions.

The detailed theory relating partial ionisation cross sections to incident photon energy is also highly complex. Relative intensities of photoelectron bands obtained using a particular photon energy may be related to partial ionisation cross sections.

West and Marr have measured absolute photoionisation cross sections and angular distributions of photoelectrons for noble gases in the UV and soft X-ray region using synchrotron radiation. [11] To date, most work on photoionisation cross sections has involved the noble gases; [11,12] however work has been published on valence d and s shells for zinc, cadmium and mercury, [13] and for some solid organometallics. [14]

All studies described in this thesis were carried out using gas-phase UVPES with both HeI and HeII photon sources, and some aspects of this particular technique will now be discussed in further detail.

1.5 THE PHOTOELECTRON SPECTRUM

In the spectrometer, an intense beam of monochromatic photons ionises atoms of sample gas in the ionisation chamber. A complete description of instrumentation used in the current study, together with a block diagram of the photoelectron spectrometer is given in Appendix 1 (page 282)

The process occurring in the ionisation chamber may be represented by equation (1)1. For HeI photons, only the valence electrons will undergo ionisation, the electrons ejected from each orbital having a characteristic ionisation energy, I_n, which is related to their kinetic energy, E_n (equation (1)3).

$$I_n = h\nu - E_n \qquad (1)3$$

The photoelectrons are analysed according to their kinetic energy and the photoelectron spectrum gives the probability distribution of the ejected photoelectrons as a function of their kinetic energy. The situation for molecular species (1)4, is more complex since there is the additional possibility of vibrational or rotational excitation on ionisation, reducing the energies of the ejected photoelectrons:

$$I_n = h\nu - E_n - E_{vibr} - E_{rot} \qquad (1)4$$

Depending on the instrument and worker, the ionisation energy scale on the chart form of the PE spectrum may increase or decrease from left to right. For all spectra reproduced in this thesis the convention of ionisation energy increasing from left to right across the chart is employed.

1.6 DISCHARGES IN HELIUM: PHOTON SOURCES FOR UVPES

HeI_α photons (21.22 eV) are produced by the transition He (1s)(2p) to the ground state He $(1s)^2$, (^1S). Higher members of this series, that is, (1s)(np) to the ground state, are also present under the conditions producing HeI_α photons, but their intensity is not more than a few per cent of the 584 Å line. The lines are designated HeI_α, HeI_β, etc., and are listed in table 1.1.

TABLE 1.1	ENERGY OF HELIUM DISCHARGE LINES	
LINE	WAVELENGTH (Å)	ENERGY (eV)
HeI_{α}	584.3340	21.2175
HeI_{β}	537.0296	23.0865
HeI_{γ}	522.2128	23.7415
$HeII_{\alpha}$	303.781	40.8136
$HeII_{\beta}$	256.317	48.3702
$HeII_{\gamma}$	243.027	51.0153
$HeII_{\delta}$	237.331	52.2397

Discharges in helium also generate a series of lines from ionised helium, He^+; these are designated HeII, and the main line, $HeII_{\alpha}$ is at 303.8 Å. These lines are produced from analogous transitions in the helium ion.

Under normal conditions in UVPES, the intensities of HeI_{β} and HeI_{γ} photons produced are not significant and are ignored in the interpretation of spectra in this thesis (2% and 0.5% of the HeI_{α} intensity, respectively). By altering the discharge conditions (section 1.3 ii)) nearly 100% of the $HeII_{\alpha}$ line at 303.8 Å may be produced, and a significant $HeII_{\beta}$ line is also produced. The $HeII_{\beta}$ satellite spectrum is about 10% in intensity of the total spectrum (from results for nitrogen, see Appendix 1), and when taking relative intensity measurements in HeII PE spectra, this effect must be taken into consideration.

Sources other than helium have been used for exciting UVPE spectra, and table 1.2 [15] shows some of the more common ones. All of these sources contain ionising radiation of several frequencies and different intensities, which complicates the assignment of spectra. The relative intensities are a rough guide for capillary discharge lamps.

TABLE 1.2 LINES FROM OTHER GASES

GAS	LINE	ENERGY (eV)	RELATIVE INTENSITY
NEON	NeI_{α}	16.6704	15
		16.8476	100
	NeI_{β}	19.6877	< 1
		19.7792	< 1
	NeII	26.8132	100
		26.9100	100
	NeII	27.6858	20
		27.7616	20
		27.7827	20
		27.8590	20
	NeII	30.4520	20
		30.5483	20
ARGON	ArI_{α}	11.6233	100
		11.8278	50
	ArII	13.3019	30
		13.4794	15
HYDROGEN	$Lyman_{\alpha}$	10.1986	100
	$Lyman_{\beta}$	12.0872	10
	$Lyman_{\gamma}$	12.7482	1

1.7 RESOLUTION

The theoretical resolution for UVPES is dependent on several factors:

(i) Conservation of momentum

The error in assuming that momentum is conserved is negligible, that is, less than one part in 10^4.

(ii) The natural linewidth of the source

(a) HEISENBERG BROADENING. The emission of electromagnetic radiation occurs on an electronic transition from a higher to a lower energy level, the loss in electron energy appearing as emitted radiation. The linewidth of the emitted radiation depends on the width of the initial and final state electron energy levels. An electron in any energy level has an uncertainty in its energy, ΔE, given by Heisenberg's uncertainty principle ($\Delta E.\tau \approx h$) (where τ is the lifetime of electron in energy level). If ΔE is taken as peak width at half height, the broadening will be approximately $4 \times 10^{-15} \tau^{-1}$ eV ($2 \times 10^{-16} \tau^{-1}$ J). The lifetime, τ, is proportional to energy^{-3}; thus with increasing energy, the linewidth will increase appreciably. Valence orbitals (0 to 20 eV) have lifetimes of the order of 10^{-8} to 10^{-10}s, giving widths of approximately 5×10^{-5} to 5×10^{-7} eV; for core orbitals (100,000 to 40 eV), lifetimes are 10^{-13} to 10^{-18} s giving linewidths of about 10^{-1} to 4×10^{-3} eV. Thus for UV sources, one would expect linewidths of less than 10^{-5} eV, and for X-ray sources, about 1 eV.

(b) LORENTZ BROADENING. The lifetime of an energy level of a gas phase molecule is affected by pressure, since collisions can shorten the lifetime; this pressure resonance, or Lorentz broadening, is generally less than 10^{-6} eV and is insignificant compared to other effects.

(c) DOPPLER BROADENING. This is due to random thermal motion of the helium source gas - the emitting molecule moves, giving rise to Doppler broadening. The hot gas in the discharge region, therefore, emits lines broadened by the Doppler effect although the broadening is reduced by the cold gas outside the discharge region. For helium at room temperature, the Doppler broadening is 6.54×10^{-5} eV.

For hydrogen sources, significant broadening arises from this effect, but for other sources of greater emitter mass and greater energy, it is negligible, since the magnitude of the broadening is proportional to the wavelength of the radiation and inversely proportional to the mass of the emitter. Doppler broadening is obviously greater for HeII sources than for HeI.

(iii) Broadening due to sample molecules

An effect analogous to the Doppler broadening due to motion of source gas molecules occurs due to the combination of the photoelectron velocity with the motion of the target molecule. The broadening (ΔE) is given in equation (1)5, where V_m is the velocity of the sample molecule and V_e the

$$\frac{V_m}{V_e} \times E \propto \Delta E \qquad (1)5$$

velocity of the emitted electron. For an electron with kinetic energy of 10 eV, the molecule of mass 100, the broadening is approximately 1.76×10^{-3} eV.

Thus the use of a cool helium discharge photon source would lead to natural line widths of the order of 10^{-3} eV, the lines being Gaussian in shape. Thus high or low resolution PES can be defined according to whether the above factors or instrumental limitations control the resolution of fine structure in the photoelectron spectrum. For high resolution work, an energy resolution of the order of 0.01 eV is required. From Appendix 1 it is seen that the instrumentation used for the current study is capable of high resolution, and the experimental limitation on resolution was the physical width of the electron energy analyser exit slits.

1.8 CALIBRATION

The energy scale of a UVPE spectrum may be calibrated by use of the spectra of the noble gases, argon, krypton, and xenon, which show two peaks each corresponding to the formation of the ion in a

$^2P_{\frac{3}{2}}$ or $^2P_{\frac{1}{2}}$ state. The widths of these peaks indicate the resolving power of the instrument.

If one of these calibrant gases is mixed with the sample under investigation in order to provide internal calibration, interpolation between the known peaks allows an estimate of the ionisation energies for individual sharp peaks to be made to at least 10 meV precision. The ionisation energies of these gases are accurately known from other spectroscopic data, and are given in table 1.3.

TABLE 1.3 IONISATION ENERGIES FOR SOME NOBLE GASES

GAS	$^2P_{\frac{3}{2}}$ (eV)	$^2P_{\frac{1}{2}}$ (eV)
ARGON	15.759	15.937
KRYPTON	14.000	14.665
XENON	12.130	13.436

The ratios of the peak heights after correction for the different band widths are Ar ($^2P_{\frac{3}{2}}$: $^2P_{\frac{1}{2}}$) 1.8, Kr, 1.7, and Xe, 1.6. These ratios may be interpreted as experimental partial photo-ionisation cross sections for the production of ions in their $^2P_{\frac{3}{2}}$ and $^2P_{\frac{1}{2}}$ states at a photon energy of 21.22 eV. The ratio of statistical weights is 2:1, and therefore this is obviously a major factor in the relative band intensities. A table of useful calibration lines is given (table 1.4) [15].

Lloyd has shown [16] that for a particular analyser (127^o electrostatic), exact linearity between electron energy and analyser potential cannot be relied on for electron kinetic energies below 5 eV. For this reason, the calibrant lines used should be as near as possible in energy to the individual peak whose ionisation energy (I.E.) is to be measured.

TABLE 1.4 USEFUL CALIBRATION LINES

	IONIC STATE	IONISING LINE	ELECTRON ENERGY (eV)	APPARENT I.E. (eV)
Ne	$^2P_{\frac{3}{2}}$	$HeII_\alpha$	19.2494	1.9681
Ne	$^2P_{\frac{1}{2}}$	$HeII_\alpha$	19.3463	2.0650
He	^2S	$HeII_\alpha$	16.2268	4.9907
Hg	$^2D_{\frac{5}{2}}$	HeI_α	6.378	14.840
Hg	$^2D_{\frac{3}{2}}$	HeI_α	4.514	16.704
N_2	$^2\Sigma^+_u$	HeI_α	2.467	18.75
N_2	$^2\Pi_u$	HeI_α	4.53	16.69
N_2	$^2\Sigma^+_g$	HeI_α	5.65	15.57

1.9 VIBRATIONAL FINE STRUCTURE

From equation (1)4 it may be seen that the vibrational energy of the final ionised state contributes to the ionisation energy as does the rotational energy. The rotational states are in general too close in energy to be resolved as separate bands in the PE spectrum. The vibrational separations though, are of the order of 0.01 eV and therefore bands in the PE spectrum of a molecule may be expected to show vibrational fine structure.

Vibrational fine structure is often visible in the UVPE spectra of small molecules, and a distinction should be made between vertical and adiabatic ionisation energies. Vibrational fine struture appears as a series of 'lines' forming a photoelectron 'band'; the highest peak of the band is generally taken to correspond to the vertical ionisation energy, and the line of highest electron kinetic energy within the band (lowest I.E.) corresponds to the adiabatic ionisation energy. Ionisation energies quoted

throughout this thesis are vertical ionisation energies.

The bonding or antibonding character of electrons ejected to form a molecular ion, may be revealed by the form of the vibrational fine structure associated with each band in the PE spectrum.

THE FRANCK CONDON PRINCIPLE

The hydrogen molecule is used as an example to illustrate the Franck-Condon principle. The potential energy curves for the H_2 molecule and the H_2^+ molecular ion are given in figure 1.1.

On ionisation of the hydrogen molecule by a photon, the nuclei find themselves in the potential field due to H_2^+, but still separated by an internuclear distance characteristic of the neutral molecule (r_e). The most probable change is thus a transition on the potential energy diagram from the ground state to a point on the potential energy curve vertically above. The Franck-Condon principle determines to which vibrational level of the molecular ion is the most probable transition.

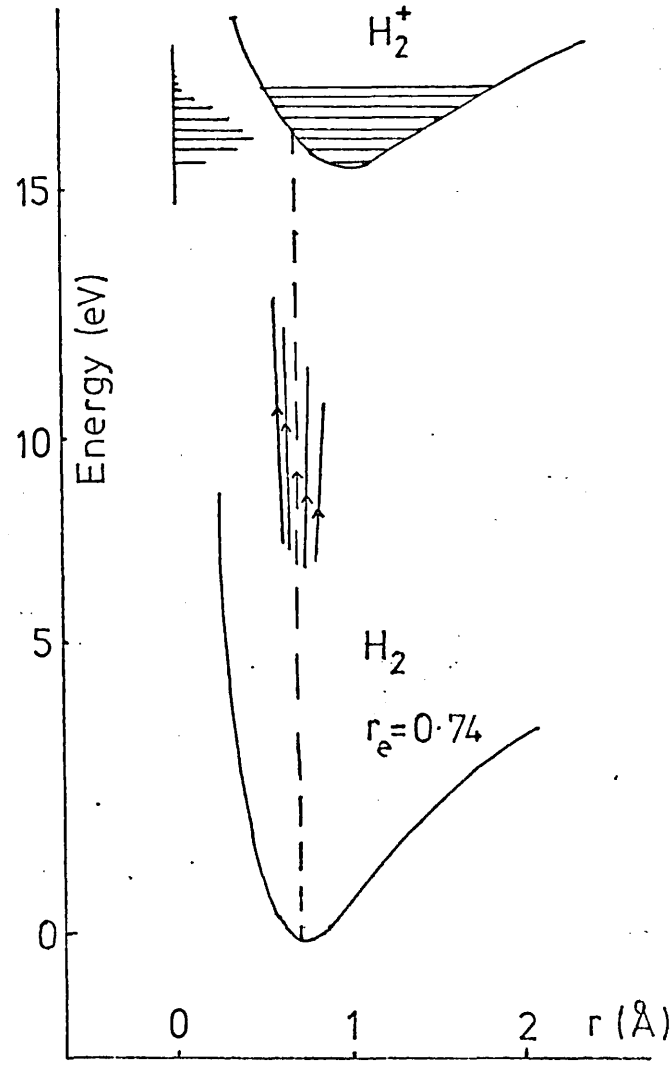

Figure 1.1 Potential energy curves for H_2 and H_2^+

Hence the transition of highest probability gives rise to the most intense band in the PE spectrum and corresponds to vertical ionisation energy (I_v). Transitions to the vibrational levels on either side of I_v are weaker, the one of lowest energy corresponding to the vibrational ground state of the molecular ion, and to the adiabatic ionisation energy.

Adiabatic ionisation energy is more strictly defined as the difference in energy between the neutral molecule in its electronic, vibrational and rotational ground state, and the molecular ion in the lowest vibrational and rotational level of a particular electronic state. Adiabatic transitions are thus often seen in PE spectra as the first vibrational lines of different bands, however they are weak when there is a large change in equilibrium molecular geometry on ionisation.

The vertical ionisation energy is the energy difference between the molecule in its ground state and the molecular ion in a particular ionic state, but with the nuclei in the same positions as in the neutral molecule, and generally corresponds to the line of maximum intensity in the photoelectron band. This is not strictly accurate, since the intensity is also dependent on other factors.

It can be seen, therefore, that experimental ionisation energies are the differences in total energy between the neutral molecule and a particular molecular ion state, suggesting that the correct way to calculate ionisation energies is to calculate the total energy for the molecular ion and for the neutral molecule and subtract. The energy for the molecular ion is sometimes calculated at its equilibrium geometry; the result must then be compared with the adiabatic ionisation energy. The PE spectrum shows the relative energies of the various states of the molecular ion formed on ionisation. However, often, Koopmans' theorem [17] is assumed, and calculated orbital energies are compared directly with experimental ionisation energies.

It should be possible from the intensity distribution in the photoelectron bands to calculate the change in internuclear separation, on ionisation, for simple molecules. Information on the bonding characteristics of a particular electron may be obtained from changes

in vibrational separation and vibrational splitting in the PE spectrum. On removal of a bonding electron, the photoelectron band corresponding to this shows wide vibrational structure with vibrational separation reduced from that in the ground state. Removal of a non-bonding electron will give rise to a band with little or no vibrational structure, since there will be little or no change in internuclear separation on ionisation; removal of an antibonding electron will give rise to a band with increased vibrational separation, relative to the ground state.

The Franck-Condon factors for ionisation to each electronically excited state are obtained from the peak heights; the extent of the Franck-Condon envelope indicates the difference in dimension between ion and molecule.

The majority of substances of interest to chemists have molecular structures of low symmetry, possessing large numbers of atoms per molecule. The resulting increase in the possible modes of vibration that can be excited on ionisation usually leads to vibrational fine structure of great complexity, which, though characteristic for a particular molecule, does not give information as to the bonding character of the electrons. The bands tend to be broad with unresolved vibrational structure.

1.10 KOOPMANS THEOREM AND MOLECULAR ORBITALS

It is possible to compare ionisation energy data from a series of related compounds by drawing energy level diagrams based on experimental vertical ionisation energies. Molecular orbital calculations should provide similar data to the PE spectrum, and the diagrams obtained from experimental ionisation energies may be likened to molecular orbital energy level diagrams. Such diagrams have been widely used in assignment of photoelectron spectra, but could only have strict equivalence on a basis of rigid adherence to Koopmans' theorem [17]. There are certain problems in adopting this approach, particularly for open shell molecules, however some use has been made of such diagrams in chapters 2 and 4, and in this particular case they have proved helpful in assignment of the spectra.

Koopmans' theorem states that for a closed shell molecule, the computed one-electron molecular orbital energy from an ab initio

self consistent field (SCF) calculation, is equal to the ionisation energy of an electron from that orbital (equation (1) 6), that is, molecular

$$I_j = -\varepsilon_{SCF_j} \qquad (1)6$$

orbital energies are defined as the difference in energy between an electron at an infinite distance from the molecular ion, and the same electron in the molecule. There are three reasons why this approximation is inaccurate; much has been written of the inaccuracy involved in comparison of experimental photoelectron data directly with results of molecular orbital calculations of all types [18-20].

(i) Reorientation approximation

In the SCF model, molecular orbitals are one electron orbitals; the electrons are each treated as moving in a field provided by fixed nuclei and average interactions of the remaining electrons. In assuming Koopmans' theorem, the approximation that electron interactions are exactly the same in the molecule and molecular ion, is introduced, and this is strictly incorrect, that is, that there is no reorientation of the remaining electrons on ionisation. The electrons in ions can always attain a more stable state than the one defined by their motions in the neutral molecule, therefore Koopmans' theorem will predict an ionisation energy that is too high. The reorientation energy is the difference between the total energies calculated for the molecule and molecular ion.

(ii) Correlation energy approximation

Even the perfect Hartree-Fock SCF limiting answer for the energy of a molecule would not equal the experimental value, because of a correlation energy error. This is inherent in the one-electron orbital approximation mentioned in section 1.9(i), which assumes that each electron experiences the effects of others only by interaction with a smoothed out average, found by squaring the one-electron wave function. In fact electrons tend to keep apart and

reduce their mutual repulsion energy: their motion is correlated. Koopmans' theorem assumes that correlation must be the same for molecule and ion, but since correlation effects arise to a large extent from pair interactions, the correlation will be different for molecule and ion, and probably less in the ion.

(iii) Relativistic approximation

The Hartree-Fock SCF method does not consider relativistic effects, and Koopmans' theorem assumes that relativistic energy is the same in molecule and ion. In fact this is not an unreasonable assumption in considering the ionisation of valence electrons (in non-degenerate molecular orbitals) with relatively small kinetic energies; however any levels showing spin-orbit coupling are relativistically affected. For inner-core electrons with large kinetic energies relativistic effects become important.

JUSTIFICATION FOR USE OF KOOPMANS' THEOREM

The errors mentioned in 1.9(i) and (ii) tend to cancel each other, in practice, and that in (iii) may be considered small in the case of UVPES since the technique is concerned with valence electrons. However, the cancellation of error is only partial since the reorientation effect is larger, resulting in calculated ionisation energies that are too high. Assignment of PE spectra is further complicated by the fact that reorientation energies for different types of orbital within a molecule may be different, changing the expected band sequence.

From the beginning of UVPES research, difficulties with the adoption of Koopmans' theorem were experienced; in the case of nitrogen,[21] application of the theorem led to qualitatively incorrect ordering of ionic levels and thus incorrect assignment of the PE spectrum. This discrepancy was sufficiently small to be attributed to experimental error; such was not the case, however, in assignment of the second and third bands of the PE spectrum of fluorine[22].

For small molecules the use of a scaling factor (equation (1)7) has met with some success in application of Koopmans' theorem [23].

$$I.E. = -0.92\varepsilon_{SCF} \qquad (1)7$$

For a series of similar organometallic complexes, such as (I) to (IV) in chapter 2 and (I) to (III) in chapter 4, it has been assumed, in assignment of the PE spectra, that, even though different relaxation effects occur for orbitals of different atomic character, the relative ordering of bands in the PE spectra of such a series would be the same.

The only way to include electron correlation in calculations of molecular orbital energies is to use the method of configuration interaction. In this method, excited state wave functions with the same total symmetry are mixed in with the ground state configuration. Mixing coefficients are found using the variation method, and if an infinite number of excited state configurations are properly mixed in, the electron correlation will be represented correctly. A good total wave function and total energy are obtained, but individual molecular orbitals have no meaning; the one-electron molecular orbitals were an approximation to begin with.

1.11 MOLECULAR ORBITAL CALCULATIONS

High speed computers are now available, and because of this a great advance in the field of molecular orbital (MO) calculation has been made. However ab initio SCF calculations are costly in computer time, and unless the model used in calculation is an SCF model carried to Hartree-Fock limits, made for both molecule and molecular ion, the calculated orbital energy, ε_{SCF}, cannot be compared reliably with the experimental ionisation energy, since only for this model is the neglect of correlation energy the only remaining serious approximation.

Two reviews of the use of molecular orbital methods for large organometallic molecules have been published recently [19, 20].

(i) Ab initio methods

Most ab initio methods for molecular orbital calculations use the Hartree-Fock SCF linear combination of atomic orbitals (LCAO) method developed by Roothaan [24], in

which the orbitals are optimised to give the 'best' many-electron wave functions. Clear details of the principles have been given [25]. Molecular orbitals, Ψ_n, are expressed as linear combinations of one-electron atomic wave functions, ϕ_i (equation (1)8).

$$\Psi_n = \sum_n C_{in} \phi_i \qquad (1)8$$

If an inadequate basis set is used, the results may be substantially removed from the Hartree-Fock limit. Inherent in this method is the approximation already mentioned (section 1.10(ii)), resulting in correlation energy error.

Except for one-electron atoms, the atomic orbitals are not simple; they are functions of radial distance, and accurate molecular orbital wave functions may be expressed as a linear combination of simple algebraic atomic functions. The most convenient functions for representing atomic orbitals are Slater orbitals [26] ((1)9),

$$\phi_{n,l,m}(k,r) = Nr^{n-1} \exp(-kr) \cdot Y_{l,m}(\theta,\phi) \qquad (1)9$$

where n is the integral principal quantum number and $Y_{l,m}(\theta,\phi)$, a spherical harmonic function.

The main computational difficulty in ab initio MO calculations lies in evaluation of the two electron integrals. Slater-type functions are successful for diatomics but for larger molecules, Gaussian type functions are used. These show a radial dependence $\exp(-kr^2)$, and have computational advantages although a larger basis set is required.

The number of two electron integrals to be evaluated is proportional to the fourth power of the number of atomic functions, and is thus very high. Symmetry considerations are often made in computational methods to identify integrals of the same value within a system. An example of the large amounts of computer time required for such calculations, is Hillier's calculation for $Mn(CO)_5H$ [27];

this took three hours of computer time on the new CDC 7600 machine.

In recent years, more effort has been made to calculate ionisation energies without use of Koopmans' theorem. Cederbaum et al use perturbation methods to treat relaxation and correlation effects, [22, 28] and have had some success with small molecules.

For molecular orbitals of different spatial character, different reorientation effects are expected on ionisation. Hillier and co-workers have applied this idea in their extensive calculations for transition metal complexes using the 'Δ SCF' method, although, as already mentioned, this method is very costly in computer time. It involves calculation of ionisation energies as the difference in total energies of the neutral molecule (ground state) and the positively charged molecular ion. Two main difficulties arise with use of this method; firstly, the ionic state involves open shell calculation in which spin orbitals must be used, thus increasing computer time, and secondly, there are greater problems with convergence in solution of the secular determinant.

Hillier has reported a large number of calculations [29-36], in which it was found that

(a) reorientation energy is much greater for orbitals localised mainly on the metal atom (eg d orbitals) than for ligand orbitals.

(b) for first row transition metals, Δ SCF calculations are better than any based on Koopmans' theorem.

Other ab initio calculations for organometallic molecules, bis $(\pi$-allyl$)_2$Ni [37], Ni $(CN)_4^{2-}$, Ni $(CO)_4$ [38], and $(\pi$-$C_5H_5)_2$ Fe [39], have been reported.

(ii) Self consistent field Xα scattered wave calculations

This method provides an alternative approach to MO calculation, taking account of orbital reorientation effects [40]. Exchange interactions are approximated in terms of a local exchange potential. 'Molecular orbitals' are generated from the numerical partial-wave solutions of Schrodinger's equation for well defined spherical regions within the molecule and its immediate environment. Orbital energies for fractionally occupied subshells may be computed, and when the orbital occupancy is reduced by half from its value in the unionised system, 'ionisation energies' may be obtained. These account for changes in correlation energy on ionisation, and for a certain amount of reorientation.

Some calculations made using this method have been compared with experimental ionisation energies obtained from photoelectron spectra; comparison of X_α results and Veillard's ab initio calculation for ferrocene is discussed in chapter 3.

Koopmans' theorem is not valid for SCF X_α calculations, but Slater's transition state concept allows the interpretation of electronic transitions in terms of one-electron orbitals and includes reorientation effects.

(iii) Approximate methods

A large number of semi-empirical methods for MO calculations exists; these are often used for treating problems beyond the capacity of ab initio calculation, and are of limited value when results are compared with experimental ionisation energies. Nevertheless, these methods are often used as an aid to assignment of PE spectra.

In these methods, the basis set is limited to the valence orbitals, giving rise to errors, although chemical properties might be expected to depend on the valence orbitals. Most methods introduce approximations and incorporate parameters to reduce the computational problems (for example ZDO, CNDO, INDO, SPINDO, MINDO, SCCC methods).

Semi-empirical Hückel calculations (HMO) and purely empirical HMO calculations are still frequently used for calculating ionisation energies, for example in the case of some cyclic dienes (see chapter 2).

Assignment of many spectra contained in this thesis was aided to some extent by empirical HMO methods, but also by Hillier's ΔSCF MO calculations.

(iv) Open shell molecules

Koopmans' theorem does not apply to the ionisation of open shell molecules; PE spectra of these may show additional bands due to the formation of more than one ionic state as removal of an electron from an orbital may give rise to more than one ion state.

This complicates the PE spectrum in that several bands may be related to a single orbital energy in the neutral molecule, and the probability of formation of the various accessible ion states must be considered. The problem has been examined in detail by Cox and Orchard [41-43] and is discussed more fully in chapter 3 which is concerned with PE spectra for a series of open shell molecules.

1.12 DEGENERATE IONIC STATES

Ionisation from a fully occupied degenerate molecular orbital gives rise to a molecular ion with an orbitally degenerate ground state. This degeneracy may be lifted in two ways; by coupling of spin and orbital angular momenta, or by Jahn-Teller distortion of the molecular ion.

Orbitally degenerate ground states may also arise from ionisation from partially occupied degenerate molecular orbitals (see chapter 3), from two electron transitions, or from ionisation from closed shells in molecules that have a partially occupied shell or shells.

If both Jahn-Teller distortion and spin-orbit coupling effects are weak, then a single band with complex vibrational structure will be

apparent in the photoelectron spectrum. If the effects are strong, there may be as many bands in the spectrum as there are pairs of electrons in the degenerate orbitals. For linear species there is no Jahn-Teller effect since there can be no molecular distortion.

(i) Spin-orbit coupling

This is well illustrated by the PE spectra of the noble gases which have an np^6 outer configuration; the ionised atom has np^5 configuration. If an unpaired electron is in a degenerate orbital, and has orbital angular momentum ($l > 0$), the spin and orbital angular momenta may combine in different ways to produce different states characterised by total angular momentum ($L + S$). The new states will have different energy since the spin and orbital magnetic moments may align to reinforce or oppose one another. All states with multiplicity ($2S + 1$) greater than 1, that is $S > 0$, and a non zero orbital angular momentum, are split by spin-orbit coupling.

This effect operates on the np^5 configuration of the noble gas ions, and the ionic states produced are designated $^2P_{\frac{1}{2}}$ and $^2P_{\frac{3}{2}}$. The states are separated in energy enough to be well resolved in the PE spectra of the gases. Because in this case, the incomplete shell is more than half filled, as indicated by Hund's rules [44], the state of lower energy is that with the higher total angular momentum (J).

The ratio of the statistical weights of these two states is 2:1, and their relative intensities as derived experimentally from the PE spectrum are quoted in table 1.5, for some of the noble gases [45].

TABLE 1.5 RELATIVE INTENSITIES FOR THE NOBLE GASES

GAS	$^2P_{\frac{3}{2}}$	$^2P_{\frac{1}{2}}$
ARGON	1.8	1
KRYPTON	1.7	1
XENON	1.6	1

For the three gases shown in table 1.5, ionisation energies are accurately known from other spectroscopic data, and so these gases are used for accurate calibration of ionisation energies in other PE spectra (section 1.8).

The area ratios for these two photoelectron bands, are, in fact, experimental measurements of $\sigma_{\frac{3}{2}} : \sigma_{\frac{1}{2}}$, the partial photoionisation cross sections for production of ions in the $^2P_{\frac{3}{2}}$ and $^2P_{\frac{1}{2}}$ states using, in this case, photons of 21.22 eV energy. A full treatment of partial cross sections for these gases has been published [46].

Examples of spin-orbit interactions in non-linear molecular ions are found in the PE spectra of tetrahedral AB_4 molecules. The interaction is negligible for CF_4^+ but substantial in CBr_4^+. Spin-orbit splitting is not generally observed in ionic states of molecules having less than a 3-fold symmetry axis, since such molecules contain no degenerate orbitals, on symmetry grounds. However it is observed in a few cases and an explanation has been proposed by Brogli and Heilbronner [47].

(ii) The Jahn-Teller effect

The Jahn-Teller theorem states that a non-linear molecule in a degenerate electronic state is unstable towards distortions that remove the degeneracy [48].

The theorem applies to both spin and orbital degeneracy, but effects due to spin are negligible. When such a state is produced on ionisation of a non-linear molecule, usually by removal of an electron from a degenerate orbital, the positive ion may distort to a lower symmetry thereby becoming more stable. Distortion is equivalent to excitation of one or more degenerate vibrational modes of the undistorted molecule; these are the Jahn-Teller active vibrations. Species of active vibrations for all important point groups are tabulated by Herzberg [49].

The Jahn-Teller stabilisation energy, hνD, is the reduction in energy on changing from the symmetrical nuclear configuration to the new equilibrium position. Jahn-Teller instability in accidental degeneracy is another limitation in the use of Koopmans' theorem.

(iii) Magnitude of Jahn-Teller distortions and spin-orbit splitting

Most states of molecular ions produced by ionisation from degenerate orbitals, therefore, are susceptible to spin-orbit splitting and/or Jahn-Teller effects. The two effects may be considered as competing to lift degeneracy, and the appearance of the PE spectrum will depend on which is predominant. Spin-orbit splitting magnitudes depend on the characteristics of the atomic orbitals involved; Jahn-Teller distortions depend on the bonding characteristics of the ejected electron.

When one of the two effects is much stronger, either normal Jahn-Teller, or spin-orbit split bands are seen in the PE spectrum, but when the effects are of about the same order of magnitude, another complication arises, known as the Ham effect [50].

The effects are summarised approximately as follows:

1) spin-orbit splitting >> Jahn-Teller distortion. In the PE spectrum, the normal spin-orbit splitting is observed.

2) spin-orbit splitting $\simeq$ Jahn-Teller distortion. In the spectrum, anomalous intensity distributions are observed, owing to intensity borrowing. Examples of this are seen in the first bands of the spectra of CH_3Br and CH_3Cl.

3) Jahn-Teller distortion > spin-orbit splitting. This is the region of the Ham effect; the same components are seen as in 1) but with anomalous

intensities as in 2), and also with shifts producing an apparent reduction of spin-orbit splitting, possibly large. No examples have yet been documented in PE spectroscopy.

4) Jahn-Teller distortion ≫ spin-orbit splitting. The spin-orbit splitting is quenched.

1.13 OTHER IONISATION PROCESSES

Ionisation by photons may occur either in a one step process, photoionisation, or a two step process, autoionisation.

(i) Photoionisation

This is an ionisation process in which a photon interacts with a molecule causing an electron to be ejected from a molecular orbital of a neutral species into the continuum, leaving a positively charged molecular ion. All common photoionisation processes are one-electron transitions, and are allowed whatever orbital the electron is in.

There are two forbidden photoionisation processes that might occur in PES; these are two-electron processes:

1) ejection of an electron together with excitation of another.

2) ejection of two electrons by one photon.

These two processes are 'forbidden' since it can be proved that, if electron motions are independent, a transition induced by radiation that changes the quantum numbers of one electron must leave the quantum numbers of all the other electrons unchanged.

Two electron transitions occur since electron motion is correlated, but these processes give rise only

to very weak effects. An example is the transition in mercury, (1)10.

$$Hg\ (5d)^{10}(6s)^2\ [^1S] \xrightarrow{h\nu} Hg^+\ (5d)^{10}(6p)^1\ [^2P] + e \qquad (1)10$$

Photo-double ionisation, in which two photoelectrons are ejected by one photon has been studied [51] and the theory developed [52]. The excess photon energy is distributed between the ejected electrons above the photo-double ionisation threshold, and no sharp peak is observed. Most thresholds are higher than 21.22 eV, and so the process is of little importance in normal HeI PE spectra.

(ii) Autoionisation

This is an indirect process in which a photon first interacts with a molecule to produce an excited state, with subsequent ejection of a photoelectron (1)11.

$$M \xrightarrow{h\nu} M^* \longrightarrow M^+ + e \qquad (1)11$$

The first step is governed by normal optical selection rules; the second step is autoionisation, and no emitted radiation is involved.

The kinetic energy of the ejected electron is not unique to this process and could be produced in a normal photoionisation process. Autoionisation, therefore, will alter the intensity distribution of the PE spectrum.

Autoionisation states have been detected in experiments using sources with differing monochromatic photon energies. They appear as peaks in plots of photo-ionisation current versus photon wavelength, and are often observed when using neon as a source.

If the frequency of the photon source matches that required for production of autoionisation, the intensity spectrum will be distorted. This is rare in PES unless the energy of the photon source is continuously varied, in which

case autoionisation states are encountered. Autoionisation states are not common in HeI PE spectra and are only rarely encountered in HeII.

There are two distinct types of autoionisation:

a) VIBRATIONAL AUTOIONISATION, in which the ejected electron is the same electron that is excited in the resonance process
b) ELECTRONIC AUTOIONISATION, in which the molecular ion is formed in a different electronic state from that of the core of the autoionising level. There is no restriction to ejection of low kinetic energy electrons, and any final state of the ion with a lower energy than the autoionising state may be produced.

This may cause changes in vibrational structure of electronic bands and in relative band intensity. If photoelectron spectra are taken at different photon energies and different band intensities are found, it is sometimes possible to conclude that different branching ratios in electronic autoionisation are the cause. However it is more likely that changes are due to variations in the direct photoionisation cross sections for different photon energies and in the angular distribution of the photoelectrons.

(iii) Fluorescence emission

This process is illustrated in (1)12. Energy is lost in fluorescence as well as an autoionisation process.

$$M + h\nu \longrightarrow M^{**} \longrightarrow M^{*} + h\nu \qquad (1)12$$
$$M^{*} \longrightarrow M^{+} + e$$

This mechanism was proposed to explain the appearance of bands at certain wavelengths that do not correlate with any known ionic state [53].

1.14 ANGULAR DISTRIBUTION OF PHOTOELECTRONS

In the photoionisation process, electrons are not emitted equally in all directions, that is, the photoelectron flux is highly anisotropic. Thus band areas in the experimental photoelectron spectra

depend on the angle at which the photoelectrons are collected and analysed with respect to the photon source; usually this angle (designated Θ) is 90° [54].

Many techniques for studying the angular distribution of photoelectrons have been described in the literature, including the use of rotating sources [55] or analyser systems. Although it is possible to measure the angular distribution of photoelectron flux, as yet there is no workable theory for molecular photoelectron angular distribution. From the angular dependence of photoelectron ejection, it has been deduced [54] that at the magic angle ($\Theta = 54.7^{\circ}$), the observed intensities are directly proportional to partial photoionisation cross sections and no correction for angular distribution effects is necessary.

The angular dependence of the photoelectron flux, $I(\Theta)$, has a simple form for gases, where molecules have random orientation. If the exciting radiation is unpolarised (as in most cases), I is of the form shown in (1)13, where Θ is the angle between photon propagation

$$I(\Theta) \propto 1 + \tfrac{1}{2}\beta\left(\tfrac{s}{2}\sin^2\Theta - 1\right) \qquad (1)13$$

and the direction of the analysed outgoing photoelectrons, and β is an asymmetry parameter ranging from -1 to +2. The largest signal is seen to be when $\Theta = 90^{\circ}$, and this is the value used for all spectra given in this thesis. For gases, the angular distribution is characterised by β, which varies according to photon energy, and the type of orbital ionisation process involved.

1.15 PHOTOELECTRON BAND INTENSITY

(i) Theory of band intensity

The intensity of bands in the photoelectron spectrum gives information useful in assignment for spectra of molecules. The areas of the bands are approximately proportional to relative probabilities of ionisation to the different ion states, but there are many reasons why this is not an exact rule, for example, distortion by autoionisation processes.

Intensity patterns depend on incident photon energy, and the detailed theory for calculation of partial photoionisation cross sections is complex. In the current study, use has been made of two different photon energies, and the changes in intensity pattern in the PE spectra of some organometallic molecules are examined.

The main factors on which the probability for ionisation depend are listed below. If Ψ_i and Ψ_f represent initial and final states of a system absorbing a photon of energy $h\nu$, then the probability (σ) that an electron from an orbital ϕ_n will be ejected into the ionisation continuum is shown in (1)14,

$$\sigma \propto \left| \langle \Psi_i | r | \Psi_f \rangle \right|^2 \qquad (1)14$$

where Ψ_i is the wave function of the ground state molecule and Ψ_f is the wave function of the molecular ion multiplied by that of the electron ejected with energy $h\nu$ - I.E. Band intensity is influenced by:

(a) the occupancy of the ground state orbital, that is, the number of electrons in the orbital from which the photo-electron is ejected. This means that ionisation from an orbital containing four electrons should be twice as probable as from an orbital containing only two. This implies that all ionisations from two electron orbitals should be of equal intensity. In fact this is only nearly true when ionisation is from molecular orbitals of similar atomic character, however it can be a useful rough guide to assignment when molecular with degenerate MOs are being examined. To a rough approximation, the higher the molecular symmetry, the fewer the bands which appear in the PE spectrum.

An example of this is the carbon tetrachloride molecule, in which the outermost orbitals are the chlorine 3p. Under tetrahedral symmetry, these combine to give t_1, t_2, and e orbitals; that is, two sets of triply degenerate, and one of doubly degenerate MOs. The relative areas under the first three bands of the PE spectrum (HeI), are 1.9:2.6:1.0, giving a strong indication that the e ionisation corresponds to the third band (1.0) although the ratios are far from the predicted

3:3:2. Comparisons with other spectra and calculations confirm the assignment.

(b) the degeneracy of the resulting state of the molecular ion, for example in spin-orbit coupling or Jahn-Teller distortion. This determines the statistical weights of the final state of the system, and the number of available channels by which the electron can escape with slightly differing kinetic energy, that is, the ionisation cross section is proportional to the statistical weights of the ionic states produced, an example being ionisation of the noble gases to give two doublet states in the ratio 2:1 (see section 1.12).

(c) The Franck-Condon vibrational overlap integrals between the molecule in its ground state and a particular vibrational state of the molecular ion. (Franck-Condon factors may be separated from their total wave functions using the Born-Oppenheimer approximation.)

(d) Autoionisation effects. Ionisation probability depends on the wavefunction of the ejected electron, and thus on ($h\nu$ - I.E.) which determines the interaction of the electron with available autoionising states of electrons in other orbitals, as it leaves the molecule. Autoionising transitions such as these can be highly probable and can be used to trap photons which ultimately result in ionisation.

(e) the size of the ground state orbital. Valence orbitals of atoms of high atomic number are large compared to those of low atomic number, and give rise to more intense PE bands. Inner shell orbitals have smaller effective cross sections and give rise to lower PE yields.

(f) the energy of the incident photons. The dependence of intensity on the energy of radiation used to excite the spectra is not simple. Experimental measurements of partial ionisation cross sections as a function of energy are currently being reported [12a,46,53,56-58] and are becoming increasingly more common with the advent of synchrotron

radiation sources [11,12b-d]. Figure 1.2 shows the variation of partial ionisation cross section for a 3s electron in argon as a function of ejected photoelectron energy [12d].

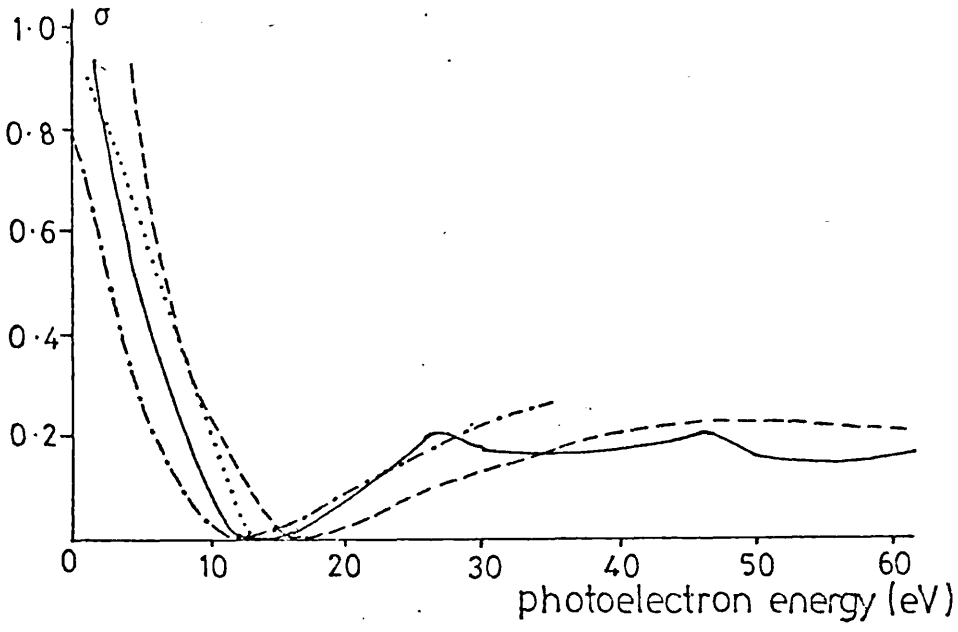

Fig 1.2 The partial photoionisation cross section of the 3s electron in argon plotted as a function of ejected photoelectron energy. ———— experimental data [12d] ..... experimental data [12a] ----, -.-.-. calculated data [59,60].

From experiment it has been found that as photon energy is varied, the partial ionisation cross section changes slowly until a threshold value is reached; here it is likely that the photon energy, $h\nu$, is of the same order of magnitude as the wavelength $h\nu'$ associated with the wave properties of an electron in the particular orbital under investigation, and when the two energies are equal, or one is at some integral multiple of the energy of the other, a periodic maximum or minimum value for ionisation cross section is reached. However, autoionisation effects may also occur; ideally synchrotron radiation provides a sufficiently continuous range of energy to detect autoionisation.

Because all one-electron photoionisations are allowed, the partial ionisation cross sections are all of the same order of magnitude. Once the threshold for a given ionisation has been passed, light of all shorter wavelengths may cause the same process. The cross section is usually at a maximum near the threshold, and then decreases with increasing photon energy, presumably until another maximum occurs.

(g) angular dependence. As mentioned previously (section 1.14), this has an effect on photoelectron band intensity. The angular dependence of an electron in a given orbital is related to the quantum numbers for the molecule and molecular ion, and the angle at which the photoelectron is detected with respect to the photon source.

(ii) Experimental band intensity measurement

The photoelectron spectra presented in this thesis are all differential spectra obtained by applying a potential sweep, linear with time, to the electrostatic analyser (Appendix 1), and simultaneously recording the first derivative of output current, as described by Turner [6]. In these spectra, the relative heights of two bands with different widths, vary with resolution of the analyser, and thus peak heights are not an appropriate measure of intensity; instead relative areas must be used.

Another difficulty arises in the variation of analyser sensitivity with electron kinetic energy; this distorts the spectrum. Electrostatic deflection analysers, such as that used in the Perkin Elmer instrument from which the spectra were obtained, are more sensitive to high energy than low energy electrons. For deflection analysers, the resolution, ΔE, and thus the energy bandwidth within which electrons are transmitted, is proportional to the electron kinetic energy. The areas of both sharp peaks, and broad bands, are proportional to ΔE, and so measured intensities may be corrected by dividing by the electron kinetic energy. The relative intensities of all spectra presented here were corrected in this way.

For the HeII spectra, in many cases, allowance was made for the $HeII_\beta$ satellite spectrum, appearing 7.56 eV to lower ionisation energy from the main $HeII_\alpha$ spectrum with 10% intensity, as seen from the HeII spectrum of nitrogen (Appendix 1).

1.16 SUMMARY

The research presented in the following chapters was carried out in an attempt to clarify the nature of ligand to metal bonding in several groups of organometallic complexes using UVPES. The HeI, and in later chapters, HeII, PE spectra of these complexes are presented and attempts are made to assign the bands with the aid of some qualitative molecular orbital diagrams, and some detailed theory and calculations published by other workers. Use has been made of the different intensity patterns obtained by using HeI and HeII photon sources. A brief summary of content is given at the beginning of each chapter.

Chapter 2

UV Photoelectron Spectra of some dienetricarbonyliron and related compounds.

2.1 SUMMARY

This chapter examines modes of bonding in a series of dienetricarbonyliron and related complexes. A brief description of their history and methods of preparation is given, and their molecular and electronic structures are examined from previously published research, together with the structures for the free dienes.

Structural evidence has been obtained from electron diffraction and X-ray crystallographic studies which are summarised. A review of the current literature concerning the structure and bonding of these complexes, including molecular orbital calculations, nuclear magnetic resonance (n.m.r.), infra-red (i.r.), Raman, and other spectroscopic data is presented, together with some chemical evidence for structure. Lastly, the PE spectroscopic data for these complexes and the free dienes published to date have been examined and the current research is presented in three sections, results, discussion, and experimental.

2.2 INTRODUCTION

Many compounds in which an unsaturated hydrocarbon ligand is bonded to a tricarbonyliron [$Fe(CO)_3$] residue have been isolated, and studies of structure, bonding and reactivity, reported.

Research on dienetricarbonyliron complexes began in 1930, when the synthesis of η^4-buta-1,3-dienetricarbonyliron, (I), was reported by Reihlen and co-workers [61]. (Figure 2.1)

The complex (I) was prepared during an attempt to formulate a structure for pentacarbonyliron; the latter compound was heated in a sealed tube with butadiene, at 150°C, for several hours, and the resulting complex analysed as $C_4H_6Fe(CO)_3$. Two alternative structures for the complex were proposed (figure 2.2), (2)1, and (2)2. In each case

Figure 2.1

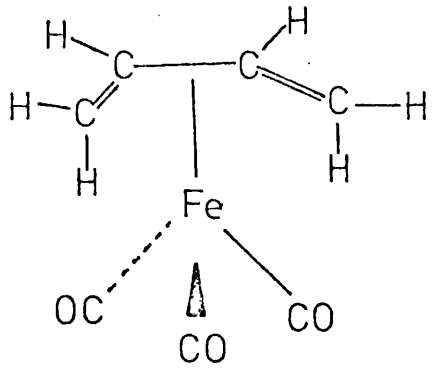

η^4-buta-1,3-dienetricarbonyliron (I)

the metal atom is considered to be bonded to the terminal carbon atoms of the diene.

Figure 2.2 Structures proposed for (I)

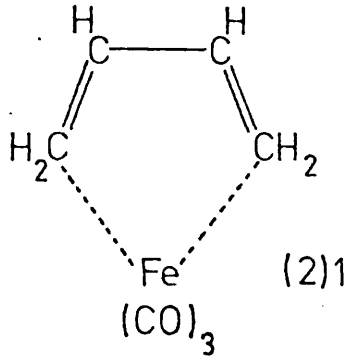

(2)1

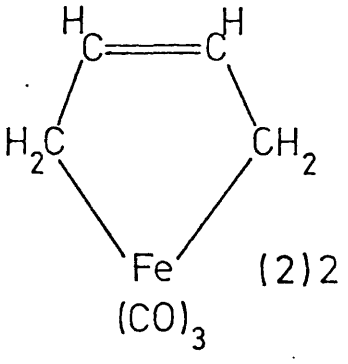

(2)2

In 1953, Reppe and Vetter reported the synthesis of organoiron complexes following reaction of acetylene with iron carbonyls [62], and in 1958, Hallam and Pauson [63] extended the study of the original complex, (I), reported by Reihlen.

More recent research has included the preparation of complexes (II) to (VIII), shown in Figure 2.3 [64-68], and the current study attempts to elucidate the nature of bonding within these complexes.

Figure 2.3 Complexes (II) to (VIII)

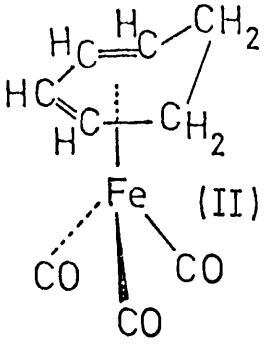

η^4-cyclohexa-1,3-dienetricarbonyliron

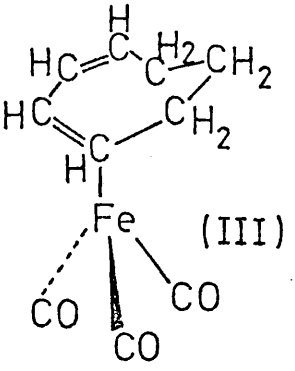

η^4-cycloheptа-1,3-dienetricarbonyliron

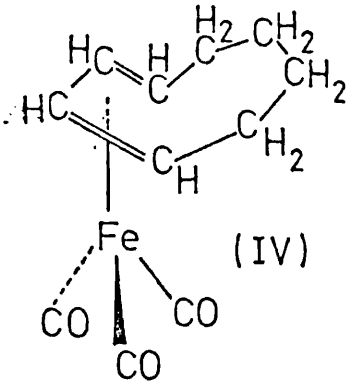

η^4-cycloocta-1,3-dienetricarbonyliron

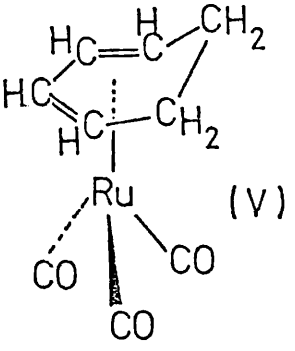

η^4-cyclohexa-1,3-dienetricarbonyl-ruthenium

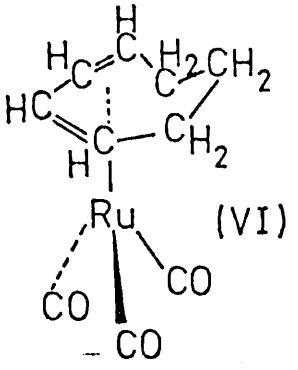

η^4-cyclohepta-1,3-dienetricarbonyl-ruthenium

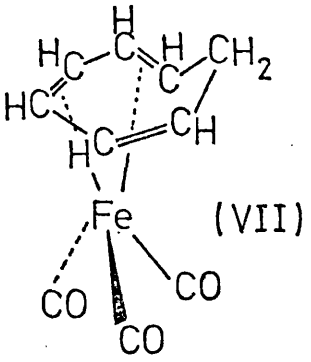

η^4-cyclohepta-1,3,5-triene-tricarbonyliron

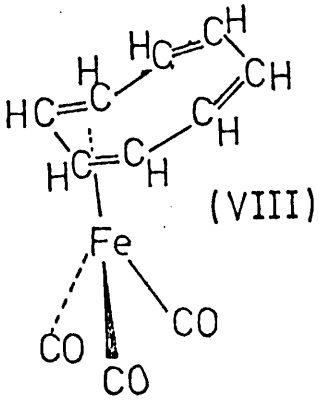

η^4-cycloocta-1,3,5,7-tetraene-tricarbonyliron

2.3 CLASSIFICATION AND SYNTHESES

The chemical behaviour of dienetricarbonyliron complexes suggests they should be separately classified from the 'ferrocene' type complexes first isolated in the early 1950s [69,70], although the general nature of metal to organic ligand bonding in both types of complex is similar.

Two valence bond structures, (2)3 [63] and (2)4 [71] (figure 2.4) were proposed. Structure (2)3 suggests that

Fig 2.4 Valence bond structures proposed for (I)

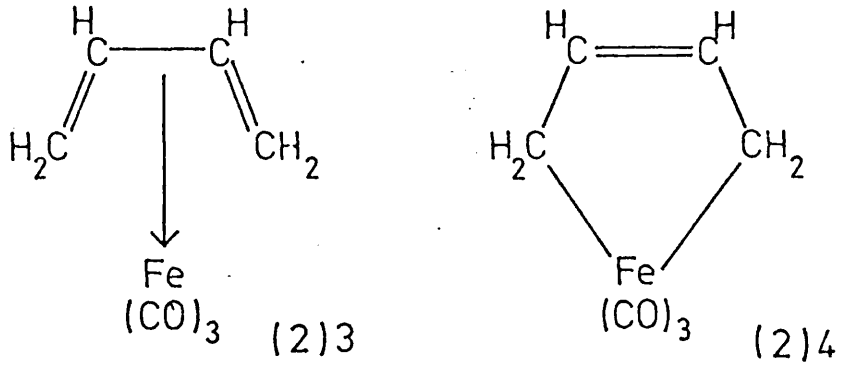

the ligand is π bonded to the metal, the ligand acting as electron donating; structure 2(4) suggests a significant amount of metal-carbon σ bonding as well as π bonding. This will be discussed more fully in section 2.5.

The general method of synthesis for complexes (II) to (VIII) is shown in figure 2.5. An iron carbonyl complex is refluxed with the relevant ligand in a suitable solvent.

Figure 2.5 General method of synthesis for (I)-(VIII)

$$Fe(CO)_5$$

$$Fe_2(CO)_9 \text{ or } Fe_3(CO)_{12} + \text{LIGAND} \xrightarrow[\text{solvent}]{\text{reflux}} \text{LIGAND} - Fe(CO)_3$$

2.4 MOLECULAR STRUCTURE

(i) Structural data for the diene ligands

(a) buta-1,3-diene

The structure of buta-1,3-diene has been determined by electron diffraction studies, and the molecule is found to exist in a planar 'trans' conformation [72]. This is not the case for perfluorobutadiene, for which a dihedral angle of 42° has been reported from photoelectron and UV spectroscopic data. This was found to be in agreement with a subsequent electron diffraction study [73].

Heilbronner [74,75] has attempted to relate the dihedral angle (that is, the angle of twist between the planes containing the double bonds) in cyclic dienes to ionisation energies, following PE spectroscopic studies of cycloalkadienes [76-78]. Infra-red studies have also been used in the determination of the conformation of some conjugated dienes by means of vibrational frequencies [79]. Calculations have been carried out to determine the minimum energy conformations of cycloalkadienes with 6,7 or 8 carbon atoms in the ring [80]. The results have been compared with electron diffraction, spectroscopic and molecular polarisability data; good agreement is generally found except for the case of cyclohepta-1,3-diene. Electron diffraction data are available for all these molecules together with experimental geometrical data.

(b) cyclohexa-1,3-diene

Calculations by Heilbronner [74,75] using photoelectron spectroscopic data [76,77], predict a dihedral angle of 18°. Other calculations predict that the most stable conformation, by 2 kcal mole^{-1}, is that in which the two planes containing the double bonds are inclined at an angle of 17.5° with respect to each other [80]. This is in good agreement with data from electron diffraction studies [81] and from a microwave investigation [82]. These results compare well with those from two other sources [83,84]. Recent i.r data give a dihedral angle of 18° [79].

(c) cyclohepta-1,3-diene

There is some disagreement over the value of the dihedral angle for this molecule. The most recent experimental data, based on i.r studies, give a value of 0° for the dihedral angle [79]. Calculations [80] suggest there are two stable forms with dihedral angles of 0° and 55°, but that the 55° form is slightly more stable [85,86]. Electron diffraction studies give a value of 0° for the dihedral angle, in agreement with the i.r. data [86]. A n.m.r. study by Crews [87] concludes that the angle is non zero, while Heilbronner's calculations give a value of 28°. UV studies provide evidence for a dihedral angle of 0° [88].

(d) cycloocta-1,3-diene

Calculations giving a dihedral angle of 65°, and the 'boat/chair' conformation as most stable, in spite of the large dihedral angle, have been published [80]. Heilbronner gives a calculated value of 59° [75]. The experimental values [89,90] derived from electron diffraction data are rather uncertain,

in view of the complete lack of symmetry in the dominant conformation. There seems to be general agreement on a dihedral angle value of approximately 60°.

The results for the cyclic dienes are summarised in table 2.1.

Table 2.1 Dihedral angles for the cyclic dienes

DIENE	CALCULATED	EXPERIMENTAL (IN DEGREES)
cyclohexa-1,3-diene	17.5 [80], 18 [75]	18 [79,81,82,83]
cyclohepta-1,3-diene	55 [80], 0 [80], 28 [75]	0 [79,85,86,88], 33 [87]
cycloocta-1,3-diene	65 [80], 59 [75]	~60 [79] uncertain [89,90]

(e) cycloheptatriene

Electron diffraction studies have determined the existence of a considerable dihedral angle, and values agree fairly well with Heilbronner's calculated angle of 50° [75]. The bond distances reported in the electron diffraction study [91] indicate a substantial amount of π electron delocalisation. Cycloheptatriene is found to exist in boat form as shown in figure 2.6.

Fig 2.6 Boat form of cycloheptatriene

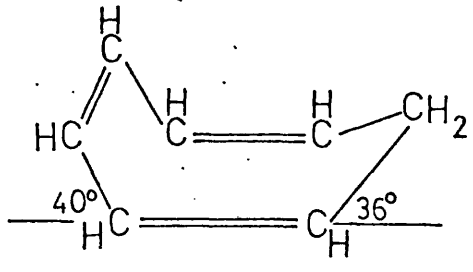

(f) cyclooctatetraene

This molecule was found by an electron diffraction study to possess D_{2d} symmetry [72]

corresponding to a boat conformation. Observed differences in bond lengths indicate a higher bond order for the single carbon-carbon bond and lower bond order for the double bond, in butadiene, compared with cyclooctatetraene. The dihedral angle is approximately 43°. Earlier X-ray diffraction [92] and electron diffraction [93] studies are in agreement.

(ii) X-ray diffraction data for the complexes

Many conjugated-diene tricarbonyliron complexes are known but X-ray crystallographic data are available for only a few; thus the exact conformations of the ligands within their tricarbonyliron complexes are not known for (II) to (VII).

X-ray crystallographic data for (I), published in 1963 by Mills and Robinson [94] showed the butadiene ligand within the molecule to be in cis-planar conformation. Bond lengths between the diene carbon atoms were found to be identical within rather large experimental limits; however the lengths of those bonds originally 'double' in butadiene itself, were undoubtedly increased within the complex. Values reported are consistent with complete delocalisation of the diene $p\pi$ electrons. The iron atom was found to lie below the plane of the diene carbon atoms and approximately equidistant from all four (2.10 $\pm$ 0.04 Å) and the plane containing the diene carbon atoms is inclined at a slight angle to that defined by the carbon atoms of the three carbonyl groups. Values for the three iron-carbon-oxygen bond angles within the complex are given as 179°, 178°, 178°.

Later X-ray crystallographic studies carried out for related complexes containing a conjugated diene-tricarbonyliron unit, have shown the same tendency towards equalisation of

the carbon-carbon bond lengths within the conjugated diene ligand [95-97].

The structures of complex (VIII), and of the related compounds (2)5, (2)6, (figure 2.7) have also been determined by X-ray diffraction [98].

Fig 2.7 Cyclooctatetraenetricarbonyliron complexes

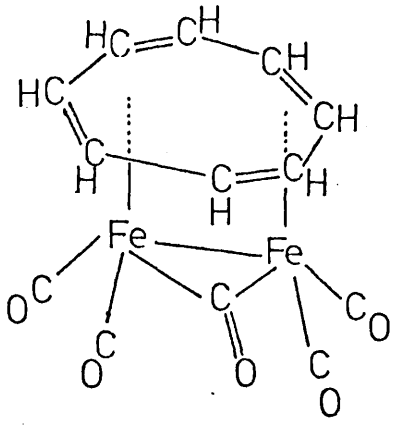

(2)5

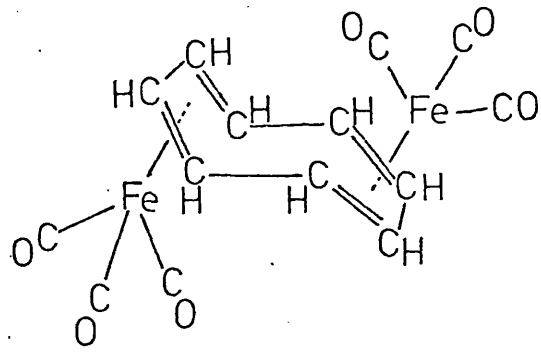

(2)6

In complex (VIII), the ligand has different geometry from the free ligand, indicating some reorganization of π electron density on coordination to the $Fe(CO)_3$ group. The cyclooctatetraene ligand was found to be coordinated to the iron atom via two double bonds only as the butadiene ligand in complex (I). There was evidence for a tendency towards equalisation of the ring carbon-carbon bond lengths, and a distortion towards planarity for the ring.

2.5 ELECTRONIC STRUCTURE

The two valence bond structures proposed for complex (I) were shown in figure 2.4 - (2)3, and (2)4. Bonding within the complex may be discussed more fully in terms of

molecular orbital theory. The synergic aspect of metal-carbonyl bonding was examined by Kettle [99]; the resulting slight polarity within the $M(CO)_3$ group (where M = metal) is a consequence of carbonyl to metal σ electron donation, assisted by metal to carbonyl back donation. The carbonyl acceptor orbitals are low lying π antibonding orbitals. Kettle also mentions possible reasons for deviation from linearity of the M-C-O bond.

A discussion of bonding within the $M(CO_3)$ fragment, together with interaction diagrams for construction of an $M(CO)_3$ molecular orbital energy level diagram, is given by Elian and Hoffmann [100] and again by Hoffmann et al. [101]. A simple molecular orbital treatment of butadiene-metal bonding has been discussed by Green [102], the two main points being:

(a) there is electron donation from the highest occupied molecular orbital of the ligand into empty metal d orbitals.

(b) this is complemented by back donation of electron density from filled d orbitals into the lowest unoccupied molecular orbital of the diene.

The relative importance of (a) and (b) is determined by the energy separation between the metal d orbitals and the highest occupied and lowest unoccupied ligand molecular orbitals, and also by the symmetry properties of the orbitals involved.

Although $Fe(CC)_3$ is not generally thought of as being an electron donating group, within complex (I), there is evidence from ab initio molecular calculations on this molecule, for a net negative charge on the butadiene ligand [29]. There is other evidence that this ligand, within the complex, tends to be electron rich [103, 104]. A recent study of the bonding in cyclopentadienyltricarbonylmanganese

and related complexes has been published [105]. With the aid of molecular orbital calculations and PE spectroscopic data, MO diagrams have been drawn showing interaction of the $Mn(CO)_3$ fragment with various ligands. The complexes studied are shown in figure 2.8.

Fig 2.8 Tricarbonylmanganese complexes

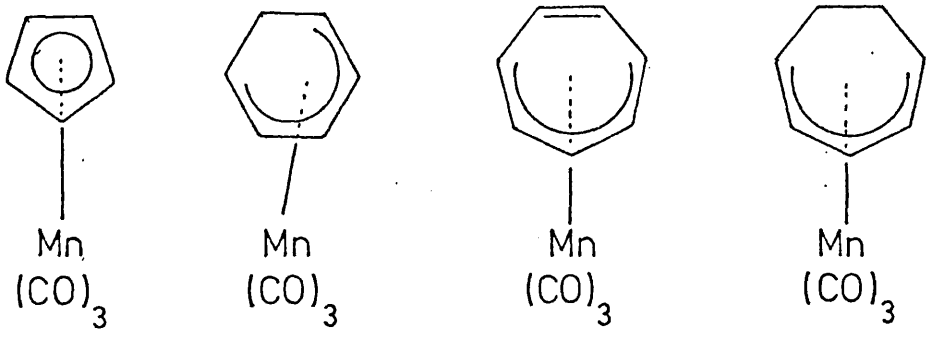

A molecular orbital treatment of conjugated olefin-metal complexes has been published by Mingos [106]. The model used appears to predict the correct trends in bond lengths for carbon-carbon bonds in metal-olefin complexes. Hückel MO theory is used and includes the metal $d\pi$ orbitals. Bond lengths are calculated from the bond orders thus obtained, using the Coulson-Golebiewski expression, (2)7 [107], where τ is the calculated bond length in Å, and p is the Hückel π bond order. For

$$\tau = 1.517 - 0.18p \qquad (2)7$$

coordinated butadiene in complex (I), the calculations suggest the carbon-carbon bonds are equal in length, and the bond length is 1.413 Å. Agreement with X-ray crystallographic data for butadienetricarbonyliron complexes is extremely good [94, 108, 109].

A simple Hückel MO treatment of the butadiene molecule will now be discussed, followed by a description in MO terms, of bonding to the $Fe(CO)_3$ group. This model will be used in discussion of the results obtained in the present study.

For buta-1,3-diene, the atomic orbitals (AOs) serving as the basis set are $2p_{z1}$, $2p_{z2}$, $2p_{z3}$, $2p_{z4}$, where the numerical subscripts refer to the carbon atoms, and the molecular plane is taken to be the xy plane. If these AOs are designated ϕ_1, ϕ_2, ϕ_3, ϕ_4, then the molecular orbitals (MOs) are given by equation (2)8 , which leads to

$$\psi_n = C_{1n}\phi_1 + C_{2n}\phi_2 + C_{3n}\phi_3 + C_{4n}\phi_4 \quad (2)8$$

the secular equations, (2)9. Zero differential overlap is assumed, even between neighbouring atoms, and α and β are the usual Hückel parameters. Consistent non trivial solu-

$$\begin{aligned}
C_{1n}(\alpha - E_n) + C_{2n}\beta &= 0 \\
C_{1n}\beta + C_{2n}(\alpha - E_n) + C_{3n}\beta &= 0 \\
C_{2n}\beta + C_{3n}(\alpha - E_n) + C_{4n}\beta &= 0 \\
C_{3n}\beta + C_{4n}(\alpha - E_n) &= 0
\end{aligned} \quad (2)9$$

tions of (2)9 are obtained when:

$$\begin{vmatrix}
\alpha-E_n & \beta & 0 & 0 \\
\beta & \alpha-E_n & \beta & 0 \\
0 & \beta & \alpha-E_n & \beta \\
0 & 0 & \beta & \alpha-E_n
\end{vmatrix} = 0 \quad (2)10$$

The solutions of determinant (2)10 give the energies of the four molecular orbitals obtained on combination of the four $2p_z$ AOs, (2)11. The coefficients, C_{in} (i = 1 to 4)(n = 1 to 4)

$$\begin{aligned} \varepsilon_1 &= \alpha + 1.62\beta \\ \varepsilon_2 &= \alpha + 0.62\beta \\ \varepsilon_3 &= \alpha - 0.62\beta \\ \varepsilon_4 &= \alpha - 1.62\beta \end{aligned} \qquad (2)11$$

give the following molecular orbitals (2)12:

$$\begin{aligned} \psi_1 &= 0.372\phi_1 + 0.602\phi_2 + 0.602\phi_3 + 0.372\phi_4 \\ \psi_2 &= 0.602\phi_1 + 0.372\phi_2 - 0.372\phi_3 - 0.602\phi_4 \\ \psi_3 &= 0.602\phi_1 - 0.372\phi_2 - 0.372\phi_3 + 0.602\phi_4 \\ \psi_4 &= 0.372\phi_1 - 0.602\phi_2 + 0.602\phi_3 - 0.372\phi_4 \end{aligned} \qquad (2)12$$

Thus a rough energy level diagram may be obtained, as shown in figure 2.9.

Fig 2.9 Approximate energy level diagram for the π orbitals of cis-butadiene showing corresponding p orbital combination

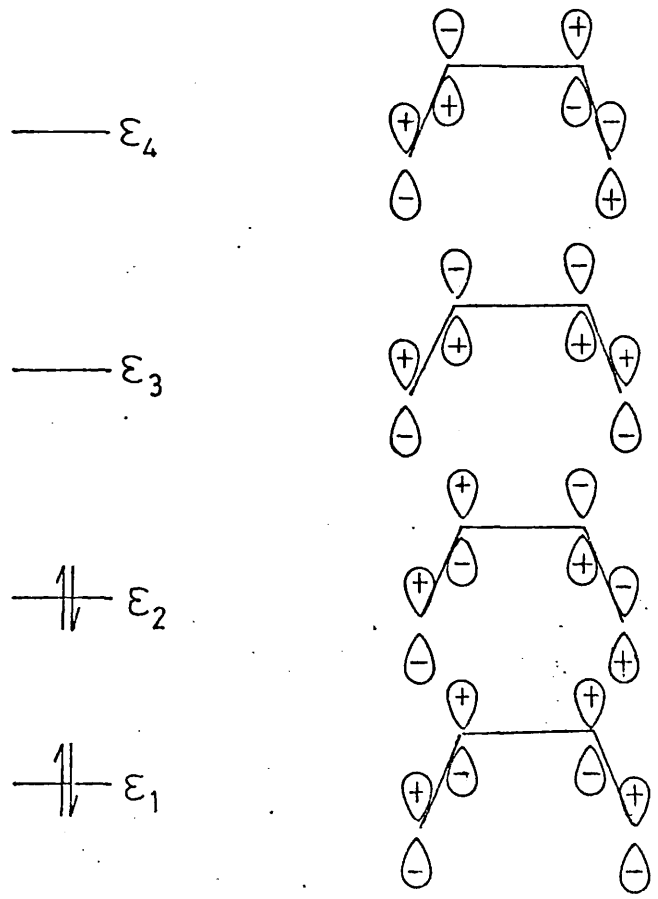

It is now a simple matter to assign symmetry labels to each of the MOs. The HMO method used makes no distinction between cis and trans buta-1,3-diene with regard to energy levels. The symmetry labels will be different for the two forms, however, since each conformation is represented by a different point group. Cis and trans butadiene differ only in the π electron interactions between carbon atoms 1 and 4; thus one would expect very little difference in the π electronic energies for the two conformations, and since the approach used here (HMO theory) is so approximate, no distinction would be expected.

Trans butadiene may be represented by the C_{2h} point group, with symmetry operations E, C_2, i, σ_h. The molecular orbitals obtained from the above calculation transform as shown in (2)13.

$$\begin{aligned} \psi_1 &\text{ as } a_u \\ \psi_2 &\text{ as } b_g \\ \psi_3 &\text{ as } a_u \\ \psi_4 &\text{ as } b_g \end{aligned} \qquad (2)13$$

Cis butadiene belongs to the group C_{2v} with molecular orbitals transforming as in (2)14.

$$\begin{aligned} \psi_1 &\text{ as } b_2 \\ \psi_2 &\text{ as } a_2 \\ \psi_3 &\text{ as } b_2 \\ \psi_4 &\text{ as } a_2 \end{aligned} \qquad (2)14$$

These symmetry labels are particularly convenient for use in discussion of MO models of the complexes (I) to (VIII), although the highest true symmetry within the complexes is C_s (E, σ_h). The symmetry labels for the diene π MOs then become a' and a" , where a' corresponds to a_2 in C_{2v} and a" to b_2, and for convenience in discussion of the bonding in complex (I), the C_{2v} labels have been adopted.

In complex (I), the butadiene MOs may be considered to interact with metal d orbitals of the same symmetry and similar energy. Possibilities for interaction on symmetry grounds alone are given in table 2.2.

Table 2.2 Symmetry properties of butadiene MOs and metal d-orbitals

Butadiene MO	Symmetry $C_{2v}(C_s)$	metal d orbital of equivalent symmetry
ψ_1	$b_2(a'')$	$d_{z^2}, p_z,$ s
ψ_2	$a_2(a')$	p_x, d_{xz}
ψ_3^*	$b_2(a'')$	p_y, d_{yz}
ψ_4^*	$a_2(a')$	$d_{x^2-y^2}$, d_{xy}

*denotes an antibonding orbital

Interaction diagrams for the $M(CO)_3$ group and its relative energy levels have been published by Elian and Hoffmann (M=Fe) [100], and by Whitesides et al. (M=Mn) [105]. The interaction diagram given by Whitesides is shown in figure 2.10.

If C_{3v} symmetry is assumed for the $M(CO)_3$ (M=Fe) fragment, with the z axis defined as the C_3 rotation axis, the 5σ carbonyl levels interact mainly with the metal d_{xz}, d_{yz} orbitals. The bonding combinations represent σ donation from the carbonyl groups to the metal. The antibonding combination is primarily d_{xz}, d_{yz} in character.

For complex (I), an approximate interaction diagram may now be constructed for the $Fe(CO)_3$ fragment and the butadiene ligand; this is shown in figure 2.11. The principal bonding interactions will be between the metal d_{xz}, d_{yz} partly occupied orbitals and the $b_2\ \pi^*$ antibonding and $a_2\ \pi$ bonding levels of butadiene. The overall symmetry of the molecule is C_s. The other dienetricarbonyliron

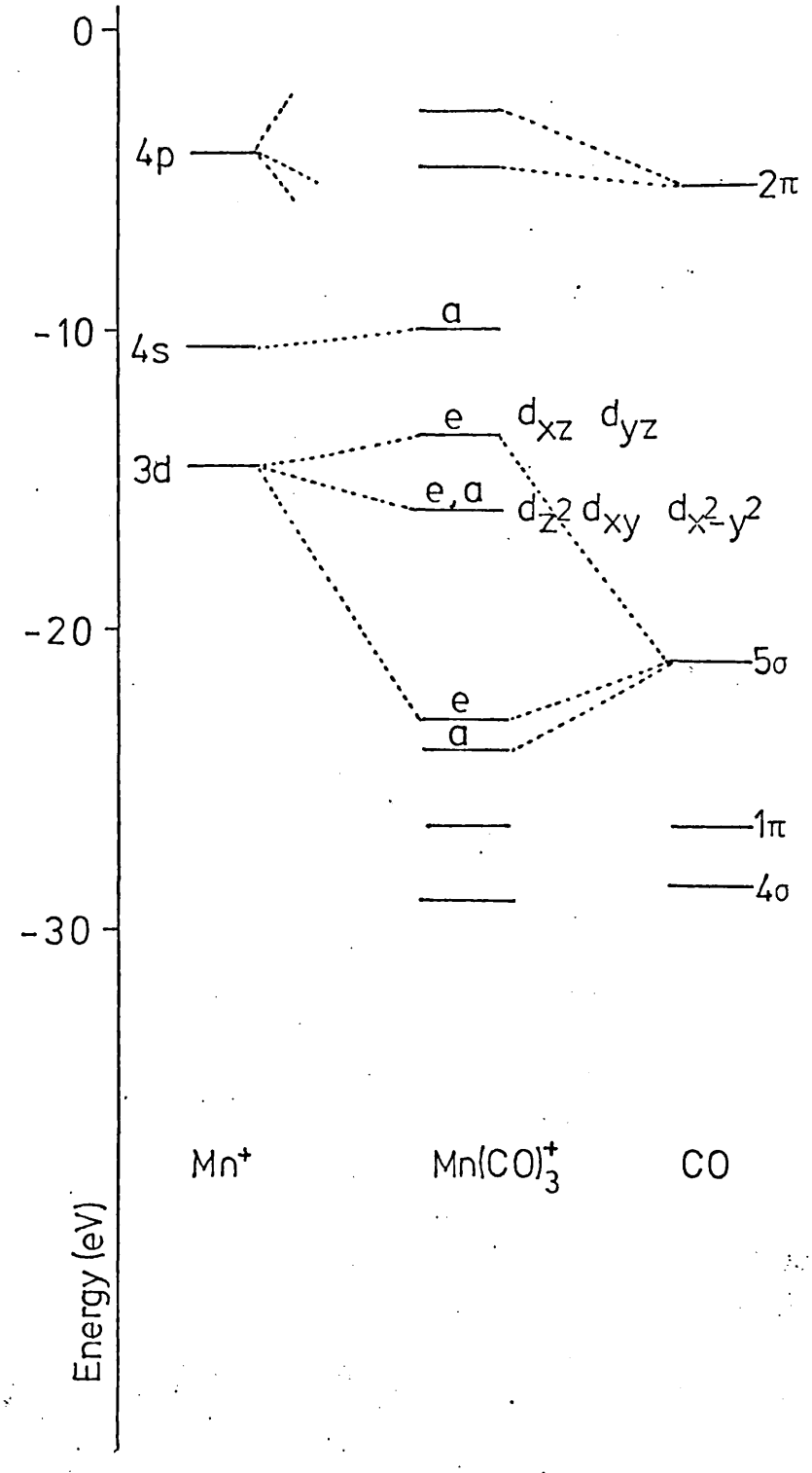

Fig 2.10 Molecular orbital interaction diagram for $Mn(CO)_3^+$ [105]

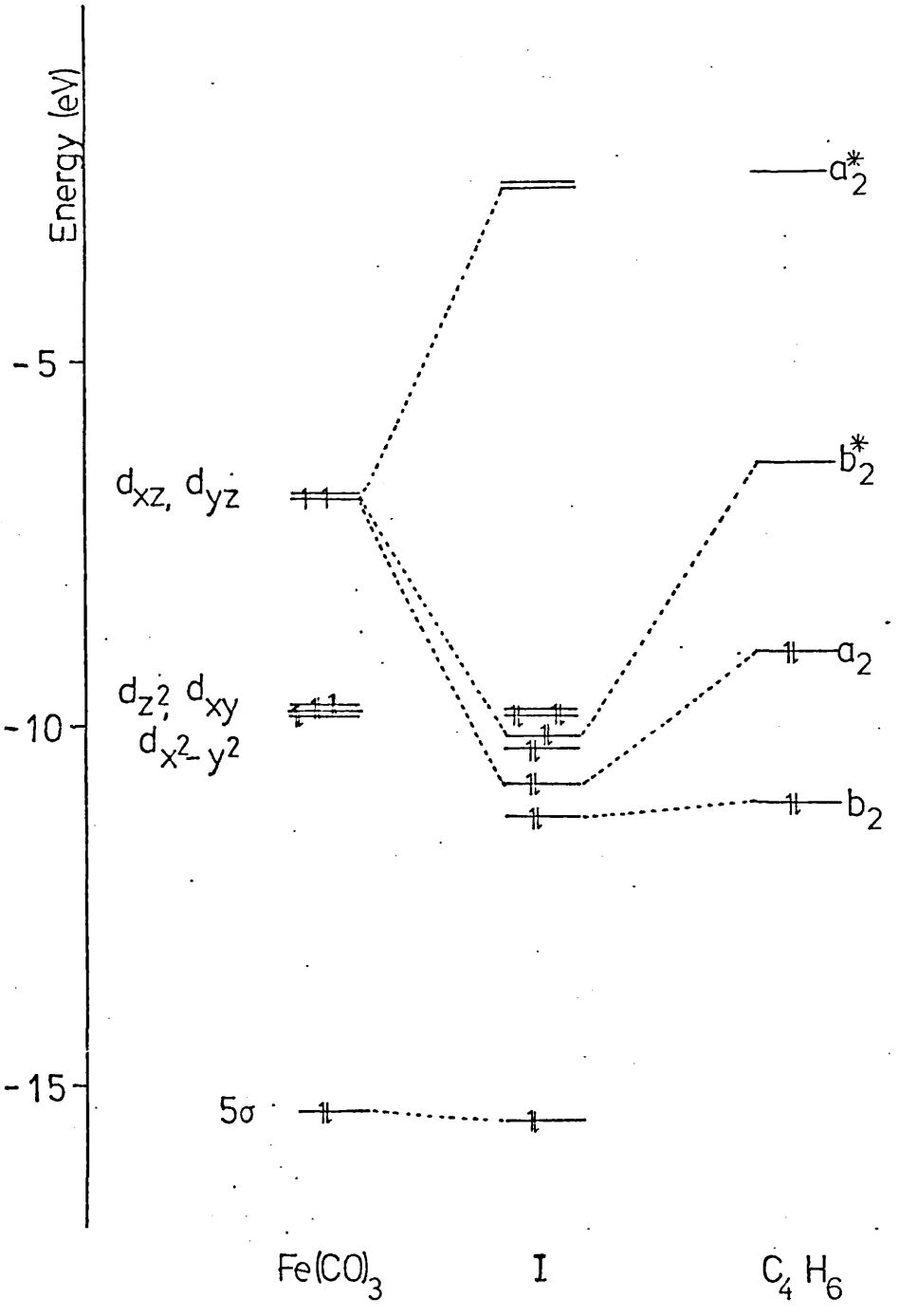

Fig 2.11 Molecular orbital interaction diagram for complex (I)

complexes, (II) to (VI), may be considered to have similar interaction diagrams, except that the further reduction in symmetry will tend to remove any residual degeneracy of the relatively non-bonding metal d levels.

2.6 OTHER SPECTROSCOPIC STRUCTURAL EVIDENCE

(i) Conjugated diene tricarbonyliron complexes

Structure (2)4 (fig. 2.4) for complex (I) was first proposed on the basis of n.m.r. data obtained by Wilkinson and co-workers [71].

In the proton n.m.r. spectrum of (I), two protons gave bands at 5.85 δ, the normal olefinic region, and two each at 1.68 δ and 0.22 δ, the aliphatic region, thus apparently favouring a structure of type (2)4. However this interpretation of the data would assume the presence of the iron atom to have no effect on the chemical shift of the protons. The same authors showed the i.r. stretching frequencies of the carbon-hydrogen bonds tending to favour sp^2 rather than sp^3 hybridised carbon atoms, and therefore considered structure (2)3 (fig. 2.4) to be a more likely representation, particularly since the effect of the $Fe(CO)_3$ group on the magnetic field was unknown.

There is obviously a contribution to the structure of (I) from both of the over simplified valence bond representations; in MO terms, structure (2)3 might be said to represent electron donation from ligand bonding orbitals to metal antibonding orbitals, and (2)4, metal d electron donation to the ligand $b_2\pi^*$ antibonding orbital. There have been many arguments as to which of the valence bond representations makes the greater contribution to the bonding, or whether or not one structure makes any significant contribution.

In 1966, two ^{13}C n.m.r. studies, concerned with establishing evidence to distinguish the structures (2)3 or (2)4 were published [110, 111]. Both favoured a structure of type (2)3 for complex (I) since the carbon-hydrogen coupling constants were more typical of values associated with sp^2 hybridised carbon atoms than sp^3. From the data it seems that there is a small rotation of the $-CH_2-$ hydrogens out of the butadiene plane. Mills and Robinson [94], in their X-ray diffraction study of complex (I), suggested that the n.m.r. results reported by Wilkinson [71] could be explained if the terminal hydrogens in the butadiene residue were bent slightly out of the butadiene plane. The authors of both the 1966 papers [110, 111] failed to comment on the significance of the appearance of a singlet in the ^{13}C n.m.r. spectrum, representing the carbonyl carbon atoms in complex (I). This was noted in a subsequent publication [112], and the same authors later published a detailed, variable temperature ^{13}C n.m.r. study of η^4-diene-tricarbonyliron complexes [113]. They stated that the single sharp resonance observed for the three carbonyl groups is inconsistent with static geometry (2)3 or (2)4, and interpreted it as a sign of intramolecular rearrangement, via carbonyl scrambling. They were able to resolve the carbonyl bands at $-90^{\circ}C$ and noted the difference in rearrangement rates for conjugated and non-conjugated diene complexes. It was argued that the increased activation barrier for carbonyl scrambling in the conjugated diene complexes was due to a significant contribution from a structure of type (2)4. A less detailed study in the same field has also been published [114].

A recent ^{13}C n.m.r. study by Pearson [115] also argues in favour of an important contribution from a structure of type (2)4. A modified bonding

model for the butadiene-metal bond is proposed; the two occupied π MOs of butadiene are localised, thus allowing retention of sp^2 character of all carbon atoms, while giving the appearance of significant contribution from a (2)4-type structure. This model appears to satisfy most of the experimental observations so far published, including the slight deviation from planarity of the diene ligand consistent with X-ray data, by allowing for partial rotation about the C_1-C_2 and C_3-C_4 bond axes. Another ^{13}C n.m.r. study reaches the same conclusions [116].

It is likely that the nature of any diene substituents will significantly affect contributions from one or other of the valence bond structures [113, 115]. Since the nature of the substituent (electron withdrawing or donating) may alter the relative energies of the π MOs, as, for example, in the case of perfluorobutadiene [73], thus having a significant influence on the structure, the relative contributions from each of the π levels to the metal ligand bond will be different.

(ii) η^4-cyclohepta-1,3,5-trienetricarbonyliron

This complex was first reported erroneously as the dicarbonyl complex in 1958 [117], but in 1961 was redescribed correctly [118]. The 'dicarbonyl' showed three strong bands in the carbonyl stretching region of the i.r. spectrum; such a spectrum was inconsistent with a simple dicarbonyl structure. Infra-red and proton n.m.r. data [118] were consistent with structure (VII), in which the tricarbonyliron group is bonded to two adjacent double bonds of the triene, while the third double bond remains uncoordinated.

(iii) η^4-cycloocta-1,3,5,7-tetraenetricarbonyliron

The room temperature proton n.m.r. spectrum of this complex in solution shows only one sharp line, and it was originally, although incorrectly, proposed that the cyclooctatetraene ring was in the form of a planar delocalised C_8 ring [119] although the X-ray diffraction data showed this not to be the case for the solid [98]. The electron diffraction study of cyclooctatetraene, (COT), has indicated a non planar 'tub' conformation [72]; this geometry is retained in the $Ag(COT)^+$ complex [120]. Cyclooctatetraene itself, fails to show aromatic character; molecular orbital calculations yield two unpaired electrons for the molecule having D_{8h} or non-planar D_{4d} symmetry.

Evidence for the existence of the η^4-diene structure of (VIII) in solution as well as in crystalline form [98], arises from an i.r. and Raman spectroscopic study of the complex both in the solid state, and in solution [121]; the spectra were found to be similar. Thus the single sharp resonance in the proton n.m.r. spectrum could not be attributed to a different geometry in solution, for the complex. The protons in compound (2)6 (figure 2.7) were found to be non-equivalent, so that any proposed exchange mechanisms for protons in (VIII) had to explain this also. Dickens and Lipscomb [98] suggested a dynamic effect amounting to permutation of the carbon atoms of the ring relative to the tricarbonyliron group; this would satisfy experimental observations.

Several temperature dependent n.m.r. studies of (VIII) were published [122-124]. Unfortunately, even at low temperatures, the proton bands failed to reach the slow exchange limit. It was suggested that the cyclooctatetraene ligand was bonded in the 1,5-position [124]. It was known that (VIII) is fluxional in solution, and the rearrangement mechanism was suggested to be by a series of 1,2-shifts of the $Fe(CO)_3$ group, around the COT ring [125]. The crystal and molecular structure of the corresponding ruthenium compound was subsequently determined [126], confirming bonding in the 1,3-position, and proton n.m.r. studies carried out on this molecule to determine a shift mechanism, since this molecule is also fluxional [127]. Since the structure of the ruthenium complex is isomorphous with (VIII) it was considered safe to regard the ruthenium complex as a close structural and dynamic analogue of (VIII), and the two were suggested to have the same shift mechanism [127]. It was possible to resolve the proton n.m.r. spectrum of the ruthenium complex at low temperatures, and a likely shift mechanism was formulated. The proposed 1,2-shift mechanism was later confirmed by a ^{13}C n.m.r. study [128], and a pulsed n.m.r. study of the molecular dynamics of (VIII) in the solid state was published [129]; the results fully substantiate conclusions drawn from earlier experiments, that there is motion in the complex in the solid state.

2.7 CHEMICAL EVIDENCE

The chemistry of dienetricarbonyliron complexes was reviewed by Pettit and Emerson in 1964 [130]. Hallam and Pauson [63] first studied the chemical reactivity of (I), and found it to be typical of the reactivity of the free diene. This led them to suggest that the buta-1,3-diene ligand remained essentially intact within the complex molecule.

Hallam and Pauson also prepared (II) from the reaction of pentacarbonyliron and cyclohexa-1,3-diene. Because the only likely conformation of the cyclic diene within the complex was that with a 'cis' arrangement of double bonds, and because of the similarity of the two complexes chemically, it was suggested that the same diene conformation was present in (I), and a structure, (2)3 (figure 2.4) was proposed.

The preference of the $Fe(CO)_3$ group for a conjugated diene, as opposed to, for example, a 1,4-, or 1,5-diene, is well known, and chemical evidence for this preference is provided by the isomerisation of some ligands during complex formation, for example as shown in figure 2.12.

Cyclohexa-1,4-diene was found to give the η^4-cyclohexa-1,3-dienetricarbonyliron complex [131], and penta-1,4-diene isomerises to give η^4-penta-1,3-dienetricarbonyliron [65]. Complexes in which the tricarbonyliron group is bonded to a

Fig 2.12 Isomerisation of some non-conjugated dienes

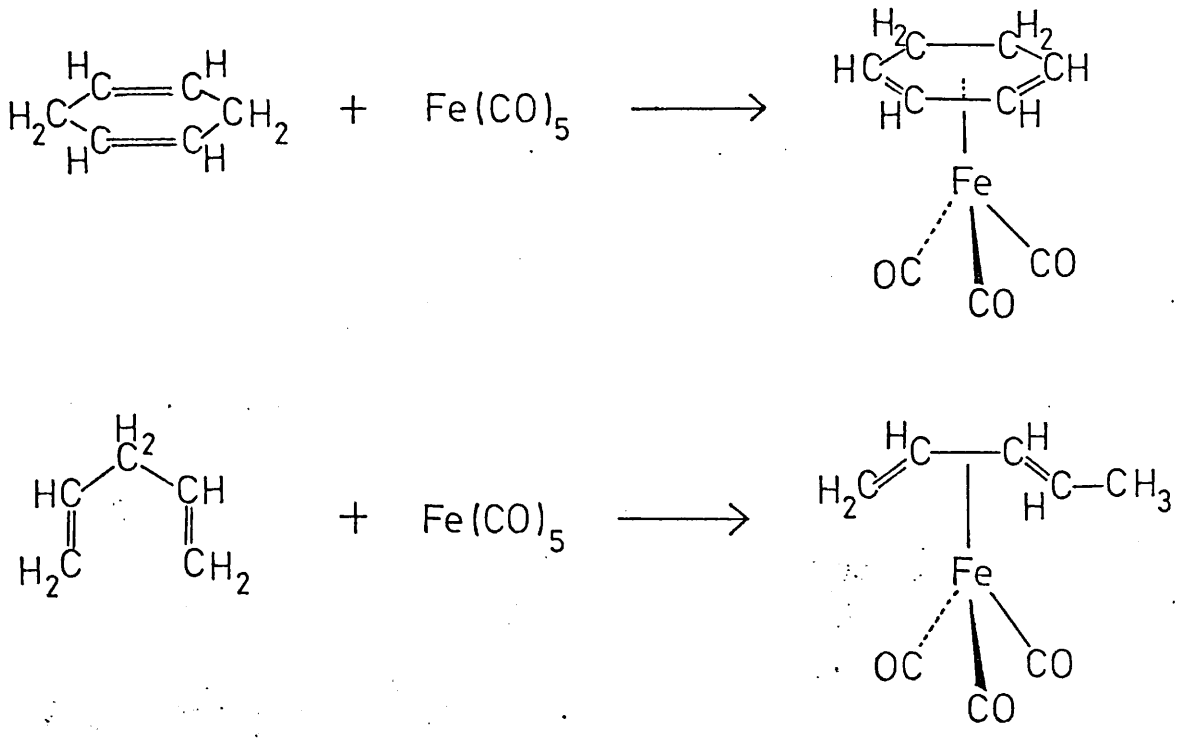

non-conjugated diene are known [132, 133, 117], but less common.

Corresponding ruthenium complexes have been isolated [134, 68] but ruthenium will readily form complexes with non-conjugated dienes [133]. The preference of the tricarbonyliron group in forming conjugated-diene complexes is discussed in molecular orbital terms by Elian and Hoffman [100], who state that, in general, any conjugated diene is a better donor or acceptor of electrons than a non-conjugated diene, in this type of complex. This is also stated by Green [102].

The reaction of cycloheptatriene with pentacarbonyliron gives three organometallic complexes; relative yields vary according to reaction conditions. The three products are (VII), a red liquid, (III), an orange liquid, and a yellow crystalline trinuclear iron complex. It was found difficult to separate the liquid products, even by repeated chromatography [118]. Dauben and Bertelli [135] published a method of preparation for (VII) in the same year as Wilkinson et al [118]. They, also, found the product to be contaminated with the diene complex (III), and the ratio of triene to diene product appeared to decrease over a period of days. They described (VII) as being sensitive to light and air. The pure diene complex (III) was readily obtained from reaction of cyclohepta-1,3-diene with pentacarbonyliron. In 1972, Lewis et al reported a preparation of pure (VII) by UV irradiation of a solution of pentacarbonyliron and cycloheptatriene in benzene [67].

Treatment of pentacarbonyliron with cyclooctatetraene, gives (VIII), (2)5, and (2)6 (figure 2.7) [136-139, 119]. For (VIII), the ligand geometry changes on complex formation, and a different chemical reactivity, more characteristic of aromatic hydrocarbons is observed, indicating some reorganisation of π electron density on coordination to the $Fe(CO)_3$ group.

2.8 PHOTOELECTRON SPECTRA

Several examples of the enhanced stability of highly reactive organic molecules by coordination to a tricarbonyliron group, for example cyclobutadiene [140], and trimethylenemethane [141] have been reported. Attempts have been made to study these organic ligands using valence region PES and molecular orbital theory [142-144].

The photoelectron spectrometer used by Dewar and Worley was of the cylindrical grid retarding potential type [145] and spectra obtained were of integral form. The ionisation energies of (I) and complexes shown in figure 2.13, (2)15 and (2)16, were recorded. There is a fairly

Figure 2.13 Cyclobutadiene- and trimethylenemethane-tricarbonyliron complexes

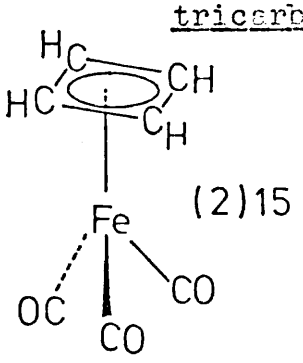

(2)15

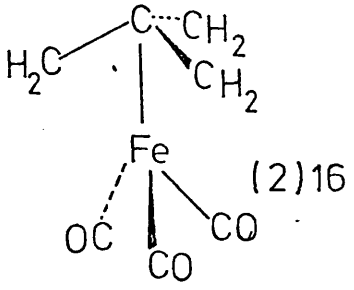

(2)16

large error inherent in the use of the above instrumentation; results obtained using a higher resolution spectrometer with magnetic or electrostatic analyser would be preferable. The study by Dewar was an attempt to examine the free organic ligands. In the case of complex (I), comparison was made with the PE spectrum of the free diene, trans-buta-1,3-diene Ionisation energies for each isomer of butadiene were predicted by calculation.

The PE spectrum of butadiene has been recorded and discussed by Turner et al [45]. There is general agreement as to the first ionisation energy of butadiene, and the high

resolution PE spectrum shows that the molecular orbital involved is rather non-bonding, and therefore likely to be the upper π orbital, $1b_g\pi$. It is known that at room temperature butadiene exists mainly in the 'trans' form with a small percentage of the 'cis' isomer present. Various studies suggest the amount is somewhere in the region of 1 to 7% [146,147] although there is no direct spectroscopic proof [148]. The ionisation energy of trans-butadiene has been determined spectroscopically as 9.062 eV [149], and calculations predict the ionisation energy of the 'cis' isomer to be greater by 0.03 to 0.14 eV [150].

Calculations performed for butadiene give varying results as to whether the second ionisation band in the PE spectrum is due to ionisation from the $a_u\pi$ orbital, or the highest σ orbital. Calculations reported by Dewar [151] place the energy of the highest occupied σ orbital between the energies of the two π orbitals, while Kato and co-workers assign the two orbitals of highest energy as π[152]. It has been suggested [75, 78] that calculations of the type used by Dewar place too much emphasis on σ levels. Heilbronner states that 'as expected from previous experience, the MINDO/2 calculation yields a much too high lying σ-level; the MINDO/2 treatment exaggerates σ/π mixing' [75].

In a more recent publication, the ionisation energies for butadiene were estimated by taking the difference between the total ground state energy for the neutral species and the total energies of the ground or excited states of a corresponding cation, according to the ΔSCF - CI method [153]. The values thus estimated are compared with experimental ionisation energies, and give the ordering $b_g\pi < a_u\pi < a_g\sigma$. Other support for this interpretation of the PE spectrum is given by Heilbronner [75]; it can be seen from the PE spectra of the dienes reported by Heilbronner, that the first two bands in each case are of similar shape and intensity, which, on the basis of simple photoionisation cross section rules, would suggest that these bands arise from ionisation from molecular orbitals of similar character. Eland

assigns the first three bands in the butadiene spectrum as π, π, and σ[154].

The photoelectron spectra of cyclohexa-1,3-diene, cyclohepta-1,3-diene, cycloocta-1,3-diene, cycloheptatriene, and cyclooctatetraene have been recorded [74-78]. The spectra of the cyclic dienes are assigned on the basis that the first two bands are due to π orbital ionisation. Although Heilbronner has also attempted to relate the dihedral angles for these conjugated dienes to data from the PE spectra [74], values obtained are not always in agreement with those given by other spectroscopic studies (table 2.1), particularly for the case of cyclohepta-1,3-diene.

Recent high resolution PE spectroscopic studies have been reported, together with ab initio MO calculations, for η^4-buta-1,3-dienetricarbonyliron [29], (I), trimethylenemethanetricarbonyliron, (2)16 [155], dibenzenechromium, and benzenetricarbonylchromium [33]. For complex (I) [29], HeI, HeII, and X-ray photoelectron data are published, and the low energy PE spectrum is interpreted taking into account apparent deviations from Koopmans' theorem. A photoelectron spectroscopic and molecular orbital study has been reported for cyclopentadienyltricarbonylmanganese, (figure 2.8) and some related compounds [105]. A linear relationship was observed between the calculated eigenvalues and the experimental ionisation energies of the complexes. This correlation suggests that deviations from Koopmans' theorem may be taken as constant for the series of similar complexes.

2.9 CURRENT RESEARCH

Complexes (I) to (VIII) were synthesised (figure 2.3) and the HeI UVPE spectra were obtained for these. Interpretation of the spectra was aided considerably by the work of Hillier et al.[29], although

qualitative MO diagrams were also used to some extent. The basis of assignment of the spectra, other than that of (I) on Hillier's work, was justified by the finding of Whitesides et al [105]; that is, that for a series of similar complexes, deviation from Koopmans' theorem may be regarded as constant. It was hoped that a clearer idea of the diene-tricarbonyliron bonding might be obtained, and that some information as to the molecular geometry of the cyclic dienes within the tricarbonyliron complexes might be inferred from the photoelectron spectra. For most of the complexes the molecular structures have not yet been confirmed. Ab initio calculations were performed for planar 'cis' and 'trans' buta-1,3-diene, using the Gaussian 70 computer package.

2.10 RESULTS

The ionisation energies obtained for each of the organic compounds are shown in table 2.3; those of the corresponding tricarbonyliron and tricarbonylruthenium complexes in table 2.4. Ionisation energies reported by Heilbronner et al.[75-77] are given in brackets. These values were taken to be more accurate for purposes of comparison with the tricarbonyliron complexes [156], since resolution in the current spectra of the ligands was extremely poor, and deteriorated as the spectra were being obtained. This is shown by the broadening, and, in some cases, doubling, of the calibration peaks, and was thought to be due to decomposition of the dienes and deposition on the analyser plates.

The spectra of two additional complexes, (IX) and (X) (figure 2.14) are reported; ionisation energies are given in table 2.5 together with values for complex (I) for comparison.

Figure 2.14 Complexes (IX) and (X)

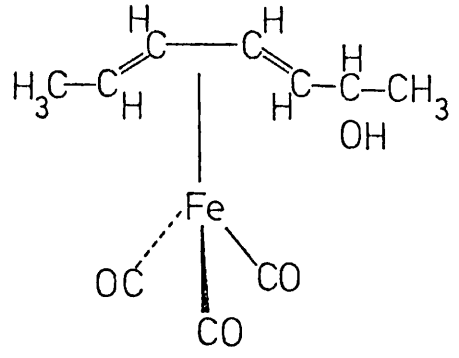

(IX)

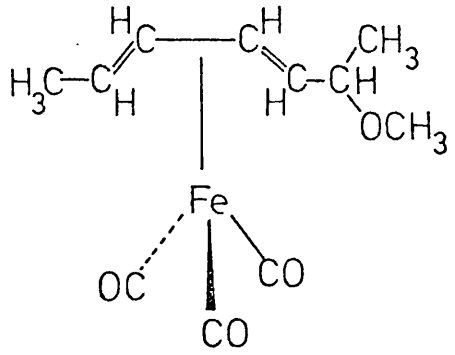

(X)

Table 2.3 Vertical Ionisation Energies (eV) for the dienes, cycloheptatriene and cyclooctatetraene

COMPOUND	IONISATION ENERGIES			
trans-buta-1,3-diene	9.08 [45] 9.09 [154]	11.34 [45] 11.55 [154]	12.2 [45]	
cyclohexa-1,3-diene	8.61(8.25)*	10.93(10.75)	11.33	
cyclohepta-1,3-diene	8.50(8.31)	10.57(10.63)	11.09	
cycloocta-1,3-diene	8.60(8.68)	9.94(10.00)	10.91(10.94)	
cyclohepta-1,3,5-triene	8.50(8.57)	9.44(9.52)	10.89(10.96)	11.67
cycloocta-1,3,5,7-tetraene	8.42(8.42)	9.78(9.78)	11.10(11.15)	11.49(11.55)

*values in brackets are those reported by Heilbronner [75-77]

Table 2.4 Ionisation Energies (eV) for complexes (I) to (VIII)

COMPOUND	VERTICAL IONISATION ENERGIES			
	A	B	C	D
(I)	8.16(sh), 8.67	9.82	11.43	12.56
(II)	7.98(sh), 8.56	9.33	11.04	12.17
(III)	7.78(sh), 8.46	9.12	10.86	11.71
(IV)	7.45(sh), 8.27	8.87	10.44	10.87
(V)	8.01, 8.91	9.39(sh)	11.01	11.83
(VI)	7.96, 8.94	9.40(sh)	10.84	11.64
(VII)	7.76(sh), 8.39	8.78, 10.23	11.10	11.82
(VIII)	7.84	8.74	10.61	11.63

(sh) = shoulder

Table 2.5 Ionisation Energies (eV) for complexes (IX) and (X)

COMPOUND	VERTICAL IONISATION ENERGIES			
	A	B	C	D
(I)	8.16(sh), 8.67	9.82	11.43	12.56
(IX)	7.72, 8.48	9.40	11.19	11.72
(X)	8.30, 8.90	9.81, 10.21	10.88, 11.40	12.43

Ab initio calculations for planar 'cis' and 'trans' buta-1,3-diene were carried out using the Gaussian 70 computer program, adapted for the London University CDC 7600 computer [157], and results are summarised in tables 2.6 and 2.7. The energies of the highest occupied molecular orbitals are given, and from these, ionisation energies have been calculated, according to equation (2)17 (that is, Koopmans' theorem has been adopted).

$$-\varepsilon_{SCF} = IE \qquad (2)17$$

Agreement with experiment is not good; however, the calculations do show the two highest occupied molecular orbitals to be essentially of π character.

Table 2.6 Gaussian 70 calculations for butadiene using normal basis set

ε_{SCF_n} in Hartrees (1 Hartree = 27.21 eV)

IE_n in eV (assuming Koopmans' theorem)

TRANS-BUTA-1,3-DIENE		CIS-BUTA-1,3-DIENE	
$\varepsilon_1 = -0.2601696$	$IE_1 = 7.08$	$\varepsilon_1 = -0.2600456$	$IE_1 = 7.08$
$\varepsilon_2 = -0.3917848$	$IE_2 = 10.66$	$\varepsilon_2 = -0.3908596$	$IE_2 = 10.64$
$\varepsilon_3 = -0.4413831$	$IE_3 = 12.01$	$\varepsilon_3 = -0.4477999$	$IE_3 = 12.18$
$\varepsilon_4 = -0.4850582$	$IE_4 = 13.20$	$\varepsilon_4 = -0.4579799$	$IE_4 = 12.46$
$\varepsilon_5 = -0.4964305$	$IE_5 = 13.51$	$\varepsilon_5 = -0.5273041$	$IE_5 = 14.35$

In fact the calculations shown in table 2.6 predict the π ionisation energies of the 'trans' form of butadiene to be slightly higher than those of the 'cis' form. For the first ionisation energy, the difference predicted is .0034 eV. Calculations shown in table 2.7 show the same trend; the differences are slightly greater.

Table 2.7 Gaussian 70 calculations for butadiene using extended basis set

ε_{SCF} in Hartrees, IE in eV.

TRANS-BUTA-1,3-DIENE			CIS-BUTA-1,3-DIENE		
ε_1 = - 0.3150399	IE_1 = 8.57		ε_1 = - 0.3131116	IE_1 = 8.52	
ε_2 = - 0.4384020	IE_2 = 11.93		ε_2 = - 0.4374724	IE_2 = 11.90	
ε_3 = - 0.4881963	IE_3 = 13.28		ε_3 = - 0.4963706	IE_3 = 13.51	
ε_4 = - 0.5384721	IE_4 = 14.65		ε_4 = - 0.5054480	IE_4 = 13.75	
ε_5 = - 0.5434406	IE_5 = 14.79		ε_5 = - 0.5728480	IE_5 = 15.59	

2.11 DISCUSSION PART 1: CALCULATIONS

The UV photoelectron spectrum of butadiene was discussed in section 2.8. There has been some disagreement as to whether the first two bands in the spectrum arise from ionisation from the two occupied π MOs, or from the highest occupied π and σ MOs. Eland assigns the first two bands as being due to ionisation from π orbitals [154], in agreement with recent calculations [153]. Heilbronner assigns the first two bands in the PE spectra of cyclic conjugated dienes as arising from π orbital ionisation. The calculations carried out using Gaussian 70 also predict this ordering, and assignment of the diene spectra has been based on this evidence. It may be seen from the spectra of the dienes that the first two bands in each case are of similar shape and intensity, which, on the basis of simple photoionisation cross section rules, would suggest that the first two bands arise from ionisation from molecular orbitals of similar type.

Although the Gaussian 70 calculations predict the π, π, σ ordering of energy levels, the ionisation energies calculated from Koopmans' approximation, (2)17, are not in good agreement with experimental values, although there is some improvement on use of an extended basis set. These latter calculations predict the first ionisation energy of the 'trans' form of butadiene to be greater than that of the 'cis', by about 0.05 eV; this is not in agreement with Dewar's calculation [150], but is in agreement with experimental data reported by Sugden and Walsh [158]. Use of the relationship (2)18 [23] gives equally poor agreement with experimental values.

$$IE_i = -0.92\,\varepsilon_{SCF_i} \qquad (2)18$$

A simple Hückel MO treatment of butadiene was discussed in section 2.5; this may be extended to describe the π MOs of the dienes in table 2.3. Due to the lowering in symmetry with respect to buta-1,3-diene, the $b_2\,\pi$ highest occupied MO of cis-butadiene will become $a''\pi$ in C_s symmetry, and the $a_2\pi$ MO of cis-butadiene, $a'\pi$. Heilbronner's ionisation energies for these dienes may be compared to those obtained in the present study by examination of table 2.3. Good agreement is seen except in the case of cyclohexa-1,3-diene, for which possible reasons were mentioned earlier.

Brundle and Robin [73] suggest that when two ethylenic groups of a conjugated diene are non-planar, the π electron energies will be very different from those of the two planar conformers of buta-1,3-diene. As the molecule twists about the central bond, the two occupied MOs, ψ_1 and ψ_2 collapse toward one another, as they both converge upon the π orbital energy of the isolated component monoolefin. Such orbital energies may be readily obtained from the PE spectrum. A simple diagram showing the relative ionisation energies of the series of dienes: buta-1,3-diene (a), cyclohexa-1,3-diene (b), cyclohepta-1,3-diene (c), and cycloocta-1,3-

diene (d), is given in figure 2.15. Heilbronner's results are shown in figure 2.16. In order to discuss trends in these energy levels it is first necessary to consider the geometries of these dienes, and, in particular, their dihedral angles. The assignments of the PE spectra of the dienes are based on those of Heilbronner [74-78].

There is evidence that all these cyclic dienes exist in 'cis' conformation [72, 80] but with varying dihedral angles as discussed in section 2.4. Although Heilbronner has attempted to relate the dihedral angle to photoelectron data [74, 75], the calculated dihedral angles are not entirely in agreement with other experimental data and calculations [72, 79].

2.12 DISCUSSION PART 2: PHOTOELECTRON SPECTRA OF THE CYCLIC DIENES

(i) cyclohexa-1,3-diene The bands in the PE spectra at 8.61 and 10.93 eV correspond to ionisation from the two π MOs. The onset of σ ionisation is at 11.33 eV Heilbronner's values for π ionisation are 8.25 and 10.75 eV.

(ii) cyclohepta-1,3-diene The π ionisa- energies measured were 8.50 and 10.57 eV, compared with Heilbronner's values of 8.31 and 10.63 eV. The first σ ionisation occurs at 11.09 eV.

(iii) cycloocta-1,3-diene The first three ionisation energies were found to be at 8.60, 9.94 and 10.91 eV. The first two bands are assigned to ionisation from π MOs and the band at 10.91 eV to ionisation from a σ MO. Agreement with Heilbronner's values of 8.68, 10.00, and 10.94 eV, is good.

Fig 2.15 Correlation diagram for the conjugated dienes

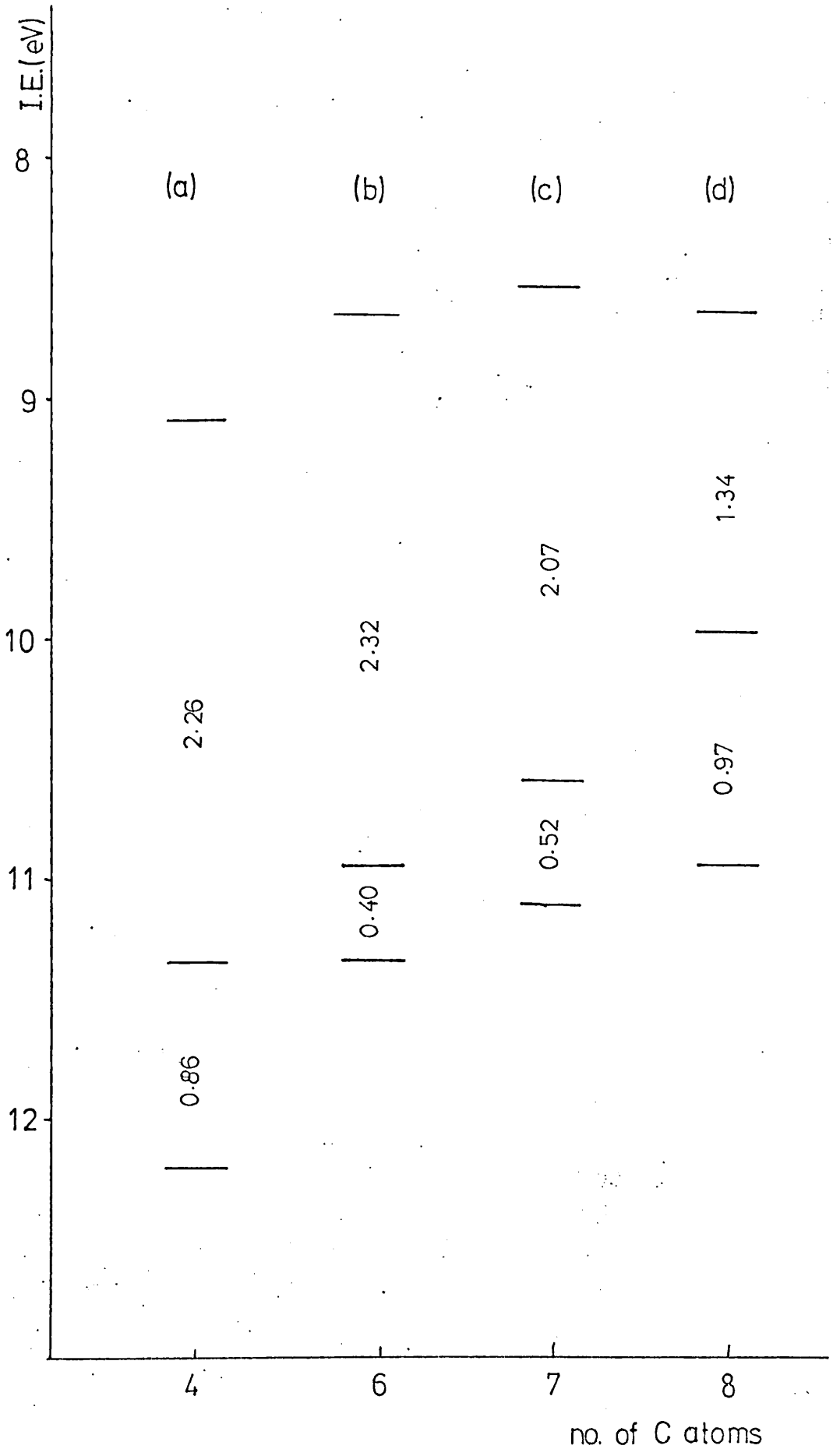

Fig 2.16 Correlation diagram for the conjugated dienes[75]

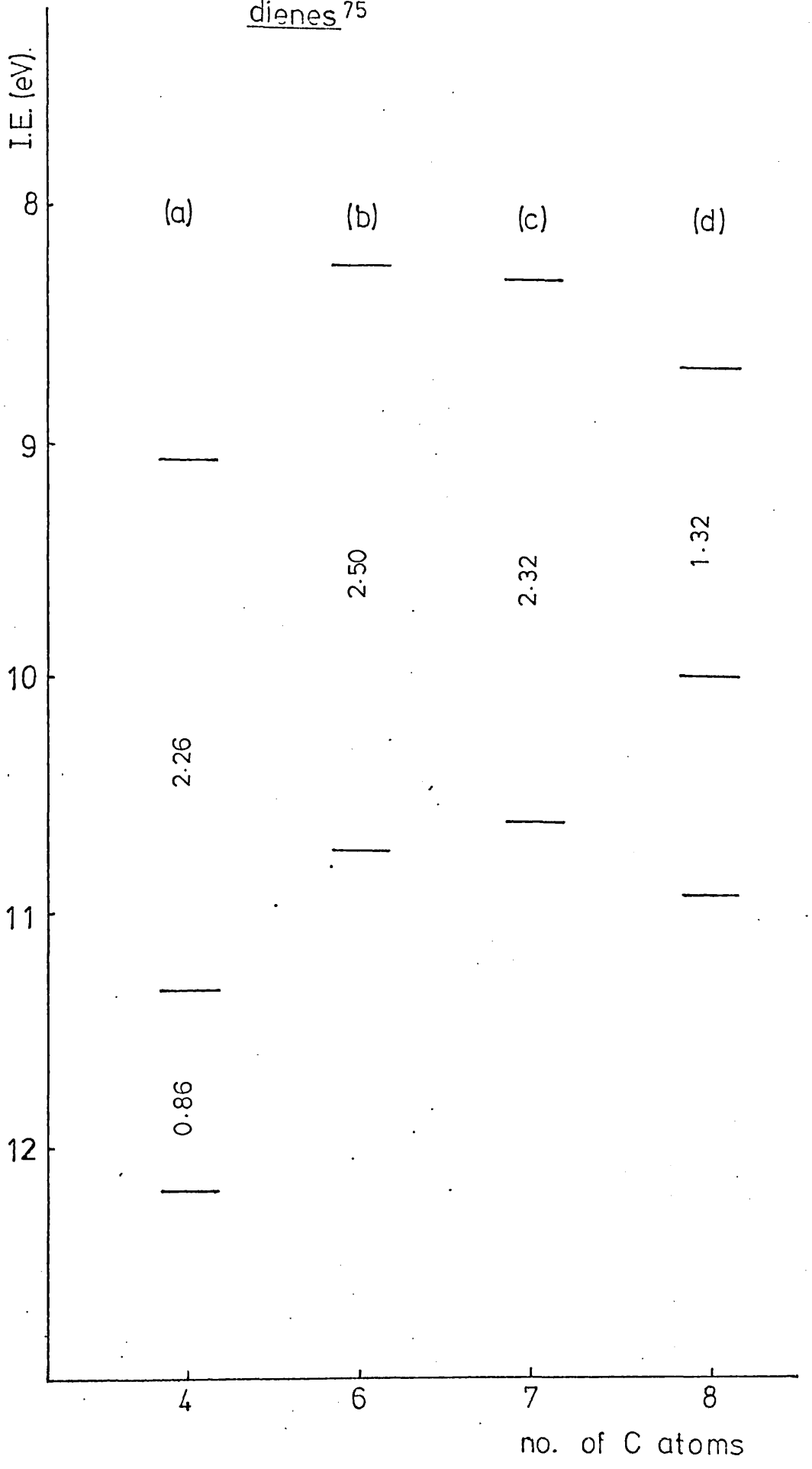

Both Heilbronner's results, and those obtained in the current study show the same general trends. It may be seen from figures 2.15 and 2.16, that the trends are as follows:

(a) there is an apparent decrease in π orbital separation as ring size increases

(b) there is an increase in separation between the lower lying π and upper σ orbital energies as the ring size increases.

Heilbronner's results show an increase in first ionisation energy with increasing ring size; the current results do not.

These apparent trends, however, may also be associated with the changing geometry of the diene. The increase in ring size would not be expected to give such noticeable changes in energy level as are observed. The change in dihedral angle, as seen from table 2.8, appears to be related to the separation of the π levels; this effect is expected, and was predicted by Brundle and Robin [73]. It appears that the two occupied π levels, ψ_1 and ψ_2, collapse towards one another in energy with increasing dihedral angle, noticeably in the case of cycloocta-1,3-diene, where the π separation is 1.34 eV. For butadiene, cyclohexa-1,3-diene, and cyclohepta-1,3-diene, the π separation is very similar (about 2.3 eV). This coincides with experimental observation that the dihedral angle is small or zero for the cyclic conjugated dienes with six or seven membered rings, and very different for cycloocta-1,3-diene.

Table 2.8 Separation of π energy levels for the conjugated dienes (eV)

COMPOUND	π SEPARATION MEASURED FROM PES (eV)	DIHEDRAL ANGLE
buta-1,3-diene	2.26 [45]	0°
cyclohexa-1,3-diene	2.32 (2.50)*	18°
cyclohepta-1,3-diene	2.07 (2.32)	0°
cycloocta-1,3-diene	1.34 (1.32)	60°

(iv) cycloheptatriene and cyclooctatetraene

Figure 2.17 is a correlation diagram showing ionisation energies for cycloheptatriene (c') and cyclooctatetraene (d'). Ionisation energies for butadiene (a), cyclohepta-1,3-diene (c), and cycloocta-1,3-diene (d) are included for comparison.

Ionisation energies found for cycloheptatriene agree well with values reported by Heilbronner [75], and the first three bands in the PE spectrum are assigned to ionisation from π MOs. The separation between these bands is small compared with butadiene in which the conjugated diene system is planar (i.e. the dihedral angle is 0°) but is not unlike the separation value found for the π levels in cycloocta-1,3-diene, which has a large dihedral angle. Thus it might be expected that the double bonds of cycloheptatriene are not nearly coplanar. The electron diffraction study [91] discussed in section 2.4 shows a large dihedral angle for this molecule, and also indicates a considerable amount of π electron delocalisation.

Fig 2.17 Correlation diagram for cycloheptatriene and cyclooctatetraene

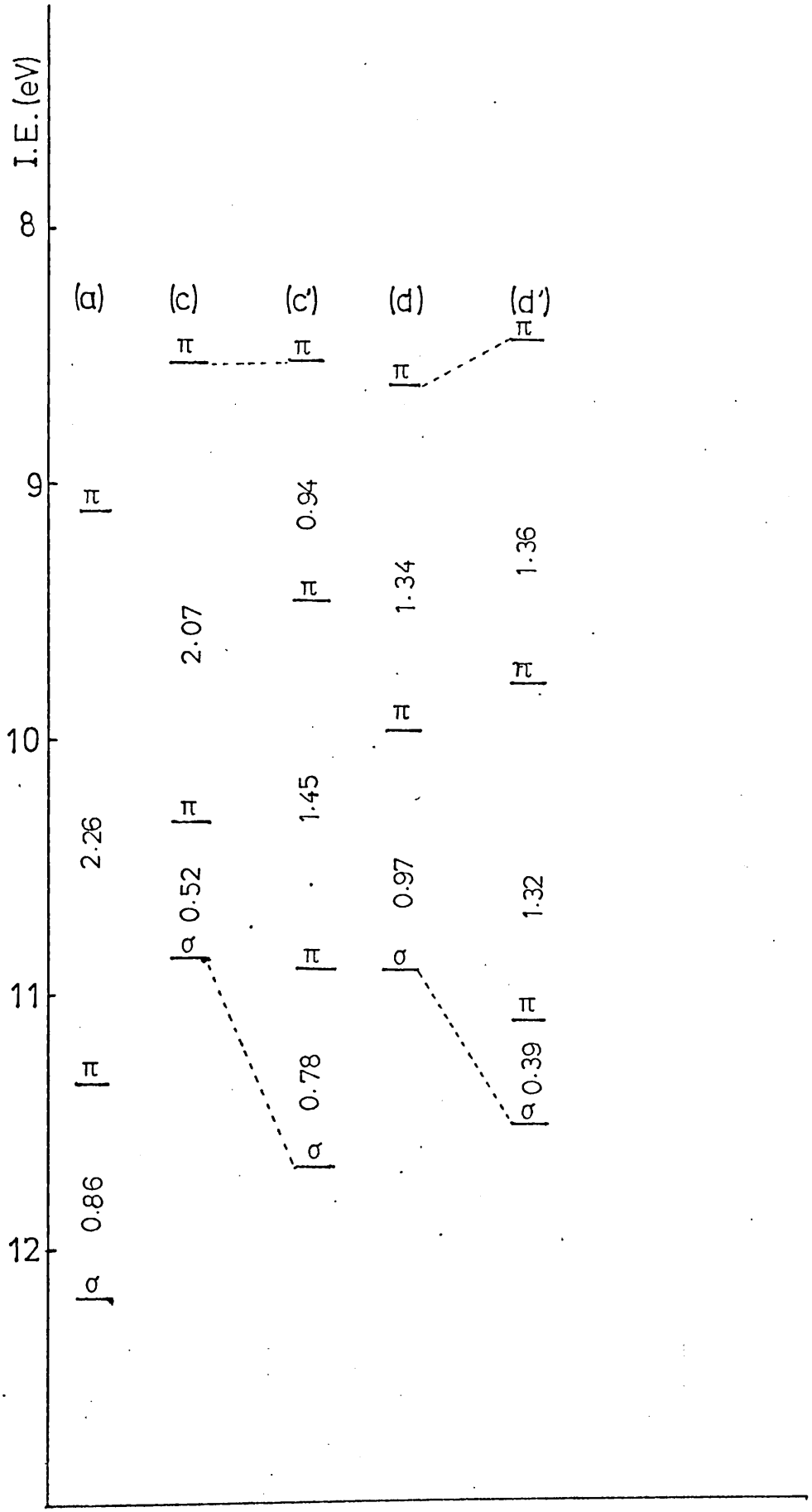

The photoelectron spectrum of cyclooctatetraene has been reported and assigned by Eland [154], and by Heilbronner [75]. The ionisation energy sequence originally proposed by Eland is confirmed by Heilbronner's data, and by the present study, on simple intensity grounds, as $\pi a_1 < \pi e_1 < \pi b_2, \sigma$. There have been other previous investigations of the PE spectrum of this compound [145, 159].

2.13 DISCUSSION PART 3: PHOTOELECTRON SPECTRA OF THE COMPLEXES

(i) η^4-buta-1,3-dienetricarbonyliron,(I)

The ionisation energies for complex (I) are listed in table 2.4. In table 2.9, these values are compared with results obtained by Dewar [142, 144] and Hillier et al. [29]. Agreement of the current values with those of Hillier is good. The quality of instrumentation used by Dewar and Worley may explain the poorer agreement with their results.

Table 2.9 Ionisation energies for complex (I) (eV)

CURRENT WORK	DEWAR AND WORLEY [142, 144]	HILLIER [29]
8.16 (sh)	8.04	8.23 (sh)
8.67		8.82
9.82	9.73	9.93
11.43	10.92	11.52
12.56	11.23	12.94

A qualitative energy level diagram constructed partly from PE data, and partly from Hückel MO calculations, for complex (I) is shown in figure 2.11; bonding was discussed in

section 2.5. The point should be made that the diagram was constructed merely as an aid to interpretation of the PE data and although the ordering of energy levels shown is the same as that found from assignment of the spectra, this ordering is not necessarily that in the neutral molecule. This would only be the case if Koopmans' theorem is obeyed, and there is some evidence from Hillier's work [29] that it is not.

The photoelectron spectrum of (I) (see PE spectrum 6 at end of chapter) is divided for convenience into regions labelled A,B,C,D [156] and has been assigned on the basis of Hillier's work [29].

Region A, of lowest ionisation energy, is associated with ionisation from molecular orbitals that are essentially of d character, that is, those arising from the iron $d_{x^2-y^2}$, d_{z^2} and d_{xy} atomic orbitals; these orbitals show little evidence of interaction with the butadiene MOs. Also in region A are ionisations from the MO arising from interaction of the partly filled d_{xz}, d_{yz} AOs with the $b_2\pi^*$ anti-bonding MO of butadiene. The ordering of these levels within region A is uncertain but it is not thought that the b_2 π^*-d orbital can be responsible for the shoulder to low IE of the first band; evidence for this is shown in the HeII PE spectrum recorded by Hillier [29]. However, according to calculations, both by Koopmans' theorem, and by the ab initio method used by Hillier, this molecular orbital is predicted to have the lowest ionisation energy.

The second region, B, consists of a band showing both metal and ligand orbital character. It is assigned to ionisation from the orbital associated with π donation from butadiene to the metal, the MOs concerned are the $a_2\pi$ (highest occupied level) of butadiene, and the partially filled d_{xz}, d_{yz} metal orbitals.

Region C consists of a band showing essentially ligand character, and may be associated with ionisation from the $b_2\pi$ occupied MO of butadiene. There is little evidence of interaction with metal d orbitals, and the ionisation energy of this level is changed very little from that of the corresponding level in the free diene.

Region D consists of bands which are due to ionisation of electrons from σ levels of the diene, and from the carbonyl ligands.

The metal d levels are presumably closer in energy to the lowest unoccupied, rather than the highest occupied MO energy level of the free diene, since there is evidence (section 2.5) that in complex (I), the tricarbonyliron fragment acts as an electron donating group.

The calculated ordering of energy levels [29] for this complex, is not at first apparently in line with the above assignments of the PE spectrum. It is found that the MOs of mainly metal character lie below the highest MOs of mainly ligand (butadiene) character. It has been suggested that orbitals of d character will show greater relaxation effects compared with p type orbitals [29, 160] and Koopmans' theorem would not be valid in this case.

(ii) η^4-dienetricarbonyl M complexes, (II)-(VI), (M=Fe, Ru)

The spectra of the remaining dienetricarbonyliron complexes, (II)-(IV) and those of corresponding ruthenium complexes, (V), (VI), have been assigned on a similar basis to that of complex (I), the justification for this being that the complexes are very similar. Thus, even if a different magnitude of orbital relaxation for orbitals of differing atomic character occurs on ionisation, this will not affect the ordering of bands in the spectrum relative to the parent compound, (I).

In the PE spectra of complexes (II) to (IV), region B is less well resolved from the metal d bands of region A, and region C occurs as a shoulder on the edge of D.

The spectra of the two ruthenium complexes, (V), and (VI), resemble those of their iron analogues, but as a consequence of the shift of band A to higher ionisation energy, B is no longer so clearly resolved, and appears as a shoulder on the edge of A. The shift to higher ionisation energy of the d levels of the ruthenium complexes is to be expected as a general trend in moving thus down a group in the periodic table; the same effect has been noted for ferrocene and ruthenocene [161], and for the neutral and singly ionised atomic species (iron and ruthenium) [162]. The intensity of the group of bands due to metal d ionisation relative to that of bands in regions C and D, increases for the ruthenium complexes compared with the iron analogues.

Similar increases in metal d orbital photoionisation cross section with increasing principal quantum number have been noted for ferrocene and ruthenocene [161].

A correlation diagram, figure 2.18, for the ionisation energies of the diene complexes is given. Figure 2.19 compares the ionisation energies of each diene with those of its corresponding tricarbonyliron complex.

(iii) General trends observed in the PE spectra of the dienetricarbonyliron complexes

For complexes (II) to (IV), all bands show a decrease in ionisation energy with increasing ring size although this is not observed in the π ionisation energies of the parent dienes. The separation between bands B and C in the iron and ruthenium complexes, (II) to (VI), is constant (1.7 ± 0.1 eV) and this may suggest that, when complexed, the cyclic dienes assume an essentially cis planar conformation, in which the dihedral angle is near zero.

If it is assumed that cyclohepta-1,3-diene has a dihedral angle of zero, the change of π ionisation energies on formation of the complex may be calculated from data shown in figure 2.20. The a_2 π ionisation energy is

Fig. 2.20 Ionisation energies for cyclohepta-1,3-diene and its tricarbonyliron complex

COMPOUND	IONISATION ENERGIES (eV)				
cyclohepta-1,3-diene			8.25	10.75	
(III)	7.78	8.46	9.33	11.04	12.17

Fig 2.18 Correlation diagram for the diene complexes

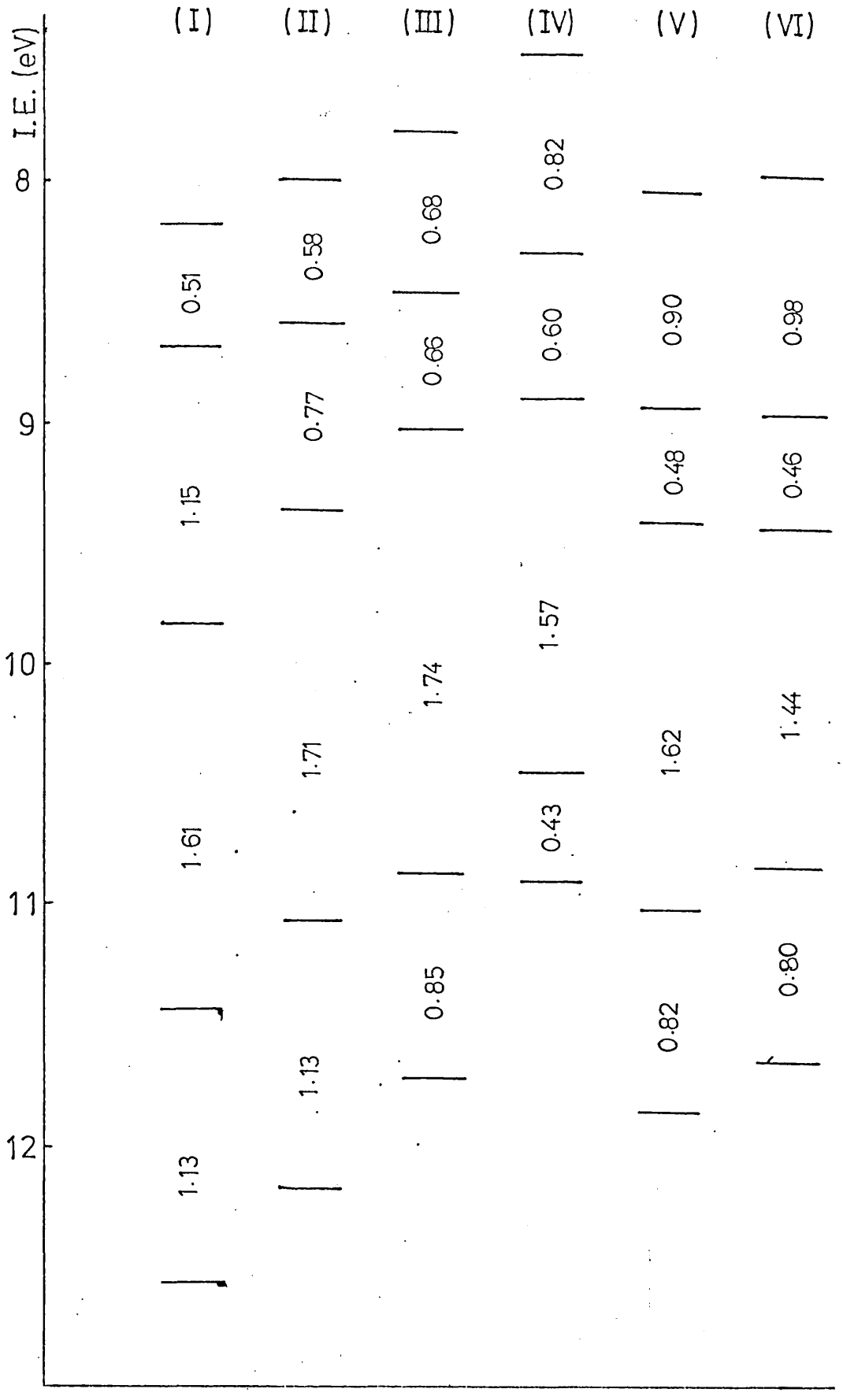

Fig 2.19 Correlation diagram for each diene with the corresponding tricarbonyliron complex

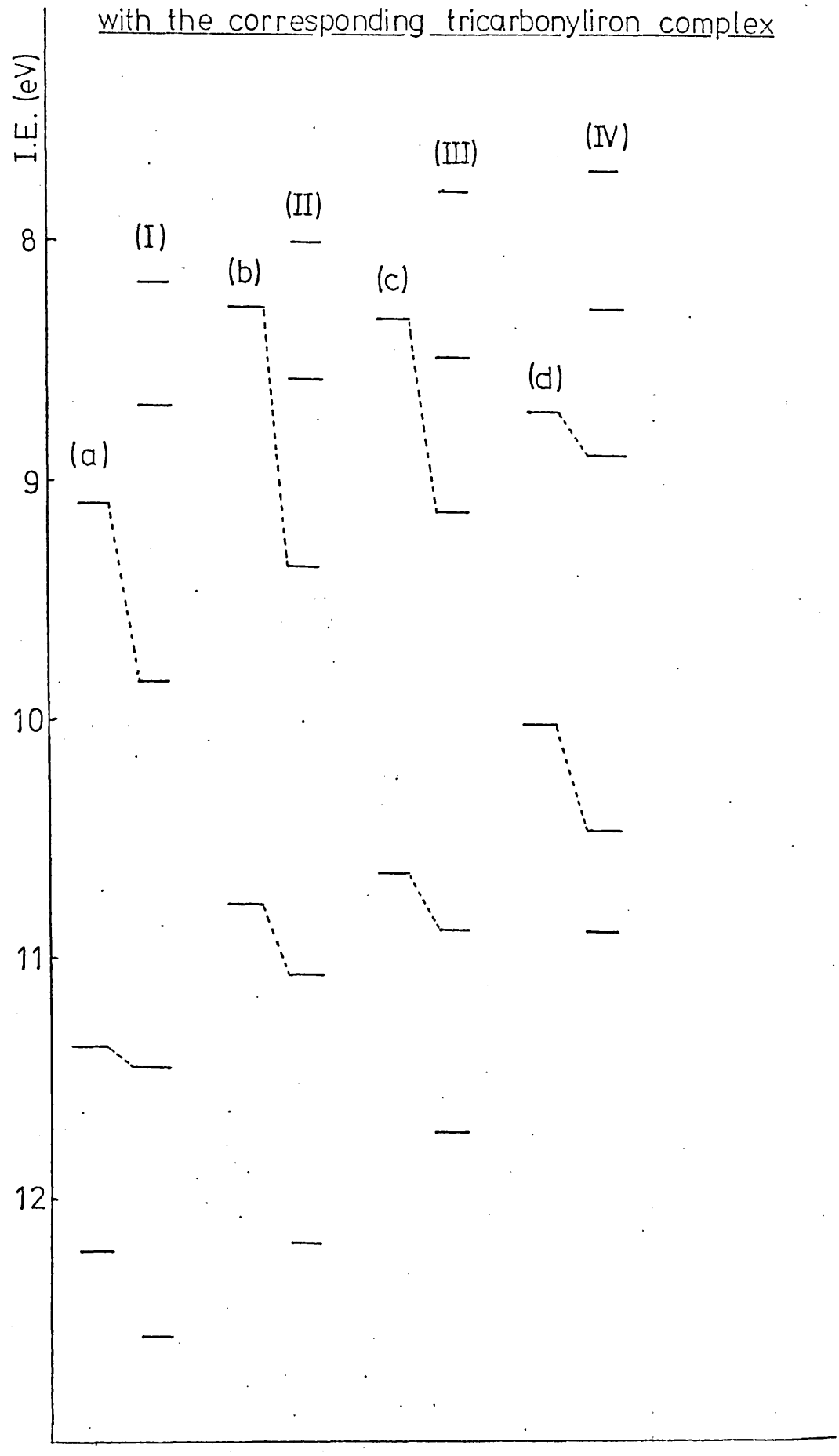

increased by 0.81 eV and the $b_2\pi$ by 0.21 eV. If a similar change in ionisation energy is assumed to occur for other dienes with dihedral angles of near zero, the energies of the free diene in its cis planar form may be predicted. This would give values of 9.01 and 11.20 eV for cis-butadiene, in good agreement with calculated values of 9.19 and 11.18 eV [150]. However, other, more recent, calculations have predicted very different values, for example the Gaussian 70 calculated values are 8.52 and 11.90 eV. For cyclohexa-1,3-diene, which has a small dihedral angle, the same argument would predict ionisation energies of 8.52 and 10.83 eV, which are in fairly close agreement with observed values.

It may be seen from figure 2.19 that the π MOs of the free dienes are considerably stabilised on complex formation, the $a_2\pi$ bonding orbital being more strongly affected than the $b_2\pi$, which appears to be relatively non-bonding except in the case of the cycloocta-1,3-diene complex, when the reverse is true. In this complex, (IV), it is seen that C is noticeably less well resolved from region D than for complexes (I) to (III). This suggests that the band due to $b_2\pi$ ionisation (C) is broader, and more bonding in character than for the other complexes. The ionisation energies of the π levels of the free diene are such that the $b_2\pi$ bonding level is closer in energy to the iron d orbitals than for (I) to (III), and therefore might be expected to contribute significantly to a metal-ligand bond. It would be apparent if HeII relative intensity data were available, whether or not band C has a significant d orbital contribution.

The question as to whether valence bond structure (2)3 or (2)4 is a more accurate representation of complex (I) does not affect assignment of the spectra, where a molecular orbital approach has been adopted. It seems to have been firmly established that neither structure gives an accurate representation of the bonding, and that the amount of contribution from each depends on the nature of the diene substituents [73, 163].

Kettle and Mason [163] state that the only difference between (2)3 and (2)4, is the contribution made by the diene lowest unoccupied MO (ψ_3^*) to the metal-diene bond; as this orbital contributes increasingly to the bonding, the structure approaches that represented by (2)3. It has been shown experimentally [94] and theoretically [106] that the diene bond lengths tend towards equalisation within complex (I) and that the diene substituents, even in the case of (I) are bent out of the diene carbon atom plane [94]. This could increase metal-ligand overlap as the p_z orbitals on the terminal carbon atoms are rotated slightly from the plane perpendicular to that of the carbon atoms. There may be some localisation of the diene π MOs as described by Pearson [115], causing slight changes in hybridisation of the terminal diene carbon atoms, leading to the effects observed in n.m.r. experiments. This, however, does not correspond to the equalisation of carbon-carbon bond lengths, which suggests a delocalised system.

It is possible that the observed decrease in ionisation energies for complexes

(II) to (IV) with increasing ring size, may be correlated with the angles of the substituents at the terminal 'diene' carbon atoms - in this case the subsequent carbon atoms of the ring - as the diene is forced to assume a planar configuration, and thus also correlated with the angle through which the p_z orbitals of these carbon atoms are rotated. This effect is unlikely to be very large, and may cause varying degrees of localisation of the 'diene' MOs, increasing as the strain increases, that is, as ring size increases.

(iv) The ruthenium complexes, (V) and (VI)

The differences in the PE spectra of (V) and (VI) and their iron analogues, (II) and (III) have already been discussed in section 2.13 ii). Since ruthenium d orbitals are known to have higher ionisation energies than the iron d orbitals, it might be expected that some minor differences in bonding would be apparent from the PE spectra. The general increase, relative to iron, of the ruthenium d orbital ionisation energies explains why, in the photoelectron spectra of (V) and (VI), band B appears as a shoulder on the edge of A, and is less well resolved than for the iron analogues. There may also be some difference in the degree of interaction with the diene $b_2\pi^*$, $a_2\pi$ and $b_2\pi$ levels, however it may be seen that the separation of bands B and C is constant in the spectra (1.7 ± 0.1 eV) and the same as for the iron complexes. The HeII spectra of (V) and (VI) might be highly informative in this respect. The two complexes were noted to be more volatile than their iron analogues.

(v) η^4-cyclohepta-1,3,5-triene-, and η^4-cycloocta-1,3,5,7-tetraene-tricarbonyliron, (VII) and (VIII)

Figure 2.21 shows the ionisation energies of complexes (VII) and (VIII) together with those of the parent ligands.

For complex (VII), as in the PE spectrum of the uncomplexed triene, there is an extra band, B'. The separation of the triene π levels appears to reverse on complexing, and all π levels are stabilised. The bonding could be described in a similar way to that of the diene complexes, that is, the tricarbonyliron group interacts with two double bonds of the ring, leaving a free ethylene unit; however it is more likely that there is considerable interaction of the tricarbonyliron group with all three double bonds of the ring. Figure 2.21 includes ionisation energies for complex (III) plus a free ethylene unit, (x), for comparison.

The photoelectron spectrum of (VIII) is surprising. The PE spectrum and geometry of the free ligand have already been discussed. The sharp peak apparent in the spectrum at 12.6 eV is due to water, present as an impurity. One might expect the spectrum to show a complexed diene system together with a free 'butadiene' unit. It is possible that these would give rise to bands close enough in energy to overlap considerably, and in fact the bands in the PE spectrum of the complex are somewhat fewer in number but broader and more intense than expected.

Fig 2.21 Correlation diagram for (c'), (d'), and corresponding tricarbonyliron complexes

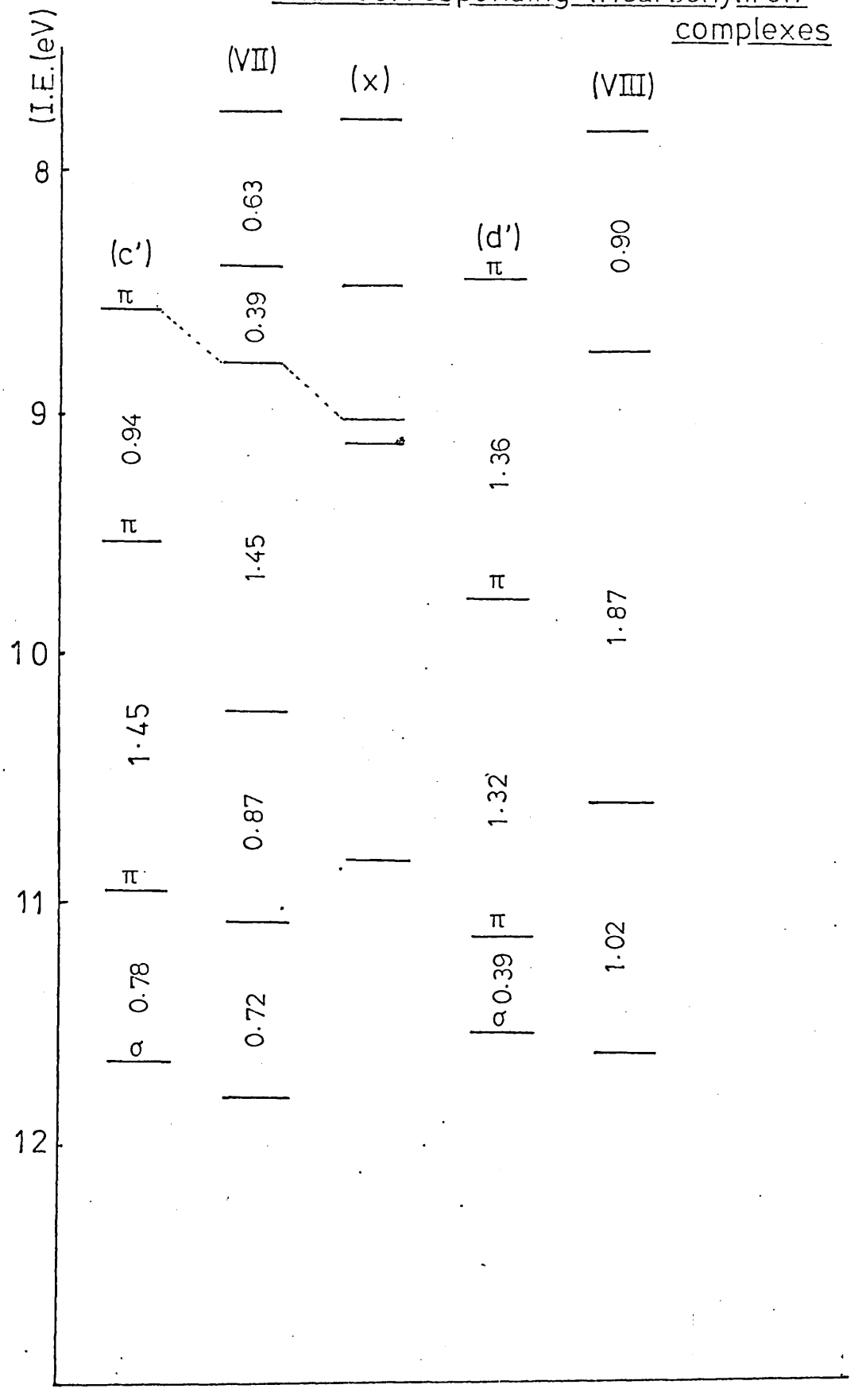

The first band, A, probably corresponds to d orbital ionisation as for the other complexes, and the second band, B, to one or more π levels, with the band at 10.61 eV also corresponding to a π double bond ionisation. It is difficult to assign the spectrum, even using relative intensity arguments. However it is likely that there is significant interaction between the tricarbonyliron unit and all double bonds; this assumption is supported by the large ring angles (135°) in the 'unbound' portion of the ring and by SCF molecular orbital calculations [98].

The HeI and HeII PE spectra of complex (VIII) were recorded at a later date, and the ionisation energies were in agreement with those reported in table 2.4. Relative intensities for the HeI and HeII spectra were calculated and are recorded in table 2.10.

Table 2.10 Relative intensity measurements for complex (VIII)

BAND:-	A	B	C	D	
HeI	0.9	0.8	1.0	5.8	10.00
HeII	1.5	1.4	1.0	2.5	7.0

In each case band C is taken as of unit intensity since this is the best separated band. Even with the aid of these relative intensity measurements it is difficult to make any further conclusions regarding the assignment, since the bands are not well enough separated for good relative intensity measurements, and the intensities have been measured

for regions rather than separate bands. The expected increases in relative intensity are observed for the first two regions, A, and B, relative to C in changing from the HeI to HeII source, since these bands arise from essentially d orbital ionisation. B is expected to show both metal d and ligand π character. Bands due to ionisation from carbonyl groups may be clearly distinguished in the HeII spectrum, and are marked CO (page 106).

(vi) PE spectra of complexes (IX) and (X)

The photoelectron spectra of complexes (IX) and (X) have been recorded and ionisation energies are given in table 2.5.

The spectrum of (IX) is very similar to that of complex (I), and may be assigned on the same basis. The ionisation energies are slightly lower than for the unsubstituted diene complex. It is interesting to note that the B-C separation is still 1.6 eV.

The PE spectrum of (X) shows two additional bands in the low ionisation energy region. Since there is an energy separation of 1.6 eV between the bands at 9.81 and 11.40 eV, these are taken to correspond to bands B and C of the parent complex, (I). The two additional bands at 10.21 and 10.88 eV may be due to the carbonyl group π orbitals. It is possible that there may be some interaction between this group and the tricarbonyliron unit.

2.14 EXPERIMENTAL

(i) Photoelectron spectra

The PE spectra were recorded using a Perkin Elmer PS 16/18 instrument, modified

to accept a heated insert probe. Spectra of the relatively volatile cyclic dienes, cycloheptatriene, and cyclooctatetraene were obtained using a volatile inlet system enabling the sample vapour to enter the ionisation chamber via a needle valve. Spectra of the tricarbonyliron complexes were obtained using the heated insert probe, but in most cases additional heating was not required. The HeI spectra were recorded; at the time of experiment, HeII facilities were not available, but at a later date, the HeII PE spectrum of complex (VIII) was recorded and is included at the end of this chapter. All spectra were calibrated using xenon and argon. Details of instrumentation are given in Appendix I.

(ii) Organic samples

Cyclohexa-1,3-diene and cyclohepta-1,3-diene were obtained from Koch Light. Commercial cis, cis-cycloocta-1,3-diene and cycloheptatriene were dried and redistilled before use, and cyclooctatetraene, obtained from Koch Light, was also dried and redistilled before use.

(iii) Organometallic complexes

(a) η^4-buta-1,3-dienetricarbonyliron (I)

η^4-buta-1,3-dienetricarbonyliron was obtained from Strem Chemicals Inc., and no further purification was carried out.

(b) η^4-cyclohexa-1,3-dienetricarbonyliron (II)

Cyclohexa-1,4-diene, obtained from the Birch reduction of benzene, was used in this preparation [164,165]. A general method for preparation

of dienetricarbonyliron complexes, described by Dauben and Lorber [64] was used thus:

The diene (5 g) was dissolved in dry diethylether (150 cm^3), and the solution heated to reflux in a nitrogen atmosphere. Diiron nonacarbonyl ($Fe_2(CO)_9$, 31.1 g) was added to the refluxing solution and heating was continued for 4.5 h. Filtration of the reaction mixture and evaporation, gave a brown oil. Distillation yielded a yellow liquid, b.p. 42°C/0.05 mm [Found: C, 49.28%; H, 3.71%; calc: C, 49.13%; H, 3.66%]

(c) η^4-cyclohepta-1,3-dienetricarbonyliron (III)

The general method described for (II) was followed; the product was a yellow liquid, b.p. 58°C/0.05 mm [Found: C, 51.13%; H, 4.46%; calc: C, 51.32%; H, 4.31%].

(d) η^4-cycloocta-1,3-dienetricarbonyliron (IV)

This was prepared following an alternative literature method [65]. Excess diene (4 g) was refluxed in benzene (150 cm^3) with triiron-dodecacarbonyl ($Fe_3(CO)_{12}$, 16 g) for 15 h under a nitrogen atmosphere. Solvent was removed, and the remaining liquid purified by column chromatography using a silica column and petroleum ether (b.p. < 40°C) as eluent. Three bands were observed on the column; the first was collected, and solvent evaporated to give yellow crystals which appeared to be slightly air sensitive. The crystals were purified by recrystallisation from degassed pentane, under nitrogen (m.p. 35.5 - 36°C) [Found: C, 53.29%; H, 4.98%; calc: C, 53.26%, H, 4.87%]

(e) η^4-cyclohepta-1,3,5-trienetricarbonyliron (VII)

Two separate methods were used for this preparation; that described by King [66], and that of Lewis [67]. In each case the complex was isolated by distillation, as a red liquid, b.p. 65°C/0.2 mm; however decomposition occurred on storing in a nitrogen atmosphere at low temperatures for any length of time. Elemental analysis was not attempted and the PE spectrum was obtained immediately after distillation.

(f) η^4-cycloocta-1,3,5,7-tetraenetricarbonyliron (VIII)

This was prepared according to the method of King [66]. On removal of the xylene solvent, a black solid remained; the product was extracted from this with benzene. On evaporation of the benzene, dark red crystals remained; these were further purified by sublimation at 80°C/0.1 mm. [Found: C, 54.6%; H, 3.5%; calc: C, 54.14%; H, 3.3%]

(g) η^4-cyclohexa-1,3-diene-, and η^4-cyclohepta-1,3-dienetricarbonylruthenium (V) and (VI)

Complexes (V) and (VI) were prepared according to a recently published literature method [68]. The starting materials were $Ru_3(CO)_{12}$ and the appropriate diene. η^4-cyclohexa-1,3-dienetricarbonylruthenium was isolated as a colourless liquid by column chromatography, and η^4-cyclohepta-1,3-dienetricarbonylruthenium as a yellow liquid by the same method.

The purity of samples was confirmed by elemental analysis (where shown), measurement of melting and boiling points, proton n.m.r., infra-red, and mass spectra, which agreed with literature data [64-68, 118, 133, 139]. All complexes, with the exception of (VII) were found to be fairly air stable when pure, but all were stored in a nitrogen atmosphere at 0°C.

2.15 PHOTOELECTRON SPECTRA

cyclohexa-1,3-diene
cyclohepta-1,3-diene
cycloocta-1,3-diene
cyclohepta-1,3,5-triene
cycloocta-1,3,5,7-tetraene

η^4-buta-1,3-dienetricarbonyliron (I)
η^4-cyclohexa-1,3-dienetricarbonyliron (II)
η^4-cyclohepta-1,3-dienetricarbonyliron (III)
η^4-cycloocta-1,3-dienetricarbonyliron (IV)

η^4-cyclohexa-1,3-dienetricarbonylruthenium (V)
η^4-cyclohepta-1,3-dienetricarbonylruthenium (VI)

η^4-cyclohepta-1,3,5-trienetricarbonyliron (VII)
η^4-cycloocta-1,3,5,7-tetraenetricarbonyliron (VIII)
(HeI; HeI & HeII)

η^4-hepta-3,5-dien-2-oltricarbonyliron (IX)
η^4-methylhexa-2,4-dien-1-oatetricarbonyliron (X)

cyclohexa-1,3-diene

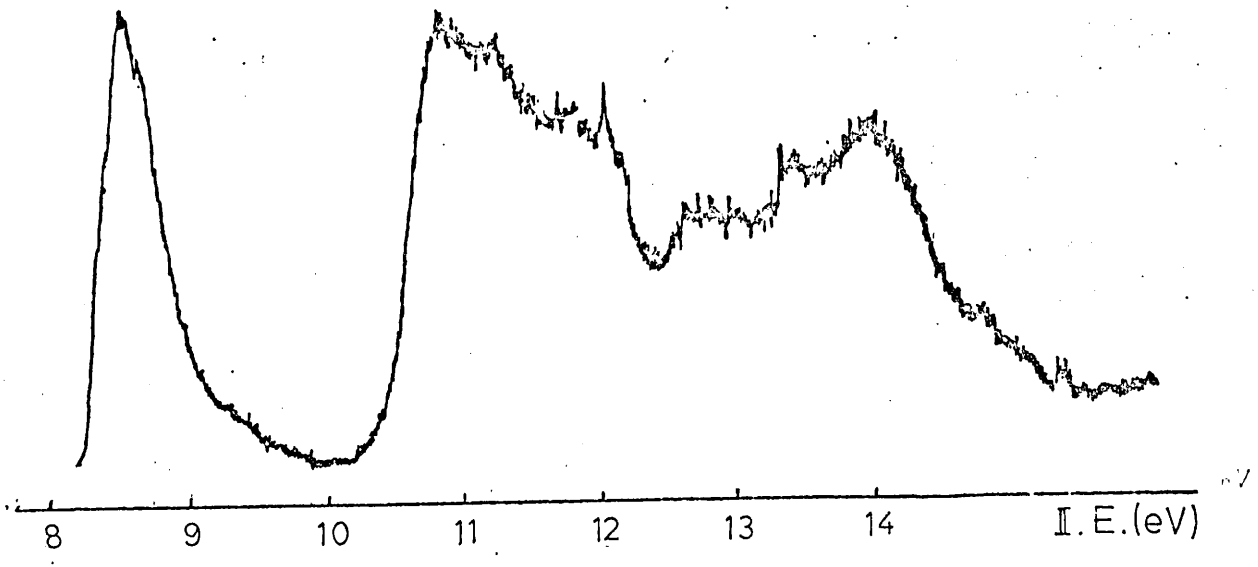

cyclohepta-1,3-diene

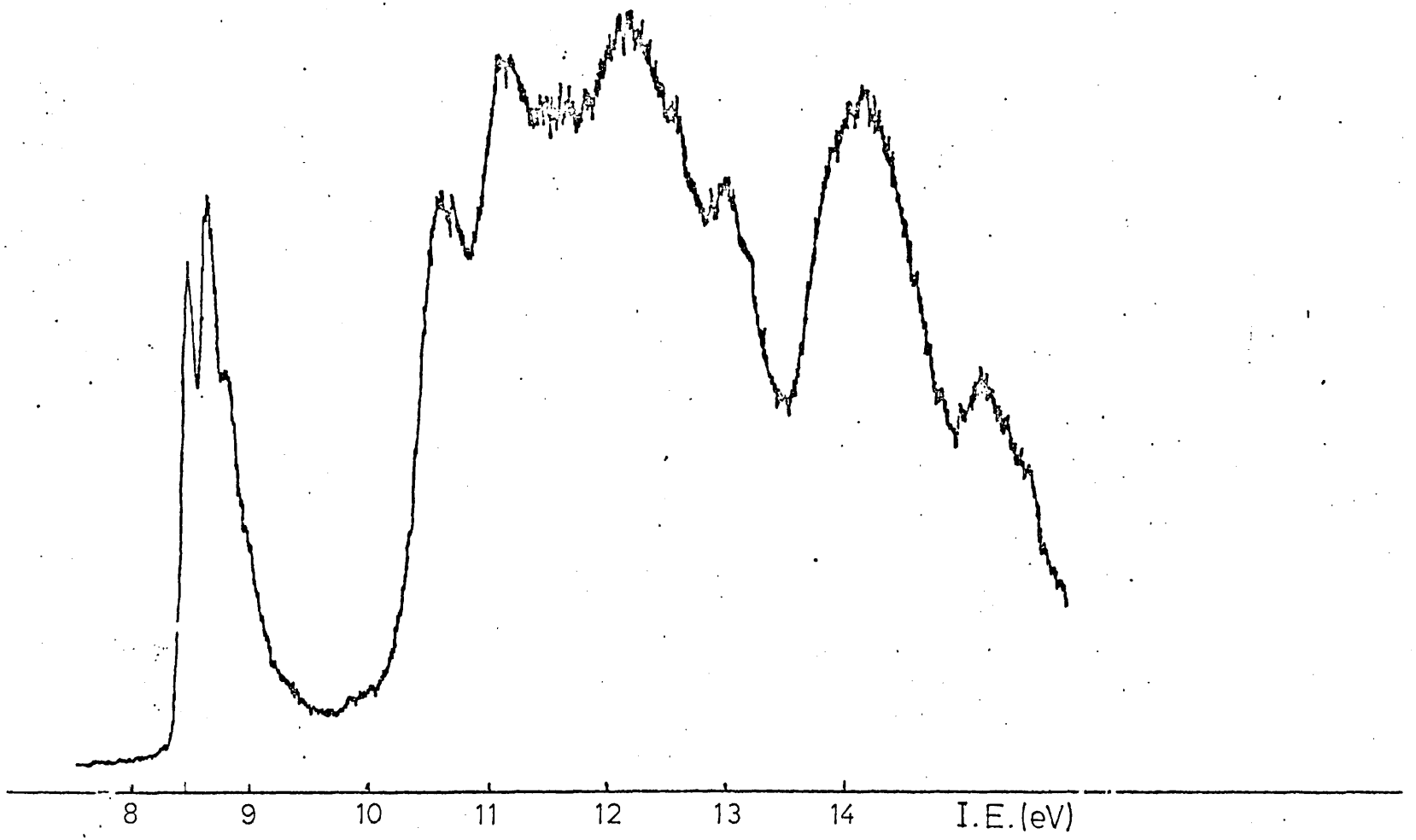

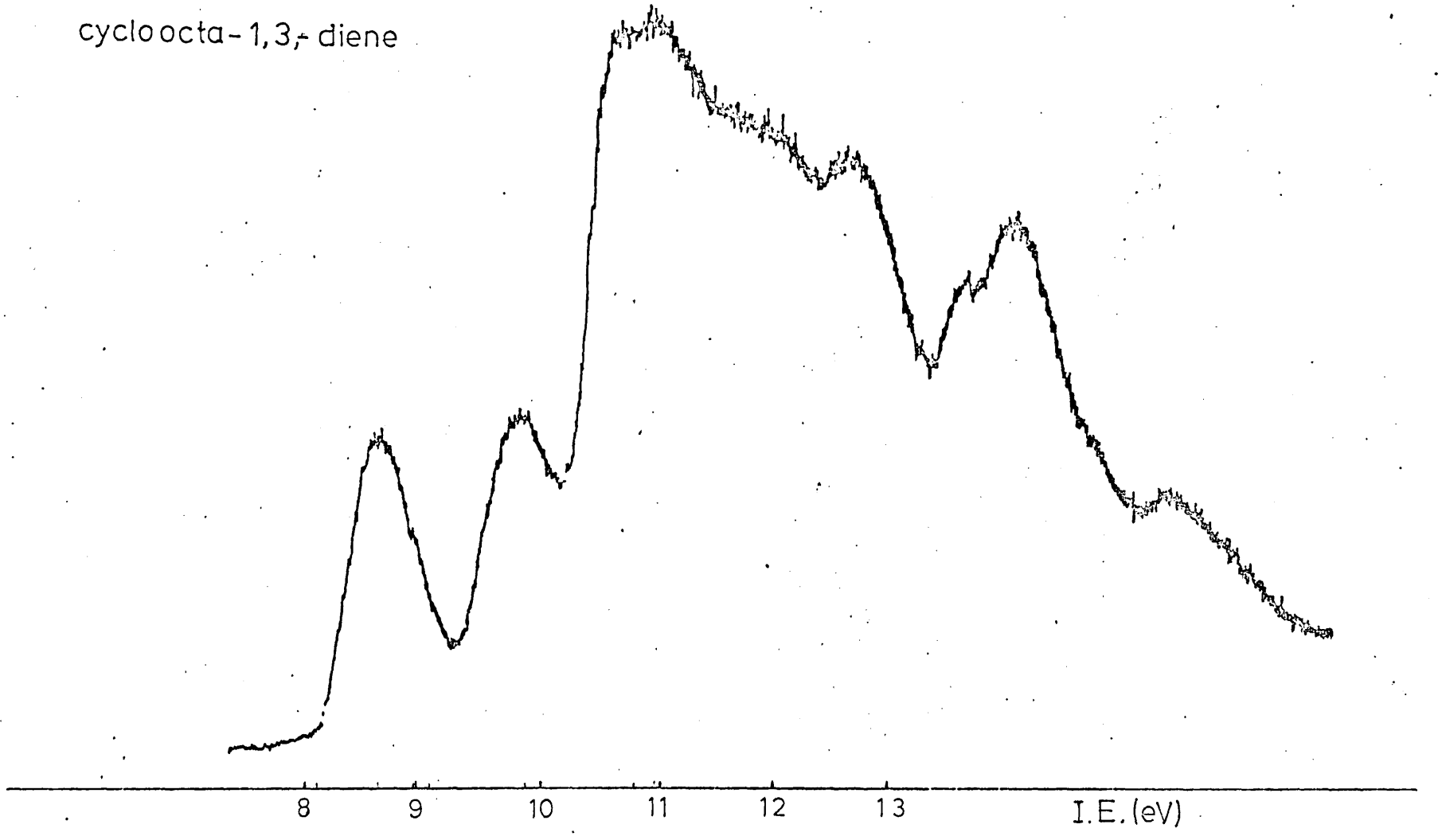
cyclooctа-1,3,- diene
8
9
10
11
12
13
I.E. (eV)

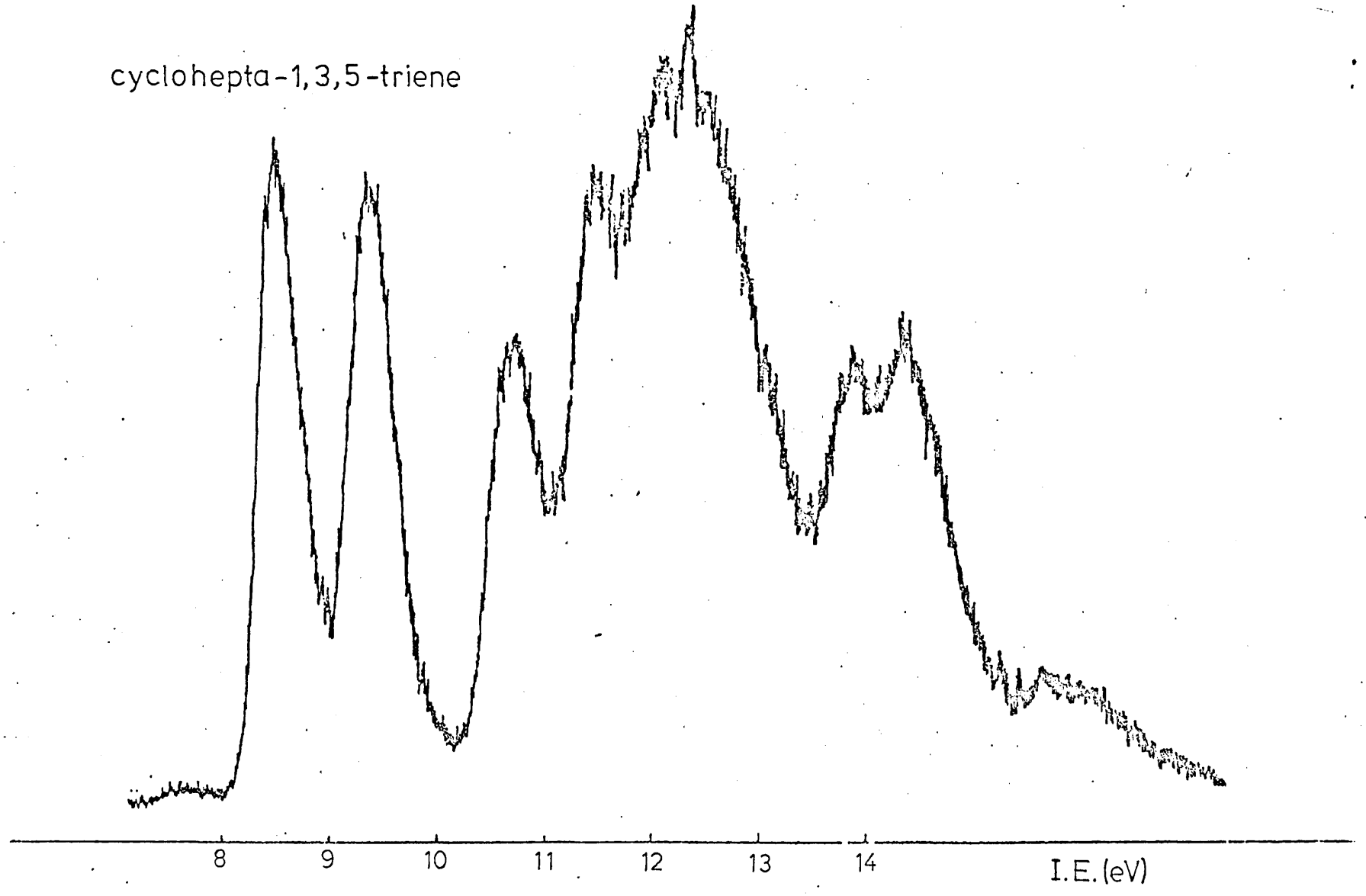
cyclohepta-1,3,5-triene
8
9
10
11
12
13
14
I.E. (eV)

cycloocta-1,3,5,7-tetraene

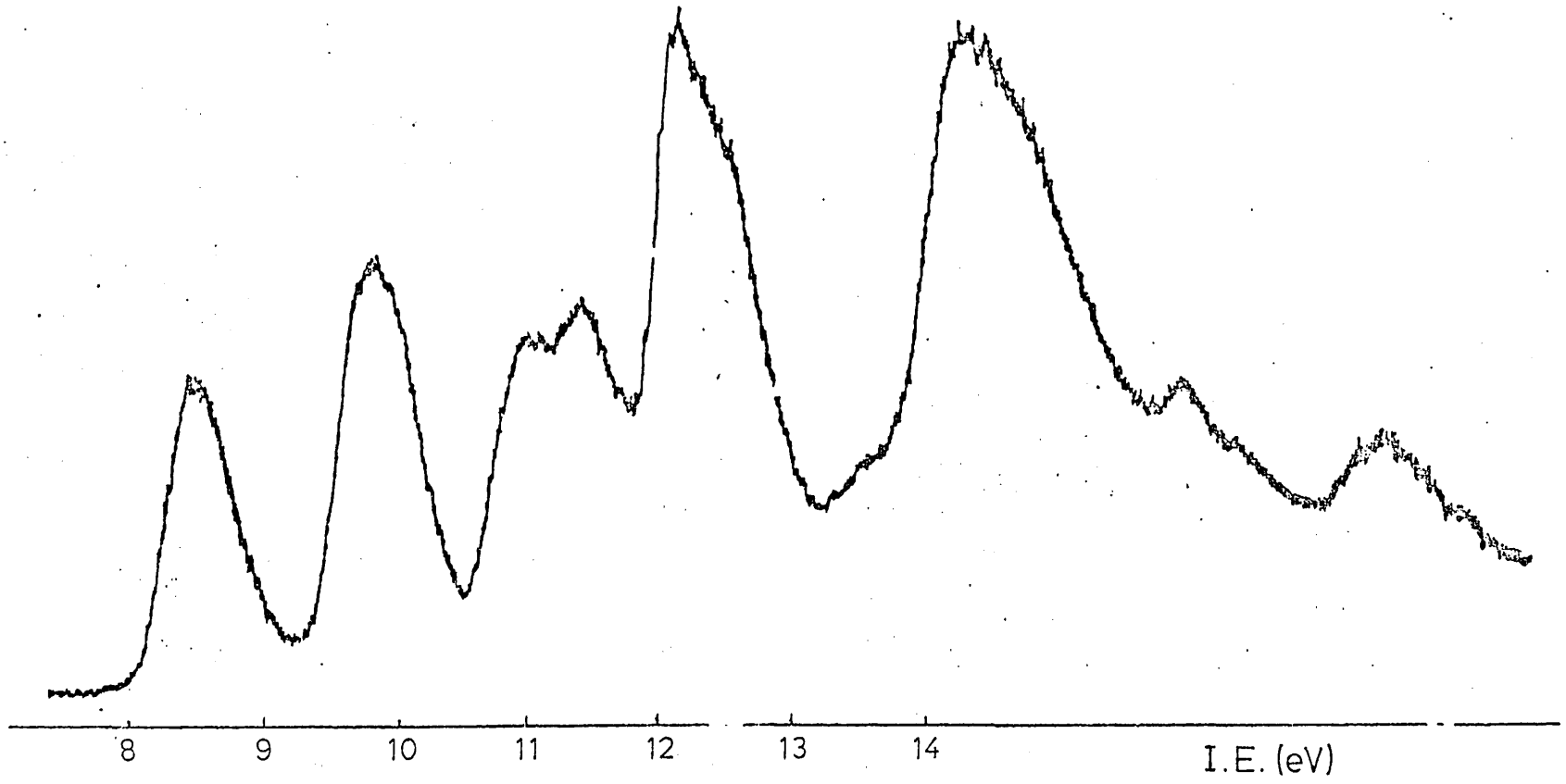

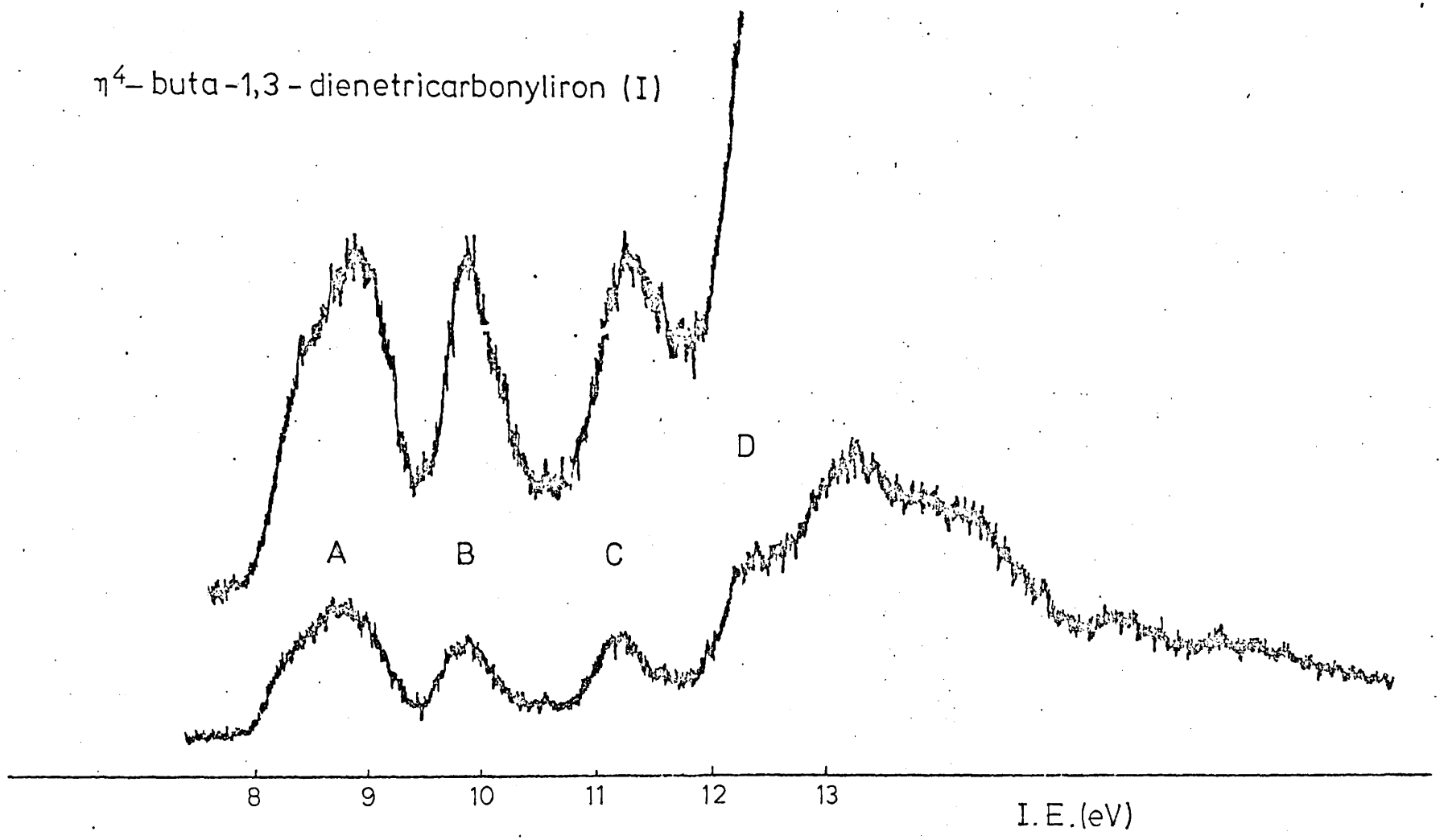
η⁴– buta-1,3-dienetricarbonyliron (I)
A
B
C
D
8
9
10
11
12
13
I.E.(eV)

η^4-cyclohexa-1,3-dienetricarbonyliron
(II)

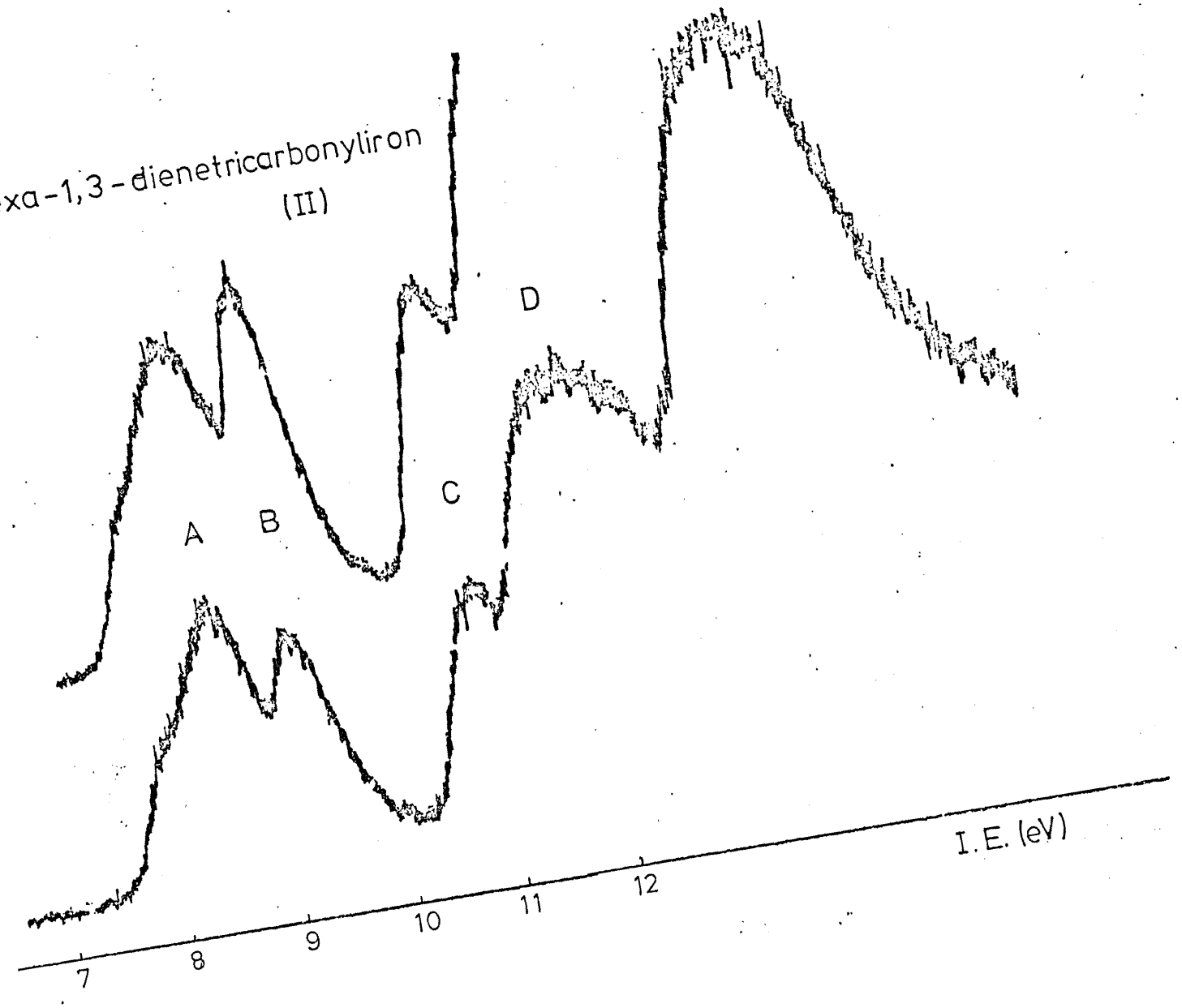

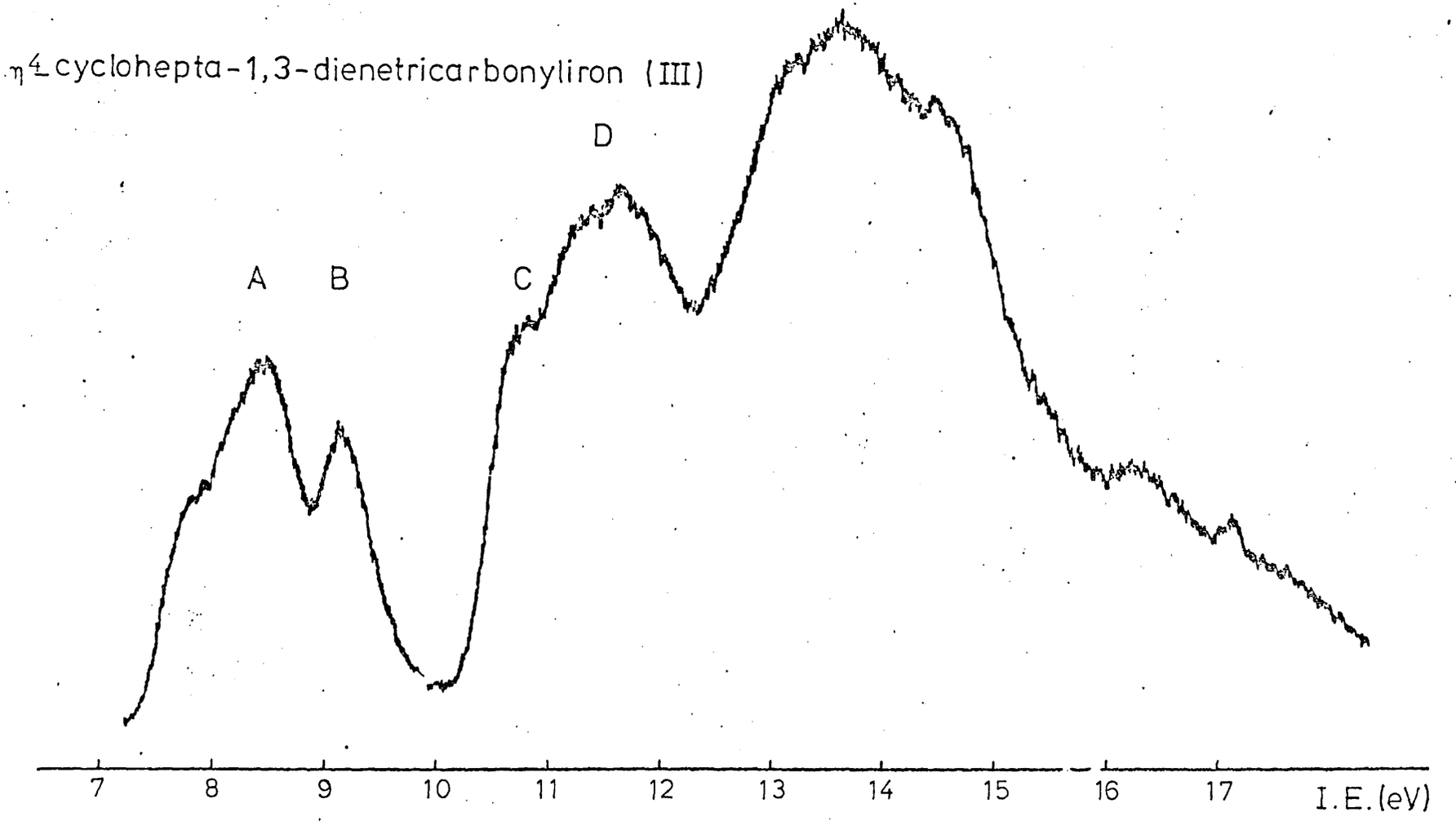
η4-cyclohepta-1,3-dienetricarbonyliron (III)
A
B
C
D
7
8
9
10
11
12
13
14
15
16
17
I.E.(eV)

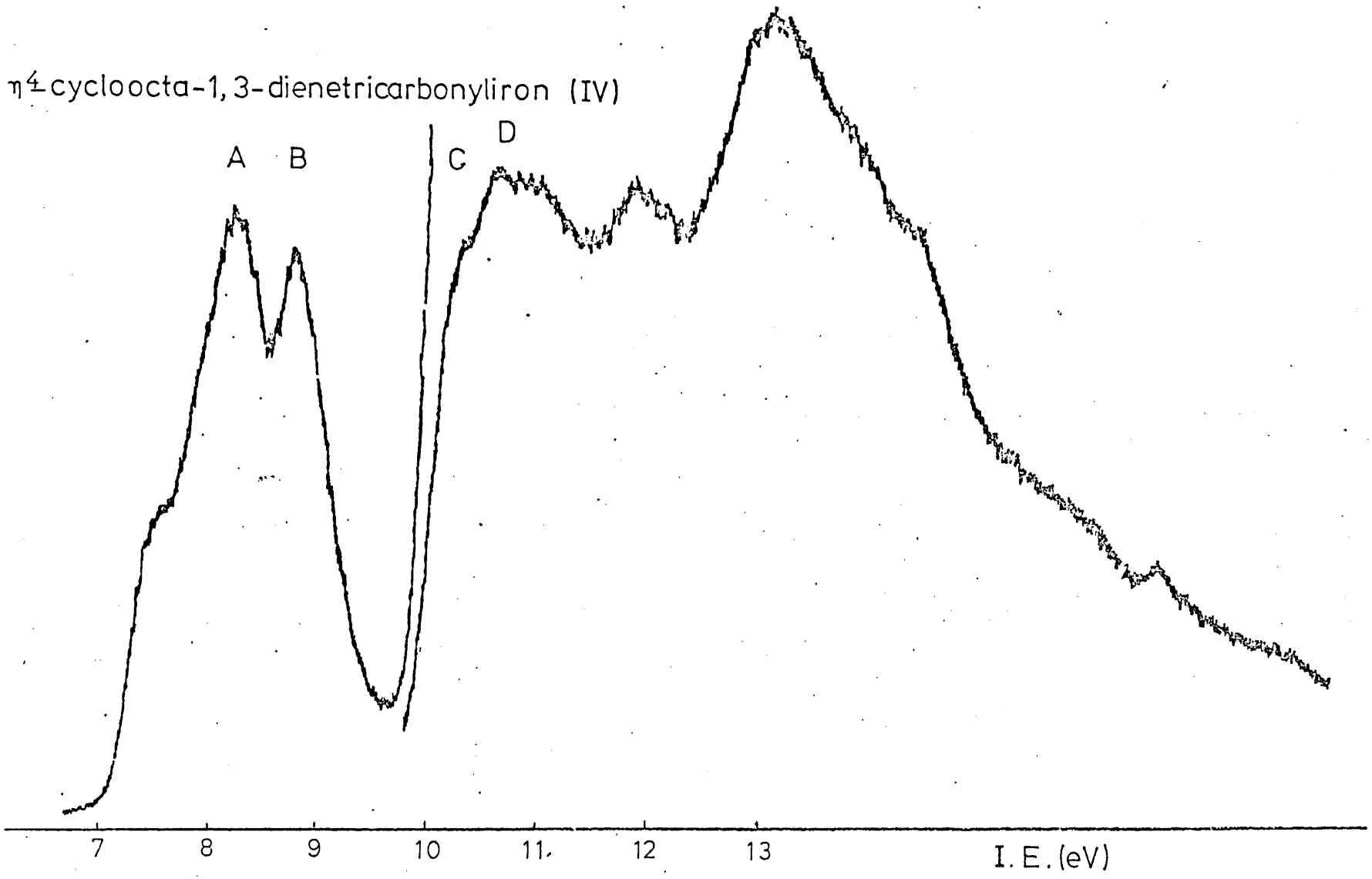
η⁴-cycloocta-1,3-dienetricarbonyliron (IV)
A
B
C
D
7
8
9
10
11
12
13
I.E.(eV)

η^4-cyclohexa-1,3-dienetricarbonylruthenium (V)

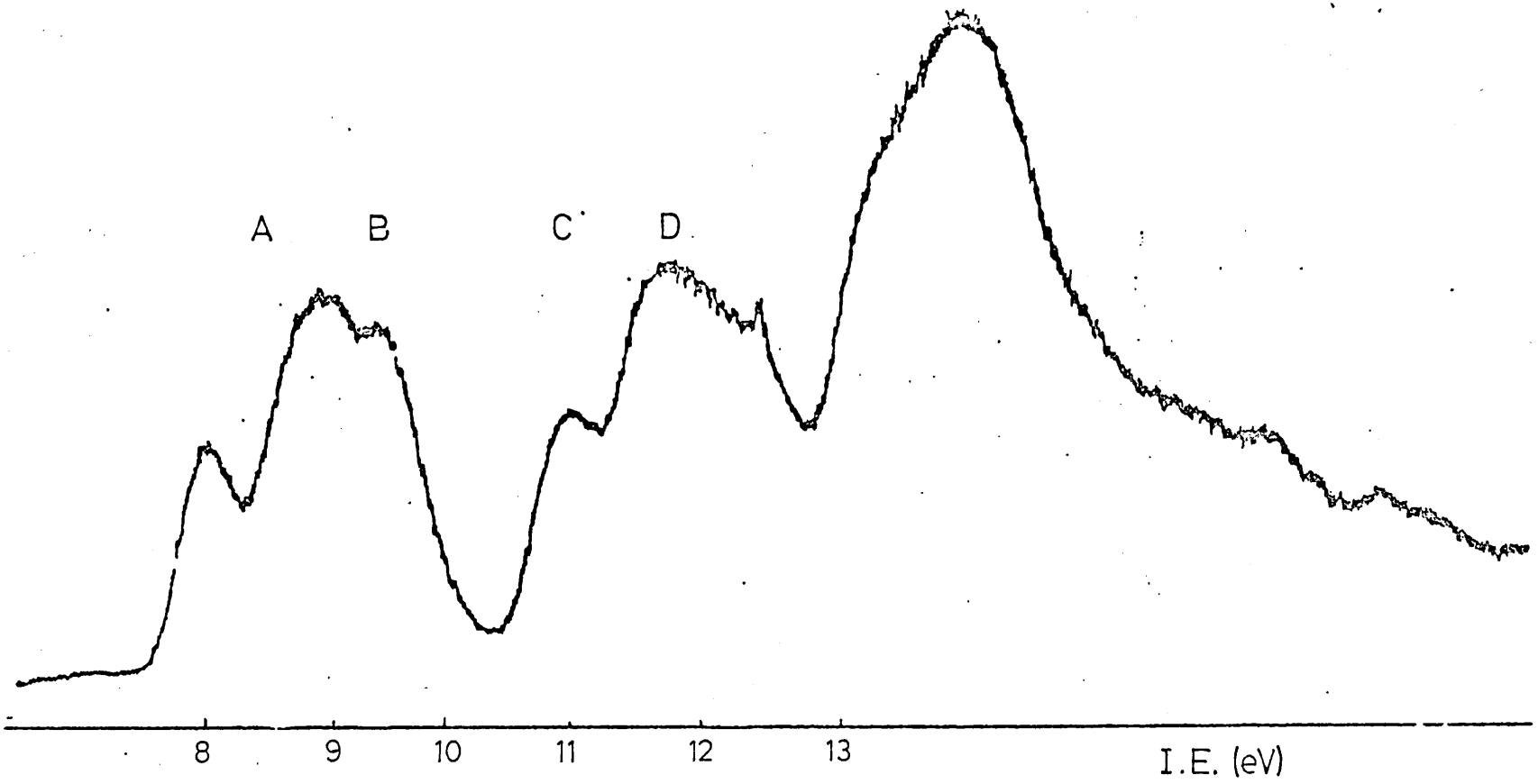

η^4-cyclohepta-1,3-dienetricarbonylruthenium (VI)

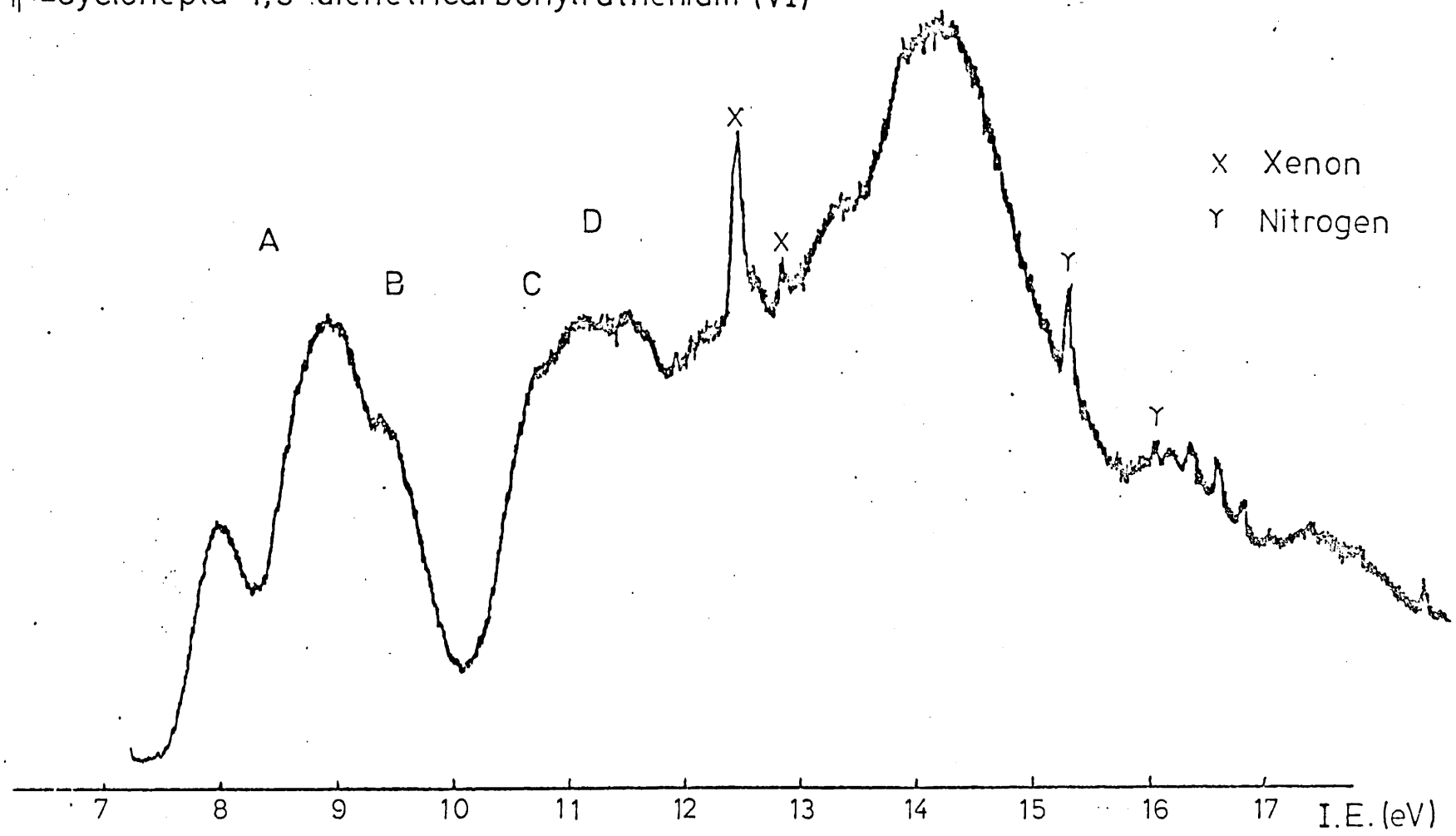

η^4-cyclohepta-1,3,5-trienetricarbonyliron (VII)

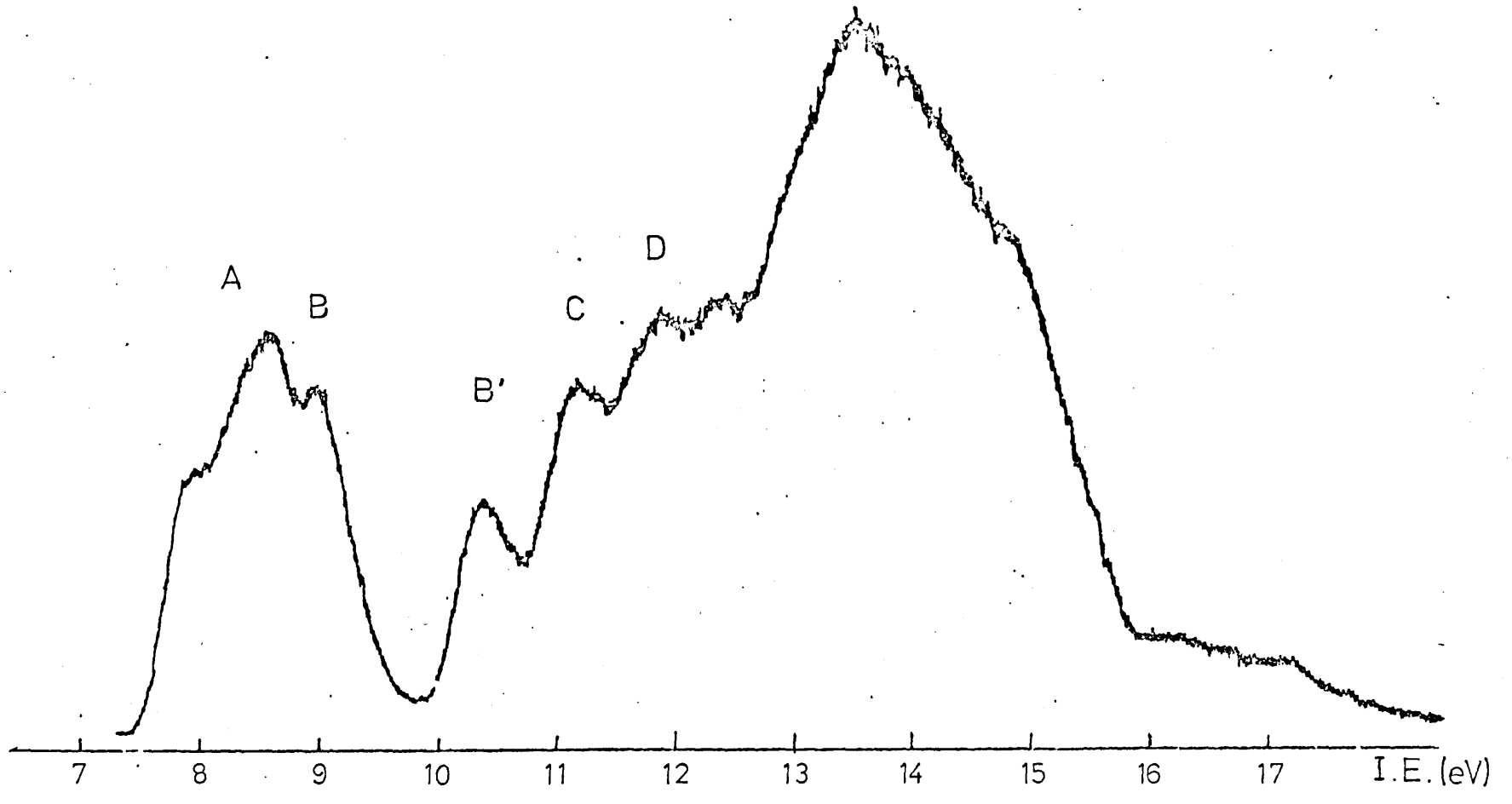

η^4-cycloocta-1,3,5,7-tetraenetricarbonyliron (VIII)

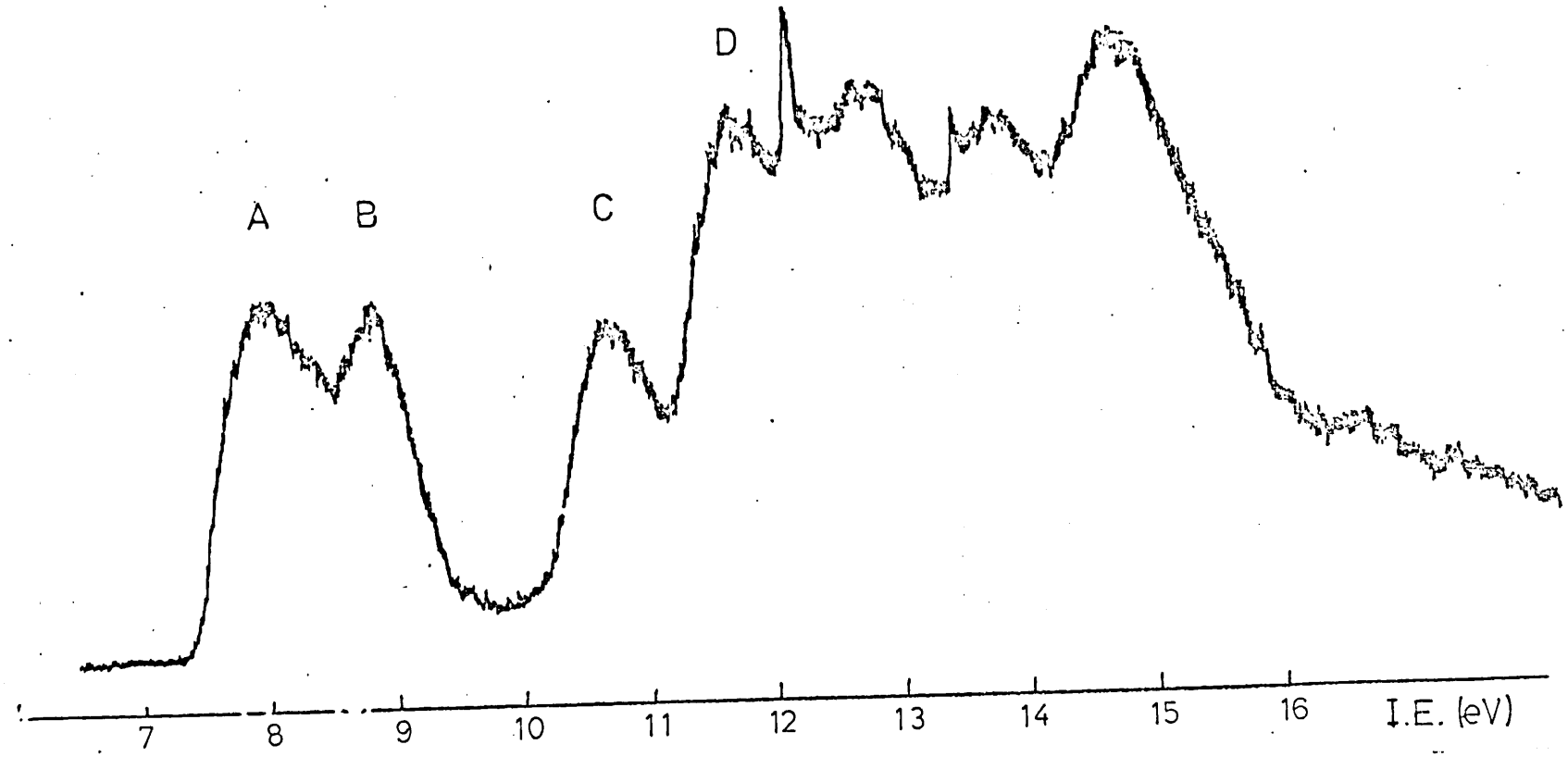

cycloocta-1,3,5,7-tetraenetricarbonyliron (VIII)

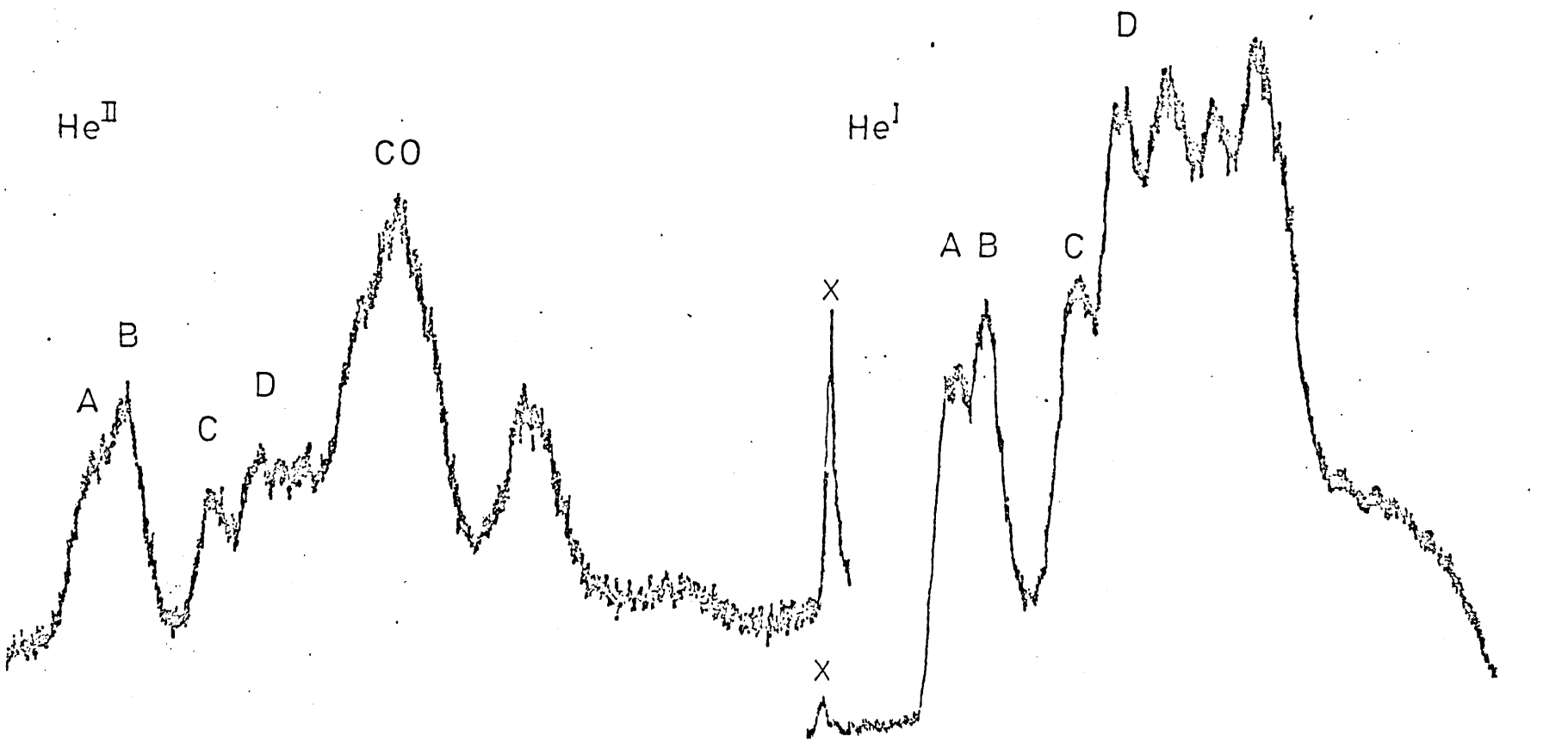

X He self ionisation

η^4 hepta-3,5-dien-2-oltricarbonyliron (IX)

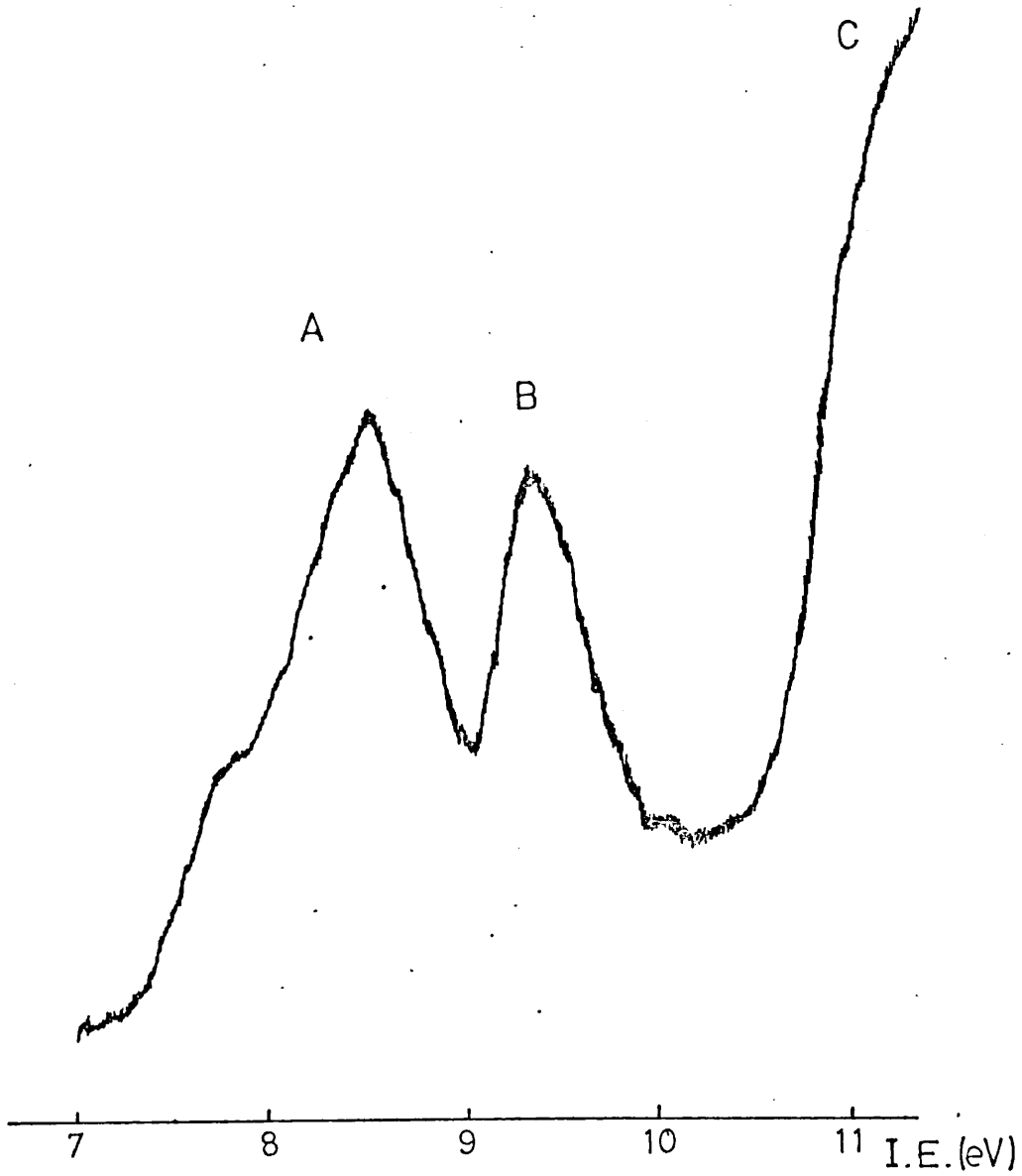

η^4-1-methyl-hexa-2,4-dien-1-oatetricarbonyliron (X)

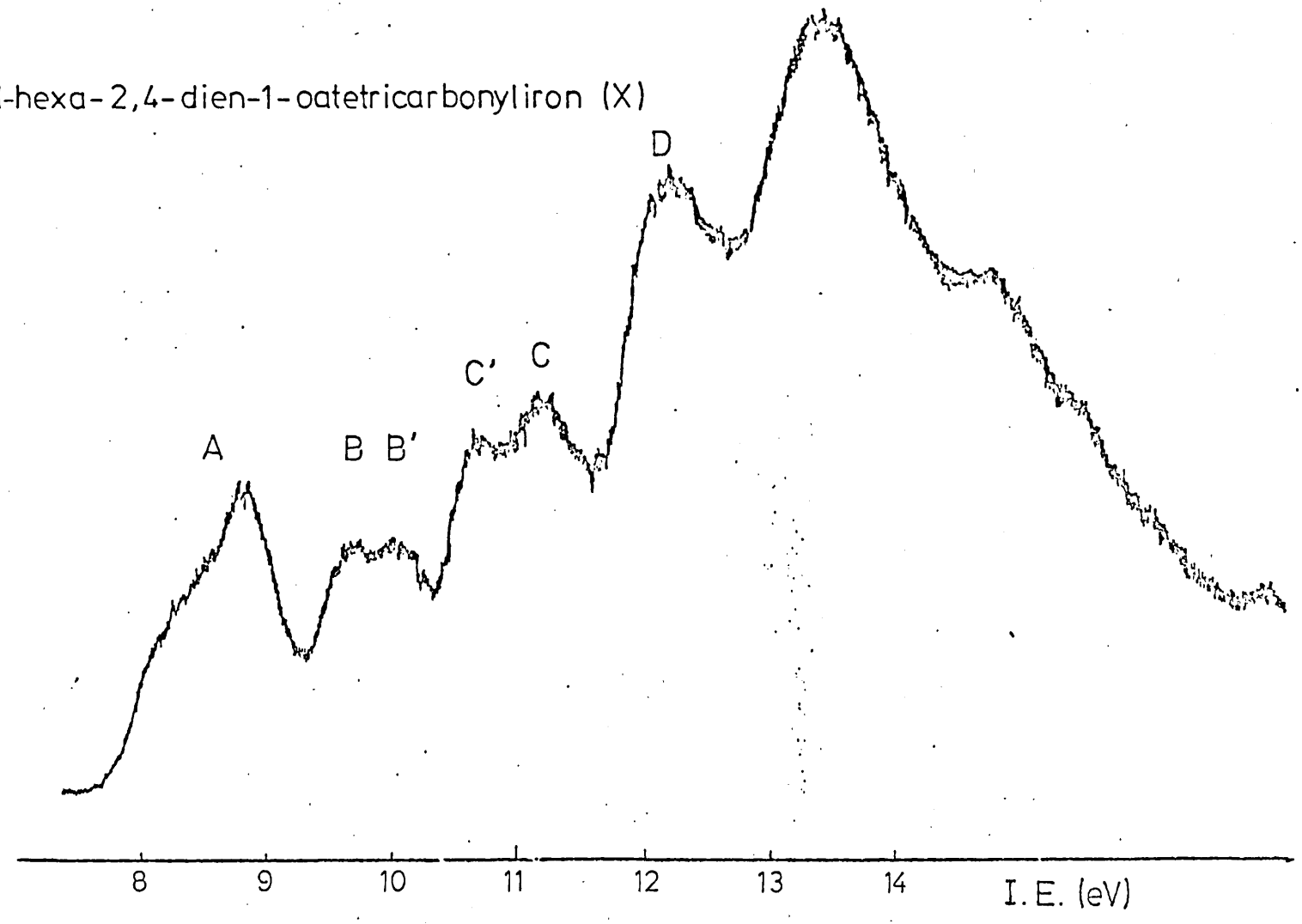

Chapter 3

Photoelectron spectra of some metallocenes and related compounds

3.1 INTRODUCTION

The HeI photoelectron spectra of the metallocenes derived from some first row transition metals and some related compounds have been reinvestigated, and the HeII photoelectron spectra are reported, in most cases, for the first time. The spectra were obtained in the hope of definitely assigning the bands in cases where current assignments are in dispute, and of confirming previous assignments in other cases.

This chapter contains an introduction to the type of complex under investigation, and a review of experimental preparative methods, physical properties, and structural characteristics. A simple molecular orbital description of the bonding is given together with a brief survey of various molecular orbital calculations published to date. The electronic ground state of each complex is discussed, as predicted by theory and confirmed (or otherwise) by experimental methods. Previous photoelectron spectroscopic data for the complexes are discussed, and compared to results obtained in the current study. Experimental details are presented at the end of the chapter.

3.2 HISTORICAL BACKGROUND

A new field of organometallic chemistry was introduced with the discovery of ferrocene in 1951, by two independent research groups [69, 70]. This led to the synthesis of several hundred compounds in which the cyclopentadienyl group is involved in bonding to a metal.

3.3 CLASSIFICATION OF COMPOUNDS

The cyclopentadienyl radical (Cp), may form three main types of complex with metals:

(i) π-cyclopentadienyl complexes. In these the Cp ring is essentially covalently bonded to the metal via the five carbon atoms, the metal atom being equidistant from all five. The Cp ring has a planar carbon skeleton (eg ferrocene, $CoCp(CO)_2$).

(ii) σ-cyclopentadienyl complexes. The Cp ring is bonded to the metal via only one carbon atom, with which the metal forms a two electron covalent bond (eg $FeCpC_5H_5(CO)_2$).

(iii) cyclopentadienide complexes. In these complexes, the bonding between metal and ring is thought to have considerable ionic character (eg $Mg^{2+}(Cp^-)_2$, Na^+Cp^-).

Examples of each type of complex are shown in figure 3.1. There is no distinct division between

Figure 3.1 Examples of complexes from groups (i), (ii) and (iii)

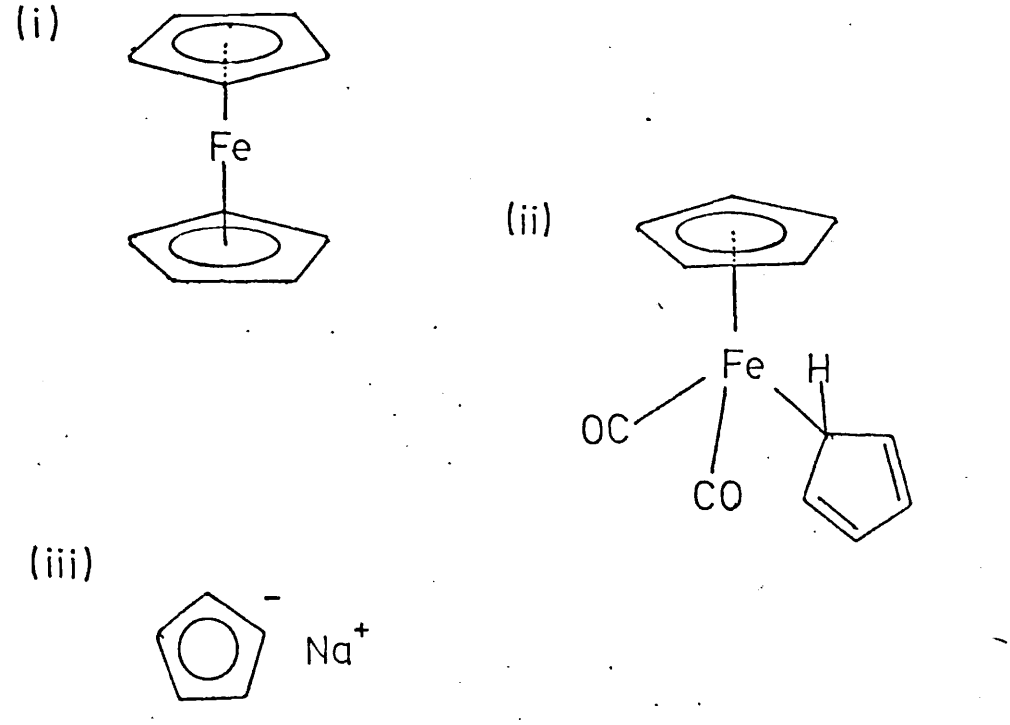

the 'ionic' and 'covalent' types of complex; many of the πCp 'covalent' complexes display considerable ionic character.

3.4 METALLOCENES

The compounds involved in the current study are some of those in which two cyclopentadienyl rings are π bonded to a metal of the first transition series. These particular biscyclopentadienylmetal complexes have the 'sandwich' structure, first proposed by Wilkinson and co-workers [166], and by Fischer and Pfab [167], in which the metal atom is arranged between the two cyclopentadienyl rings, equidistant from each, the ring planes being parallel.

The complexes of the first transition series, Cp_2M, are shown and numbered in figure 3.2, together with the related complexes studied. Throughout this chapter they will be referred to by their trivial names derived from metallocene; that is, cobaltocene, ferrocene, etc. Complexes (I) to (VIIa) are all electronically

Figure 3.2 Metallocenes (Cp_2M)

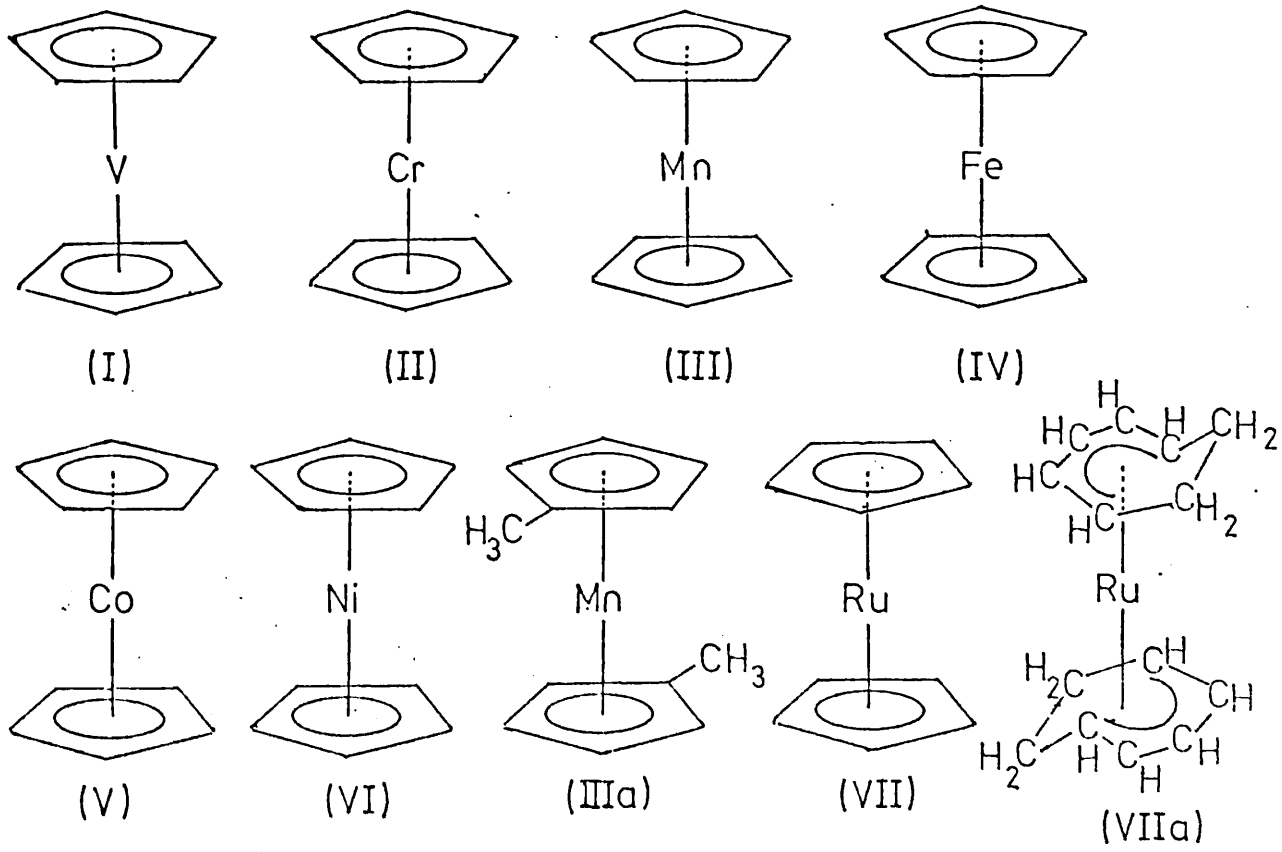

Figure 3.2 cont. Metallocenes (Cp_2M)

(I)	vanadocene
(II)	chromocene
(III)	manganocene
(IV)	ferrocene
(V)	cobaltocene
(VI)	nickelocene
(III a)	dimethylmanganocene
(VII)	ruthenocene
(VII a)	biscycloheptadienylruthenium

neutral species, although cationic species of many are known. Table 3.1 shows the transition metal metallocenes with their melting points [102], and also 'metallocenes' derived from main group metals [168].

3.5 SYNTHESES

Preparative details are given in two useful reviews [66, 168]. The general methods are evolved from those originally used by Wilkinson et al [169] to prepare the metallocenes of most of the first row transition metals in order to compare their chemical and magnetic properties.

Two general methods of preparation are described below:

(i) Reaction of alkali metal cyclopentadienides with metal complexes

This involves reaction of freshly prepared alkali metal cyclopentadienide (usually sodium cyclopentadienide) with anhydrous metal halides (or other suitable salts) in a solvent, usually tetrahydrofuran (THF)

Table 3.1 Melting point data for metallocenes

Compound (Main group)	Melting point (°C)	Colour	Compound (transition metal)	Melting point (°C)	Colour
Cp_2Be	59-60	colourless	$[Cp_2Ti]_2$	> 200 (dec.)	green
Cp_2Mg	176-178	colourless	$[Cp_2Zr]_2$	> 300 (dec.)	purple-black
Cp_2Ca	dec.	colourless	Cp_2V	167-168	purple
Cp_2Sr	dec.	colourless	Cp_2Cr	172-173	scarlet
Cp_2Ba	dec.	colourless	Cp_2Mn	172-173	brown (amber)
Cp_2Zn	dec. 100-130	colourless	$[Cp_2Tc]_2$	155	yellow
Cp_2Hg	83-85 (dec.)	yellow	Cp_2Fe	173	orange
Cp_2Sn	104-105	colourless	Cp_2Ru	199-200	pale yellow
Cp_2Pb	132-135	yellow	Cp_2Os	229-230	white
			Cp_2Co	173-174	purple
			Cp_2Rh	-	-
			Cp_2Ir	-	-
			Cp_2Ni	173-174 (dec.)	green

or 1,2-dimethoxyethane, as shown in (3)1:

$$2NaCp + MCl_2 \xrightarrow[\text{reflux}]{THF} \pi Cp_2M + 2NaCl \qquad (3)1$$

More recently, thallium cyclopentadienide has been commonly used as the metal cyclopentadienide reagent, since it may be handled conveniently in air, although it is light and heat sensitive on storage, and extremely toxic.

(ii) Reaction between cyclopentadiene and metal salts.

In some cases, direct treatment of a metal halide with cyclopentadiene in the presence of a base such as diethylamine or piperidine, results in elimination of an acidic methylene hydrogen from cyclopentadiene, as shown in (3)2:

$$NiBr_2 + 2C_5H_6 \xrightarrow{\text{base}} \pi Cp_2Ni + BH^+Br^- \qquad (3)2$$
$$B = \text{base}$$

The 1,1'-dimethyl substituted derivatives of the metallocenes were first prepared and discussed by Reynolds and Wilkinson [170]. Preparations were by analogous methods.

3.6 SOME GENERAL PROPERTIES

With the exception of those complexes in the iron group (ferrocene, ruthenocene, osmocene) all the metallocenes (I) to (VII) are very air-sensitive and suitable precautions must be taken in preparation and handling. The complexes sublime at temperatures of about 80 - 150°C at 0.1 mm Hg. Chromocene (II), and manganocene (III), (IIIa), react violently with moisture.

The complexes are thermally stable, many of them melting without decomposition. Metallocenes derived from the first transition row metals are generally considered to show covalent bonding between metal and Cp ring, with the covalent character of the bonding increasing across the series. Manganocene is an exception; the bonding shows considerable ionic character.

3.7 MOLECULAR STRUCTURE

The 'sandwich' structure of the metallocenes has been confirmed by a number of X-ray crystallographic and electron diffraction studies.

X-ray diffraction shows that crystalline ferrocene and its substituted derivatives have the anti-prismatic (staggered) conformation of Cp rings, while ruthenocene and osmocene exist in the eclipsed form [171] (figure 3.3).

Figure 3.3 Staggered and eclipsed conformation of sandwich type structures

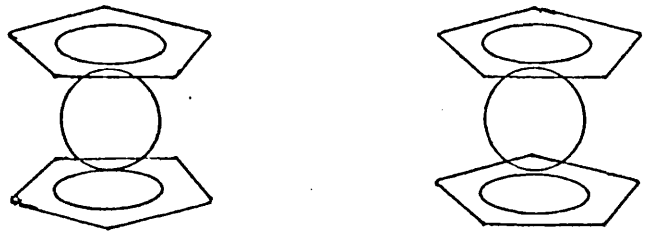

Staggered Eclipsed

It is suggested that inter-ring repulsions are less in the latter compounds than in ferrocene; this is in agreement with the larger inter-ring distances for ruthenocene and osmocene. The crystalline complexes

Cp_2M (M = V, Cr, Fe, Co, Ni), were found to be isomorphous and of monoclinic form.

There are many X-ray crystallographic and electron diffraction studies of these complexes; table 3.2 gives a summary of metal-carbon bond distances and inter-ring distances found by these methods. There is evidence for rotation of the rings about the common orthogonal axis; this was mentioned in one of the earliest electron diffraction studies of ferrocene [172]. This study also noted that the inter-ring distance found for ferrocene was similar to that found in graphite, it thus being unlikely that direct bonding occurred, to much extent, between the Cp rings.

The trends in bond lengths and inter-ring distances across the first transition series may be seen from table 3.2. Magnesium dicyclopentadienide has been included for comparison, since manganocene is also thought to possess considerable ionic character.

In the gas phase, all the first row metallocenes appear, from electron diffraction studies, to adopt the eclipsed (D_{5h} symmetry) conformation, although there is evidence for the staggered conformation (D_{5d}) in the crystalline state. Dimethylmanganocene is found to have two structures in the gas phase, corresponding to two spin isomers; this will be discussed more fully in the section 'electronic structure'. A general structural feature found from these studies is that the Cp hydrogens are bent towards the metal.

Figure 3.4 shows the structure of cobaltocene found by a gas phase electron diffraction study [173], and this structure is typical for the first row metallocenes.

Table 3.2 Structural data for the metallocenes

Bond distances are in Å

Estimated standard deviations given in parentheses in units of the last digit

Compound	Metal-Carbon	C-C (ring)	Inter-ring	Type of Study	Probable Symmetry	Ref.	Date
$MgCp_2$	2.339 (4)	1.432 (2)	4.016 (8)	electron diffraction	D_{5h}	174 a, b	1975, 1974
	2.304 (8)			X-ray crystallography		175	1974
VCp_2	2.280 (5)	1.434 (3)	3.856 (12)	electron diffraction	D_{5h}	176	1975
$CrCp_2$	2.169 (4)	1.431 (2)	3.596 (8)	electron diffraction	D_{5h}	176, 174 b	1975, 1974
$MnCp_2$	2.383 (9)	1.429 (5)		electron diffraction	D_{5h}	177	1967
$Mn(CpMe)_2$	2.42 (2)			electron diffraction	$^6A_{1g}$	178 a	1977
	2.14 (1)				$^2E_{2g}$		
	2.433 (8)			electron diffraction*	$^6A_{1g}$	178 b	1978
	2.144 (12)				$^2E_{2g}$		

* The high spin $^6A_{1g}$ state was concluded to be the more abundant species.

Table 3.2 (continued)

Compound	Metal-Carbon	C-C (ring)	Inter-ring	Type of Study	Probable Symmetry	Ref.	Date
$FeCp_2$	2.03 (2)	1.43 (3)	3.25	electron diffraction	D_{5h}	172	1955
	2.045 (10)	1.403 (20)	3.32	X-ray crystallography	D_{5d}	179	1956
	2.064 (3)	1.440 (2)		electron diffraction	D_{5h}	180	1968
	2.056 (2)	1.429 (3)	3.319 (15)	electron diffraction	D_{5h}	181	1966
	2.07 (1)	1.42 (1)		electron diffraction	D_{5h}	182	1961
$RuCp_2$	2.21 (1)	1.43 (1)	3.68 (1)	X-ray crystallography	D_{5h}	183	1959
	2.196 (3)	1.439 (2)		electron diffraction	D_{5h}	180	1968
$OsCp_2$	2.22		3.71			184	1959
$CoCp_2$	2.119 (3)	1.429 (2)	3.478 (4)	electron diffraction	D_{5h}	173	1976
	2.113 (3)	1.430 (3)	~3.5	electron diffraction	D_{5h}	185	1975
$NiCp_2$	2.160 (5)	1.41 (1)		electron diffraction	D_{5h}	186	1969
	2.196 (8)	1.430 (3)		electron diffraction	D_{5h}	187	1970

Figure 3.4 Molecular structure of cobaltocene

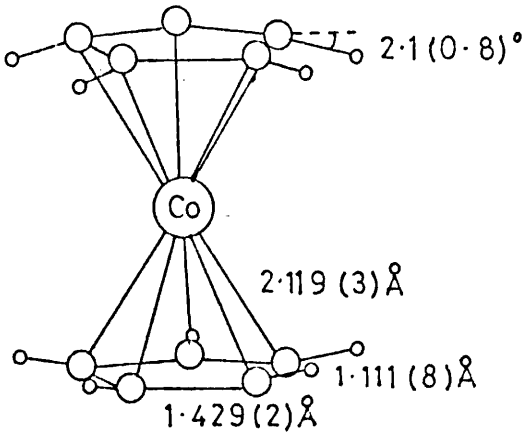

However, many metal sandwich compounds are known or suspected to show distortions from pseudo-axial symmetry. Degenerate systems showing orbital contributions to the magnetic moment must necessarily be Jahn-Teller unstable, and their D_{5d}, D_{5h}, or D_{6h} geometries should thereby be lowered to C_{2h}, C_{2v}, or D_{2h} respectively thus lifting the degeneracies of the E_{1g}, E_{2g} levels.

3.8 ELECTRONIC STRUCTURE

An important feature of the electronic structure of the metallocenes of the first transition row elements, is the unit increase in the number of d electrons available for bonding, in passing across the series. This, in some cases, gives rise to several possibilities for ground state configuration which will be discussed after a simple molecular orbital approach to the bonding has been described. The metallocenes from VCp_2 to $NiCp_2$, with the exception of ferrocene, all have at least one unpaired electron in the ground state, that is, they are paramagnetic.

The same MO approach is used here, as for the bonding in η^4-butadienetricarbonyliron of the previous chapter.

The electronic structure of the cyclopentadienyl group is first considered; the Cp fragment is approximately planar and therefore of D_{5h} symmetry. According to HMO calculations, the five $2p_z$ atomic orbitals of the ring carbon atoms may be combined to give five π molecular orbitals; the relative energies of these MOs and their wave functions may be calculated (figure 3.5). The

Figure 3.5 Molecular orbital diagram for the cyclopentadienyl fragment

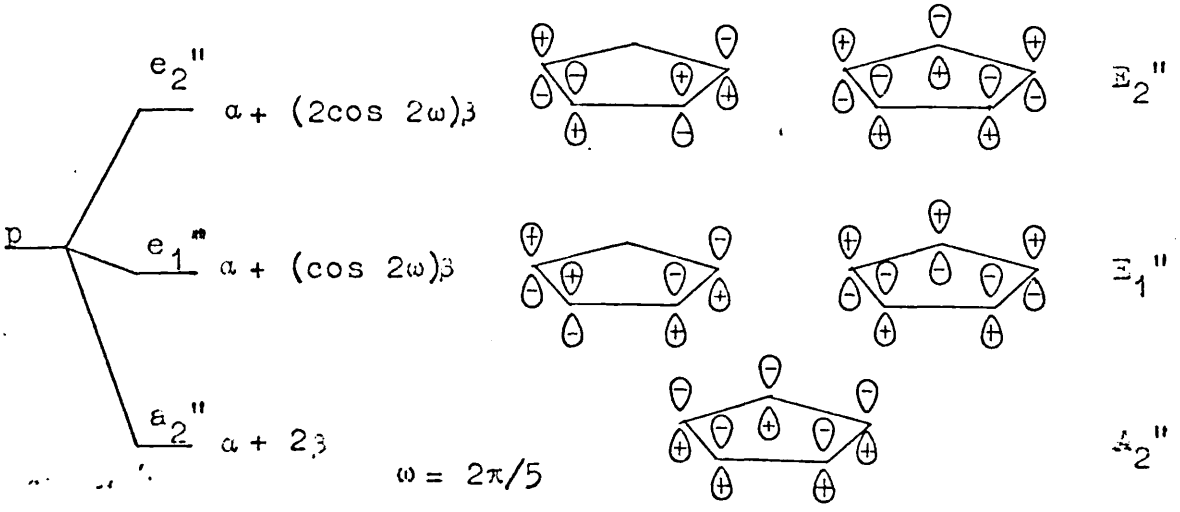

symmetry properties of the MOs are also indicated in figure 3.5. α and β are the usual HMO symbols.

This HMO model predicts the same π energy level order as does LCAO MO SCF theory for benzene with which Cp is isolectronic, and may thus be justified as a reasonable model. Probably the highest occupied σ level lies between the e_1 and a_1 π levels, as shown in other examples [188-190].

Since the metal atom interacts with a pair of cyclopentadienyl rings, the Cp_2 framework may now be considered under D_{5h} symmetry, since this is the symmetry

found in the gas phase. The Cp MOs of the same rotational symmetry are combined in pairs (figure 3.6); the 'symmetric' combination of a pair of equivalent MOs will give a stabilised energy level, and the 'antisymmetric' combination will give rise to a destabilised level with respect to the π MOs of the non-interacting rings. These energy splittings are unlikely to be large or of the same order of magnitude as the separations of the π orbitals of each ring; the σ interactions should be even smaller. The combinations of the pairs of Cp MOs are shown diagrammatically in figure 3.6 together with D_{5h} and D_{5d} symmetry labels, and an energy level diagram is given in figure 3.7.

Figure 3.7 Energy level diagram for the π orbitals of the Cp_2 framework

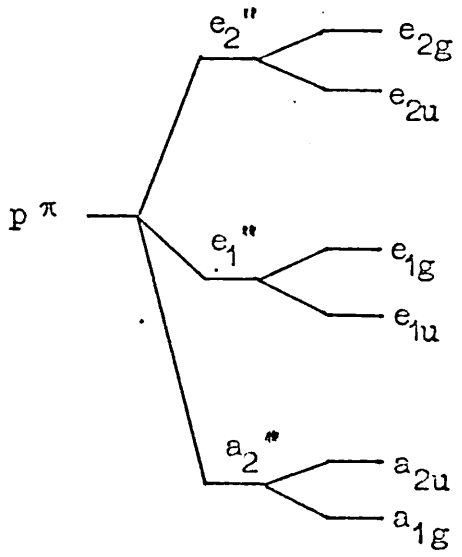

The two Cp planes are parallel within the complexes, as shown by electron diffraction, with the metal atom situated on a C_5 rotation axis. Although the first row metallocenes assume the staggered (D_{5d}) conformation in crystalline form, evidence suggests the D_{5h} conformation in the vapour phase. For most

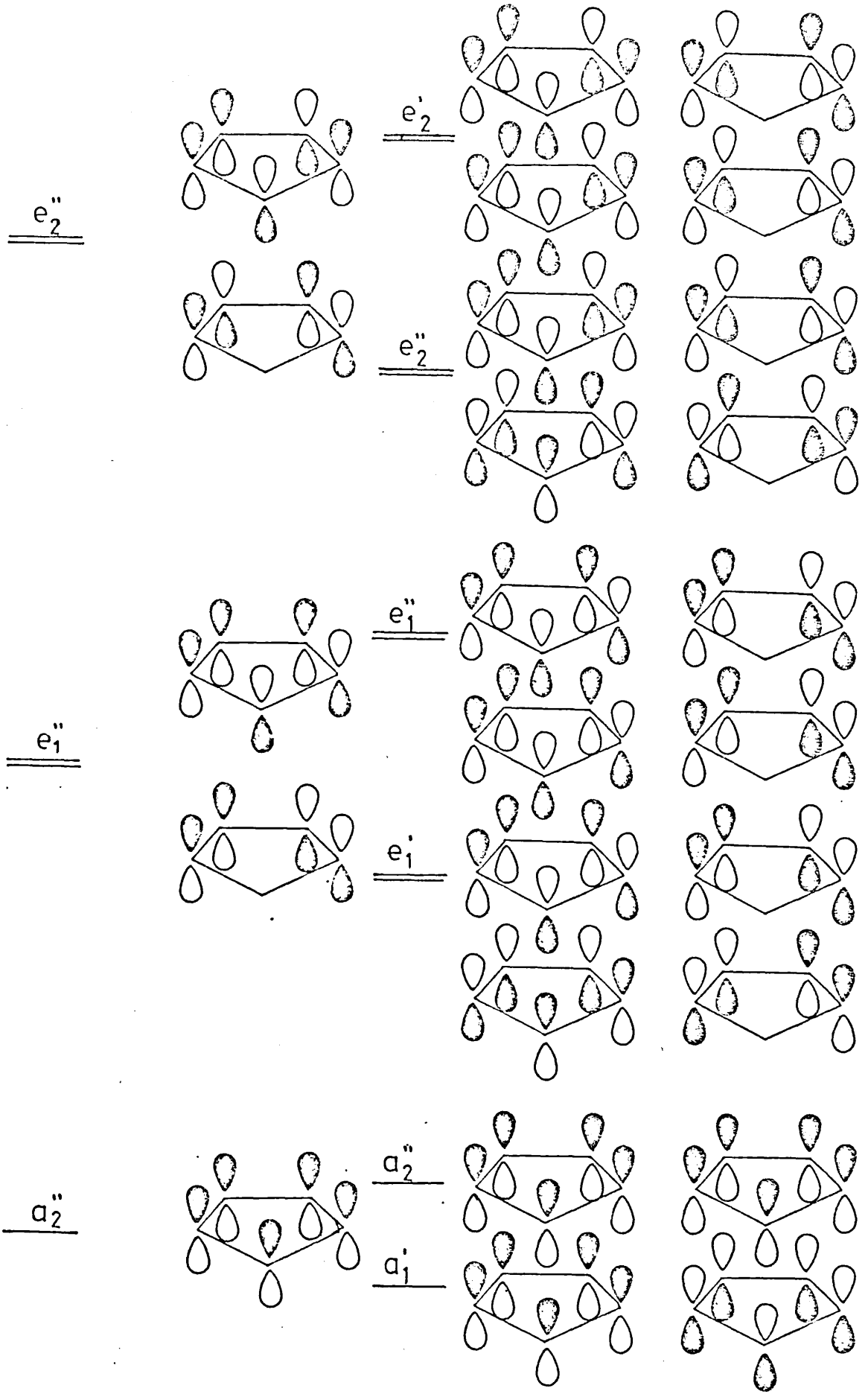

Figure 3.6 Combinations of pairs of cyclopentadienyl MOs

purposes, analysis of the orbital electronic structure in terms of D_5, the subgroup common to D_{5d} and D_{5h} is adequate. The relationship between the relevant irreducible representations of D_{5d}, D_{5h}, D_5 and $D_{\infty h}$, are given in table 3.3 [161] together with the metal d orbital transformations with respect to the relevant group.

Table 3.3 metal orbital transformations under D_{5d}, D_{5h}, D_5, $D_{\infty h}$

metal orbital	D_{5d}	D_{5h}	$D_5(C_{5v})$	$D_{\infty h}$
s	a_{1g}	a'_1	a_1	σ_g^+
p_z	a_{2u}	a''_2	a_2, a_1	σ_u^+
p_x, p_y	e_{1u}	e'_1	e_1	π_u
d_{z^2}	a_{1g}	a'_1	a_1	σ_g^+
d_{xz}, d_{yz}	e_{1g}	e''_1	e_1	π_g
$d_{x^2-y^2}$, d_{xy}	e_{2g}	e'_2	e_2	δ_g

Since most studies to date, concerning the electronic structure of these complexes, have assumed the staggered (D_{5d}) conformation in accordance with solid state structure, the D_{5d} point group notation has been generally adopted for discussion, and will be used here. The various possible metal (d) - ligand combinations of orbitals on symmetry grounds alone are shown in table 3.4.

Table 3.4 Metal (d)-ligand orbital combinations possible on symmetry considerations

metal orbital	symmetry	ligand orbital[a]
d_{z^2}	a_{1g}	a_{1g} (a_1')
d_{xz}, d_{yz}	e_{1g}	e_{1g} (e_1'')
$d_{x^2-y^2}$, d_{xy}	e_{2g}	e_{2g} (e_2')

a Symbols in brackets refer to D_{5h} symmetry properties.

Figure 3.8 shows a molecular orbital diagram for ferrocene, of the same type as that presented for η^4-butadienetricarbonyliron. The relative energies of the ligand and metal orbitals are only approximate, but likely interactions between metal and ligand are shown, and some attempt has been made to correlate the diagram with data arising from recent MO calculations.

Figure 3.8 Approximate MO interaction diagram for $FeCp_2$

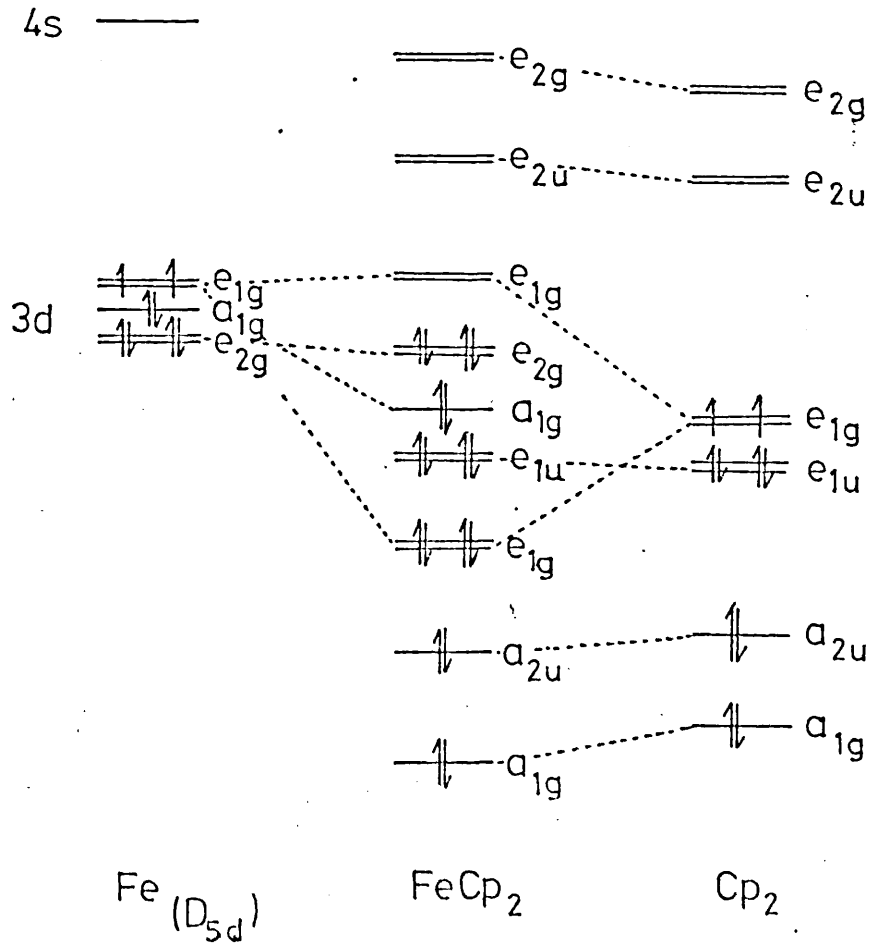

Ferrocene is the only 'closed shell' molecule of the first transition series metallocenes. An approximate MO description of the bonding may be given as follows:- The Cp ring has donor-acceptor characteristics; the e_{2g} antibonding orbital acts as an electron accepting orbital for the e_{2g} (d_{xy}, $d_{x^2-y^2}$) metal d orbitals. However the Cp ring in general is a poor electron acceptor in this type of complex, possibly due to the large difference in energy between metal d and ligand e_{2g} orbitals. Thus the e_{2g} MO of the complex will have largely metal d character. Donation of electrons from the ring π orbitals to empty metal d orbitals is represented by combination of the d_{xz}, d_{yz} (e_{1g}) metal orbitals and the ligand degenerate e_{1g} orbital. The ligand e_{1u} orbital is less likely to interact on symmetry grounds.

Since the relative energies of the d_{z2} (a_{1g}) metal orbital and the a_{1g} ring orbitals are very different there is likely to be little interaction between these levels. The metal 4s and $4p_z$ atomic orbitals are of the correct symmetry to interact with the ring a_{1g} and a_{2g} orbitals, but again, energy differences are large, so interaction is likely to be small. The eighteen electrons from the bonding orbitals of iron and Cp_2 may be placed in the nine MOs of lowest energy (fig 3.8), and it is noted that the metal d_{z2} (a_{1g}) and $d_{x^2-y^2}$, d_{xy} (e_{2g}) orbitals are rather non-bonding in character.

For other first row metallocenes, the symmetry treatment is the same, although the relative d orbital energies will vary slightly as the metal changes and the numbers of electrons will vary. It is assumed that in other cases, essentially the same orbitals as in ferrocene contribute to the bonding.

3.9 MOLECULAR ORBITAL CALCULATIONS

There exists a large number of MO calculations for ferrocene, most of the earlier treatments being of an approximate nature [34, 191-196]. Early calculations by Shustorovich and Dyatkina [191] focussed attention on the transition metal-ligand interactions. D_{5d} symmetry was assumed, and a molecular orbital diagram of the type shown in figure 3.8 was produced. The ligand MOs of e_{1g} and e_{1u} symmetry were both considered as bonding, and as donating (e_{1u}) and accepting (e_{1g}) electrons. Shustorovich and Dyatkina placed the e_{2g} (metal) orbital as highest in energy of the occupied MOs and calculated a positive charge of + 0.69e on the iron atom, while Dahl and Ballhausen calculated a negative charge on the iron atom.

Recently, more sophisticated MO calculations for ferrocene have been published [39, 161, 197-201]; the question of the correct ordering of the mainly d molecular orbitals is still unresolved. All calculations agree that the anti-bonding metal (e_{1g}*) level lies well above the a_{1g} and e_{2g} metal orbitals, but the ordering of the latter is still a matter of contention. Virtually all the calculations indicate that the πe_{1g} metal-ligand interaction is dominant in the metal to ring bonding. The validity (or otherwise) of Koopmans' theorem in predicting ionisation energies for ferrocene is another point discussed in many of these studies.

Veillard et al [39] have published an ab initio calculation for ferrocene, and have estimated ionisation potentials in two different ways: from the difference in total energy between the neutral molecule and the positive ion, and also from SCF eigenvalues for the neutral molecule. The former method gives the same sequence of ionisation energies as found by experimental PES measurements [161, 201]; that is, $(a_{2u}) > e_{1g} > e_{1u} > a_{1g} > e_{2g}$, although the

calculated ionisation energies were consistently some 2eV higher. The second method gave the ordering of ionisation energies as $a_{1g}(d) > e_{2g}(\sigma Cp) \sim a_{2u}(\pi Cp) \sim e_{2u}(\sigma Cp) > e_{2g}(d) > e_{1g}(\pi Cp) \sim e_{1u}(\pi Cp)$ with two predominantly σ ligand levels included in the sequence. Veillard et al concluded that disagreement regarding the orbital sequence is the result of a misplaced confidence in Koopmans' theorem. They suggest the theorem is not valid for ferrocene due to the differing extent of electronic reorganisation occurring on ionisation, depending on the type of orbital involved. For a ligand orbital, little electronic rearrangement was predicted compared to that for a d-type orbital. As a consequence of this, similar ionisation energies would be expected for the ligand orbitals from both methods, as was found, while those for the metal orbitals differed by as much as 6eV.

The extended HMO calculation for ferrocene of Botrel et al [197] gave the orbital sequence $e_{1g}^* > (a_{1g})^2 > (e_{2g})^4 > (e_{1u})^4 > (e_{1g})^4 > (a_{2u})^2 > (a_{1g})^2$, that is, the ionisation energy sequence $a_{2u} > e_{1g} > e_{1u} > e_{2g} > a_{1g}$. Rosch and Johnson [198] report a SCF X_α scattered wave calculation for ferrocene, giving the ionisation energy sequence as $e_{1g} > e_{1u} > e_{2g} > a_{1g}$. They suggest that the photoelectron spectrum [161, 201] has been incorrectly assigned, since the calculated ordering is in agreement with visible optical absorption spectral data [202, 203], which give the ordering $(e_{1g})^* > (e_{2g})^4 > (a_{1g})^2$, that is, the ionisation energy sequence $e_{2g} > a_{1g}$.

A recent ab initio calculation for ferrocene and the ferricinium cation [199] was found to agree with that of Veillard et al. The results obtained are applied to prediction of Mössbauer isomer shifts and ionisation energies, the calculated ordering of the latter being $e_{2u} \sim a_{2u} < e_{1u} \sim e_{1g} < a_{1g} < e_{2g}$. The conclusions differ from those of Johnson and Rosch.

The ionisation energies for manganocene have been calculated from the total energy differences between the neutral molecule and relevant $MnCp_2^+$ ions [200]. Good numerical and sequential agreement with experiment was obtained. Again, it is concluded that Koopmans' theorem is not valid, due to considerable electronic redistribution on ionisation. INDO SCF MO calculations for $FeCp_2^+$ also give good agreement with experiment.

A general theoretical interpretation of ground and excited state properties of the metallocenes has been attempted [204]. The CNDO MO formalism is used for first row metallocenes, and the multi-electron configuration interaction method [205] applied to the calculation of ionisation energies and absorption spectra. Agreement with experiment is satisfactory.

Results giving some calculated energy levels for ferrocene are summarised in table 3.5.

Table 3.5 Calculated energy level sequences for ferrocene

Author:	Veillard [39]		Botrel [197]	Bagus [199]	Johnson [198]
Method:	LCAO SCFMO ΔSCF (ab initio)		EHMO	ab initio	Xα
		e_{1g}^*			e_{1g}^*
Highest	$a_{1g}(d)$	$e_{2g}(d)$	a_{1g}	e_{2g}	a_{1g}
Occupied	$e_{2g}(\sigma Cp)$	$a_{1g}(d)$	e_{2g}	a_{1g}	e_{2g}
level	$a_{2u}(\pi Cp)$	$e_{1u}(\pi Cp)$	e_{1u}	e_{1g}	e_{1u}
	$e_{2u}(\sigma Cp)$	$e_{1g}(\pi Cp)$	e_{1g}	e_{1u}	e_{1g}
	$e_{2g}(d)$		a_{2u}	a_{2u}	
	$e_{1g}(\pi Cp)$			e_{2u}	
	$e_{1u}(\pi Cp)$				

3.10 ELECTRONIC GROUND STATES FOR THE METALLOCENE SERIES

The general outer molecular orbital sequence for the neutral metallocenes, vanadium to nickel, is found to be $e_{1g}^{*} > a_{1g} \gtrsim e_{2g}$, although the relative ordering of a_{1g} and e_{2g} is not certain. The electronic ground state of each complex will now be discussed. Table 3.6 gives a summary of the most probable ground state configuration in each case, together with magnetic data, determined from magnetic susceptibility measurements. Electron spin resonance (e.s.r.) data are also available. Other evidence for the electronic configuration of ground states is from measurement of absorption spectra. On the whole, the ground states are well characterised, and the most likely ground state configurations for the gas phase are given.

Table 3.6 Ground state electronic configurations

complex	g.s. configuration	unpaired spins	μ_{so}	μ(expected)	μ(experimental)
Cp_2V	$(a_1)^1(e_2)^2$	3	3.87	~3.87	3.84±0.04
					3.20±0.16
Cp_2Cr	$(a_1)^1(e_2)^3$	2	2.83	>2.83	3.10
					3.27
	$(a_1)^2(e_2)^2$	2	2.83	2.83	2.80±0.17
Cp_2Mn	$(a_1)^1(e_2)^2(e_1)^2$	5	5.92	5.92	7.18 [169]
Cp_2Fe	$(a_1)^2(e_2)^4$	0	0	0	0
Cp_2Co	$(a_1)^2(e_2)^4(e_1)^1$	1	1.73	~1.73	1.76±0.07
Cp_2Ni	$(a_1)^2(e_2)^4(e_1)^2$	2	2.83	~2.83	2.86±0.11

μ = magnetic moment
BM = Bohr magneton
so = spin only

(i) Vanadocene, d^3

For vanadocene, the $^4A_{2g}$ ground state $(e_{2g})^2(a_{1g})^1(e_{1g})^0$ is indicated by the value of the magnetic moment [206]. This is in agreement with calculation [194, 195] and experiment [207, 208]. The e.s.r. spectrum of vanadocene confirms the presence of three unpaired electrons [209].

(ii) Chromocene, d^4

There is still controversy over the ground state electronic configuration of chromocene. Calculations have predicted both the $^3A_{2g}$ ground state $(a_{1g})^2(e_{2g})^2$ [204], and the $^3E_{2g}$ ground state [210]. Engelmann [211] reported a magnetic moment of 3.20 ± 0.16 BM between 90 and 295°K, and a solution measurement by n.m.r. gave a value of 3.10 BM [212]. These results, together with those of Gordon and Warren [213] give support to the assumption of a $^3E_{2g}$ ground state $(a_{1g})^1(e_{2g})^3$, with orbital contribution to the magnetic moment. Anderson and Drago interpreted their n.m.r. data in terms of a $^3E_{2g}$ ground state [214]. However the experimental value of 2.80 ± 0.17 BM found between 88 and 293°K suggests a $^3A_{2g}$ ground state [215]. There is no e.s.r. signal for the d^4 chromocene system which suggests it possesses an orbitally degenerate ground state. Photoelectron spectroscopic data have so far failed to settle the question of a ground state [216].

(iii) Manganocene, d^5

There is also a great deal of controversy over the ground state configuration of manganocene. There are three possibilities:

$^6A_{1g}$ $(a_{1g})^1(e_{2g})^2(e_{1g})^2$

$^2E_{2g}$ $(a_{1g})^2(e_{2g})^3$

$^2A_{1g}$ $(a_{1g})^1(e_{2g})^4$

INDO SCF MO calculations by Clack [200] predict the high spin $^6A_{1g}$ ground state in agreement with the photoelectron spectroscopic assignment of Orchard et al [216]. However Armstrong et al [204] predict the $^2E_{2g}$ ground state configuration, in agreement with the interpretation of Rabalais [201] of the photoelectron spectrum.

Early e.s.r. [217] and magnetic moment [169] measurements were interpreted in terms of a high spin $^6A_{1g}$ ground state, but more recent measurements [218, 219] have suggested that $MnCp_2$ must lie very close in energy to the high spin - low spin crossover point, and can be induced to exhibit either ground state, depending on the molecular environment. Current evidence, then, suggests that manganocene should exhibit high spin behaviour in solution [219, 220] and electronic spectra are examined and discussed on this assumption [221].

$MnCp_2$ and its derivative, 1,1'-dimethylmanganocene ($Mn(MeCp)_2$), show complex temperature dependent magnetic susceptibility; the first satisfactory study dates from 1956 [169] and showed that in ether or benzene solutions at room temperature, $MnCp_2$ gave a magnetic moment of ~ 5.8 BM corresponding closely to the spin only value of 5.92 BM, that is to a $^6A_{1g}$ ground state. Solid manganocene shows two crystalline forms, an amber brown rhombic form, stable up to a transition temperature of 432°K and a pink monoclinic form,

stable up to the melting point of 445°K. For the solid above 432°K, and the melt below 445°K, Wilkinson et al [169] found the spin only magnetic moment, but below the transition temperature, the effective moment decreased rapidly with temperature to a value of 2.49 BM at 77°K. However, in solid solutions in $MgCp_2$, (8% $MnCp_2$), the spin only value was again observed, and it was concluded that manganocene possesses the high spin $^6A_{1g}$ ground state configuration. The anomalous behaviour of the solid was attributed to antiferromagnetism.

The magnetic properties of 1,1'-dimethylmanganocene have been investigated [169]; the spin only magnetic moment value was found for solutions, but similar behaviour to that of manganocene was observed for the solid. The measurement of the magnetic moment of $Mn(MeCp)_2$ in toluene [218] by n.m.r. methods showed evidence for the existence of a thermal equilibrium of the two spin isomers, $^6A_{1g}$ and $^2E_{2g}$. On this basis, the observed temperature dependence of the magnetic moment could be reproduced on the assumption that the low spin $^2E_{2g}$ state lay lower in energy, with the higher $^6A_{1g}$ level being thermally populated with increasing temperature.

A recent X-ray diffraction study of manganocene has shown this system to consist of a polymeric chain structure, with no discreet sandwich molecules [175]. Thus a $^2E_{2g}$ - $^6A_{1g}$ equilibrium is not applicable for the brown solid form of $MnCp_2$; this structure might well show approximate low spin behaviour. The molecular structures of high spin ($^6A_{1g}$) and low spin ($^2E_{2g}$) $Mn(MeCp)_2$ have been determined by electron diffraction [178].

Combined evidence from magnetic and e.s.r. data shows manganocene to possess the high spin $^6A_{1g}$ ground state in various organic solvents or in solid solution in $MgCp_2$. It is generally true that ferromagnetic and antiferromagnetic interactions are decreased when the magnetic species are separated from one another physically - thus when the magnetic behaviour of a solid shows the effects of interionic coupling, such as the case for $MnCp_2$, solutions of the same substance will be free of such interactions. The energy difference between the two states $^6A_{1g}$ and $^2E_{2g}$ in manganocene is probably small, and the process of dissolution in various solvents or in a host system favouring large metal-ring distance, is sufficient to produce a high-spin ground level (solid solution of $MnCp_2$ in $FeCp_2$ shows a low spin $^2E_{2g}$ ground state). Manganocene might be expected to exhibit high spin behaviour in the vapour phase.

(iv) Ferrocene, d^6

This is the only 'closed-shell' neutral metallocene of the first transition series, having a singlet $^1A_{1g}$ ground state arising from the electronic configuration $(e_{2g})^4(a_{1g})^2$.

(v) Cobaltocene, d^7

For this system, either a quartet or doublet ground state configuration is theoretically possible; early magnetic susceptibility measurements [211, 222] showed values for the magnetic moment corresponding to one unpaired spin,

thus confirming the $^2E_{1g}$ ground state. More recent magnetic susceptibility data [223a, b] suggest that the effective moment is rather less than the spin only value first reported, but this does not invalidate the conclusion concerning the ground state which is also in accordance with e.s.r. evidence. Cobaltocene shows considerable distortions from pseudo-axial symmetry due to its degenerate ground state [224]. The magnetic moment obtained by Engelmann [211] is supported by n.m.r. solution methods which also gave the spin only value.

(vi) Nickelocene, d^8

The electronic configuration $(e_{2g})^4 (a_{1g})^2 (e_{1g})^2$ corresponds to a $^3A_{2g}$ ground state, for which there is evidence both from experimental magnetic susceptibility data [225] and from calculation [204]. Of the first row transition series metallocenes, this is the most stable next to ferrocene, and thus has been extensively studied. For d^8 systems with D_{5d} symmetry a $^3A_{2g}$ ground state is to be expected. The magnetic moment for nickelocene is essentially temperature independent above $\sim 70^\circ K$ and corresponds closely to the spin only value for two unpaired spins [222, 225]. Nickelocene signals for e.s.r. have not been observed.

3.11 PHOTOELECTRON SPECTRA OF OPEN SHELL MOLECULES

The UV PE spectra of open shell molecules such as most of the metallocenes, are more complex than those for closed shell molecules since each electronic subshell, filled or partly filled, will, in general, give rise to more than one state of the molecular ion. The problem of identification of the states visible in the PE spectrum will

then arise; this has been investigated by Cox [41-43] and the following rules formulated:

(a) If a closed shell is ionised, all states arising from the coupling of the positive hole with the ground term will be realised, the relative cross sections for production of these states being in proportion to their spin-orbital degeneracies.

(b) If a unique open shell is ionised, the relative probabilities of producing different ion states will reflect the squares of the fractional parentage coefficients which may, but in general will not, be proportional to the spin orbital degeneracies.

(c) If there is more than one open shell, it is necessary also to take into account the pre-determined coupling that exists between the different open shells. This involves Racah coefficients as additional proportionality factors in the expressions for the ionisation cross sections.

(d) If orbitals belonging to different subshells are assumed to have the same one electron cross sections, the integrated cross section of a particular subshell is simply proportional to the occupancy of that subshell in the molecule.

However, the most serious approximation on which these rules are based, is the neglect of configuration interaction, which may upset theoretical considerations even in the simplest cases.

Selection rules formulated by Cox [41-43] state

that:

(a) the intensity of the ionised state is zero unless the total spin changes by $\pm \frac{1}{2}$

(b) the direct product of the orbital representations of the final and initial states must contain the orbital representation of the ionised shell.

The states arising for any particular ionisation from a given ground state are readily determined by group theory, however the relative intensity of the resulting bands will not depend on orbital occupation in the neutral species, but, as shown by Cox [41-43], on the nature of the ground state and the coefficients of fractional parentage connecting the ionised states. The molecular ion states that are accessible on photoionisation, given the ground states in table 3.6, are shown in table 3.7 [216] and the relative probabilities for the production of these states are also given [41]. From the above listed rules, the relative areas under bands in the photoelectron spectra should bear some relation to the predicted relative probabilities for the production of particular ion states, provided that the levels are separated well enough in energy to be resolved.

3.12 CRYSTAL FIELD APPROACH

The d orbital energies of ferrocene are found to have the ordering $a_{1g} > e_{2g}$ from some MO calculations, whereas other calculations give the ordering $e_{2g} > a_{1g}$ in agreement with conclusions from photoelectron spectroscopy [161] which is not the ordering expected from crystal field or ligand field considerations, since the d_{z^2} (a_{1g}) orbital is more strongly directed towards the ligands.

Crystal field theory should permit a direct analysis of the relative energies of the various states of the molecular

Table 3.7 Ion states produced on ionisation of the metallocenes (and their relative probabilities)

metallocene	ground state	orbital ionisation	ion configuration	ion states produced
Cp_2V	$^4A_{2g}\ (a_{1g})^1(e_{2g})^2$	a_{1g}	$(e_{2g})^2$	$^3A_{2g}\ (k_{a1})^a$
		e_{2g}	$(a_{1g})^1(e_{2g})^1$	$^3E_{2g}\ (2)$
Cp_2Cr	$^3A_{2g}\ (a_{1g})^2(e_{2g})^2$	a_{1g}	$(a_{1g})^1(e_{2g})^2$	$^4A_{2g}\ (\frac{4}{3}k_{a1}) + {}^2A_{2g}\ (\frac{2}{3}k_{a1})$
		e_{2g}	$(a_{1g})^2(e_{2g})^1$	$^2E_{2g}\ (2)$
or	$^3E_{2g}\ (a_{1g})^1(e_{2g})^3$	a_{1g}	$(e_{2g})^3$	$^2E_{2g}\ (k_{a1})$
		e_{2g}	$(a_{1g})^1(e_{2g})^2$	$^4A_{2g}\ (\frac{4}{3}) + {}^2A_{2g}\ (\frac{1}{6}) + {}^2A_{1g}\ (\frac{1}{2}) + {}^2E_{1g}\ (1)$
Cp_2Mn	$^6A_{1g}\ (a_{1g})^1(e_{2g})^2(e_{1g})^2$	a_{1g}	$(e_{2g})^2(e_{1g})^2$	$^5A_{1g}\ (k_{a1})$
		e_{2g}	$(a_{1g})^1(e_{2g})^1(e_{1g})^2$	$^5E_{2g}\ (2)$
		e_{1g}	$(a_{1g})^1(e_{2g})^2(e_{1g})^1$	$^5E_{1g}\ (2k_{e1})$
	$^2E_{2g}\ (a_{1g})^2(e_{2g})^3$	a_{1g}	$(a_{1g})^1(e_{2g})^3$	$^3E_{2g}\ (\frac{3}{2}k_{a1}) + {}^1E_{2g}\ (\frac{1}{2}k_{a1})$
		e_{2g}	$(a_{1g})^2(e_{2g})^2$	$^1E_{1g}\ (1) + {}^1A_{1g}\ (\frac{1}{2}) + {}^3A_{2g}\ (\frac{3}{2})$

Table 3.7 (continued)

metallocene	ground state	orbital ionisation	ion configuration	ion states produced
Cp_2Mn cont.	$^2A_{1g}\ (a_{1g})^1(e_{2g})^4$	a_{1g}	$(e_{2g})^4$	$^1A_{1g}\ (k_{a1})$
		e_{2g}	$(a_{1g})^1(e_{2g})^3$	$^3E_{2g}\ (3) + {}^1E_{2g}\ (1)$
Cp_2Fe	$^1A_{1g}\ (a_{1g})^2(e_{2g})^4$	a_{1g}	$(e_{2g})^4$	$^2A_{1g}\ (k_{a1})$
		e_{2g}	$(a_{1g})^2(e_{2g})^3$	$^2E_{2g}\ (4)$
Cp_2Co	$^2E_{1g}\ (a_{1g})^2(e_{2g})^4(e_{1g})^1$	a_{1g}	$(a_{1g})^1(e_{2g})^4(e_{1g})^1$	$^3E_{1g}\ (\frac{3}{2}k_{a1}) + {}^1E_{1g}\ (\frac{1}{2}k_{a1})$
		e_{2g}	$(a_{1g})^2(e_{2g})^3(e_{1g})^1$	$^3E_{1g}\ (\frac{3}{2}) + {}^1E_{1g}\ (\frac{1}{2}) + {}^3E_{2g}\ (\frac{3}{2}) + {}^1E_{2g}\ (\frac{1}{2})$
		e_{1g}	$(a_{1g})^2(e_{2g})^4$	$^1A_{1g}\ (k_{e1})$
Cp_2Ni	$^3A_{2g}\ (a_{1g})^2(e_{2g})^4(e_{1g})^2$	a_{1g}	$(a_{1g})^1(e_{2g})^4(e_{1g})^2$	$^4A_{2g}\ (\frac{4}{3}k_{a1}) + {}^2A_{2g}\ (\frac{2}{3}k_{a1})$
		e_{2g}	$(a_{1g})^2(e_{2g})^3(e_{1g})^2$	$^4E_{2g}\ (\frac{8}{3}) + {}^2E_{2g}\ (\frac{4}{3})$
		e_{1g}	$(a_{1g})^2(e_{2g})^4(e_{1g})^1$	$^2E_{1g}\ (2k_{e1})$

a) Relative probabilities are given in brackets.
k_{a1} and k_{e1} are ionisation cross sections for the a_{1g}(d) MO and one e_{1g}(d) MO respectively, relative to either of the e_{2g}(d) MOs.

ion; these parameters are directly given by the photoelectron spectrum.

For the molecular ion, $FeCp_2^+$, the energy separation of the e_{2g} and a_{1g} levels is defined as $\Delta(e_2, a_1)$. The molecular orbital energy level diagram for the iron d orbitals (as verified by photoelectron spectroscopy) is shown in figure 3.9. Evaluating electron repulsion energies for

Figure 3.9 Energy level scheme for the metal d orbitals in ferrocene as found by UV PES

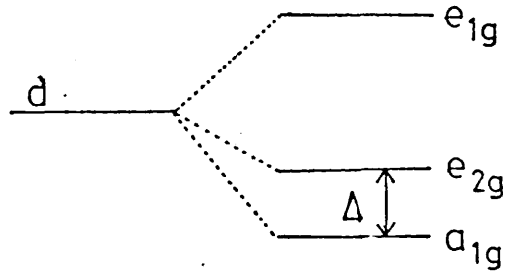

the two states $^2A(e_2^4\ a_1^1)$ and $^2E_2(e_2^3\ a_1^2)$, it can be seen that [226], in general (3)2:

$$E(^2A_1)-E(^2E_2) = \Delta(e_2, a_1)+3Je_2e_2 - Ke_2e_2-Ja_1a_1-2Ja_1e_2 + Ka_1e_2 \qquad (3)2$$

where E is the energy of a state and J and K are the usual coulomb and exchange integrals. For pure d orbitals, J and K may be expressed in terms of Racah parameters ((3)3) [226]. In the case of ferrocene, it is known experimentally that $E(^2A_1) - E(^2E_2) = 380$ meV (~ 3000 cm^{-1}), while $20B \simeq 2$eV.

$$E(^2A_1) - E(^2E_2) = 20B + \Delta(e_2, a_1) \qquad (3)3$$

Thus from equation (3)3, $\Delta(e_2,a_1)$ must be negative, which suggests that the predictions of crystal field theory do not agree with some molecular orbital calculations, and the UV PES data [161]. That is, crystal field theory predicts the energy level ordering a_1 (d_{z^2}) > $e_2(d_{x^2-y^2}, d_{xy})$.

Crystal field theory may be used as an aid to interpretation in the case of PE spectra for the open shell metallocenes. The crystal field energy level diagram, with positive Δ_1, Δ_2, is shown in figure 3.10 [216].

Figure 3.10 Crystal field energy level diagram for the d orbitals of the metallocenes

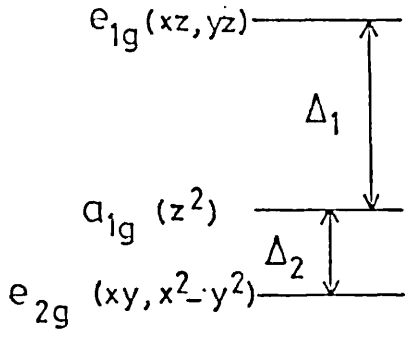

The most likely ground states for the metallocenes were discussed in section 3.10, and the accessible molecular ion states were given in table 3.7 together with the relative probabilities for the production of these states. Orchard's work [216] includes a crystal field analysis of the molecular ion states and the relevent energy expressions obtained in this work are shown in table 3.8. Values for the crystal field parameters A, B, C, Δ_1 and Δ_2 are not available for the molecular ions of the metallocenes, but their likely magnitude may be assessed by studying values found for the neutral complexes from electronic spectra. The relative energies of the molecular ion states in terms of these parameters may be obtained theoretically

Table 3.8 Energies of molecular ion states for the metallocenes

Compound	State and configuration	Energy expression
Cp_2V^+	$^3A_{2g} : (e_{2g})^2$	$A + 4B$
	$^3E_{2g} : (a_{1g})^1(e_{2g})^1$	$A - 8B + \Delta_2$
Cp_2Cr^+	$^4A_{2g} : (a_{1g})^1(e_{2g})^2$	$3A - 12B + \Delta_2$
	$^2A_{2g} : (a_{1g})^1(e_{2g})^2$	$3A + 3C + \Delta_2$
	$^2E_{2g} : (a_{1g})^2(e_{2g})^1$	$3A + 8B + 2\Delta_2$
	$^2A_{1g} : (a_{1g})^1(e_{2g})^2$	$3A - 8B + 5C + \Delta_2$
	$^2E_{1g} : (a_{1g})^1(e_{2g})^2$	$3A - 8B + 3C + \Delta_2$
	$^2E_{2g} : (e_{2g})^3$	$3A + 12B + 4C$
Cp_2Mn^+	$^5E_{1g} : (a_{1g})^1(e_{2g})^2(e_{1g})^1$	$6A - 21B + 2\Delta_2 + \Delta_1$
	$^5E_{2g} : (a_{1g})^1(e_{2g})^1(e_{1g})^2$	$6A - 21B + 3\Delta_2 + 2\Delta_1$
	$^5A_{1g} : (e_{2g})^2(e_{1g})^2$	$6A - 21B + 2\Delta_2 + 2\Delta_1$
	$^3E_{2g} : (a_{1g})^1(e_{2g})^3$	$6A - 8B + 5C + \Delta_2$
	$^1E_{2g} : (a_{1g})^1(e_{2g})^3$	$6A + 7C + \Delta_2$
	$^3A_{2g} : (a_{1g})^2(e_{2g})^2$	$6A - 16B + 5C + 2\Delta_2$
	$^1A_{1g} : (a_{1g})^2(e_{2g})^2$	$6A - 16B + 9C + 2\Delta_2$
	$^1E_{1g} : (a_{1g})^2(e_{2g})^2$	$6A - 16B + 7C + 2\Delta_2$
	$^1A_{1g} : (e_{2g})^4$	$6A + 24B + 8C$
Cp_2Fe^+	$^2E_{2g} : (a_{1g})^2(e_{2g})^3$	$10A - 20B + 10C + 2\Delta_2$
	$^2A_{1g} : (a_{1g})^1(e_{2g})^4$	$10A + 10C + \Delta_2$

Cp_2Co^+	$^1A_{1g} : (a_{1g})^2(e_{2g})^4$	$15A - 20B + 15C + 2\Delta_2$
	$^3E_{1g} : (a_{1g})^2(e_{2g})^3(e_{1g})^1$	$15A - 26B + 12C + 3\Delta_2 + \Delta_1$
	$^1E_{1g} : (a_{1g})^2(e_{2g})^3(e_{1g})^1$	$15A - 14B + 14C + 3\Delta_2 + \Delta_1$
	$^3E_{2g} : (a_{1g})^2(e_{2g})^3(e_{1g})^1$	$15A - 32B + 12C + 3\Delta_2 + \Delta_1$
	$^1E_{2g} : (a_{1g})^2(e_{2g})^3(e_{1g})^1$	$15A - 32B + 14C + 3\Delta_2 + \Delta_1$
	$^3E_{1g} : (a_{1g})^1(e_{2g})^4(e_{1g})^1$	$15A - 13B + 12C + 2\Delta_2 + \Delta_1$
	$^1E_{1g} : (a_{1g})^1(e_{2g})^4(e_{1g})^1$	$15A - 11B + 14C + 2\Delta_2 + \Delta_1$
Cp_2Ni^+	$^2E_{1g} : (a_{1g})^2(e_{2g})^4(e_{1g})^1$	$21A - 31B + 18C + 3\Delta_2 + \Delta_1$
	$^4E_{2g} : (a_{1g})^2(e_{2g})^3(e_{1g})^2$	$21A - 43B + 14C + 4\Delta_2 + 2\Delta_1$
	$^2E_{2g} : (a_{1g})^2(e_{2g})^3(e_{1g})^2$	$21A - 34B + 17C + 4\Delta_2 + 2\Delta_1$
	$^4A_{2g} : (a_{1g})^1(e_{2g})^4(e_{1g})^2$	$21A - 31B + 14C + 3\Delta_2 + 2\Delta_1$
	$^2A_{2g} : (a_{1g})^1(e_{2g})^4(e_{1g})^2$	$21A - 28B + 17C + 3\Delta_2 + 2\Delta_1$

by the strong field approximation; this is discussed by Warren [221] for the metallocenes, in terms of $C_{\infty v}$ molecular symmetry. Some crystal field parameters deduced from electronic spectra are given in figure 3.11.

Figure 3.11 Crystal field parameters deduced from electronic absorption spectra [207]

	Cp_2V	Cp_2Fe	Cp_2Ni
Δ_2(eV)	0.475	0.84, 0.89 [227]	0.50
Δ_1(eV)	1.15	2.80, 2.75	1.85
B (eV)	0.055	0.051, 0.049	0.074

3.13 PHOTOELECTRON SPECTRA

The UV gas phase PE spectra of the metallocenes (M = Cr, Mn, Fe, Ni) were obtained by Rabalais et al [201],

and a more detailed investigation including the vanadium and cobalt derivatives was published by Orchard et al [216]; the same group had previously carried out a detailed UV PES study of some closed shell metallocenes [161]. Similar studies were published for some bis-arene and mixed sandwich complexes [228-231].

The high energy (X-ray) PE spectra of the open shell metallocenes were obtained by Hillier et al [232]. From this study it was concluded that in all cases there is a net electron transfer from the metal to the ligand rings, giving a positive charge of between 0.8 and 1.0 on the metal. A study of some chromium complexes also suggests that this is the case for chromocene [233]. The high energy PE spectra of the metallocenes were also investigated by Jolly et al., and the core binding energies tabulated [234], and molecular core binding energies for the metallocenes (M = Cr, Fe, Co, Ni) were also reported by Clark and Adams [235].

The He^{I} and He^{II} UV PE spectra of the biscyclopentadienyl derivatives of mercury, thallium, tin and lead have been reported [236]. The authors suggest that all systems with centrally bonded rings have a significant degree of π bonding with the exception of purely ionic compounds. Main group elements such as Mg, Be, and Li are assumed to use their vacant p orbitals for π bonding interactions, and the same is considered true for the compounds of In, Tl, Sn and Pb studied by Cradock and Duncan.

3.14 CURRENT RESEARCH

Complexes (I) to (VIIa) were synthesised (figure 3. 2) and the HeI and HeII UV PE spectra were obtained for each complex. Relative intensities and ionisation energies were obtained from each PE spectrum and tabulated. The HeI data were generally in good agreement with previous work.

The aim of this work was to obtain HeII data for this series of first row transition metal complexes for the

following reasons:

(a) to establish a pattern of HeI:HeII relative intensities
(b) to look for a change in the 3d ionisation cross section along the transition series
(c) to examine previous assignments in the light of new data.

3.15 RESULTS

Vertical ionisation energies obtained for the complexes (I) to (VIIa) are given in table 3.9. Table 3.10 gives previously reported values for comparison purposes; agreement with these values is generally good. Table 3.11 (i) - (viii) shows the relative intensities obtained from HeI data by Orchard et al [161, 216] and those from the current study. Relative intensity data from HeII spectra are also shown. Table 3.12 shows data obtained for complex (VIIa), bis-cycloheptadienylruthenium. The HeI PES resolution was 40-60 meV, measured from the nitrogen spectrum. For the metallocene spectra, labelling consistent with that adopted by Orchard et al is used. The PE spectra of complexes (I) to (VIIa) are found at the end of chapter 3.

Table 3.9 Vertical ionisation energy data (eV) for the metallocenes

Region	Cp_2V	Cp_2Cr	Cp_2Mn	$MeCp_2Mn$	Cp_2Fe	Cp_2Ru	Cp_2Co	Cp_2Ni
A'	6.81	5.70 (a)*	6.26 (a')	6.06 (a')	6.86	7.45	5.55 (a)	6.50 (a)
			7.01 (a)	6.68 (a)				
		6.90 (b)		7.10 (b')	7.21	7.68	7.15	
		7.20 (c)		7.47 (c')			7.65 (c)	
		(7.49)(d)					7.99 (d)	
A''	8.35	8.54	8.85 (b)	8.55 (b)	8.77	8.47	8.72 (e)	8.40 (b)
	8.64	(8.78)	10.25 (c)	9.83 (c)		(8.85)		8.81 (c)
	8.78	(9.20)	10.57 (d)	10.29 (d)		9.94		9.08 (d)
	9.00	(9.58)	11.10 (x)	-	9.28	10.29	9.92 (f)	10.23 (e)
B	12.46	(11.78)	12.38	12.21	12.2	(11.61)	12.34	12.46
	12.84	12.25	(13.14)	13.01	13.3	12.43	13.43	13.38
	13.38	12.92				13.52		
		13.20						
C	16.62	16.7	16.82		16.6	17.07	16.98	16.75

* small letters a,b,c,d etc. are band labels (see spectra)
figures in brackets are approximate values for poorly defined bands

Table 3.10 Experimental ionisation data (eV)

	i) VANADOCENE (I)		ii) CHROMOCENE (II)		
	Orchard et al [216]	current	Orchard et al [216]	Rabalais et al [201]	current
A'	6.78	6.81	5.71	5.69	5.70
			7.04	7.02	6.90
			7.30	7.3	7.20
			(7.58)	~ 7.4-7.9	7.49
A''	8.40	8.35	8.55		8.54
	8.65	8.64	(8.87)	~ 9.0	(8.78)
	8.79	8.78	(9.25)		(9.20)
	9.02	9.00	(9.57)		(9.58)
B	(11.85)		(11.89)		(11.78)
	12.37	12.46	12.25		12.25
	12.62	12.84	(12.82)		12.92
	13.35	13.38	13.44		13.2
C	16.8	16.62	16.8		16.7

Table 3.10 cont.

v) FERROCENE (IV)

	Orchard et al [161]	Rabalais et al [201]	current
A'	6.88	6.86	6.86
	7.23	7.23	7.21
A''	8.72	8.72	8.77
	(8.87)		
	9.14		
	9.39	9.38	9.29
B	12.30	12.2	12.2
	13.00		13.3
	13.46	13.6	
C	16.5	16.4	16.6

vi) RUTHENOCENE (VII)

	Orchard et al [161]	current
A'	7.45	7.45
	(7.63)	7.68
A''	8.51	8.47
	(8.80)	(8.85)
	9.93	9.94
	(10.23)	10.29
B	(11.8)	11.97
	12.3	12.43
	13.4	13.52
C	16.8	17.1

Table 3.10 cont.

iii) MANGANOCENE (III)

	Orchard et al [216]	Rabalais et al [201]	current
A'	6.26 (a')		(6.26)
	6.91 (a)	(6.70	7.01
		(6.85	
		(7.10	
A''	8.76 (b)		8.85
	10.10 (c)	7.9-9.3	10.25
	10.51 (d)		10.57
	(x)		11.10
B	12.37		12.38
	13.18		13.14
C	16.71		16.82

iv) DIMETHYLMANGANOCENE (IIIa)

Orchard et al [216]	current
6.01 (a')	6.06
6.58 (a)	6.68
7.15 (b')	7.10
(7.36)(c')	(7.47)
8.42 (b)	8.55
9.90 (c)	9.88
10.23 (d)	10.29
12.47	12.21
13.09	13.01

Table 3.10 cont.

vii) COBALTOCENE (V)

	Orchard et al [216]	current
A'	5.56 (a)	5.55
	7.18 (b)	7.15
	7.63 (c)	7.65
	8.01 (d)	7.99
A''	8.66 (e)	8.72
	(8.94)	
	(9.31)	
	9.88 (f)	9.95
B	12.24	12.34
	13.99	13.43
C	15.57	16.98

viii) NICKELOCENE (VI)

	Orchard et al [216]	Rabalais et al [201]	current
A'	6.51	6.40	6.50
A''	8.43	6 bands,	8.40
	8.78	8.2-10.9	8.81
	9.22		9.08
	10.33		10.23
B	12.25	12.4	12.46
	(12.84)		
	13.27	13.6	13.38
C	16.59	17.2	16.8

Table 3.11 Relative intensity data for the metallocenes

Results obtained previously by Orchard et al [161, 216] are given in brackets.

i) VANADOCENE (I)

Band:	A'	A"	B	C	D
HeI	1.0	4.1	14.7	4.9	
	(1.0)	(4.2)			
HeII	1.0	2.7	7.5	3.5	1.2

ii) CHROMOCENE (II)

Band:	a	(b+c+d)	A"
HeI	0.152	0.233	1.00
	(0.154)	(0.205)	(1.00)
HeII	0.17	0.24	1.00

iii) MANGANOCENE (III)

Band:	a' + a	b	c	d	B	C
HeI	0.25	1.00	0.08	0.20	7.8	1.7
	(0.20)	(1.00)	(0.06)	(0.18)		
HeII	0.57	1.00	0.16	0.36	5.8	2.3

iv) DIMETHYLMANGANOCENE (IIIa)

Band:	a' + a + b' + c'	b	c + d	B
HeI	0.27	1.00	0.54	5.9
HeII	0.8	1.00	0.9	4.8

v) FERROCENE (IV)

Band:	A'	A"	B	C	D
HeI	1.0	2.1	11.4	5.7	
	(1.0)	(2.1)	(11.1)	(2.4)	
HeII	1.0	1.2	3.6	1.7	0.9

Table 3.11 cont.

vi) RUTHENOCENE (VII)

Band:	A'	A''	B	C	D
HeI	1.1	1.0, 0.8	7.3	2.1	
	2.3	2.0, 1.5	15.2	4.3	
	(2.3)	(2.0, 1.2)			
HeII	2.0	1.0, 1.2	3.6	2.4	

vii) COBALTOCENE (V)

Band:	a	b + c + d	e + f	B	C
HeI	0.08	0.38	1.00	5.6	1.8
	(0.08)	(0.35)	(1.00)		
HeII	0.24	0.74	1.00	3.0	

HeI:- b : c : d - 0.24 : 0.08 : 0.08
(0.22):(0.06):(0.06)

viii) NICKELOCENE (VI)

Band:	a	b + c + d + e	B	C
HeI	0.15	1.00	4.5	1.00
	(0.14)	(1.00)		
HeII	0.3	1.00	1.9	0.9

Table 3.12 Experimental ionisation energy data and relative intensity data for biscyclopentadienylruthenium (VIIa)

IONISATION ENERGY (eV)		RELATIVE INTENSITY	
		HeI	HeII
7.07	(a))	1.5	1.1
7.53	(b))		
8.16	(c)	1.0	1.0
9.15	(d))	0.8	0.35
9.55	(e))		
(10.50))			
11.10)		7.9	3.2
12.00)			
13.13)			
14.07		3.0	3.5
16.08		0.5	0.9

3.16 DISCUSSION

The HeI PE spectra of the metallocenes have been discussed fully by Orchard [161, 216] and Rabalais [201], as mentioned in section 3.13. Labels adopted by Orchard et al for the photoelectron bands will be used throughout the following discussion. The labelling is generally based on the HeI PE band assignment for ferrocene [161]; region A' represents ionisation from essentially metal d orbitals, and A'', ionisation from the mainly ligand π orbitals, (that is, the e_{1u} and e_{1g} MOs). Region B is correlated with ionisation from higher energy ligand π orbitals and region C, with ionisation from ligand σ orbitals. For the open shell metallocenes, regions A' and A'' are not so clearly divisible into regions corresponding to mainly d or mainly ligand ionisations, and in many cases the bands in these areas have been separately labelled.

The HeII PE spectra are subdivided in a similar manner. In many cases the bands are not so clearly resolved as in the HeI spectra, and the relative intensities are quite different from those seen in the HeI spectra. In particular, the bands associated with ionisation from metal orbitals of essentially d character are considerably enhanced in the HeII spectra relative to the bands associated with ligand π ionisation. This effect has been noted in previous studies [29, 229].

Region B of the HeII spectra, therefore, is generally much reduced in intensity, relative to the metal 'd' bands, while the intensity of region C is less dramatically reduced, possibly due to the orbitals involved in ionisation having greater s character; s orbitals are known to have a higher cross section for ionisation by HeII photons [8].

An additional band, D, is observed in the HeII spectra, and is probably due to further ligand ionisation. Since the HeII photons are not filtered from the HeI photons, further HeII PE bands toward lower kinetic energies may be observed that are not completely masked by ionisations due to HeI photons. The sensitivity of UV PES using HeI photons is about one order of magnitude higher than for HeII photons, and thus the HeII spectrum in the HeI region is negligible compared to the HeI spectrum, and will not interfere with calculated relative intensities.

Although, strictly speaking, Koopmans' theorem cannot be assumed in consideration of open shell ionisations, Orchard [216] makes use of the approximation on the grounds that deviations should be reasonably systematic within a series of electronically similar isostructural molecules, such as the metallocenes. Thus valid conclusions may be reached concerning orbital energy trends; however the individual PE spectra must be assigned in terms of states of the molecular ions, using the rules formulated by Cox [41-43].

Ionisation cross section scale factors, k_{a1} and k_{π} as defined by Orchard [161] were calculated from both HeI and HeII relative intensity data. The factor k_{a1} is defined as the one-electron ionisation cross section of the a_{1g} (d) orbital relative to that of the e_{2g} (d) orbital, and is found to differ with varying photon energy, as is the analogous factor, k_{π}, the 'average' of the e_{1u} (π) and e_{1g} (π) ligand MO cross sections, relative to the e_{2g} (d) cross section. The symbols k_{a1}II and k_{π}II will be used to refer to those factors calculated from HeII data. Allowances for differences in cross section between the a_{1g}, e_{1g} and e_{2g} 'd' orbitals due to different amounts of ligand-metal mixing should be made; one would expect relative

HeI cross sections to be in the order $e_{1g} > e_{2g} > a_{1g}$.

Throughout the following discussion, in assignment of PE bands to ionisation from specific orbitals, an attempt is made to correlate the relative intensities of the bands with occupancy and degeneracy of the orbitals from which ionisation has occurred, (with the aid of rules stated in section 3.11 [41-43]) and thus to verify previous assignments using HeII data, or, in the cases where assignment was undecided, to decide between alternative assignments.

The magnitudes of photoionisation cross sections are not well understood and substantial variations in ionisation cross section have been found for the same ionisation with photon sources of different energy [14, 237]. The spectra are discussed in turn.

(i) Ferrocene (IV)

The PE spectrum of ferrocene is, as expected, less complex than spectra of the open shell metallocenes, since each ionisation leads to only one molecular ion state. The PE spectra of ferrocene, ruthenocene, and osmocene were previously studied in detail by Orchard et al [161].

Figure 3.12 shows the PE spectra of ferrocene and biscyclopentadienylmagnesium obtained by Orchard et al [161]. The bands observed for ferrocene were divided into regions A', A'', B and C, as shown; the PE spectrum of the magnesium complex is included for comparison, since obviously, for this complex, there are no bands due to essentially d ionisations, and thus such bands in ferrocene may be clearly distinguished.

Figure 3.12 Photoelectron spectra of ferrocene (a) and biscyclopentadienylmagnesium (b)

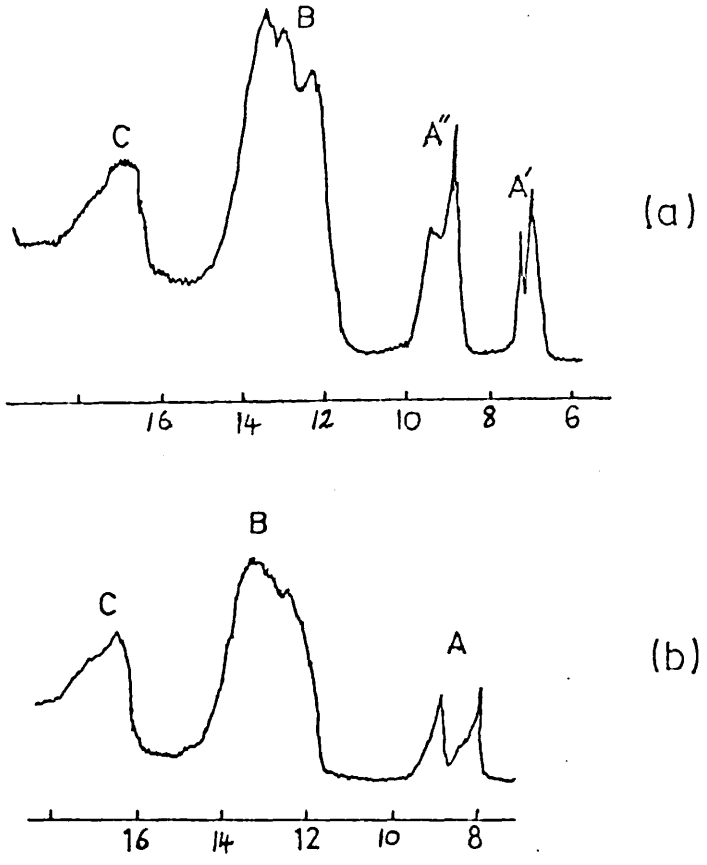

Region A' was assigned [161] to d orbital ionisation from the e_{2g} and a_{1g} molecular orbitals. Since the relative intensity of bands in the spectrum should be in proportion to the degeneracies of the orbitals, the relative intensities of the bands due to ionisation from the e_{2g} and a_{1g} levels in ferrocene should be in the ratio 2:1, according to simple theory. The first two bands in the spectrum were assigned accordingly by Orchard et al who observed a relative intensity ratio of 5:2 for the two bands in region A'; the band at lowest ionisation energy being due to ionisation from e_{2g} (d) levels, and the next band, to ionisation from the a_{1g} d orbital. This assignment was in agreement with some of

the more recent MO calculations (section 3.9) and also with the assignment of Rabalais et al.

Band A" was assigned to ionisation from mainly ligand π orbitals; that is, the e_{1u} and e_{1g} MOs. The e_{1u} level, thought to be rather non-bonding in character, weakly mixing with metal p_x and p_y orbitals, was identified with the sharper peak to lower ionisation energy, of band A". Ionisation from the e_{1g} level, which is expected to be strongly mixed with the metal d_{xz}, d_{yz} levels, is represented by the higher IE band of A". However the opposite assignment, $e_{1g} > e_{1u}$, is preferred by Rabalais et al [201].

Region B was associated with ionisation from lower energy ligand π orbitals, while band C was assigned to ionisation from ligand σ orbitals.

The assignment of Orchard et al [161], is confirmed by the current study. A relative intensity ratio of 5:2 was found for the two bands in region A', in agreement with previous work [161], giving a value for k_{a1} of 0.8. It was noted by Orchard et al [216], that intensity ratios of bands due to ligand + metal ionisations were in less good agreement with ratios expected from simple degeneracy considerations than the essentially d ionisation intensity ratios. It was suggested that the ligand ionisation cross sections were greater than metal d cross sections by about 60% (for a HeI photon source).

The first two bands of the HeII PE spectrum of ferrocene, gave a value for k_{a1}II of 1.2, that is, assuming the same assignment

as Orchard, the a_{1g} d orbital is found to have a relatively high cross section for ionisation by HeII photons, higher than that for the e_{2g} d orbital. The HeII value for k_πII is surprising. The HeI value for k_π is found to be 1.47, in excellent agreement with that reported by Orchard et al [161], but k_πII = 0.98, indicating that the metal d and ligand π orbitals have almost equal cross sections for HeII ionisation.

Since k_{a_1}II = 1.2 and k_π II = 0.98, an intensity ratio for A':A" close to that predicted by simple degeneracy considerations is expected, that is, A"/A' = 8/6 = 1.33. The experimental value from the HeII data is 7.2/6 = 1.2 which is slightly low, probably due to the fact that the a_{1g} d ionisation cross section is slightly greater than that for an e_{2g} d orbital.

This result indicated that HeII relative intensity data might be useful for assignment purposes since the relative ionisation cross sections may not vary substantially through a series of spectra obtained using one photon energy.

From the HeII PE spectrum of ferrocene, it appears that the second band in region A" (due to ionisation from the cyclopentadienyl e_{1g} π orbital thought to be a metal-ligand bonding orbital) is more intense, relative to the e_{1u} π Cp band, than in the HeI spectrum; this suggests that the e_{1g} band indeed has some metal d character.

The series of twelve vibrational bands claimed by Rabalais [201] for the lowest ionisation

energy band of ferrocene were not observed despite fairly good resolution.

The spacing of the $^2E_{2g}$ and $^2A_{1g}$ levels of the molecular ion, $FeCp_2^+$ is found experimentally to be 0.35 eV, from the PE spectrum. Theoretically, the energy difference expressed in terms of Racah and crystal field parameters Δ_1, Δ_2, defined in section 3.12, is $20B - \Delta_2$, and the opposite ordering of levels is predicted to that found from the PE spectrum. Using the experimental data of Prins and van Voorst [207] or Sohn et al [227], values of + 0.18 eV and + 0.09 eV for $20B-\Delta_2$ are calculated; these values are not in agreement with those found from the PES data.

(ii) Vanadocene (I)

For this complex, only a single band was observed by Orchard [216] in the A' region, although the $(a_{1g})^1 (e_{2g})^2$ ground state configuration would be expected to give rise to $^3A_{2g}$ and $^3E_{2g}$ levels in the molecular ion. Crystal field treatment [221] shows that the $^3A_{2g} - {}^3E_{2g}$ energy separation is $12B-\Delta_2$ ($\simeq$ 0.2 eV). Orchard [216] assigns the single band to both d ionisations. The remaining bands are similar to those of ferrocene but A" should be rather more diffuse, owing to the larger number of ion states that may be produced.

The current PE data are in good agreement with those of Orchard et al, as are the relative intensity data for A':A". The relative intensities for regions A' and A"

from the HeII spectrum of vanadocene are A':A" = 1.0:2.7 or 3.0:8.1, which are exactly those expected for the ionisation of three d and eight π electrons, if, as has been shown for ferrocene, the ionisation cross sections for the d and π orbitals are approximately equal, and if, as has been assumed by Orchard et al [216], both the e_2 and a_1 metal d ionisations give rise to the first band in the PE spectrum and are not resolved separately.

Thus the assignment adopted by Orchard [216] is confirmed, and A' is due to ionisation from the d a_{1g} and e_{2g} orbitals giving rise to the $^3A_{2g}$ and $^3E_{2g}$ molecular ion states. These are too close in energy for resolution, using the current instrumentation. Further confirmation is given by the considerable increase in intensity of A' relative to A" in the HeII spectrum. The assumption of a 1:1 3d:2p ratio for ionisation cross section, therefore, appears to hold for ferrocene and vanadocene. For these two cases, the relative energies of the various ion states calculated by crystal field theory and data from electronic spectra, appear to bear little relation to those observed experimentally by UV PES.

(iii) Chromocene (II)

The ground state is still uncertain in this case. The UV PE spectrum has been examined by Orchard [216] and by Rabalais [201]. Rabalais suggests that the $^3E_{2g}$ ground state, that is $(a_{1g})^1 (e_{2g})^3$, provides the best interpretation of the observed bands, giving rise to five ionic states. The sharp peak at

5.69 eV is assigned to the $^2E_{2g}$ ion state and the three peaks at around 7 eV to ionisation to the states $^4A_{2g}$, $^2E_{1g}$, $^2A_{2g}$ and $^2A_{1g}$ as follows: (7.02 eV) $^4A_{2g}$, (7.3 eV) $^2E_{1g}$, (7.4-7.9 eV) $^2A_{1g}$, $^2A_{2g}$. The predicted relative intensities $^2E_{2g}$: $^4A_{1g}$:$^2E_{1g}$:$^2A_{2g}$:$^2A_{1g}$ are 1:$\frac{1}{3}$:1: $\frac{1}{6}$: $\frac{1}{2}$. Rabalais claims that good agreement is found, except in the case of the $^2E_{2g}$ band, which is of unexpectedly high intensity; this is suggested to be due to the variation in cross section for the a_{1g} and e_{2g} orbitals. In this same region of the PE spectrum (A'), Orchard et al [216] observe at least four distinct ionisation processes; bands corresponding to these are labelled a, b, c and d. On these grounds, the possibility of a $^1A_{1g}$ ground state, that is $(e_{2g})^4$, is discarded by both sets of authors, since this would give rise to only one molecular ion state on ionisation of the outer electrons. The possibility of a $^3A_{2g}$, $(a_{1g})^2(e_{2g})^2$, ground state is also rejected by Rabalais [201], since this would lead to only three ion states, however, although Orchard is in favour of the $^3E_{2g}$ ground state, in agreement with Rabalais, there is still a possibility, on energetic grounds, of a $^3A_{2g}$ ground state.

Ionisation energies and relative intensities for the current HeI PE spectrum of chromocene were in good agreement with those previously observed [201, 216]. Of the four bands in region A', if band d was attributed to impurity, or to a shake-up process, the assignment possibilities on energetic grounds, assuming the $^3A_{2g}$ ground state would be as follows:

$a(^4A_{2g})$; b, c$(^2E_{2g})$, $(^2A_{2g})$ (3)4

$a(^2E_{2g})$; b$(^4A_{2g})$; c$(^2A_{2g})$ (3)5

The predicted relative intensities are:

$$(\tfrac{4}{3}\,k_{a1})\ {}^4A_{2g} : (\tfrac{2}{3}\,k_{a1})\ {}^2A_{2g} : (2)\ {}^2E_{2g}$$

Taking the values of k_{a1} found for ferrocene, the predicted HeI relative intensities are ($k_{a1} = 0.8$):- 1.1($^4A_{2g}$) : 0.53 ($^2A_{2g}$) : 2.0 ($^2E_{2g}$), and the HeII ($k_{a1}II = 1.2$):- 1.6 ($^4A_{2g}$) : 0.8 ($^2A_{2g}$) : 2.0 ($^2E_{2g}$). However, it has proved impossible to obtain experimental intensity ratios for the separate bands accurately from current data, since the bands overlap considerably, and only the collective band area ratio for (b+c+d) : a is available. The experimental relative intensities are compared with predicted values in table 3.13.

Table 3.13 Calculated and observed relative intensities for chromocene

	EXPERIMENTAL [a : (b+c+d)]	CALCULATED	ASSIGNMENT
HeI	1.0 : 1.5	1.0 : 2.4	(3)4
		1.0 : 0.8	(3)5
HeII	1.0 : 1.4	1.0 : 1.75	(3)4
		1.0 : 1.2	(3)5

Thus neither of the assignments 3(4) or 3(5) appears to be in line with observed relative intensity values, and the possibility of the $^3A_{2g}$ ground state for chromocene is rejected.

The most probable ground state, is, therefore the $^3E_{2g}$, $(a_{1g})'(e_{2g})^3$, which gives rise to five ion states, and assignment of the

PE spectrum will now be discussed on this basis.

The five possible ion states are $^2E_{2g}$, $^4A_{2g}$, $^2E_{1g}$, $^2A_{2g}$ and $^2A_{1g}$. Four possible assignments of the PE spectrum have previously been proposed assuming a $^3E_{2g}$ ground state for chromocene [216]; these are shown in table 3.14 (1-4) together with an alternative assignment (5).

Table 3.14 Possible assignments for the PE spectrum of chromocene

ASSIGNMENT	a	b	c	d	predicted intensity a : (b+c+d)
1	$^4A_{2g}+^2E_{2g}$	$^2E_{1g}$	$^2A_{1g}$	$^2A_{2g}$	$(4+3k_{a1}):5$
2	$^2E_{2g}$	$^4A_{2g}$	$^2E_{1g}$	$^2A_{1g}+^2A_{2g}$	$k_{a1}:5$
3^x	$^4A_{2g}$	$^2E_{1g}$	$^2A_{1g}$	$^2A_{2g}$	4:5
4^y	$^4A_{2g}$	$^2E_{1g}+^2E_{2g}$	$^2A_{1g}$	$^2A_{2g}$	$4:(5+3k_{a1})$
5	$^4A_{2g}$	$^2E_{1g}$	$^2E_{2g}$	$^2A_{1g}+^2A_{2g}$	$4:(5+3k_{a1})$

x - The $^2E_{2g}$ band is assumed to be included in the first ligand band system (A'')

y - The $^2E_{1g}$ band may be elsewhere in the system.

Of these assignments, Rabalais et al [201] favour assignment 2, since relative intensity measurements obtained are in good agreement with those predicted.

Table 3.15 gives the predicted and experimental intensity ratios a : (b+c+d), assuming values of k_{a1} and k_{a1}II found experimentally for ferrocene.

Table 3.15 Theoretical and experimental relative intensity ratios for chromocene

ASSIGNMENT		THEORETICAL a : (b+c+d)	EXPERIMENTAL a : (b+c+d)
1	HeI	1.0 : 0.78	
	HeII	1.0 : 0.66	
2	HeI	1.0 : 3.75	
	HeII	1.0 : 2.50	
3	HeI	1.0 : 1.25	1.0 : 1.5
	HeII	1.0 : 1.25	1.0 : 1.4
4	HeI	1.0 : 1.85	
	HeII	1.0 : 2.15	
5	HeI	1.0 : 1.85	
	HeII	1.0 : 2.15	

From the experimentally determined relative intensity ratio, a : (b+c+d), values of k_{a1} and $k_{a1}II$ may be estimated for each proposed assignment. On these grounds, assignment 1, which would require negative values for k_{a1} and $k_{a1}II$, may be discarded. Assignment 2 would give $k_{a1} \simeq k_{a1}II > 2$, which is unlikely, since other evidence suggests that the a_{1g} 3d ionisation cross section is not expected to be twice that for an e_{2g} 3d orbital. Assignments 4 and 5 give values for $k_{a1} = 0.3$ and $k_{a1}II = 0.2$, which are rather low.

Region A" has been assigned to the ligand e_{1g}, e_{1u} ionisations; however there is a possibility that the small shoulder to the high ionisation energy side of the ligand band e, labelled f, may be due to ionisation from a d type orbital, although HeI data obtained for the

dimethyl substituted complex suggest that f is a ligand band, due to its shift.

HeII data give an intensity ratio of $\simeq$ 5 : 12 for A' :A". On the basis of observations made for ferrocene and vanadocene, that is, that the 3d and ligand 2p π ionisation cross sections are approximately equal in the HeII spectrum, the expected intensity ratio would be 4 : 8, which is very near the experimental value.

From the HeI and HeII PE spectra of $CrCp_2$, it can be seen that band c shows an increase in relative intensity in the HeII spectrum, even relative to the other 'd' ionisations. This strongly suggests that band c is due to the $^2E_{2g}$ ionic state, arising from ionisation of the a_{1g} electron, since it has been shown that, in the case of ferrocene, the a_{1g} cross section is greater than that for an e_{2g} orbital. From this argument, assignment 5 is favoured. The experimental intensity ratios found for a : (b+c+d) do not agree well with any of the ratios expected from the five proposed assignments, however assignments 3,4, and 5 are in slightly better agreement than 1 or 2.

The crystal field predictions as to the relative energies of the ion states produced may be examined in relation to assignments 3 to 5. Since it has not proved possible to measure relative band areas for b,c and d separately, accurate assignment is further complicated. The energies of each ion state produced relative to the $^4A_{2g}$ ion state are given in table 3.16, together with the experimental relative energies found assuming assignments 3, 4, and 5. If it is assumed that

Table 3.16 Relative energies of the ion states produced on ionisation from the $^2E_{2g}$ ground state

ION STATE	ENERGY RELATIVE TO $^4A_{2g}$ STATE	eV	CALCULATED ENERGY (eV) 3	4	5
$^2E_{2g}$	24B + 4C - Δ_2	2.6-Δ_2	2.8	1.2	1.5
$^2A_{2g}$	12B + 3C	1.56	1.8	1.8	1.8
$^2A_{1g}$	4B + 5C	1.56	1.5	1.5	1.8
$^2E_{1g}$	4B + 3C	1.04	1.2	1.2	1.2

C=4B [207], and a value of 520 cm^{-1} (0.065 eV) is substituted for B [221], the approximate energy of each ion state relative to the $^4A_{2g}$ ion state may be calculated, and these values are also given in table 3.17. Since Δ_2 is likely to be fairly large compared with B, the energy separation between the $^4A_{2g}$ and $^2E_{2g}$ ion states is likely to be less than that expected from assignment 3, and thus assignments 4 or 5 are more likely. Since assignment 5 predicts exactly the correct ordering of bands, with the $^2A_{2g}$ and $^2A_{1g}$ ion states having the greatest (and equal) energy separation from the $^4A_{2g}$ ion state, and with the additional relative intensity evidence that band c is due to production of the $^2E_{2g}$ ion state, this assignment is proposed as being the most likely, although assignment 4 cannot be ruled out.

(iv) Cobaltocene (V)

The four low ionisation energy bands, a-d, have been attributed to ionisation of metal d electrons, since the intensity ratio A" : (a+b+c+d) was consistent with this assignment [216].

The ground state electronic configuration of cobaltocene is well established as $(e_{2g})^4(a_{1g})^2(e_{1g})^1$, corresponding to a $^2E_{2g}$ state.

The first band, a, in the PE spectrum, at 5.56 eV was assigned by Orchard [216] to ionisation from the $(e_{1g})^1$ orbital, giving the $^1A_{1g}$ molecular ion state. The width of this band is greater than for bands due to d orbital ionisation in ferrocene, indicating the antibonding nature of the e_{1g} electron; the ionisation energy of this electron is remarkably low. Assignment of bands b-d was attempted with the aid of relative intensity measurements and crystal field theory, but has remained tentative [216]. Band e was assigned as being due to ligand ionisation, and the weak band f, could possibly represent d ionisation; however by comparison of the PE spectrum with that of the 1,1'-dimethyl substituted derivative [216], band f is more likely to be due to ligand ionisation. For cobaltocene, as with the other metallocenes, regions B and C were found to be similar to bands B and C in ferrocene.

Table 3.17 shows the relative intensity ratios found experimentally for A'(a+b+c+d) : A" (e+f). The HeI relative intensity data give a ratio of approximately 4 : 8 for (a+b+c+d) : A"; the expected value is 7 : 8. The HeII result is nearer, but gives a very high relative intensity for region A'. This is probably due to the very high ionisation cross sections found for the e_{1g} d orbitals, with HeII photons.

Table 3.17 Relative intensity data for cobaltocene

	a	b	c	d	a+b+c+d	e+f
HeI	0.08	0.24	0.08	0.08	(0.48)	1.00
HeI [216]	0.083	0.220	0.063	0.063	(0.43)	1.00
			0.346			
HeII	0.24		0.74		(0.98)	1.00

The ionic states produced on loss of a d electron for cobaltocene, together with their predicted relative intensities, are: $(k_{e1})\ ^1A_{1g}$, $(\frac{3}{2}\ k_{e1})\ ^3E_{1g}$, $(\frac{1}{2}\ k_{a1})\ ^1E_{1g}$, $(\frac{3}{2})\ ^3E_{1g}$, $(\frac{1}{2})\ ^1E_{1g}$, $(\frac{3}{2})\ ^3E_{2g}$, $(\frac{1}{2})\ ^1E_{2g}$. Possible assignments suggested by Orchard et al are given in table 3.18.

Table 3.18 Possible assignments for the PE spectrum of cobaltocene

ASSIGNMENT	a	b	c	d	predicted intensity b : c : d
1	$^1A_{1g}$	$^3E_{2g}+^3E_{1g}$	$^1E_{2g}$	$^1E_{1g}$	$3 : \frac{1}{2} : \frac{1}{2}$
2	$^1A_{1g}$	$^3E_{2g}+^3E_{1g}$	$^1E_{2g}+^1E_{1g}$	$^3E_{1g}$	$3 : 1 : \frac{3}{2}k_{a1}$
3	$^1A_{1g}$	$^3E_{2g}+^3E_{1g}$	$^3E_{1g}$	$^1E_{2g}+^1E_{1g}$	$3 : \frac{3}{2}k_{a1} : 1$
4	$^1A_{1g}$	$^3E_{2g}+^3E_{1g}$	$^1E_{2g}+^1E_{1g}$	$^3E_{1g}+^1E_{1g}$	$3 : 1 : 2k_{a1}$

In assignment 1 it is assumed [216] that the $^1E_{1g}$ second ionisation occurs in the region of the ligand π ionisations, as for chromocene, however there appears to be evidence that this is not the case, from the shift in the corresponding band in the HeI PE spectrum of 1,1'-dimethyl-cobaltocene.

Crystal field parameters give the energy separation of the two $^3E_{1g}$ states as 13B- Δ_2, which is small, and therefore configuration interaction is likely to be significant. The energy separation of the $^3E_{2g}$ and $^3E_{1g}$ ion states, of 6B, suggests that these bands are unlikely to be resolved in the PE spectrum. From this it was concluded [216] that the fairly intense band, b, is due to the $^3E_{1g}$ and $^3E_{2g}$ states. The HeI relative intensity for bands a and b, is 1 : 3, which is consistent with this assignment. Unfortunately bands b, c and d are not well enough resolved in the HeII PE spectrum for their separate relative intensities to be calculated.

Bands c and d are suggested to relate to the $^1E_{2g}$ and $^1E_{1g}$ ion states, but their intensities relative to band b are too high, and are, in fact, even higher in the HeII spectrum. This assignment would place both of the states $^3E_{1g}$ and $^1E_{1g}$, produced on a_{1g} ionisation, under the ligand band system. Although it is just possible that f is due to the $^1E_{1g}$ state, that both bands should be obscured by the ligand band system A" is unlikely on intensity grounds. Thus assignment 1 does not seem likely although it gives $k_{e1} = 0.8$.

Assignments 2,3 and 4 are more satisfactory on intensity grounds, but none is wholly satisfactory. Assignment 4 would require $k_{a1} = 0.5$ to fit the intensity data (no detailed HeII data are available); assignment 2 requires $k_{a1} = 0.6$, but is unlikely on crystal field grounds, since ionisation to the second $^1E_{1g}$ state would be expected to occur before band e. Assignment 3 requires $k_{a1} = 0.7$ which is the nearest to the experimental k_{a1} value observed for ferrocene, and an experimental value calculated approximately for

k_{c1} (from (b+c+d) : a, assuming $k_{a1} \simeq 1$) is 1.2 which seems reasonable, when compared with k_{c1} values obtained for manganocene and nickelocene.

It is not possible for a definite assignment to be made even with the aid of the HeII relative intensity data; these give a : (b+c+d) as 1 : 3 which can really only be consistent with assignment 1, and k_{c1}II is found to be ~ 2, which is in agreement with the high ionisation cross sections found for the e_{1g} d orbitals in nickelocene and manganocene, for HeII ionisation. However, the assignment of band e as being due to ligand ionisation is confirmed by its reduction in relative intensity in the HeII spectrum, although band f is still clearly visible as a shoulder to the high ionisation energy side of e. This band is not clearly resolved and it is difficult to say whether its intensity relative to e has increased in the HeII spectrum. Bands a, c and d show distinct increases in intensity relative to b.

(v) Nickelocene (VI)

Bands due to metal d ionisations and π Cp ionisations in the PE spectrum of nickelocene, appear to overlap considerably.

As for cobaltocene, there is a band at low ionisation energy, a, which is assigned to ionisation of the two e_{1g} d electrons. The molecular ion ground state, $^2E_{1g}$, is subject to Jahn-Teller distortion, however only slight asymmetry of the PE band is noted.

The HeI intensity ratio, (b+c+d+e) : a, is found to be 6.7, in fairly good agreement with previous work [216], and the predicted value is 7.

The HeII intensity data, however, give (b+c+d+e) : a as 1 : 0.3, or 3.3, thus suggesting a high ionisation cross section for the e_{1g} d orbital, as was found for cobaltocene. In fact if $k_{a_1}II$ and $k_{\pi}II$ are taken to be $\simeq 1$, a value for $k_{e_1}II$ of 1.5 is obtained.

From the HeII information it may be seen that band c is due to ligand ionisation as predicted by Orchard et al from HeI data [216], and bands b and d are clearly due to metal d ionisations. Band e is similar in appearance to band f of cobaltocene; it does not show signs of a decrease in intensity relative to band d in the HeII PE spectrum, and therefore is likely to be due to metal d ionisation. However, there is some evidence, as with cobaltocene, from PE data for the 1, 1'-dimethyl substituted analogue [216], that this band is due to ligand ionisation. Band b is tentatively assigned [216] to ionisation of an e_{2g} d electron to give the $^4E_{2g}$ ion state; this leaves the $^4A_{2g}$, $^2A_{2g}$ and $^2E_{2g}$ states unaccounted for in the PE spectrum. Of these, the $^4A_{2g}$ and $^2E_{2g}$ would be expected to have approximately the same relative intensity, with the $^2A_{2g}$ much lower in intensity. Thus a tentative assignment might be that band d is due to the $^4A_{2g}$ and $^2E_{2g}$ molecular ion states, and band e to the $^2A_{2g}$.

Assignment by Rabalais et al [201] of the HeI PE spectrum of nickelocene is restricted to the first band only, and is in agreement with conclusions drawn here.

(vi) Manganocene (III) and 1,1'-dimethyl manganocene (IIIa)

There is much evidence that manganocene exists in the high spin $^6A_{1g}$ ground configuration

as the solid, and in solution, and a satisfactory interpretation of the gas phase UV PE spectrum may be made on assuming a $^6A_{1g}$ ground state for the gas phase. The PES data of Rabalais et al [201] were interpreted in terms of a $^2A_{1g}$ ground state; this assignment was criticised by Warren [224b] who noted that the data are more applicable to a $^6A_{1g}$ ground state. Orchard et al [216] assigned the PE spectrum in terms of a high spin ground state, in agreement with calculations by Clack [200]. The spectrum is complex and was divided [216] into regions a-d, x, B and C.

The first band, a, at 7.01 eV is assigned to e_{1g} ionisation to give the $^5E_{1g}$ ion state; the band is similar in appearance to the e_{1g} bands in the cobaltocene and nickelocene spectra. The weaker band system in the 10-11 eV region of the spectrum is also assigned to d orbital ionisation; band c to the production of the $^5A_{1g}$ state, and band d to the $^5E_{2g}$ state. The "impurity" band, x, is hardly visible as a separate band in the current study. However band d is very broad; x was assigned by Orchard as being due to cyclopentadiene present as impurity. Band b was assigned to the various ligand ionisation processes generating $^7E_{1u}$, $^5E_{1u}$, $^7E_{1g}$, $^5E_{1g}$ states.

The HeII PE data show bands c and d as relatively more intense and therefore confirm that they are due to d orbital ionisation, whereas band b is shown to be due to ligand ionisation. Certainly bands c and d are not so weak that they may be ignored as in the assignment of the HeI PE spectrum by Rabalais et al [201]. Rabalais found band a to have three distinct peaks, and found no structure at c and d; manganocene was assumed to

have the $^2A_{1g}$ ground state which would produce three ion states. The $^6A_{1g}$ ground state also gives rise to three ion states, $^5A_{1g}$, $^5E_{2g}$ and $^5E_{1g}$. The assignment of Rabalais is not in agreement with crystal field theory which would predict a large energy difference ($\sim 28B - \Delta_2$) between the $^3E_{2g}$ and $^1A_{1g}$ ion states, with the $^3E_{2g}$ state lower in energy. The first band of the PE spectrum is assigned by Rabalais to closely spaced $^1A_{1g}$, $^3E_{2g}$ and $^1E_{2g}$ ion states in that energy sequence.

The HeI relative intensities were found to be a : b : c : d = 0.25 : 1.00 : 0.08 : 0.2; the relative intensities of c and d cannot be obtained with great accuracy from current data. These data give $k_{e1} = 1.2$ and $k_{a1} = 0.8$, as for ferrocene. The HeII relative intensities are a : b : c : d = 0.57: 1.00 : 0.16 : 0.36, giving $k_{e1}II = 2$ and $k_{a1}II = 0.9$. These $k_{a1}II$ and $k_{e1}II$ values are consistent with the predicted relative intensities for bands a, c and d, and again the e_{1g} d orbital is seen to possess a high ionisation cross section for HeII ionisation. The ratio a+c+d : b from HeII data, is therefore rather higher than expected due to the large value for k_{e1}.

The energy separations of the ionic states as measured from the PE spectrum by Orchard et al [216], were in reasonable agreement with the predictions of crystal field theory.

A small band just to the low ionisation energy side of a was observed; this was relatively very low in intensity, being only just visible. This small band is taken as evidence for the existence of manganocene as an equilibrium mixture

of different spin isomers, being due to ionisation from the $^2E_{2g}$ ground state.

The PE spectrum of 1,1'-dimethylmanganocene (IIIa) was obtained by Orchard et al., and found to be more complex than that of its unsubstituted analogue. Recent n.m.r. [218] and electron diffraction [178] studies have shown (IIIa) to exist as an equilibrium mixture of high and low spin isomers in solution and in the gas phase, and the PE spectrum would therefore be expected to show evidence of this. Orchard et al observed three bands corresponding to those assigned for $MnCp_2$ to e_{1g}, a_{1g} and e_{2g} ionisations, and also several additional bands. Calculations indicate a $^2E_{2g}$ ground state for the low spin form; the bands labelled a', b' and c' are assigned speculatively [216] as arising from the $^2E_{2g}$ ground state.

The HeI PE spectrum of (IIIa) obtained in the current study is in good agreement with previous work [216]. The three bands a, c and d, assigned to metal d ionisation in the PE spectrum of manganocene, and arising from the $^6A_{1g}$ ground state, are found to be analogous with bands a, c and d in the spectrum of (IIIa) and may be assigned in the same way. However the relative intensity of the c, d region to a, is higher in the PE spectrum of (IIIa) than for (III) and several extra bands are observed, a', b' and c'. Of these, a' has a very weak counterpart in the manganocene spectrum. The $^2A_{1g}$ ground state may be rejected since the c'-a' energy separation of ~ 1.4 eV is too large for a singlet triplet splitting as would be produced by the $^2A_{1g}$ ground state to give ionic states $^3E_{2g}$ + $^1E_{2g}$. Bands a', b' and c' are therefore assigned as arising from a $^2E_{2g}$ ground state.

The HeI PE spectrum for bands a', a, b' and c' was obtained with the sample chamber at a range of temperatures: 45, 71, 92, 117, 165, 250, 300 and 325°C. As the temperature was increased, bands a', b' and c' were reduced in intensity, and at the highest temperatures, a' was only just visible. Thus the $^2E_{2g}$ and $^6A_{1g}$ states must lie very close in energy with the $^2E_{2g}$ state slightly lower, and at high temperatures thermal energy is available for increased population of the $^6A_{1g}$ level. It is not possible from current PE data to determine the relative proportions of the two isomers.

The HeII data confirm the assignments of bands a, a', b', c' and c to ionisation of metal d electrons and band b to ionisation of ligand π electrons but it was not possible to calculate accurately the relative intensities of these bands separately. However the overall relative intensities for (a'+a+b'+c'+c+d) : b are 0.81 : 1.00 (HeI) and 1.7 : 1.0 (HeII), both values giving rather high relative intensity values for metal d ionisations. This may be due to the relatively large ionisation cross section for e_{1g} d orbitals as noted for cobaltocene and nickelocene.

It is not surprising that complex (IIIa) should exist with a different ground state to complex (III); the electron donating characteristics of the methyl group are greater than for hydrogen, and so in comparing (III) and (IIIa), the donor character of the ligands in the latter may be significantly increased, and thus cause spin pairing. It might be expected that the bis-pentamethyl substituted analogue would exist in the low spin form.

(vii) Ruthenocene (VII)

The PE spectrum of ruthenocene was obtained by Orchard et al [161], and found to be similar in appearance to that of ferrocene, except that the band structure in region A' is unresolved, and that in A" is completely resolved. This latter feature is the most significant, and corresponds to a large separation between the e_{1g} and e_{1u} mainly ligand ionisations. This is suggested by Warren [221] to be due to an increasing metal-ligand interaction (hence increase in ionisation energy) between the metal and ligand e_{1g} orbitals. The same effect was observed for osmocene [161].

The HeI spectrum obtained in the current study is in good agreement with that of Orchard et al [161].

As expected from earlier data for the atomic species [162], the a_{1g} (d) and e_{2g} (d) ionisation energies increase significantly from iron to ruthenium; this effect was also noted for complexes studied in chapter 2.

The a_{1g}-e_{2g} d orbital energy separation is found to be less for ruthenocene than ferrocene; this effect may be due to the increased covalency of ruthenocene, that is, stabilisation of the e_{2g} level by interaction with $e_2\pi^*$. From crystal field theory, the decrease in $^2A_1 - {}^2E_2$ energy separation in ruthenocene may be explained since B is expected to be smaller for ruthenocene ($^2A_1 - {}^2E_2 = 20B - \Delta_2$). This effect is similar in nature to the general increase noted in (Δ e, t_2) separation for analogous first and second row octahedral complexes; both effects tend to diminish $^2A_1 - {}^2E_2$

separation.

The PE spectra of the isoelectronic complexes CpMn (C_6H_6) and $(C_6H_6)_2Cr$ have been examined [229], and the sequence of $^2A_1$ and $^2E_2$ ion states is reversed relative to ferrocene, in both complexes; the actual $^2E_2 - {}^2A_1$ separations observed were 0.36 eV for the manganese compound and ~ 1.0 eV for $(C_6H_6)_2Cr$.

Orchard et al [161] found that the combined a_{1g} and e_{2g} d ionisation cross section, k_d, steadily increases relative to k_π in the series Fe → Ru → Os; this is apparent from the HeI spectra.

The increased $\pi e_{1u} - \pi e_{1g}$ separation in ruthenocene compared to ferrocene may be attributed to an increase in stabilisation of the $e_{1g}\pi$ bonding MO through interaction with the empty metal e_{1g}* d orbital. This is in agreement with the noted decrease in $e_{2g} - a_{1g}$ d separation.

From HeII relative intensity data, the lower ionisation energy band of region A" may be immediately assigned to ionisation from the e_{1u} ligand level, while the higher ionisation energy band is seen to be due to ionisation from the mainly ligand e_{1g} orbital, having significant d character; this shift of the e_{1g} π ionisation energy to a higher value reflects the stabilisation of this level with increased covalency.

Since the ligand πe_{1u} band is separated from the e_{1g} ligand band, relative intensity measurements may be used to calculate more accurate values for k_d, since the πe_{1u} band is unlikely to

have significant d character. An estimate of the d character of the πe_{1g} band may also be obtained. The relative intensities, A' : A" (e_{1u}) : A" (e_{1g}) together with k_d values are given in table 3.19.

Table 3.19 Relative intensity data for $FeCp_2$ and $RuCp_2$

$FeCp_2$ A' : A"	(HeI)	1.0 : 2.1	k_d = 0.65
	(HeII)	1.0 : 1.2	k_dII = 1.13
$RuCp_2$			
A' : A"	(HeI)	1.0 : 1.6	k_d = 0.83
	(HeII)	1.0 : 1.1	k_dII = 1.21
A' : A" (e_{1u}) : A" (e_{1g})			
	(HeI)	1.1 : 1.0 : 0.8	k_d = 0.73
	(HeII)	2.0 : 1.0 : 1.2	k_dII = 1.33

It may be seen from table 3.19 that for ionisation by HeI photons, the ruthenocene 4d orbitals, have a higher average ionisation cross section than the iron 3d orbitals, however in neither case is the 'd' cross section greater than the ligand π cross section. For HeII ionisation both the 3d and 4d orbitals show an increase in ionisation cross section relative to the ligand π orbitals; in both cases the 'd' cross section is higher than the π orbital cross section, and the 4d average ionisation cross section is greater than that for the 3d orbitals, giving a value for ruthenocene of k_dII = 1.33. It may also be seen from table 3.19 that the e_{1g} ligand band of ruthenocene has considerable metal d character, calculated at 121% with respect to band A'. This abnormally large apparent d character is possibly due to the very high ionisation cross sections observed for e_{1g} d ionisations.

(viii) bis (η^5-cycloheptadienyl)ruthenium (VIIa)

The PE spectrum is very different in appearance from that of ruthenocene, and the first band, a, shows a much lower ionisation energy (7.07 eV).

The structure of this complex has not been examined by X-ray crystallography, but n.m.r. data have been obtained [238], and both ligands are assumed to have equivalent geometries with respect to the metal atom, and are bonded via five consecutive carbon atoms of the ring. The highest possible symmetry is C_{2h}.

The first three bands, a, b and c may be assigned to ionisation of metal d electrons from the HeI and HeII relative intensities; bands d and e are seen to be due to ligand π ionisation. The reduction in symmetry of (VIIa) compared to ruthenocene, will tend to remove the e_{2g} d orbital degeneracy, and these levels are now separated enough to be resolved in the PE spectrum. The relative intensities (a+b+c) : (d+e) are shown in table 3.20, together with the calculated values of the factor k_d, analogous to k_d in ruthenocene. The k_d values obtained in this way are exceptionally high even if bands (d+e) are assumed to arise from ionisation of two non-degenerate levels (ie 4 electrons) instead of two almost degenerate levels (8 electrons). Reasonable values could only be possible if bands e and f were due to ionisation from just one non-degenerate level. If this were the case, the k_d values would be in fairly good agreement with those found for ruthenocene; however it is unlikely

Table 3.20 Relative intensity data for (VIIa)

(a+b+c) : (d+e)	HeI	3.1 : 1.0	k_d = 2.09
	HeII	6.0 : 1.0	k_dII = 4.00

since bands d and e are well resolved.

3.17 SUMMARY

Figure 3.13 shows the ionisation energies for metallocenes of the first row transition elements, from vanadium to nickel.

Agreement of many previous assignments of PE spectra for these complexes, with current assignments made using HeII relative intensity was, in many cases, extremely good. Assignment of the spectra using this data was aided by the observation that metal a_1 and e_2 3d orbitals and ligand 2p π orbitals all have approximately equal ionisation cross sections for HeII ionisation, and by the unusually large value observed for k_{e1}, the e_{1g} d ionisation cross section. In some cases a satisfactory assignment was reached, though assignments for chromocene, cobaltocene, and nickelocene are still uncertain. Values for the factors k_{a1}, $k_{a1}II$; k_{π}, $k_{\pi}II$ and k_{e1}, $k_{e1}II$; or k_d, k_dII, were determined experimentally from the spectra wherever possible; however in many cases it was not possible to obtain accurate relative intensity data for the HeII spectra, due to poor resolution, or overlapping bands. The relative changes of k_{a1}, k_{π} and k_d between the HeI and HeII spectra were a useful aid to assignment; the ionisation cross sections seemed to be fairly constant for different metals.

The variation of ionisation energy across the series is noted to be very irregular, and, in general, the result of interelectronic repulsion in the various open shell configurations involved.

3.18 EXPERIMENTAL

Photoelectron Spectra

The spectra were obtained using the same instrumentation as in chapter 2, but with HeII facilities (see

Fig 3:13 Correlation diagram showing ionisation energy trends for the metallocenes

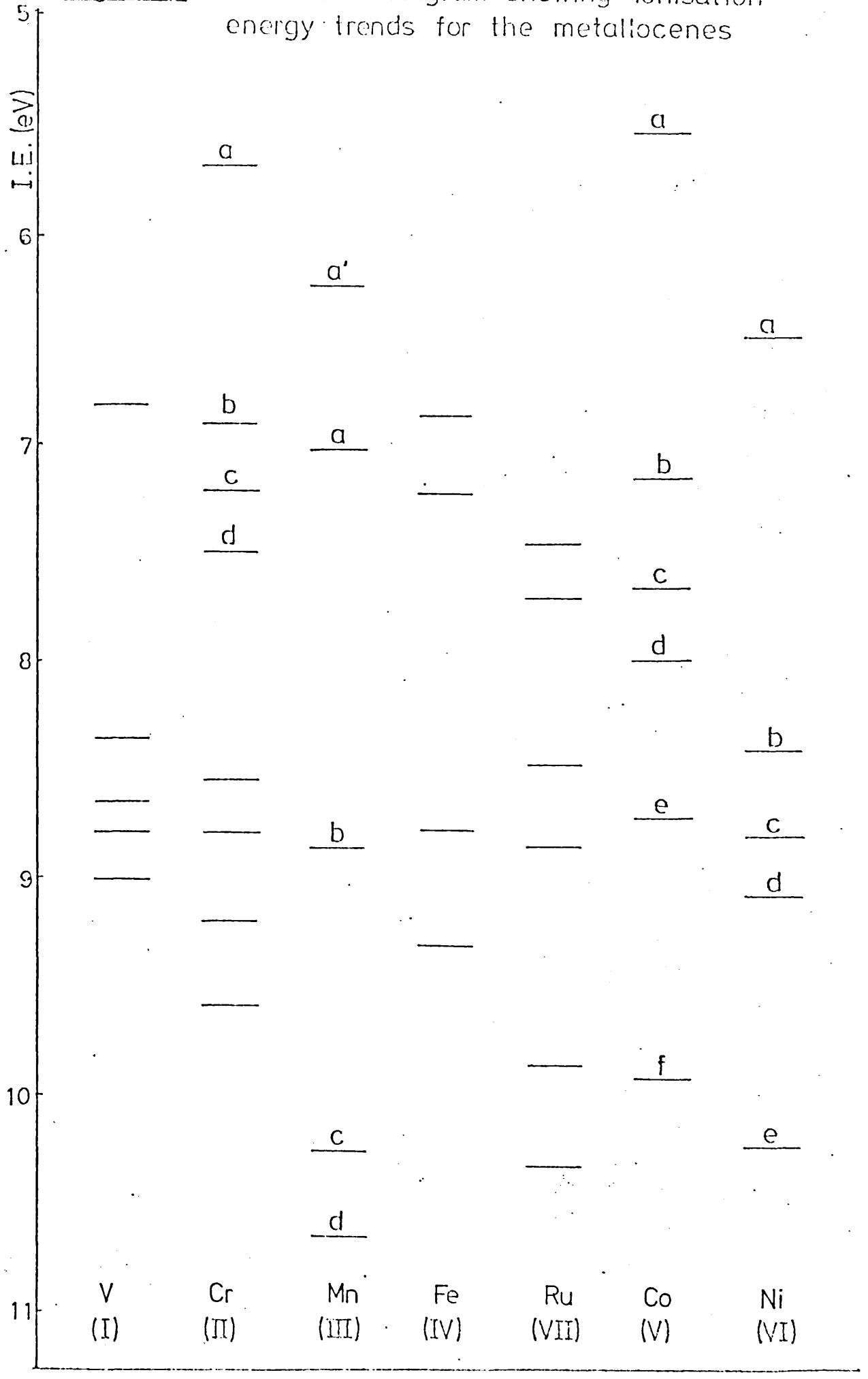

appendix 1), HeI and HeII spectra being recorded at least in duplicate for each complex.

The air sensitive samples were sealed under vacuum in glass tubes of the correct diameter to fit the heated insert probe, and the tubes were broken open at the time of inserting the sample. Contact with air was therefore minimal, with very little surface area of the sample exposed. This method was found to be satisfactory for all cases except 1,1'-dimethylmanganocene (IIIa). This complex was stored in a nitrogen atmosphere at low temperatures, and introduced into the spectrometer via the 'volatile' inlet system, directly from a Schlenk tube. Xenon and Nitrogen were used as calibration gases, and the He self ionisation peak was used as an additional calibration check.

Relative intensities were calculated by three independent methods by measurement of areas under bands. In estimating HeII relative intensities, care was taken to correct for the $HeII_{\beta}$ satellites which appear with approximately 10% intensity of the $HeII_{\alpha}$ spectra displaced by 7.56 eV. For example, a shadow of the main band appears in the region of $\simeq$ 5-6 eV.

Methods of Preparation

Except for the iron group, the complexes (I) to (VIIa) are very air sensitive, and in all cases special handling precautions were taken.

1. Sodium cyclopentadienide

This was used as a reagent in most syntheses, and was prepared according to the method described by King [66]. The general preparation is described; this was modified in some cases:

The reaction was carried out in a 1 litre,

three necked round bottomed flask, with motor stirrer, reflux condenser, nitrogen inlet, and pressure equalised dropping funnel. The apparatus was flushed through with nitrogen and charged with 11.5 g (0.5 mole) of sodium metal, and about 150 ml of sodium dried xylene. The mixture was heated to the boiling point of xylene, and the sodium dispersed into a sand by vigorous stirring which was halted below reflux temperature. The flask was then cooled to room temperature and the xylene was siphoned off and replaced by 250 ml of freshly distilled THF. The suspension of sodium in THF was treated dropwise with 50-60 ml of freshly prepared cyclopentadiene to dissolve the sodium forming a solution of sodium cyclopentadienide. [Colour of this solution varied from a very pale straw colour to deep red, due to partial oxidation; pure sodium cyclopentadienide in THF is colourless. It is difficult to prevent a small amount of oxidation, but this does not significantly affect the yield] . The reaction mixture is then ready for reaction with transition metal salts to give metallocenes.

2. Tetrahydrofuran (THF)

This was always used freshly purified. Sodium and benzophenone were added and the mixture refluxed until deep blue. THF was then distilled off, collected under nitrogen, and added immediately to the dispersed sodium via stainless steel tubing.

3. Cyclopentadiene

This was always freshly prepared from dicyclopentadiene, by thermal dedimerisation, using

apparatus of the type shown in Figure 3.14. The apparatus was flushed with nitrogen prior to loading; the cyclopentadiene was collected in an ice-cooled flask and used within 0.5 hr.

Figure 3.14 Apparatus for preparation of cyclopentadiene

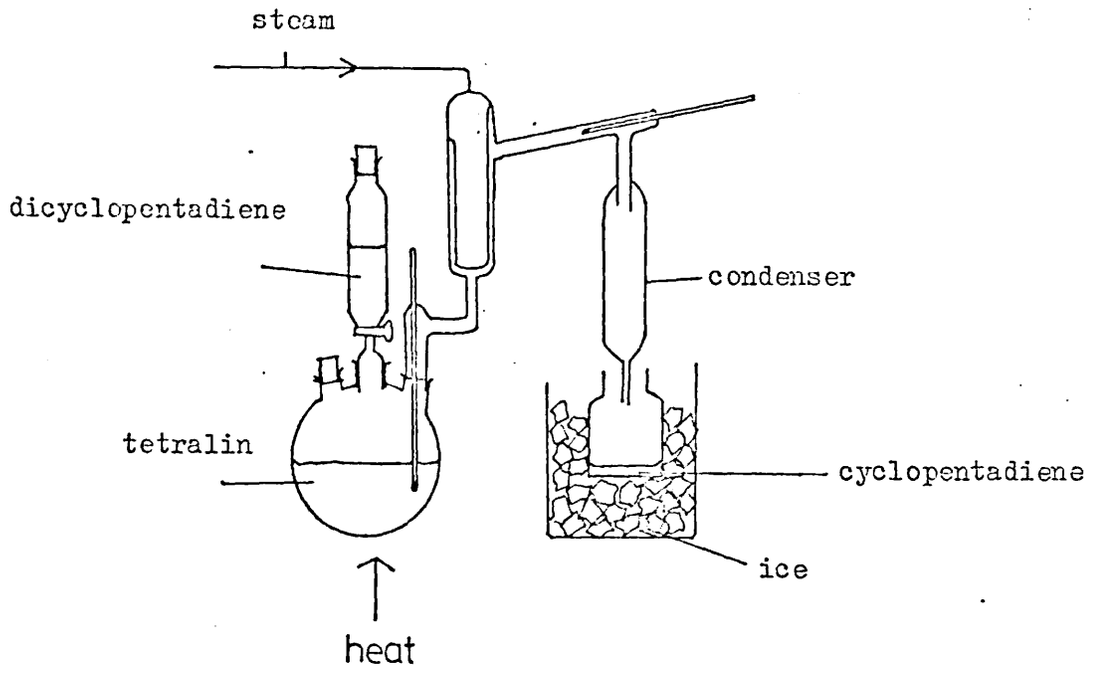

4. Vanadocene (I)

Anhydrous VCl_3 (23.6 g, 0.5 mole) was added to freshly prepared sodium cyclopentadienide solution. The vanadium trichloride was purified by refluxing with thionyl chloride [239] and storing in a desiccator. The reaction mixture was refluxed for about 4 hr, and allowed to cool. THF was removed by pumping, and the dark residue remaining was transferred to a sublimation apparatus, in a nitrogen filled glove bag. The residue gave purple air sensitive crystals on sublimation (100-180°, 0.1 mm).

5. Chromocene (II)

The above procedure was used, but all stages of the reaction were carried out in Schlenk tubes. The anhydrous chromium chloride had been prepared by dropping carbon tetrachloride on to hydrated chromium chloride [240] at high temperature. This form of chromium trichloride does not hydrate rapidly in air. The reaction residue obtained as above was sublimed (80-150°C, 0.1 mm) to give dark red crystals, which were immediately transferred, under nitrogen, to sample tubes which were sealed under vacuum. This complex was found to be far more air sensitive than vanadocene, and is also water sensitive.

6. Manganocene (III)

This was prepared by reaction of sodium cyclopentadienide in THF, with manganese dibromide prepared from manganese and bromine in 1,2-dimethoxyethane, as described by King [66]. As much of the dimethoxyethane as possible was decanted from the manganese dibromide before addition of sodium cyclopentadienide solution in a previously measured volume, via stainless steel tubing. Care was taken to admit no air to the reaction vessel. The solvents were removed in vacuum, leaving a dark residue which was transferred to a sublimation apparatus in a glove bag which had been evacuated and filled with nitrogen several times. It was found necessary to use a vacuum of 10^{-3} τ for the product to sublime from the residue (50°C). The product sublimed as pale yellow crystals, turning light brown on contact with dry nitrogen. The complex was sealed under vacuum in sample tubes

immediately, and was found to be the most air and water sensitive of the metallocenes.

7. 1,1'-dimethylmanganocene (IIIa)

A sample was donated by the Inorganic Chemistry Laboratory, Oxford, and was purified by redistillation, to give a dark red liquid, b.pt. ~100°/0.1 mm. This complex was at least as air sensitive as manganocene and was stored in a nitrogen atmosphere.

8. Ferrocene (IV)

Ferrocene was obtained commercially from Koch-Light, and purified by resublimation at 80°-100°/0.1 mm to give orange, air stable crystals.

9. Ruthenocene (VII)

A sample was prepared using a recently reported and very simple method [238]. Zinc dust was added to a mixture of freshly prepared cyclopentadiene and ruthenium chloride hexahydrate in ethanol, and the mixture was stirred for 0.5 hr. The solution was filtered, the filtrate evaporated down, and the solid product recrystallised from n-pentane at -78°C, and sublimed at 90-100°/0.1 mm to give pale yellow air stable crystals.

10. bis(η^5-cycloheptadienyl)ruthenium (VIIa)

This complex was donated, having been prepared by the same method as ruthenocene. In this case the reaction mixture was refluxed for 1 hr. Purification by sublimation at 90-100°C/0.1mm gave yellow, slightly air sensitive crystals.

11. Cobaltocene (V)

Anhydrous cobalt chloride was prepared by heating a hydrated sample in vacuo until completely blue and anhydrous. This was added to sodium cyclopentadienide solution and allowed to reflux overnight. Purple crystals of cobaltocene were purified by sublimation 80-150°/0.1 mm.

12. Nickelocene (VI)

Nickel bromide was prepared from nickel and bromine in 1,2-dimethoxyethane; diethylamine and freshly prepared sodium cyclopentadienide solution were added, and the reaction mixture was stirred overnight at room temperature. The solvent was removed in vacuo, and the residue transferred under nitrogen to a soxhlet extraction apparatus, and extracted with refluxing hexane. Green crystals separated from the hexane extract, were removed by filtration and purified by sublimation at 100°C/0.1 mm. Nickelocene may be handled in air, but was stored under nitrogen.

3.19 PHOTOELECTRON SPECTRA

1. vanadocene (I)
2. chromocene (II)
3. chromocene (II) HeII
4. manganocene (III) HeI
5. manganocene (III) HeII
6. ferrocene (IV)
7. ferrocene (IV) (1st two bands, HeI & HeII)
8. cobaltocene (V)
9. nickelocene (VI)
10. 1,1-dimethylmanganocene

11. ruthenocene (VII) HeI
12. ruthenocene (VII) HeII
13. bis (η^5-cycloheptadienyl)ruthenium (VIIa)
14. bis (η^5-cycloheptadienyl)ruthenium (VIIa) HeII

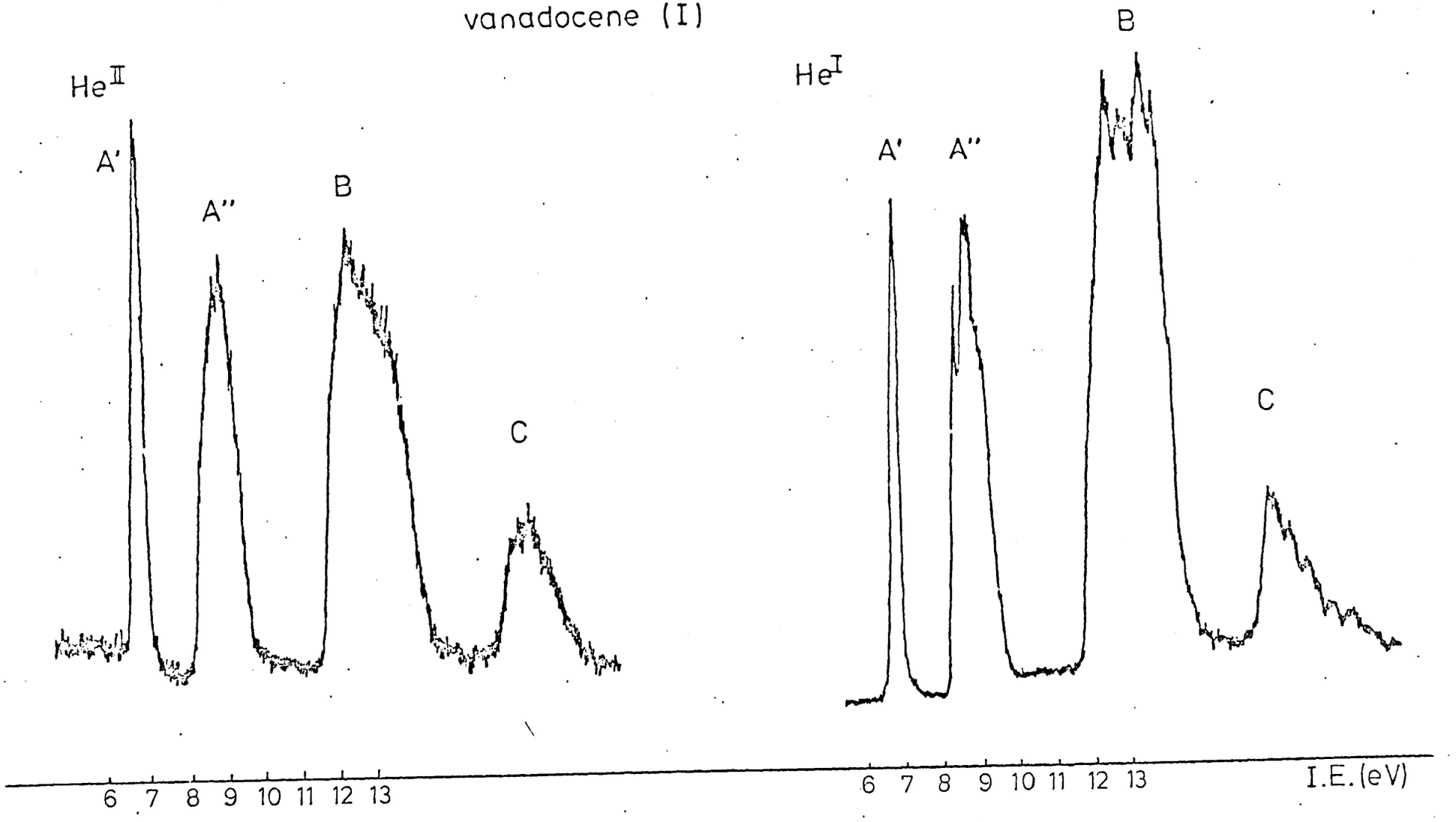
vanadocene (I)
He II
A'
A''
B
C
He I
A'
A''
B
C
6 7 8 9 10 11 12 13
6 7 8 9 10 11 12 13
I.E. (eV)

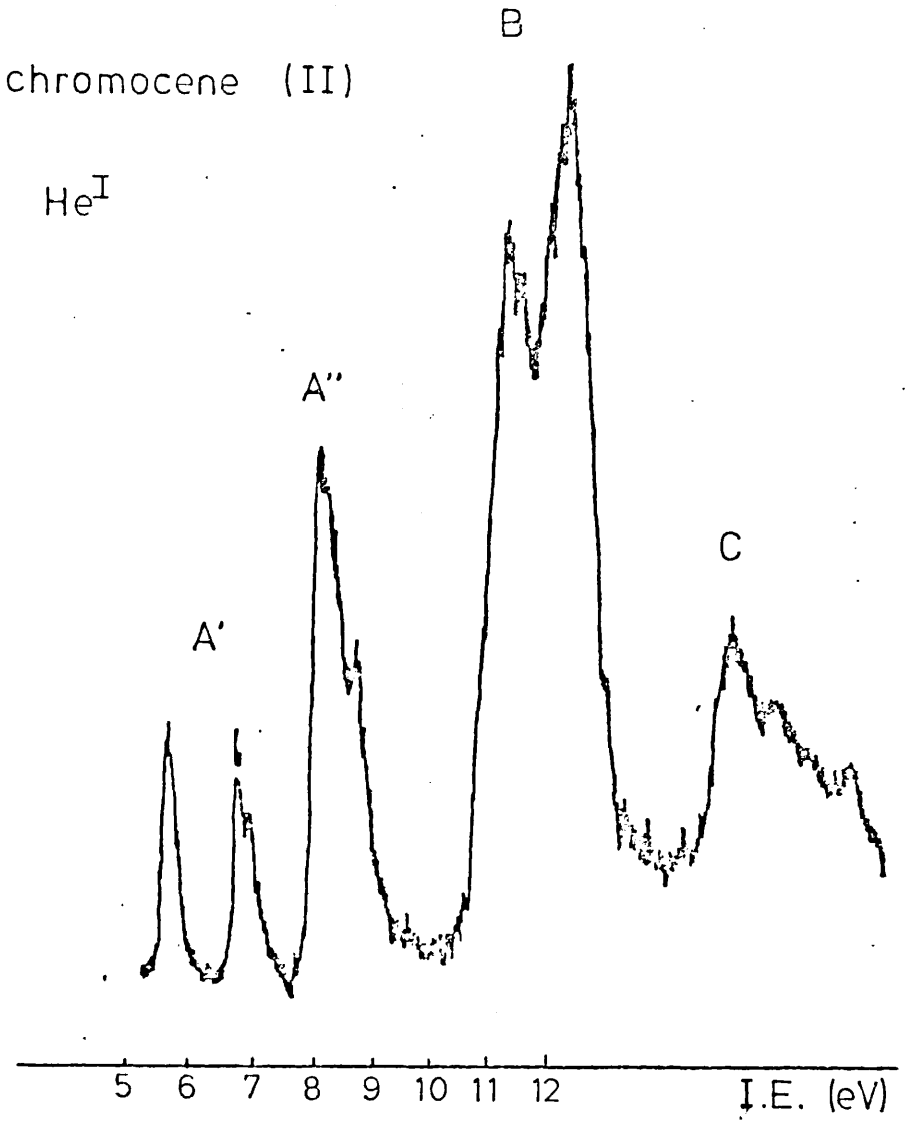
chromocene (II)
He^I
A'
A''
B
C
5 6 7 8 9 10 11 12
I.E. (eV)

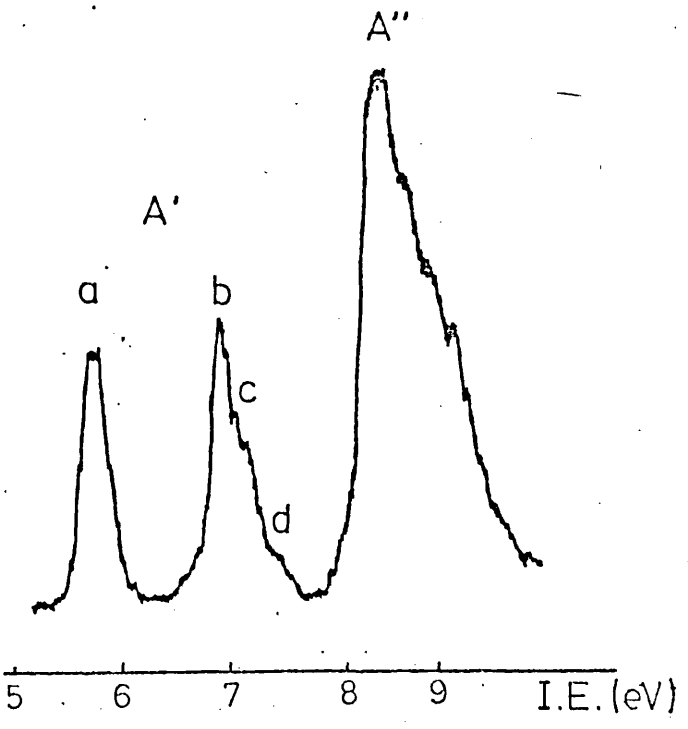
A''
A'
a
b
c
d
5 6 7 8 9
I.E. (eV)

chromocene (II)

He^{II}

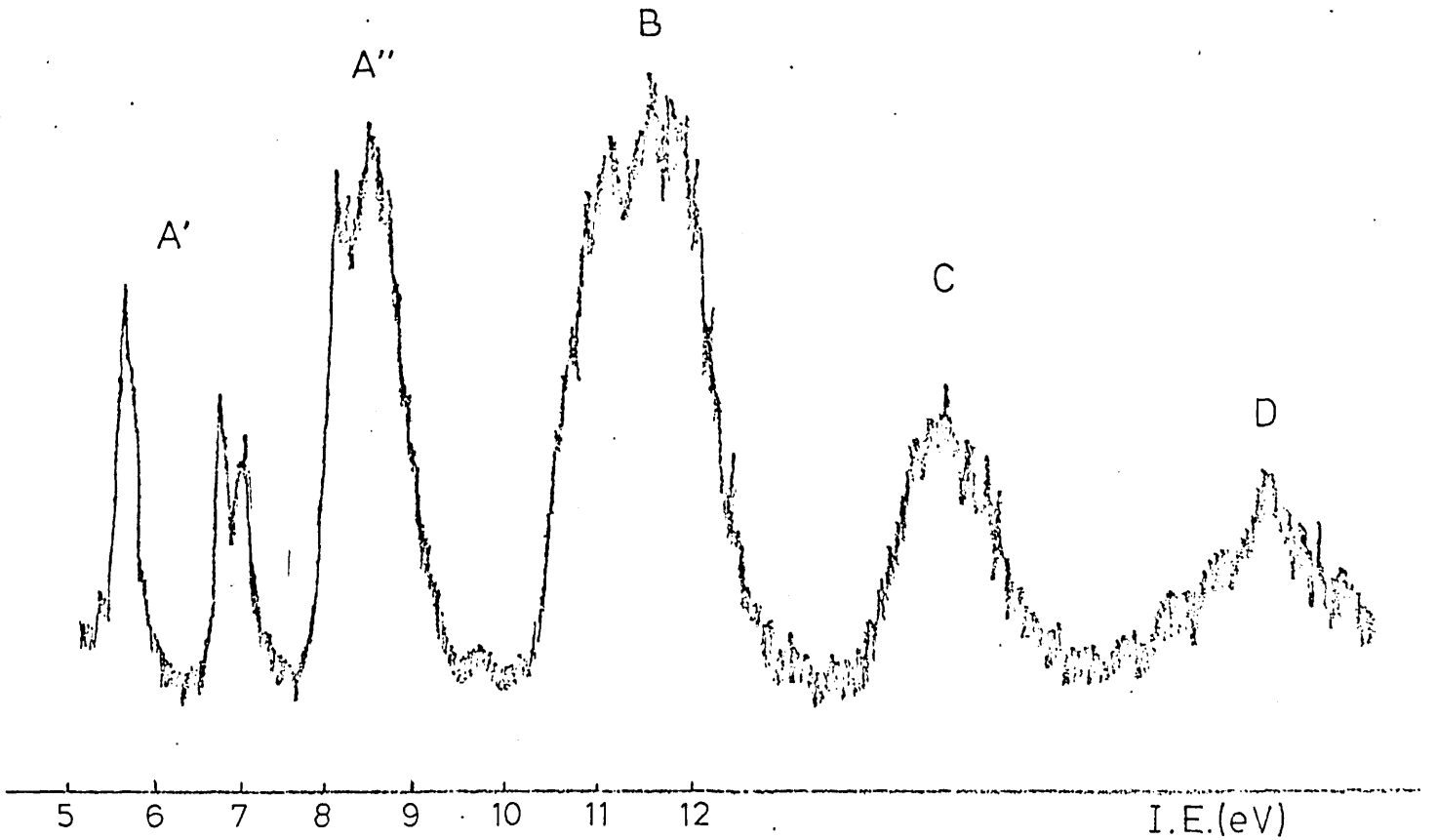

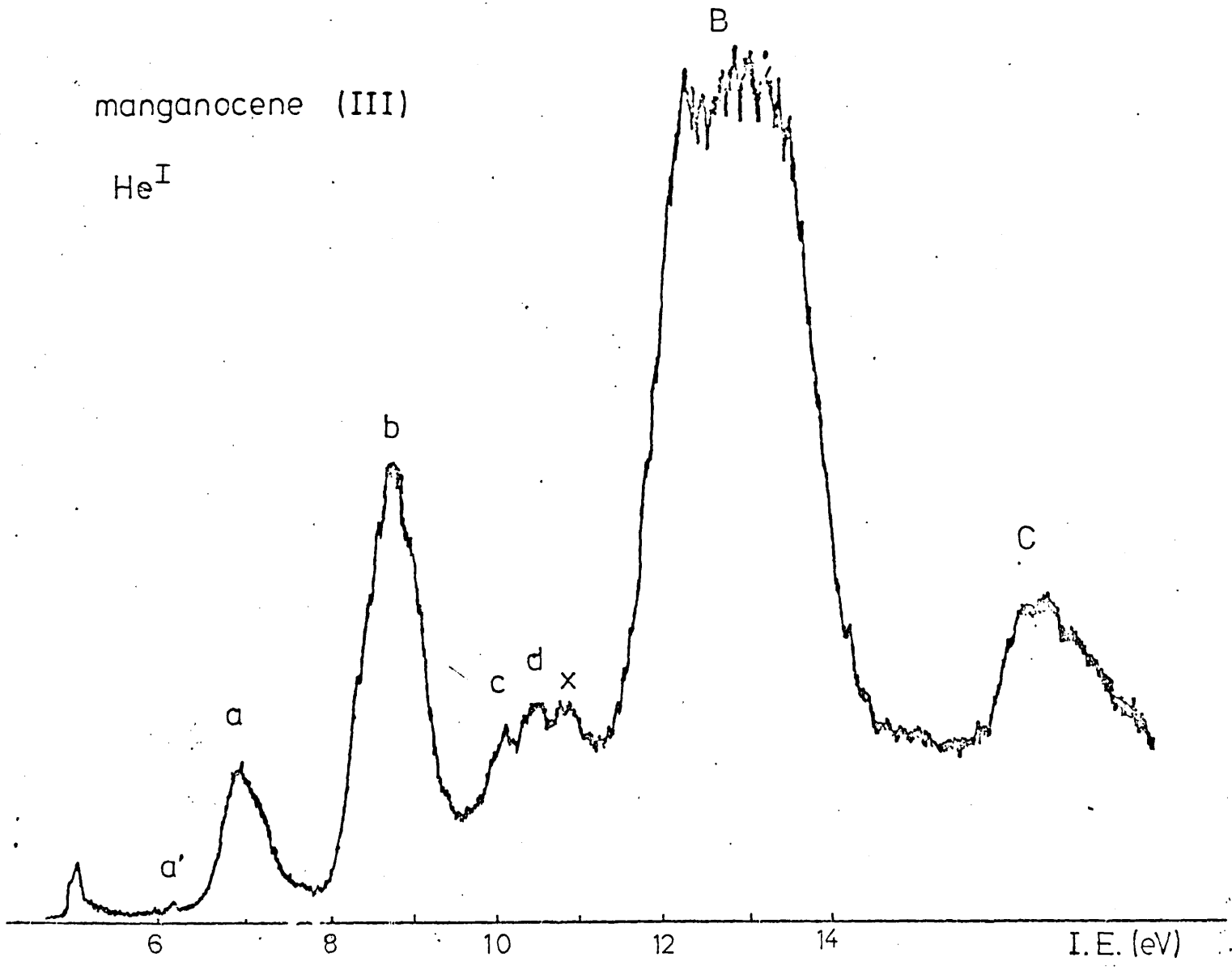
manganocene (III)
He^I
B
b
C
a
c
d
x
a'
6
8
10
12
14
I.E. (eV)

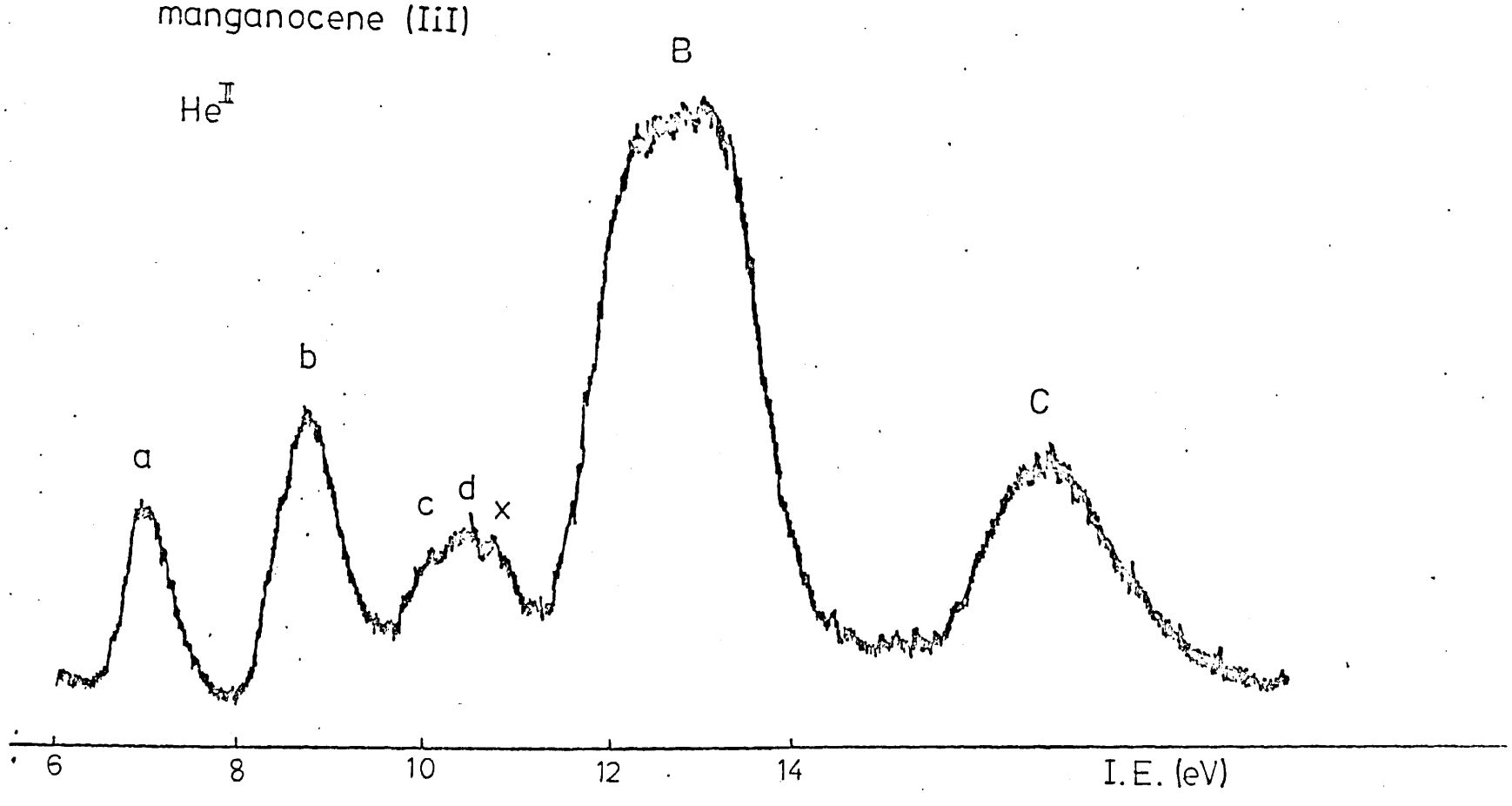
manganocene (IiI)
He^{II}
a
b
c
d
x
B
C
6
8
10
12
14
I.E. (eV)

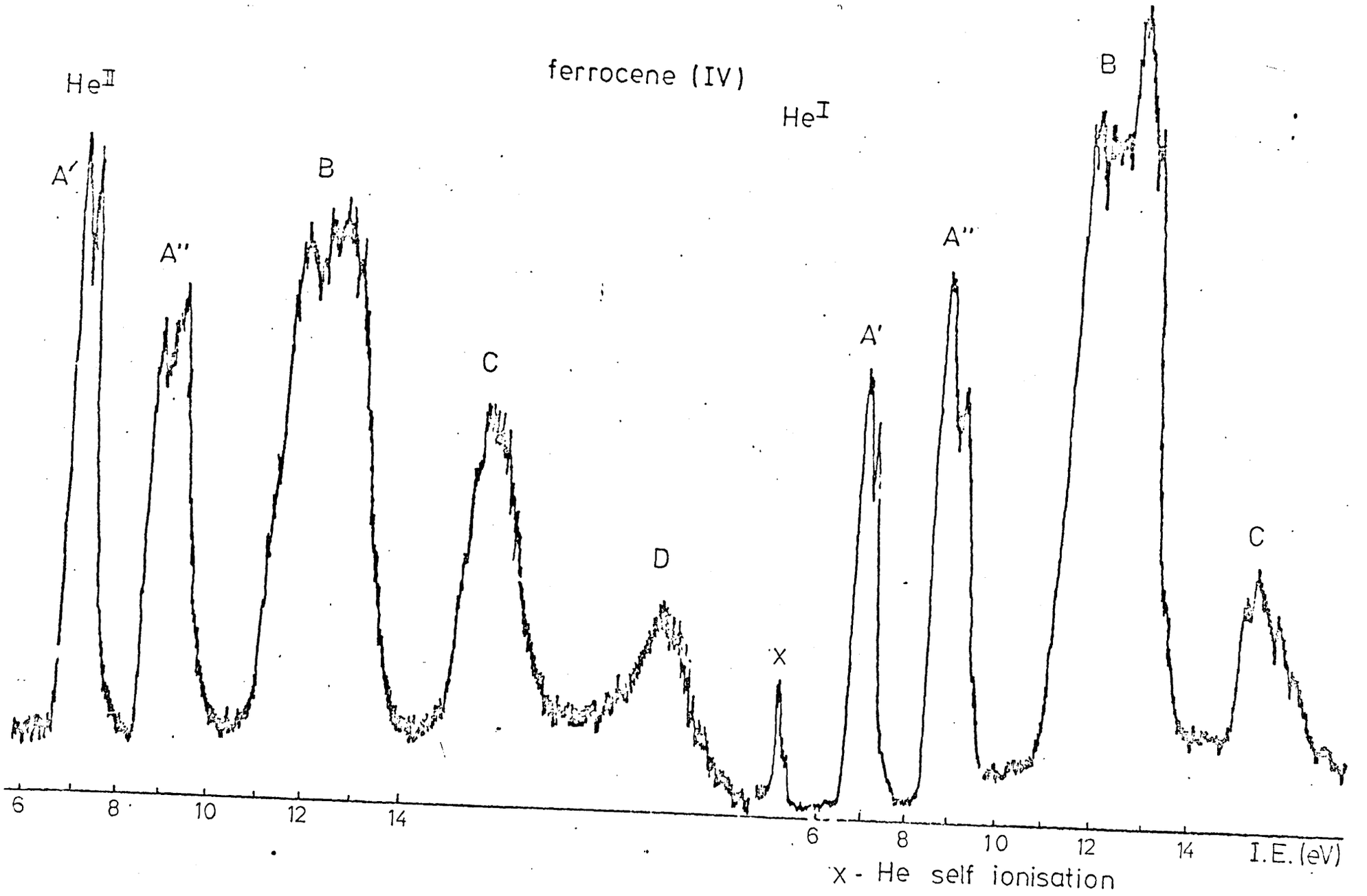
ferrocene (IV)
He II
He I
A'
A''
B
C
D
X
A'
A''
B
C
6
8
10
12
14
6
8
10
12
14
I.E. (eV)
X - He self ionisation

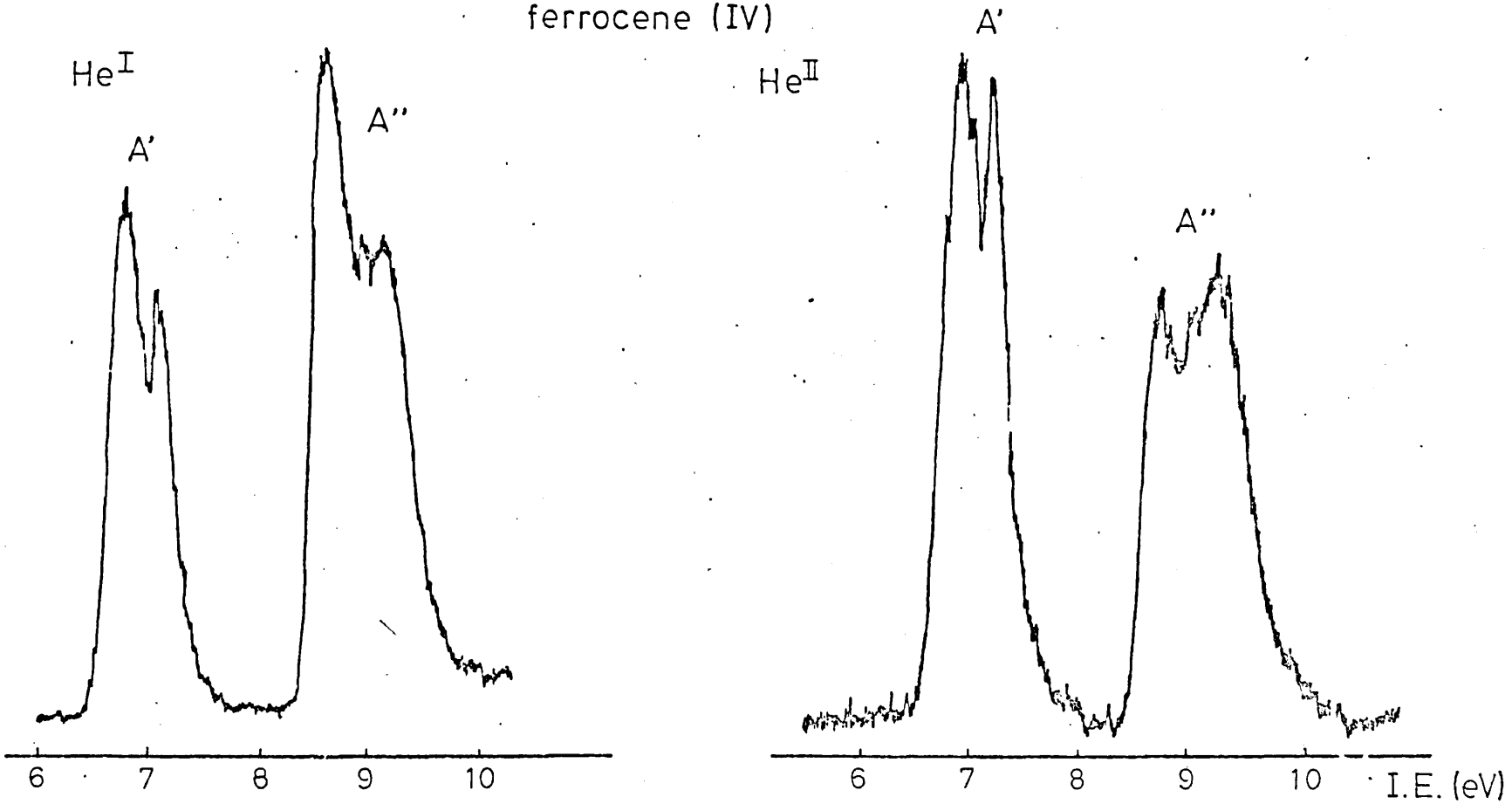
ferrocene (IV)
He^I
A'
A''
He^II
A'
A''
6
7
8
9
10
6
7
8
9
10
I.E. (eV)

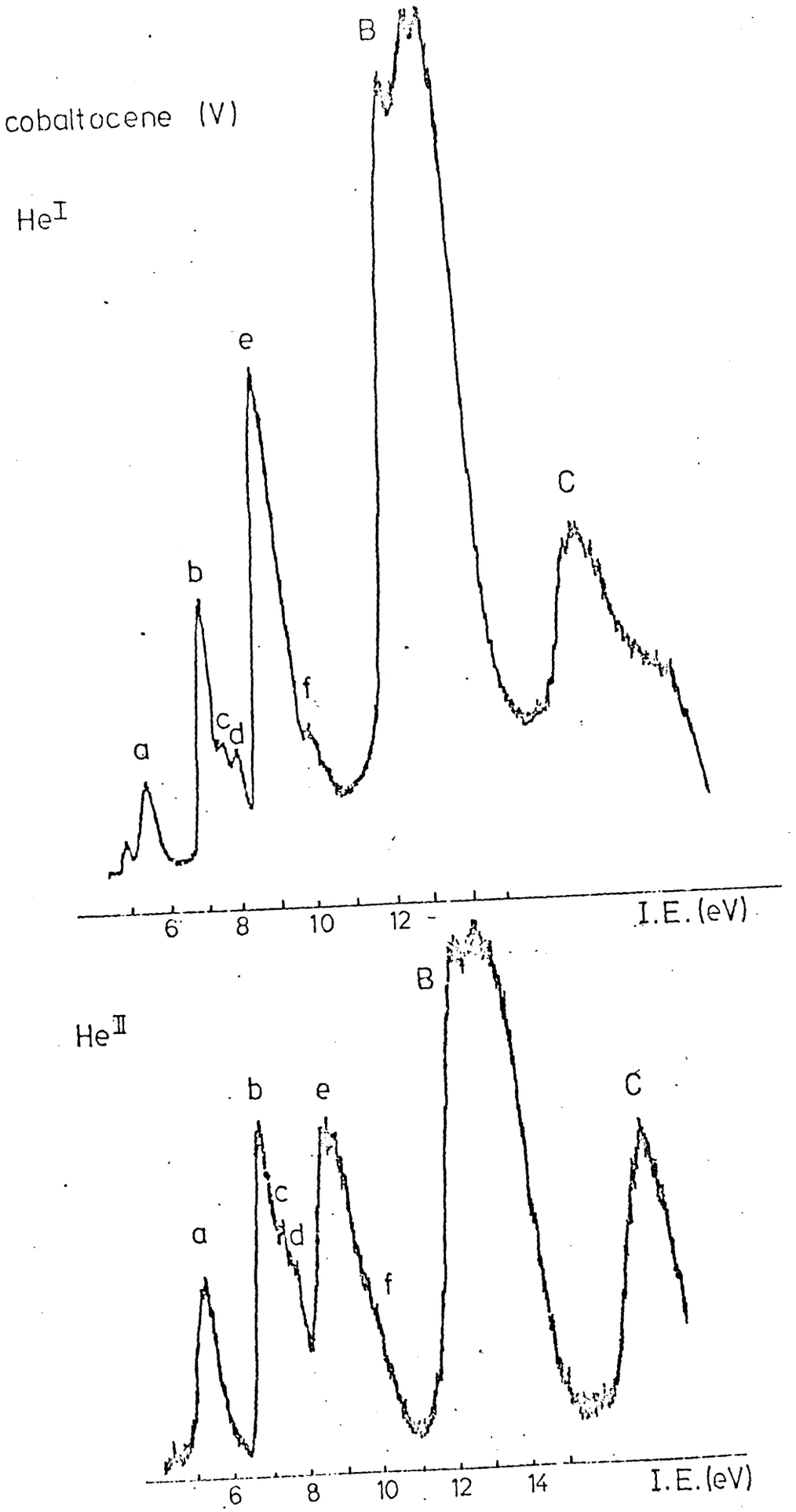
cobaltocene (V)
He^I
B
e
C
b
f
c
d
a
6
8
10
12
I.E. (eV)
He^II
B
b
e
C
c
a
d
f
6
8
10
12
14
I.E. (eV)

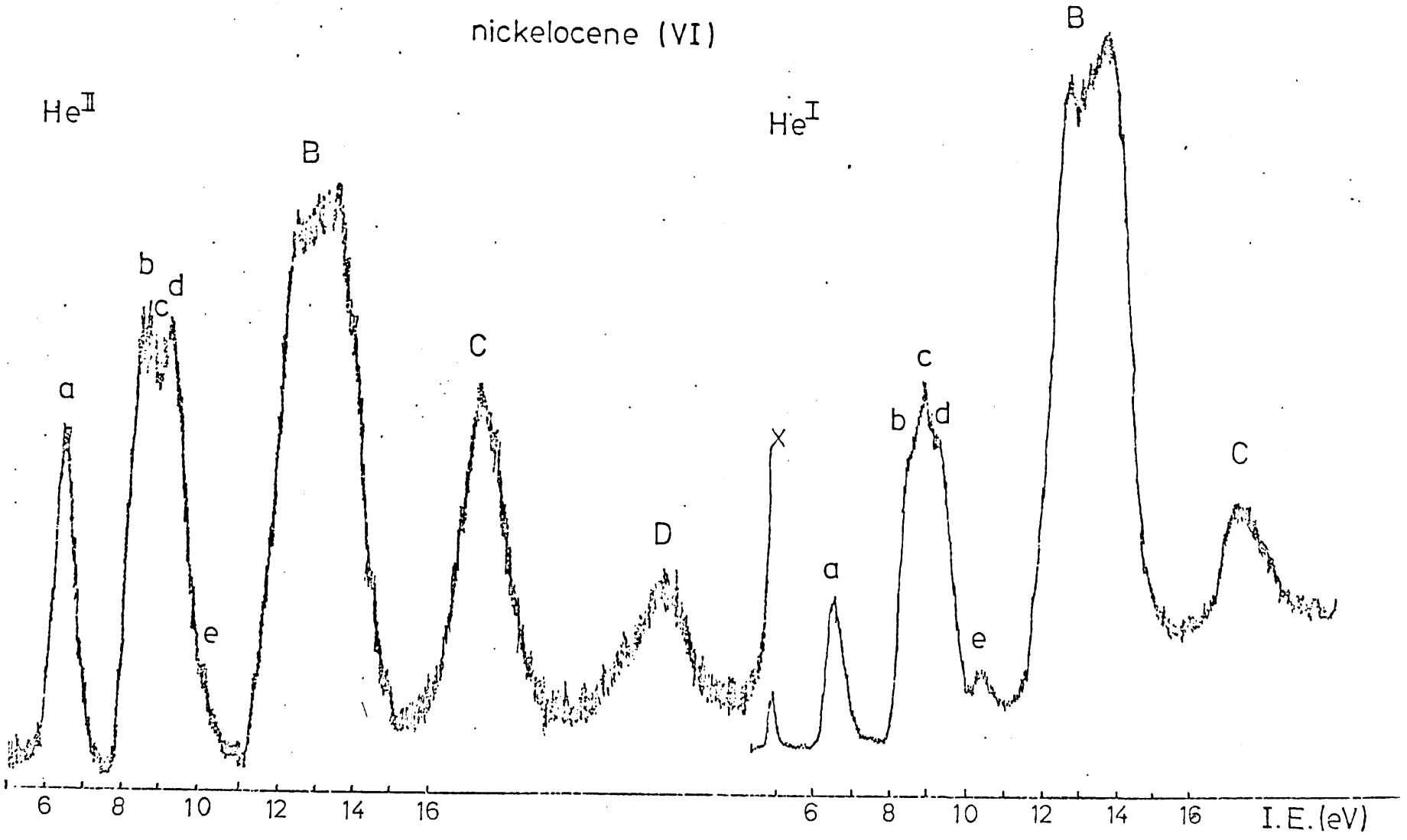
nickelocene (VI)
He II
He I
a
b
c
d
e
B
C
D
X
6
8
10
12
14
16
I.E.(eV)

1,1'-dimethyl manganocene (IIIa)

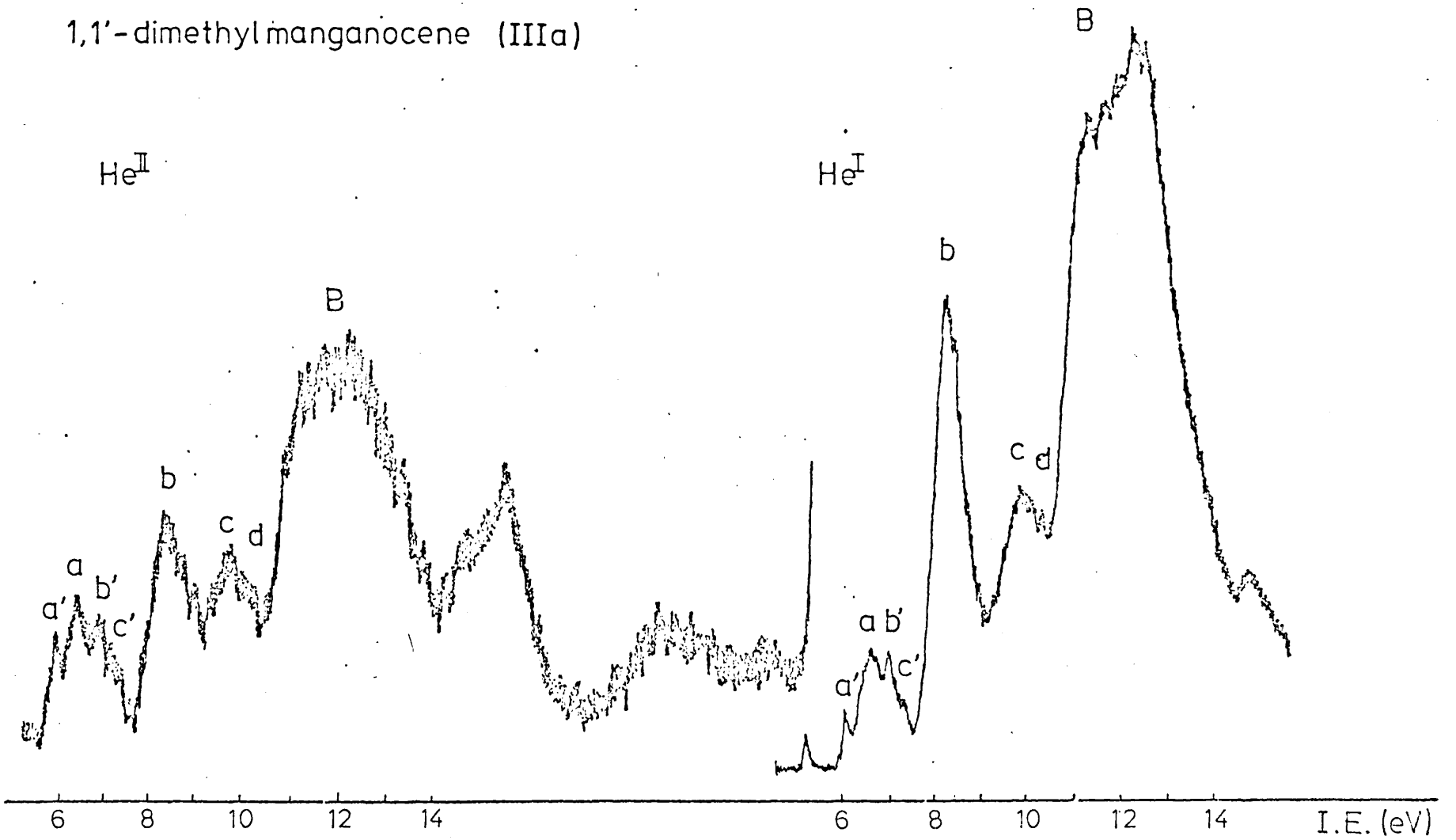

ruthenocene (VII)

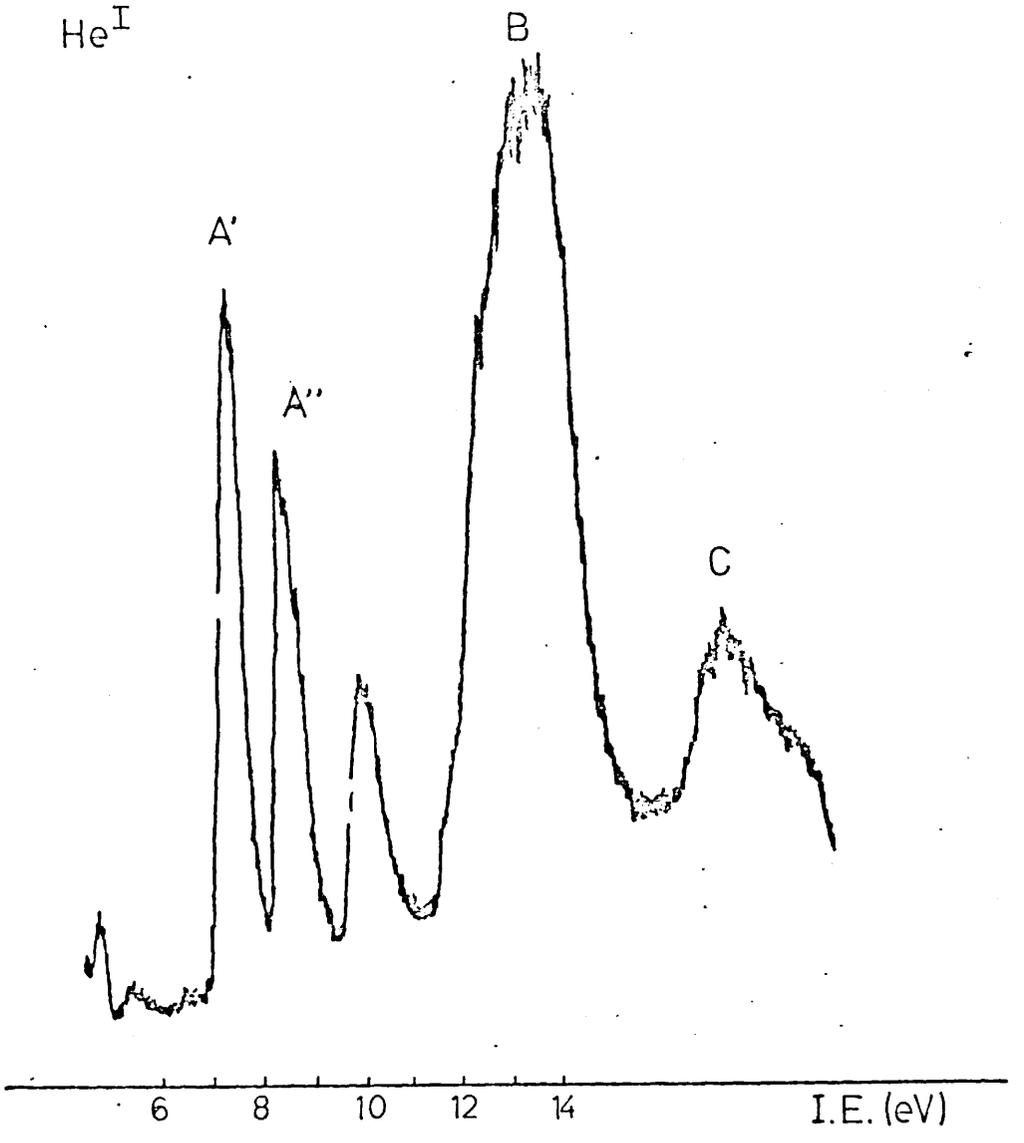

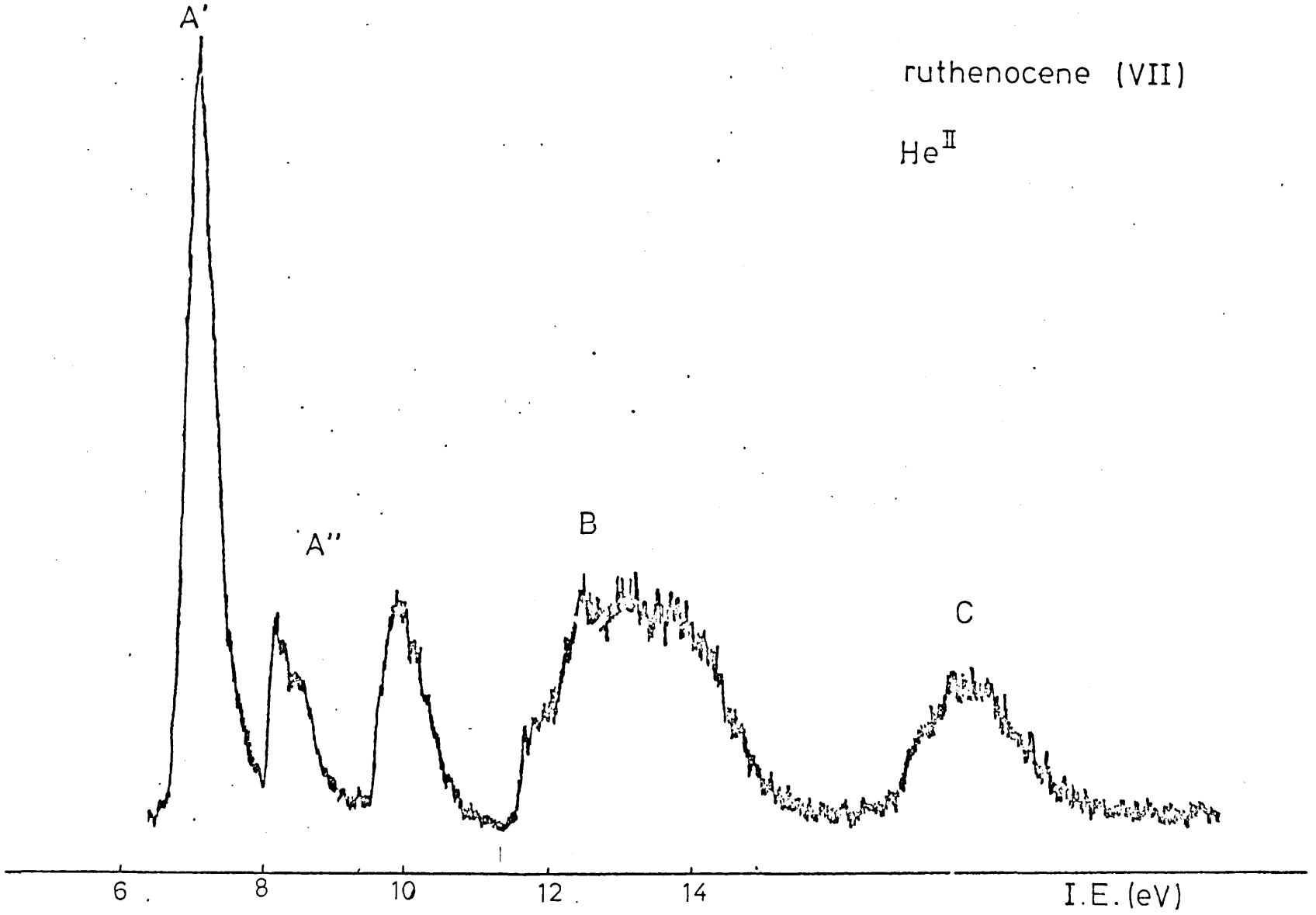
A'
A''
B
C
ruthenocene (VII)
He II
6
8
10
12
14
I.E. (eV)

bis-(cycloheptadienyl)ruthenium (VIIa)

He^{I}

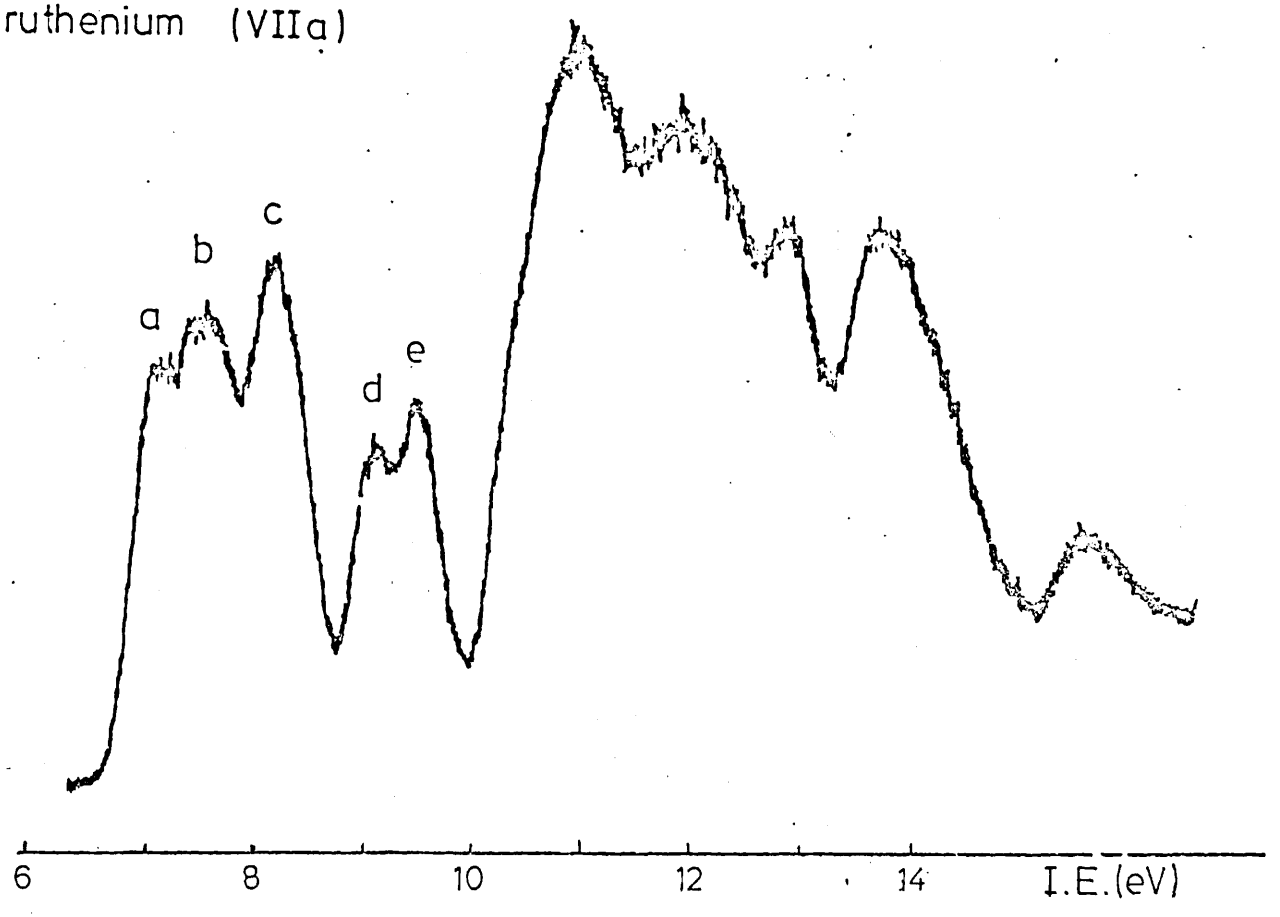

bis-(cycloheptadienyl) ruthenium (VIIa)

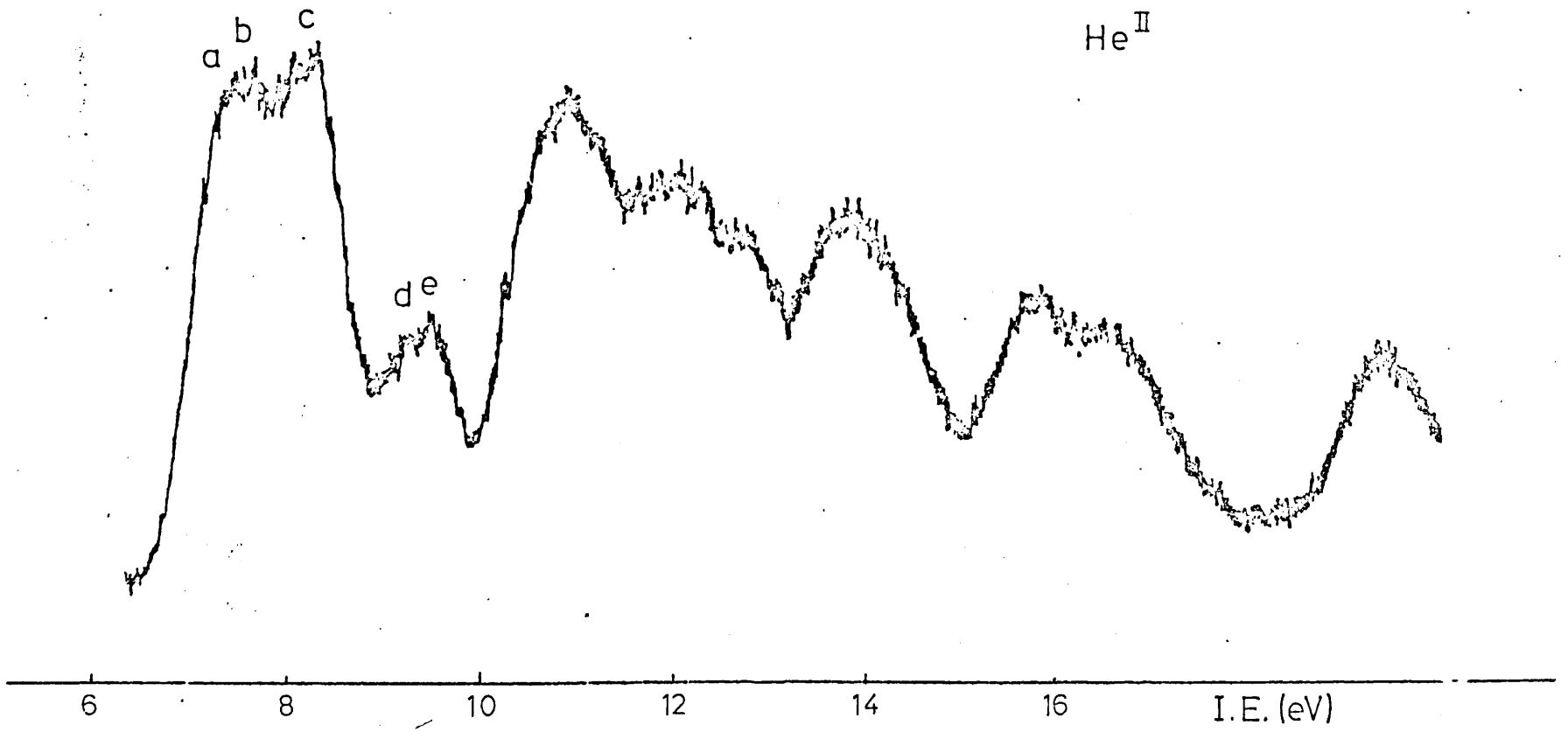

Chapter 4

Photoelectron spectra of some diene-cyclopentadienylmetal complexes

4.1 INTRODUCTION AND SUMMARY

This chapter is concerned with the study of bonding in some complexes of cobalt, rhodium and iridium, containing both the η^5-cyclopentadienyl ligand and a diene, bonded directly to the metal.

Complexes (I) to (XII) were synthesised (fig 4.1), and their HeI and HeII UV PE spectra recorded. Assignment of the spectra with the aid of simple molecular orbital diagrams and relative intensity data, is attempted, and the assignments are used in a discussion of some aspects of the bonding in the complexes. Where possible, comparison is made with PE spectra of complexes discussed in earlier chapters.

Figure 4.1 η^5-cyclopentadienyldieneM complexes (M = Co, Rh, Ir)

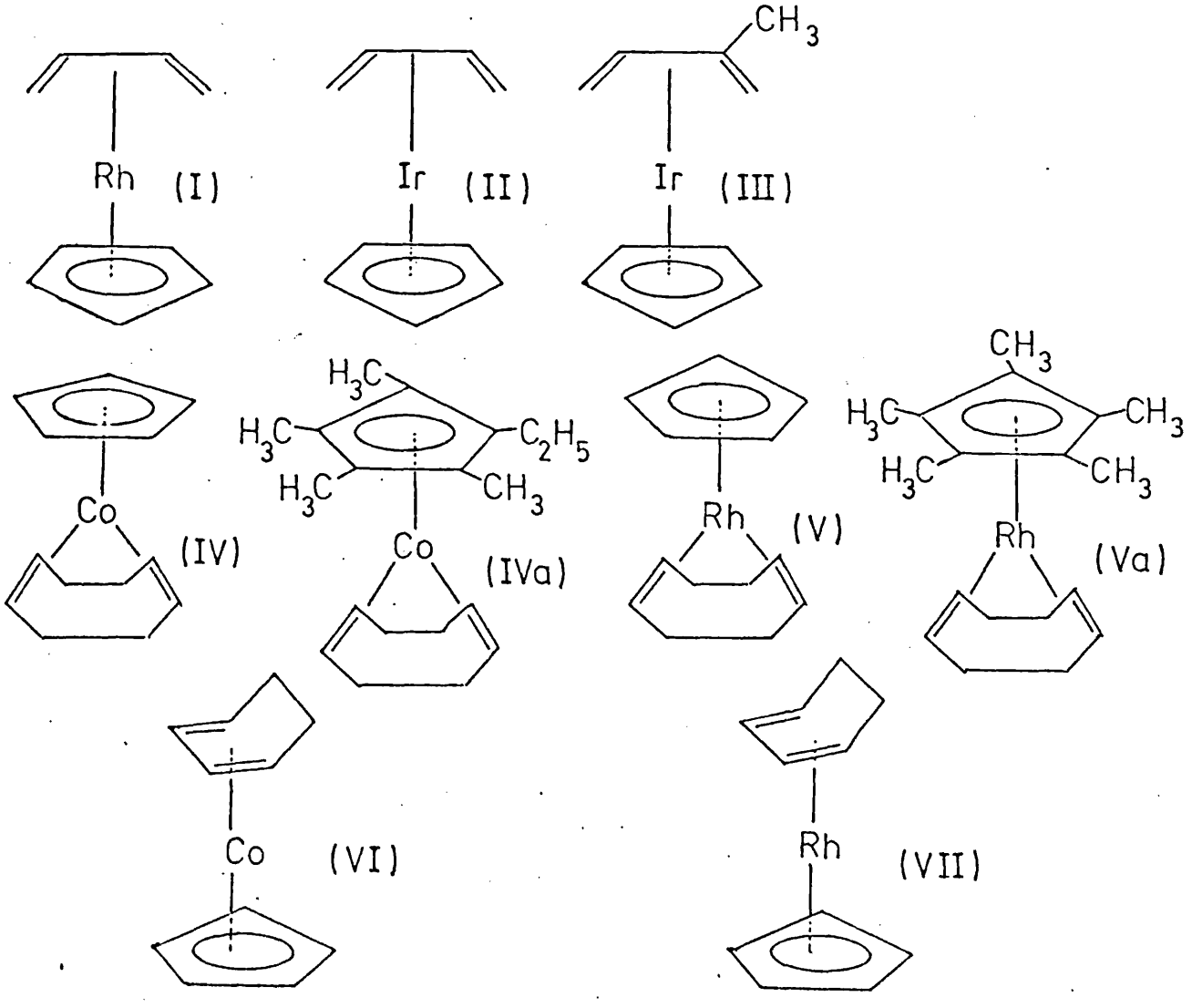

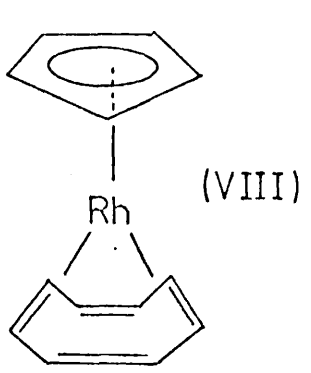

(VIII)

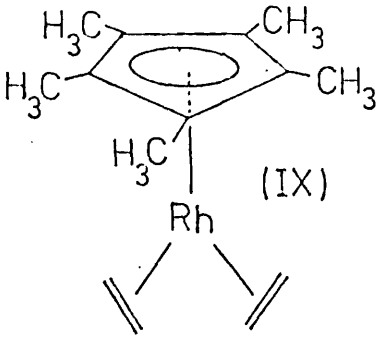

(IX)

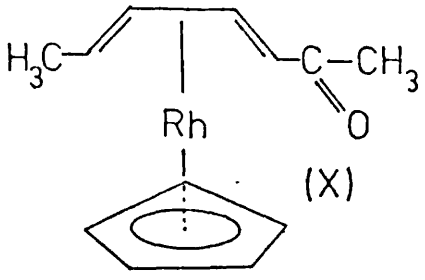

(X)

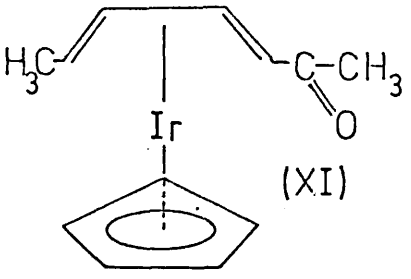

(XI)

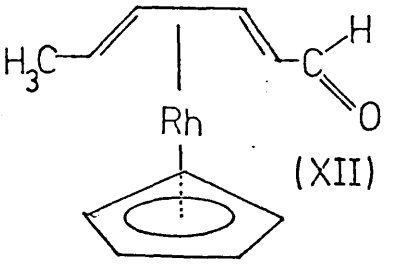

(XII)

(I) (η^5-cyclopentadienyl)(η^4-buta-1,3-diene)rhodium

(II) (η^5-cyclopentadienyl)(η^4-buta-1,3-diene)iridium

(III) (η^5-cyclopentadienyl)(η^4-2-methylbuta-1,3-diene) iridium

(IV) (η^4-cycloocta-1,5-diene)(η^5-cyclopentadienyl)cobalt

(IVa) (η^4-cycloocta-1,5-diene)(η^5-tetramethylethylcyclo-pentadienyl)cobalt

(V) (η^4-cycloocta-1,5-diene)(η^5-cyclopentadienyl)rhodium

(Va) (η^4-cycloocta-1,5-diene)(η^5-pentamethylcyclopenta-dienyl)rhodium

(VI) (η^4-cyclohexa-1,3-diene)(η^5-cyclopentadienyl)cobalt

(VII) (η^4-cyclohexa-1,3-diene)(η^5-cyclopentadienyl)rhodium

(VIII) (η^4-cycloocta-1,3,5,7-tetraene)(η^5-cyclopentadienyl) rhodium

(IX) (η^5-pentamethylcyclopentadienyl)(bisethylene)rhodium

(X) (η^4-hepta-3,5-dien-2-one)(η^5cyclopentadienyl)rhodium

(XI) (η^4-hepta-3,5-dien-2-one)(η^5cyclopentadienyl)iridium

(XII) (η^4-hexa-2,4-dien-1-al)(η^5cyclopentadienyl)rhodium

4.2 HISTORICAL BACKGROUND

In 1956, Chatt and Venanzi reported the first organo-rhodium complex, prepared by refluxing an ethanolic solution of rhodium trichloride (hydrated) with an excess of cycloocta-1,5-diene [241]. The orange solid, $C_8H_{12}RhCl$, was found to be dimeric, diamagnetic, and a non-electrolyte in benzene; structure (4)1 was assigned.

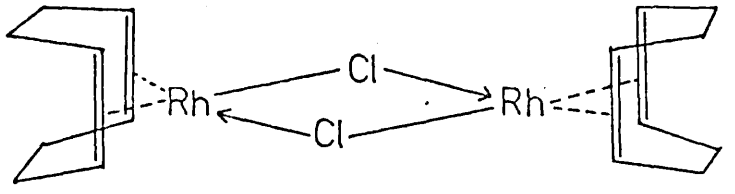

(4)1

From this complex, the mononuclear complex (4)2 was obtained by reaction with sodium cyclopentadienide [242]; however, attempts to obtain analogous complexes with other olefins and diolefins met with little success. Bonding

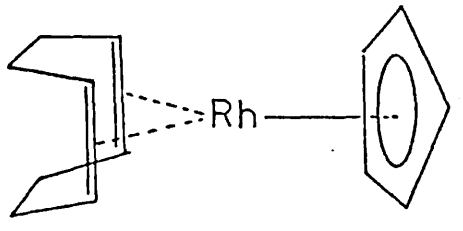

(4)2

between the cyclopentadienyl ring and the metal was thought to be similar to that in ferrocene.

This work led to an interest in organorhodium chemistry and many reports of reactions of these complexes and preparations of related complexes, appeared.

The first report of the cobalt analogue of (4)2 was published in 1961 (4)3 [243].

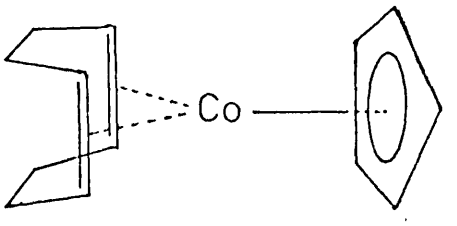

(4)3

This complex was prepared by an entirely different method (from η^5-cyclopentadienyldicarbonylcobalt and the diene) since the cobalt analogue of (4)1 is unknown.

Some reactions of these rhodium and cobalt complexes were investigated in 1967 by Lewis and Parkins [244]. The work by King [243] was an attempt to prepare cobalt complexes analogous to the tricarbonyliron-diene compounds which were being reported at the time [63, 65]. (η^5-cyclopentadienyl)(η^4-cyclopentadiene)cobalt [71] and (η^5-cyclopentadienyl)(η^4-cycloocta-1,3,57-tetraene)cobalt [245a) b)] were already known.

The η^5-cyclopentadienyl cobalt complexes proved to be more difficult to characterise than the corresponding tricarbonyliron ones, and although (η^4-cyclohexa-1,3-diene)(η^5-cyclopentadienyl)cobalt, (VI), was reported by King [243], attempts to isolate (η^5-cyclopentadienyl)(η^4-buta-1,3-diene)cobalt failed.

Nakamura and Hagihara proposed structure (4)4 for the cyclooctatetraene complex [245a)] on the basis of i.r., UV, and proton n.m.r. spectroscopic data, and chemical reactivity. The structure was confirmed in 1962, when the rhodium analogue was also described and shown to have a similar structure [246].

(4)4

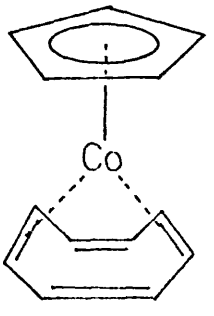

In 1962 the first synthesis of a rhodium complex with a mono-olefin was reported [247], (4)5, together with X-ray diffraction data, and in 1963, King prepared (η^5-cyclopentadienyl)(bisethylene)rhodium, (4)6, from reaction of (4)5 with sodium cyclopentadienide [248].

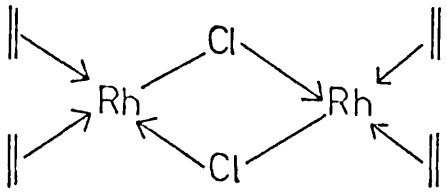

(4)5

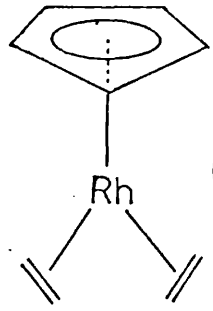

(4)6

Complex (4)6 was believed to have a structure analogous to (4)2, with the two ethylene units replacing the coordinating diene. However, the unexpected presence of two resonances from the ethylene protons could not be explained until further structural studies were reported in 1964 [249]. Many compounds of type (4)7 have been prepared and their reactions studied [250 a) b) c)].

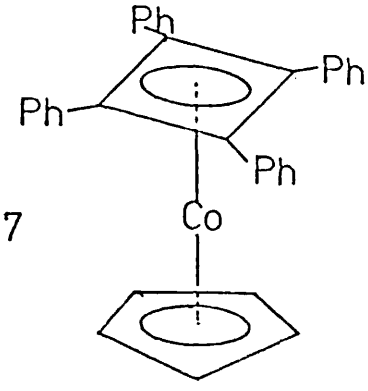

(4)7

Ph = C_6H_5

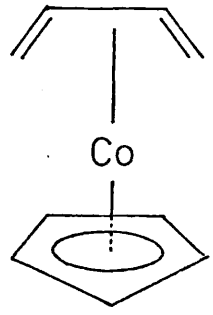

(4)8

Complex (4)8 has been reported [251], but no satisfactory method for preparation and isolation exists. King failed to characterise the complex, and it has been suggested [252] that it is formed as an intermediate in a catalytic reaction sequence, involving polymerisation of

butadiene. The rhodium analogue is well known [253] and the iridium complex has been described recently [254].

In 1965, the first example of a rhodium complex with an acyclic diene was reported [255 a) b)], together with X-ray diffraction data. Two methods of preparation were described:

a) direct reaction of rhodium trichloride with butadiene
b) reaction of rhodium trichloride with cyclo-octene, and treatment of the resulting complex with butadiene.

The product is bisbutadienerhodium chloride.

In 1968, a novel ring contraction reaction [256], whereby hexamethyldewarbenzene was converted to a pentamethylcyclopentadienylrhodium complex, was published (4)9. From this product, mononuclear rhodium complexes, analogous

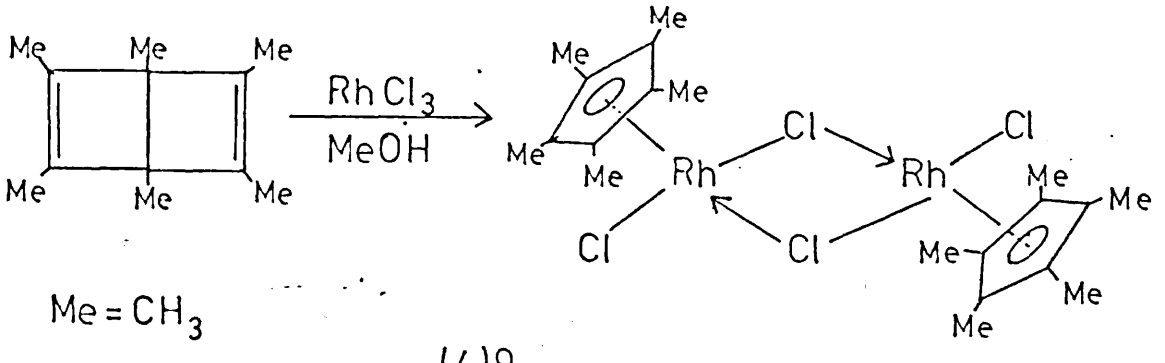

(4)9

to the Chatt and Venanzi compound (4)2, were readily available.

Further work on these complexes was published in 1969 [257, 258], in which it was reported that cycloocta-1,3-, 1,4-, and 1,5-dienes all reacted with the dimeric complex (product in (4)9) to give a 1,5-diene complex, and a similar reaction was found to occur for iridium. (η^4-cyclohexa-1,3-diene)(η^5-pentamethylcyclopentadienyl)rhodium was also

prepared; in this case, the starting material, cyclohexa-1,4-diene isomerised to give the 1,3-diene complex. Reactions of the substituted cyclopentadienylrhodium complex were reported in 1973 [259]; here the preparative method involved displacement of ethylene from $[Rh(C_2H_4)_2Cl]_2$ [247].

Further studies of the pentamethylsubstituted compounds were reported in 1976 together with a new method of synthesis for the cyclooctatetraene complex [260]. Some reactions of the cyclopentadienylrhodium complex (VII) and preparations of the cobalt and iridium analogues have been reported by Lewis et al [261]. Other iridium complexes have also been described recently [254, 261, 262].

Following the work described here (although this is not intended as a comprehensive review), many reactions of similar complexes have been studied, and general methods of preparation (used in synthesis of new complexes) have evolved. For example, it is now more usual to treat a dimeric complex of type (4)1 with thallium cyclopentadienide, than with sodium cyclopentadienide, to obtain a mononuclear complex of type (4)2, containing an unsubstituted cyclopentadienyl group. The mononuclear pentamethylcyclopentadienyl complexes are prepared by a different method, from the dimeric complex (4)9 [263].

A convenient starting material for preparation of many of the cyclopentadienyl-diene complexes, used in the current work is chlorobis(cyclooctene)rhodium [255] for which a convenient synthesis is given by A.van der Ent and A. L. Onderdelinden [264]. This complex has not been proved to be dimeric, and is represented as $[RhCl(C_8H_{14})_2]_n$. The iridium analogue is also described; molecular weight measurements suggest a dimeric structure, $[IrCl(C_8H_{14})_2]_2$.

4.3 MOLECULAR STRUCTURE

The structure of the cyclooctatetraene complex, (4)4, was assigned [245 a)] on the basis of n.m.r., i.r. and

UV spectroscopic data and confirmed by further n.m.r. studies [246], which indicated a similar structure for the rhodium analogue and also for the (η^4-cycloocta-1,5-diene)(η^5-cyclopentadienyl) complexes of rhodium and cobalt, (IV) and (V). It is likely that complexes (IVa) and (Va) have similar structures.

X-ray diffraction data were published in the early 1960s for the complexes $[(C_8H_{12})_2Rh_2Cl_2]$ [265], and $[RhCl(CO)_2]_2$ [266], and also for complex (4)5 [247]. The complex was expected to be structurally similar to $[RhCl(CO)_2]_2$; in the latter complex the rhodium atoms and bridging chlorine atoms lie in two planes forming an angle of 124°, and the $[RhCl(CO)_2]_2$ units appear to be connected by Rh - Rh bonds.

The first X-ray diffraction data for a mononuclear complex of this type were published in 1965 for bisbutadienerhodium chloride [255]. The structure in the solid state is shown in figure 4.2, with a Rh - Cl bond distance of 2.45 (3) Å and an average Rh - C distance of 2.20 (5) Å. Molecular symmetry is C_{2v}.

Figure 4.2 Bisbutadienerhodium chloride

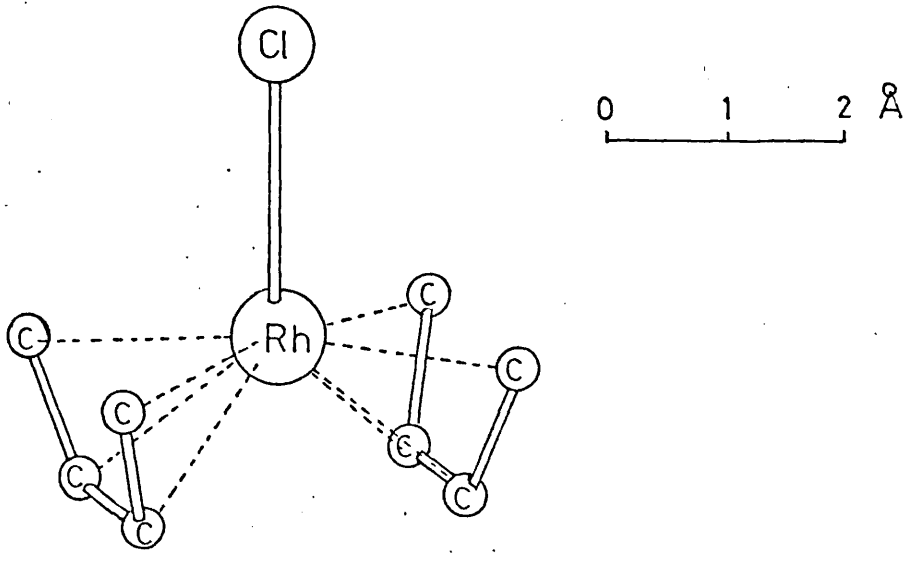

X-ray diffraction data are not available for any of the complexes listed in figure 4.1, but most of the structural features are fairly well established from X-ray diffraction studies or n.m.r. studies of similar complexes.

Variable temperature proton n.m.r. studies of (η^5-cyclopentadienyl)(bisethylene)rhodium, (4)6 [249] have shown that the ethylene groups rotate about the rhodium-ethylene bond axis with a rotational energy barrier of ~ 6 kcal. mole^{-1}. However these ethylene groups do not exchange with free ethylene molecules, and thus remain bonded to the metal as they rotate. In this study the molecule is pictured as octahedral, with the cyclopentadienyl group centred on one face, and co-ordinated with the three apices of that face. Ethylene is bonded at two other corners, while an unshared electron pair occupies the sixth apex (fig 4.3).

Figure 4.3 Structure of (η^5-cyclopentadienyl)(bisethylene)-rhodium

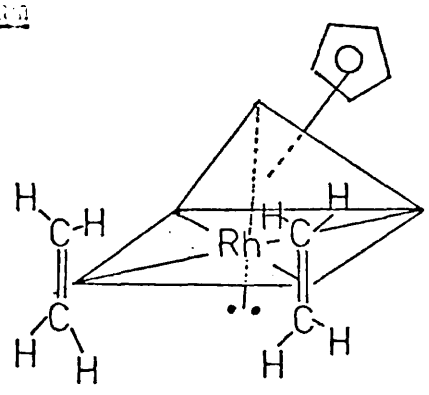

The crystal structures of (η^5-cyclopentadienyl)(η^4-2,3-dichlorobutadiene)rhodium and (η^5-cyclopentadienyl)(η^4-2,3-dimethylbutadiene)rhodium have been reported [267] and the structures of the unsubstituted butadiene complexes (I) and (II), and of the monomethyl substituted complex (III) are assumed to be similar.

The molecules have approximate mirror planes (σ_1) (figure 4.4) through atom C_5 and the mid point of the $C_2 - C_3$ and $C_7 - C_8$ bonds. The cyclopentadienyl and butadiene groups

Figure 4.4 Projection of complex of type (I) onto the cyclopentadienyl ring

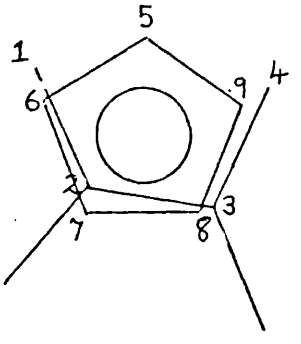

are planar, and the C_5 end of the cyclopentadienyl ring is inclined towards the plane of the diene, the two planes intersecting at approximately 11°. There are no significant variations in carbon-carbon bond distances for the butadiene unit; values reported are: C_1-C_2, 1.43 (2) Å; C_2-C_3, 1.44 (2) Å; C_3-C_4, 1.41 (2) Å. Inequalities were noted in the cyclopentadienyl ring carbon-carbon bond distances; C_7-C_8 is the shortest bond, and C_7 and C_8 lie furthest from the metal atom. The two longest bonds, C_5-C_6 and C_5-C_9, are between those carbon atoms lying closest to the metal.

4.4 ELECTRONIC STRUCTURE

Early theoretical studies of bonding in ethylene-rhodium complexes [268, 269] suggested that tetra-coordinated Rh(I) but not hexa-coordinated Rh(III), has a vacant p_z orbital, which, by combination with the metal d_{xz} and d_{yz} may form hybrid orbitals suitable for forming strong dative π bonds with the antibonding orbitals of a diene.

From the time of the first isolation of complex (4)2 in 1957 [242], the cyclopentadienyl ring was thought to be sandwich bonded to the metal, as in ferrocene. Detailed studies of complexes of the type (η^5-cyclopentadienyl) (η^4-cyclopentadiene)M (where M = Co, Rh) [71], showed that one cyclopentadiene ring is bonded to the metal via a conjugated diene system, while the other is bonded via a ring delocalised π system.

Bonding in the mono η^5-cyclopentadienyl transition metal carbonyls is discussed by Green [102]. A procedure that is commonly adopted when this type of bonding is encountered is the separate treatment of the cyclopentadienyl-metal- or carbonyl-metal-fragment followed by consideration of its interaction with the rest of the molecule. This approach was used for η^4-buta-1,3-dienetricarbonyliron in Chapter 2.

The tricarbonyl group attached to a transition metal, is known to have strong electron donating/accepting characteristics, and a net negative charge has been found to exist on the butadiene ligand of η^4-buta-1,3-dienetricarbonyliron [23], indicating that the butadiene ligand acts, in this complex, as a strong electron acceptor, and weaker donor. That is, the metal d - $b_2^*\pi$ is the dominant interaction, and bands in the PE spectrum due to ionisation from this orbital would be expected to show a large amount of ligand p character compared to the d character of those arising from the weaker $a_2\pi$ - d^* interaction.

By comparison with the tricarbonyl group, the Cp ring (local D_{5h} symmetry) has strong donor properties but in general is a poor electron acceptor. This is illustrated by the PE spectra and energy level diagrams for the metallocenes (chapter 3). Under D_{5h} symmetry the main ligand-metal bonding interactions are likely to be the ligand $e_{1g}\pi$ - metal e_{1g}d combination, representing ligand to metal donation, and the

metal e_{2g}d - ligand e_{2g} π combination, representing metal to ligand donation. Of these, the latter interaction is expected to be relatively small, since the $e_{2g}\pi$ antibonding orbital is not the lowest unoccupied ligand level, and there is likely to be a relatively large energy difference between this orbital and the e_{2g}d level. This prediction is confirmed by the PE spectra of the metallocenes, particularly ruthenocene, in which the e_{1g} π and e_{1u} π ligand levels are resolved, showing the e_{1g} π orbital to have a large amount of d character. The e_{2g} d level does not show a correspondingly large increase in ligand character. This reasoning leads to prediction of a net positive charge on the cyclopentadienyl rings with respect to the metal atoms at variance with the generally accepted view of the metallocenes having the metal in oxidation state 2, although in agreement with some molecular orbital calculations.

Thus comparing complex (I) with η^4-butadiene-1,3-tricarbonyliron, the net negative charge on the butadiene ligand would be relatively greater.

An X-ray photoelectron spectroscopic study of some transition metal carbonyl and cyclopentadienyl complexes gives the charge distribution for these molecules [235]. For the metallocene-type complexes it was found that the cyclopentadienyl rings sustained a slight overall positive charge; for η^5-cyclopentadienyltricarbonylmanganese, there is an observed net electron transfer from the ring to the carbonyl groups via metal d orbitals, and the observed shift of the ring carbons to higher binding energy, compared with the metallocenes, implies even greater ligand (Cp) to metal donation, which seems reasonable, in view of the fact that the tricarbonyl group has strong acceptor properties.

Complexes (I) to (XII), may be divided into three main categories as far as their electronic structure is concerned; in each case the η^5-cyclopentadienylmetal unit

is expected to bond to the olefin in a slightly different way.

(i) The conjugated diene cyclopentadienyl metal complexes

The bonding of a conjugated diene to the cyclopentadienylmetal group may be considered similar to that observed in the tricarbonyliron complexes of chapter 2. The same arguments arise as to the relative contributions of the σ and π valence bond structures, or in MO terms, the relative importance of the metal d-ligand π^* and the ligand π-metal d^* contributions.

A detailed study of the bonding in two cobalt complexes of this type was published by Kettle and Mason [163] (figure 4.5), and the relative importance of the π and σ valence bond contributions to the bonding was discussed.

Figure 4.5 Metal-ligand bonding in two η^5cyclopentadienylcobalt complexes

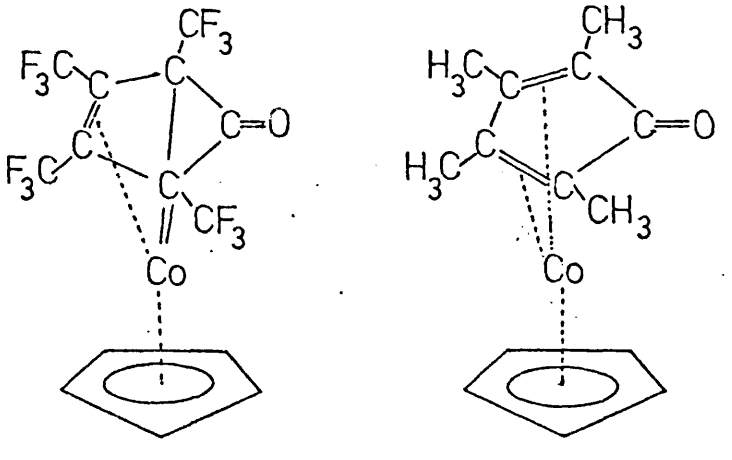

In complex (a) the σ structure was thought to be dominant (in MO terms, electron donation from filled metal d orbitals to the ligand π antibonding orbitals), while for (b), the π structure was thought to show the more important contribution (that is, electron donation from the highest occupied ligand π orbital to metal d antibonding orbitals). The discussion suggests that the change in geometry induced by the electron withdrawing $-CF_3$ groups encourages contribution from the σ valence bond structure, that is, increased metal to ligand donation, as observed by Brundle and Robin [73].

The PE spectrum of complex (I), therefore, might be expected to show similar features to that of η^4-butadienetricarbonyliron, except that the metal d to ligand b_2 π^* donation is likely to be more important in complex (I), since the η^5-Cp group acts as a strong donor and poor acceptor of electrons, although this effect may also increase the ligand to metal ($a_2\pi$ - d*) contribution. The relative net negative charges on the butadiene ligand compared to the metal, in each of these complexes have not been compared.

Photoelectron spectroscopic data have not been published for complexes (I) to (XII); however data for the diene ligands are available and were fully discussed in chapter 2. The MO diagram for the Cp group in D_{5h} symmetry is well known, and a qualitative molecular orbital diagram (figure 4.6), similar to that for η^4-butadienetricarbonyliron, has been constructed for complex (I). The CpM unit has been considered separately [101]; the d orbitals split into three sets under the five-fold symmetry, and there is

Fig 4.6 Molecular orbital interaction diagram for complex (I)

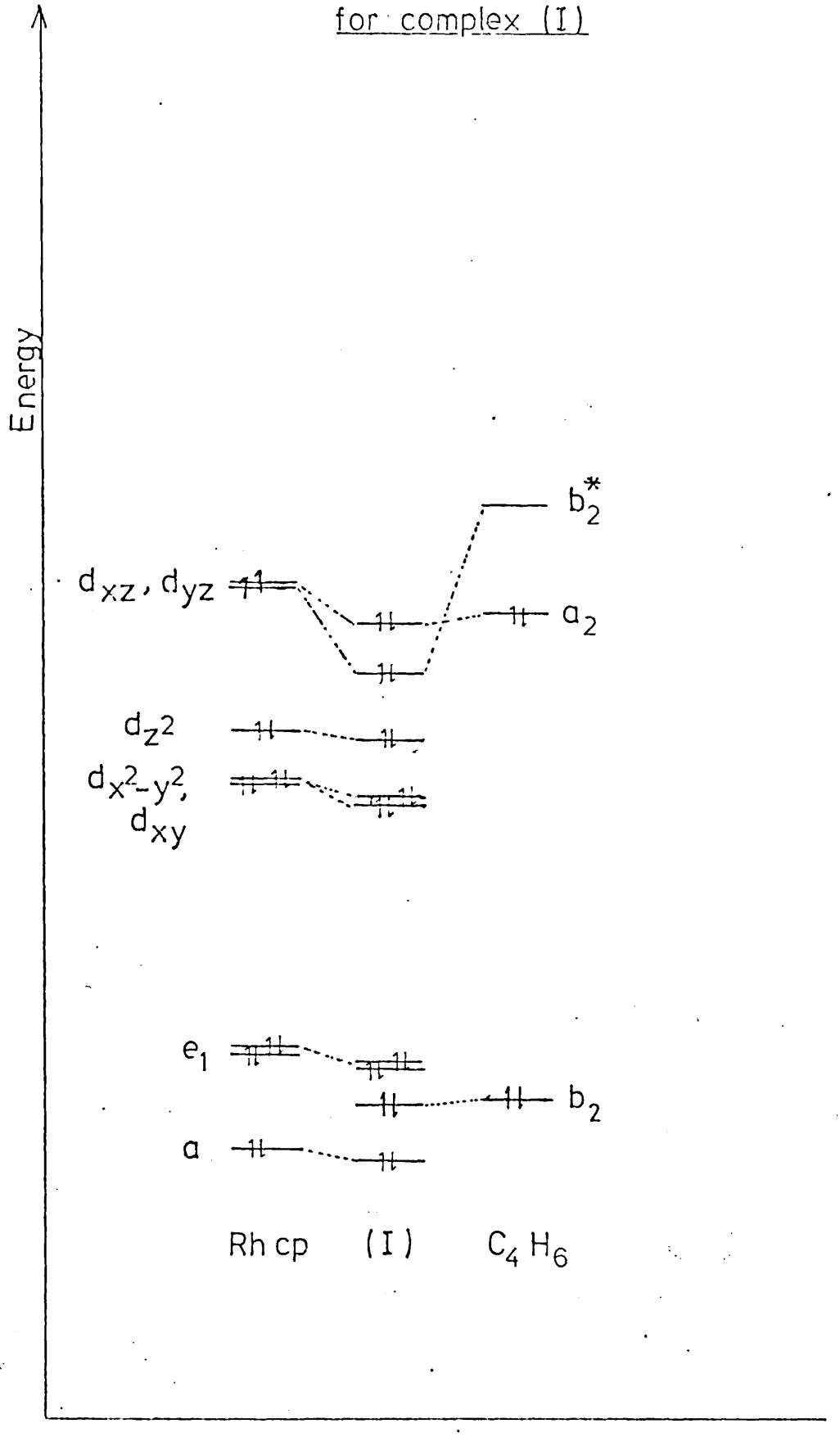

some interaction with the e_1 and a ring molecular orbitals. The C_5 rotation axis was defined as the z axis. To the right of figure 4.6 are shown the butadiene MO energy levels* according to values obtained from PE spectra [45].

As for the tricarbonyliron complexes, interaction is expected between the $\psi_2(a_2)$ butadiene level and the partly filled metal d_{xz} orbital, and between the $\psi_3^*(b_2)$ butadiene level, and the d_{yz} metal orbital. The diagram is qualitative; it is not possible to determine the ordering of the molecular orbitals from the information available. There are no reports of detailed MO calculations for any of these molecules.

The appearance of the PE spectrum of complex (I) may be predicted to some extent, and compared with that of η^4-butadienetricarbonyliron. The d_{xy} and $d_{x^2-y^2}$ levels will not be at the same energy relative to the a_2 and b_2 diene levels and should appear as distinct bands. Due to the lowering in symmetry of this complex compared to the metallocenes, it is unlikely that the 'metal' $d_{x^2-y^2}$ and d_{xy}, and the 'cyclopentadienyl' e_1 levels will remain degenerate. The π Cp e_1 levels are predicted to give rise to a PE band in the same region as the butadiene b_2 π bonding orbital. The $a_2\pi - d_{xz}^*$ and $b_2\pi^* - d_{yz}$ ionisations will both give rise to bands in the same region as metal d

*For the butadiene energy level diagram, the C_2 rotation axis was taken as z axis, thus resulting in symmetry labels a_2 and b_2 as shown in chapter 2. Taking the z axis perpendicular to the plane of the carbon atoms results in the labelling a_1 (equivalent to a_2) and b_2.

ionisations, but their energies relative to the corresponding bands in the PE spectrum of η^4-butadienetricarbonyliron, cannot be predicted.

An additional consideration for the rhodium complexes is that the metal p orbitals may now contribute to the bonding; p_z may interact with $\psi_1(b_2)$, although the energy difference is likely to be large, p_y with $\psi_3(b_2^*)$ and p_x with $\psi_2(a_2)$.

(ii) The (bismonoene)cyclopentadienylmetal complex

A general description of the bonding of the ethylene ligand to transition metals is given by Green [102]. If ϕ_1 and ϕ_2 are the two $2p_z$ atomic orbitals of ethylene, the π MOs are represented as:-

$$\psi_1 = \frac{1}{\sqrt{2}}(\phi_1 + \phi_2)$$
$$\psi_2^* = \frac{1}{\sqrt{2}}(\phi_1 - \phi_2) \qquad (4)10$$

The combinations of ligand (ethylene) and metal orbitals that may interact on symmetry grounds may be easily found. A convenient representation of the metal-ethylene bond, originally proposed by Dewar [270], and modified by Chatt [269] is shown in figure 4.7.

The bonding in the unsubstituted analogue of complex (IX), that is, η^5-cyclopentadienyl(bis-ethylene)rhodium, has been investigated by Cramer [249]. N.m.r. evidence is presented to show that the co-ordinated ethylene groups may rotate about the metal-ethylene co-ordination bond axis, and the energy barrier to rotation is small (~ 6 kcal mole^{-1}).

Figure 4.7 Conventional representation of a metal-olefin bond

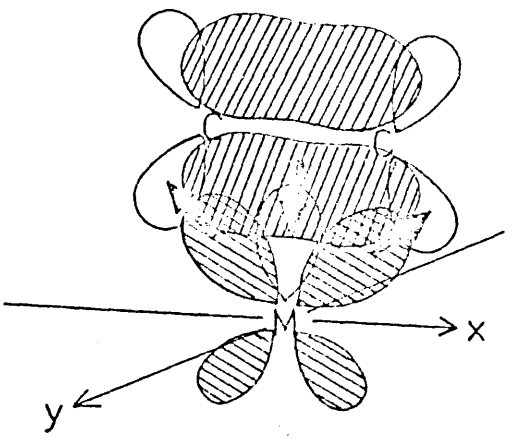

Shaded areas denote filled orbitals; arrows, the direction of electron donation

From X-ray studies of crystalline $[PdC_2H_4Cl_2]_2$ [271], $[Pt(C_2H_4)(HN(CH_3)_2)Cl_2]$ [272], $K[Pt(C_2H_4)Cl_3]H_2O$ [273], and other platinum complexes [274], the olefin double bond is found to be perpendicular to the co-ordination plane as shown in figure 4.8, with the d_{xz} metal orbital involved in the π bond. However it is also possible that the d_{yz} metal orbital could participate in a similar bond (fig. 4.9).

Figure 4.8 MO representation of metal d_{xz}-olefin bond

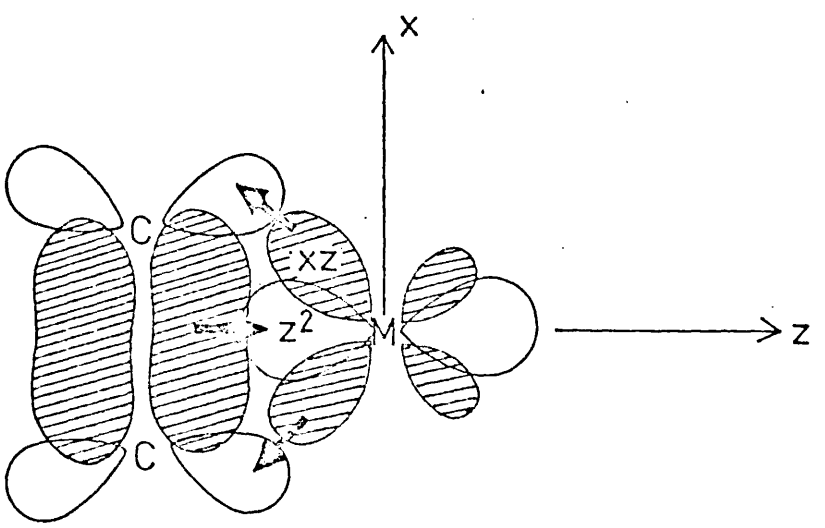

Figure 4.9 LO representation of metal d_{yz}-olefin bond

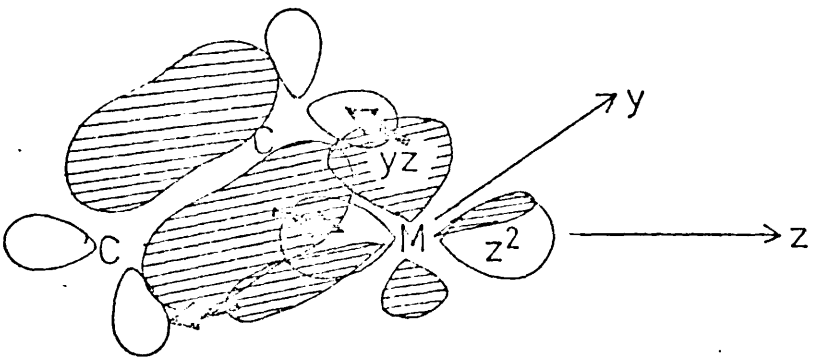

It was concluded that the ethylene group is free to rotate about the co-ordination bond axis without the bond being broken at any instance, and with different combinations of metal d orbitals forming the bond with the ethylene MOs.

Recently, the SCF X_α scattered wave calculation for Zeise's salt (figure 4.10) has been published [275], based on C_{2v} molecular geometry. It was found that the π orbital of ethylene makes the most significant contribution to metal-olefin bonding by mixing with platinum d orbitals of the correct symmetry (d_{z^2}, $d_{x^2-y^2}$). A significant degree of mixing of these orbitals was found. However it was also concluded that the metal p orbitals are not involved in the bonding to any significant extent.

Figure 4.10 Zeise's salt

$K^+[Pt(C_2H_4)Cl_3]^-.H_2O$

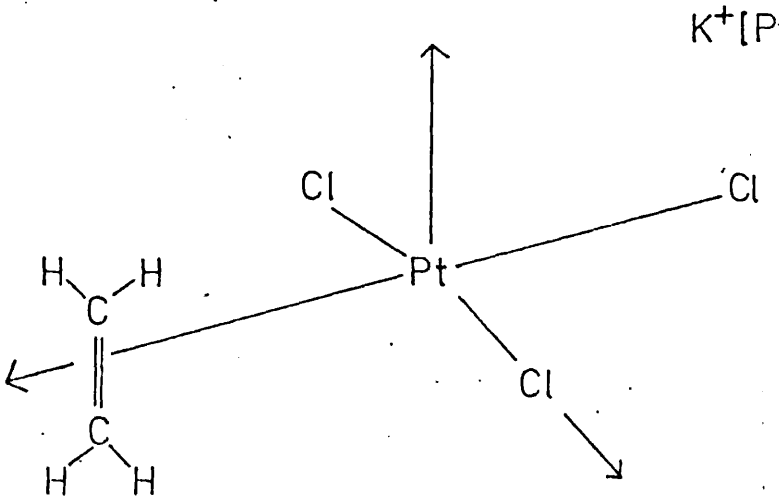

(iii) The non-conjugated dienecyclopentadienylmetal complexes

The non-conjugated dienes might be expected to bond to the cyclopentadienylmetal group in the same way as the ethylene units in complex (IX); however there will be no free rotation about the metal-ligand bond axis.

4.5 CHEMICAL REACTIONS

In 1967, work was published on the reactions of (η^4-cycloocta-1,5-diene)(η^5-cyclopentadienyl)cobalt, and its rhodium analogue [244]. Differences in reactivity of the two complexes towards the triphenylmethyl cation were noted. With the cobalt complex, electrophilic attack on the cycloocta-1,5-diene ring occurs, (4)11

$$\underset{\text{(1 mole)}}{C_8H_{12}CoC_5H_5} + \underset{\text{(1 mole)}}{Ph_3C^+BF_4^-} \longrightarrow [C_5H_5CoC_8H_{11}]^+BF_4^- \quad \text{(red crystals)} \qquad (4)11$$

Hydride abstraction from the ring occurs to give a red crystalline salt and triphenylmethane. In contrast to this, is the reaction of the rhodium complex, (4)12

$$\underset{\text{(1 mole)}}{C_8H_{12}RhC_5H_5} + \underset{\text{(1 mole)}}{Ph_3C^+BF_4^-}$$

Ph = C_6H_5

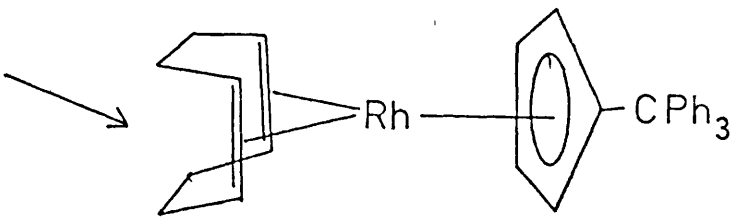

(4)12

In this case, electrophilic substitution of the cyclopentadienyl ring occurs; with two moles of triphenylmethyltetrafluoroborate, a cation is formed by hydride abstraction from the cyclooctadiene ring - $[Ph_3C.C_5H_4RhC_8H_{11}]^+$.

The marked difference between the rhodium and cobalt complexes towards triphenylmethylcation emphasises the importance of the metal in affecting the course of reaction. From this evidence too, one might expect the PE spectra of the two neutral complexes to show some differences in the bonding region.

From the above results, Lewis and Parkins concluded that initial electrophilic attack of the triphenylmethylcation on the $C_8H_{12}MC_5H_5$ complexes, proceeds by two competitive routes:

(a) electrophilic attack on the cyclopentadienyl ring

(b) hydride abstraction from the cycloocta-1,5-diene ring

and the proposed sequence was:

$$C_8H_{12}MC_5H_5 + Ph_3C^+ \longrightarrow Ph_3C.C_5H_4MC_8H_{12} + H^+$$

$$Ph_3C.C_5H_4MC_8H_{12} + Ph_3C^+ \longrightarrow Ph_3CH + [\, Ph_3C.C_5H_4MC_8H_{11} \,]^+$$

With the cobalt complex, hydride abstraction occurs preferentially; once the cation $[\, C_5H_5CoC_8H_{11} \,]^+$ is formed, no further attack by the triphenylmethyl cation appears possible It was found that the electrophilic substitution reaction does occur with the cobalt complex, but to a minor extent.

It has been shown [275] that (η^4-cyclohexa-1,3-diene)(η^5-cyclopentadienyl)cobalt and its rhodium analogue react with the triphenylmethyl cation to give $[\, C_5H_5CoC_6H_6 \,]^{2+}$ and $[\, C_5H_5RhC_6H_6 \,]^{2+}$, although with the tricarbonyliron complex, hydride abstraction occurs to give a dienyl complex.

Reactions of the (η^4-cyclohexa-1,3-diene)(η^5-cyclopentadienyl)metal complexes were studied, where M=Ir, Rh, Co [261, 176, 277], also reactions of the pentamethylcyclopentadienyl substituted rhodium and iridium analogues [257, 258, 278]. Until recently, cobalt complexes containing the fully substituted cyclopentadienyl ring were unknown, but (η^4-cycloocta-1,5-diene)(η^5-tetramethylethylcyclopentadienyl) cobalt has now been synthesised [279].

It was found [261] that for (η^4-cyclohexa-1,3-diene)(η^5-cyclopentadienyl)metal (M=Rh,Ir) complexes, protonation (with trifluoroacetic acid occurred first at the metal centre, followed by reversible transfer of the proton to form a cationic π-allylic complex. This seems to be in agreement with the theory of a net electron transfer from the cyclopentadienyl ring to the metal, so that the region of greatest electron density is where electrophilic attack occurs. For ferrocene, also, electrophilic attack has been proposed to occur first at the metal [280, 281]; however Friedel-Crafts substitution occurs at the cyclopentadienyl rings. Although the cobalt complex was synthesised [261] according to King's method [243], no mention was made by Lewis et al of its reactions.

Unlike the tricarbonyliron group, the η^5-cyclopentadienylmetal group (M=Co,Rh,Ir) appears to form complexes readily with non-conjugated dienes, without isomerisation of these dienes to the conjugated form. Cycloocta-1,3-, 1,4-, and 1,5-dienes react with $(C_5(CH_3)_5MCl_2)_2$, (M=Rh,Ir), to give (η^4-cycloocta-1,5-diene)(η^5-pentamethylcyclopentadienyl)M [257], with isomerisation of the 1,3- and 1,4-diene. $(C_5(CH_3)_5MCl_2)_2$, (M=Rh) reacts with cyclohexa-1,4-diene, to give the product (η^4-cyclohexa-1,3-diene)(η^5-pentamethylcyclopentadienyl)rhodium [258].

4.6 RESULTS AND DISCUSSION

The vertical ionisation energies for complexes (I) to (XII) are given in a series of tables together with relative intensity data and correlation diagrams. The PE spectra of the complexes are discussed in groups.

The rhodium and iridium complexes

Compounds (I) to (III) are expected to show a more complex set of bands in the low ionisation energy region than the corresponding tricarbonyliron compounds, since the cyclopentadienyl e_1 orbitals are expected to give rise to bands in this region.

The interaction between the CpM unit and the diene is expected to be different from that between the $(CO)_3M$ unit and the diene , as discussed in section 4.4. Ionisation energies and relative intensity data for the three CpM complexes are given in table 4.1.

Table 4.1 Ionisation energy data (eV) for complexes (I) to (III)

Complex		A	B	B'	C	D	E
(I)		7.26	8.32	8.81	10.17	10.99	13.05
Relative	(HeI)	1.0	1.6	1.9	1.5	0.9	16
Intensity:	(HeII)	1.0	2.7	3.5	1.8	0.8	5.4
(II)		7.13	8.02, 8.29	8.71, 9.02	10.52	10.93	12.85
Relative	(HeI)	1.0	2.0	2.3	1.7	0.9	14
Intensity:	(HeII)	1.0	2.8	3.2	1.8	0.8	6
(III)		7.21	8.00, 8.29	8.76, 9.08	10.50	-	12.73
Relative	(HeI)	1.0	1.9	2.1	2.5		17
Intensity:	(HeII)	1.0	2.1	3.1	2.3		6

The PE spectra of complexes (I) to (III) are essentially very similar. The most unexpected feature is that the band of lowest ionisation energy, A, is clearly not due to

ionisation from mainly metal d orbitals as was the case for all complexes studied in chapters 2 and 3. The bands in the spectra are assigned with the aid of molecular orbital considerations mentioned in section 4.4.

Band A is assigned in each case to ionisation from an orbital of mainly ligand character, the butadiene ψ_2 (a_2) bonding orbital, which interacts with the metal d_{xz} partly filled level to some extent; this MO represents ligand to metal donation and this level is destabilised in complexes (I) to (III) relative to the tricarbonyliron complex. This effect is not unexpected since the metal centre is more electron rich in complexes (I) to (III), and in valence-bond terms corresponds to a decrease in 'π' contribution to the metal-diene bond. However the butadiene ψ_3 (b_2*) antibonding-metal d_{yz} interaction gives rise to a molecular orbital that is relatively stabilised in complexes (I) to (III); ionisation from this MO is likely to be included under band B. This may be deduced from the relative intensity data for A:B:B'.

Bands B and B' also represent ionisation from the mainly metal $d_{x^2-y^2}$, d_{xy} and d_{z^2} levels. In the iridium complexes (II) and (III) bands B and B' are split, that is, the four expected energy levels are all separately resolved although they are not in the rhodium complex. One would expect larger ligand field splitting and spin orbit coupling effects from third row transition elements than for second row metals.

Bands C and D are assigned to ionisation from mainly ligand orbitals, with band C being due to the cyclopentadienyl e_1 level and band D to the bonding ψ_4 (b_2) diene level. Band D is not resolved from C in the spectrum of complex (III) and is only visible as a shoulder to the high IE side of C in the spectrum of complex (II). It is seen from the PE spectra that band D is more sensitive to methyl substitution in complex (III), therefore assignment of this band as arising from the $b_2\pi$ diene level is confirmed.

Relative intensity data are reasonably consistent with the above assignment, except that the ligand bands seem unusually low in intensity in the HeI spectra compared with those in first row complexes. This effect is predicted however, since 4d orbitals have been shown to have a higher cross section for ionisation by HeI photons than 3d orbitals (see chapters 2 and 3). The HeII relative intensities are essentially the same for all three complexes.

Figure 4.11 shows the relative ionisation energies for complexes (I) to (III) and butadiene. It should be noted that whereas the a_2 and $b_2\pi$ IEs are increased in the $Fe(CO)_3$ complexes compared to the free ligand, the opposite situation is found for complexes (I) to (III) if the assignments are correct. In fact the a_2 and b_2 diene levels are seen to be considerably destabilised on formation of the complexes (I) to (III); this suggests that the diene $b_2\pi^*$ antibonding-metal d combination is stabilised; this represents a relative increase in metal to ligand elcctron donation which is not unexpected.

Table 4.2 gives ionisation energy data for complexes (I), (VII), and (X) to (XII).

Table 4.2 Ionisation energy data (eV) for complexes (I), (VII), (X)-(XII)

Complex		A	B	B'	C	D	E
(I)		7.26	8.32	8.81	10.17	10.99	13.05
Relative Intensity	HeI	1.0	1.6	1.9	1.5	0.9	16
	HeII	1.0	2.7	3.5	1.8	0.8	5.4
(VII)		7.21	8.11	8.54	9.87	10.40	11.47(e')
Relative Intensity	HeI	1.0	1.8	2.2	1.8	1.0	2.6 (e')17
	HeII	1.0	3.0	4.1	3.1		1.6 (e')6
(X)		7.40	8.27	8.68	10.17	10.99	12.93, 13.93
Relative Intensity	HeI	1.0	5.7		1.4	0.9	41
	HeII	1.0	7.5		1.6	1.2	11

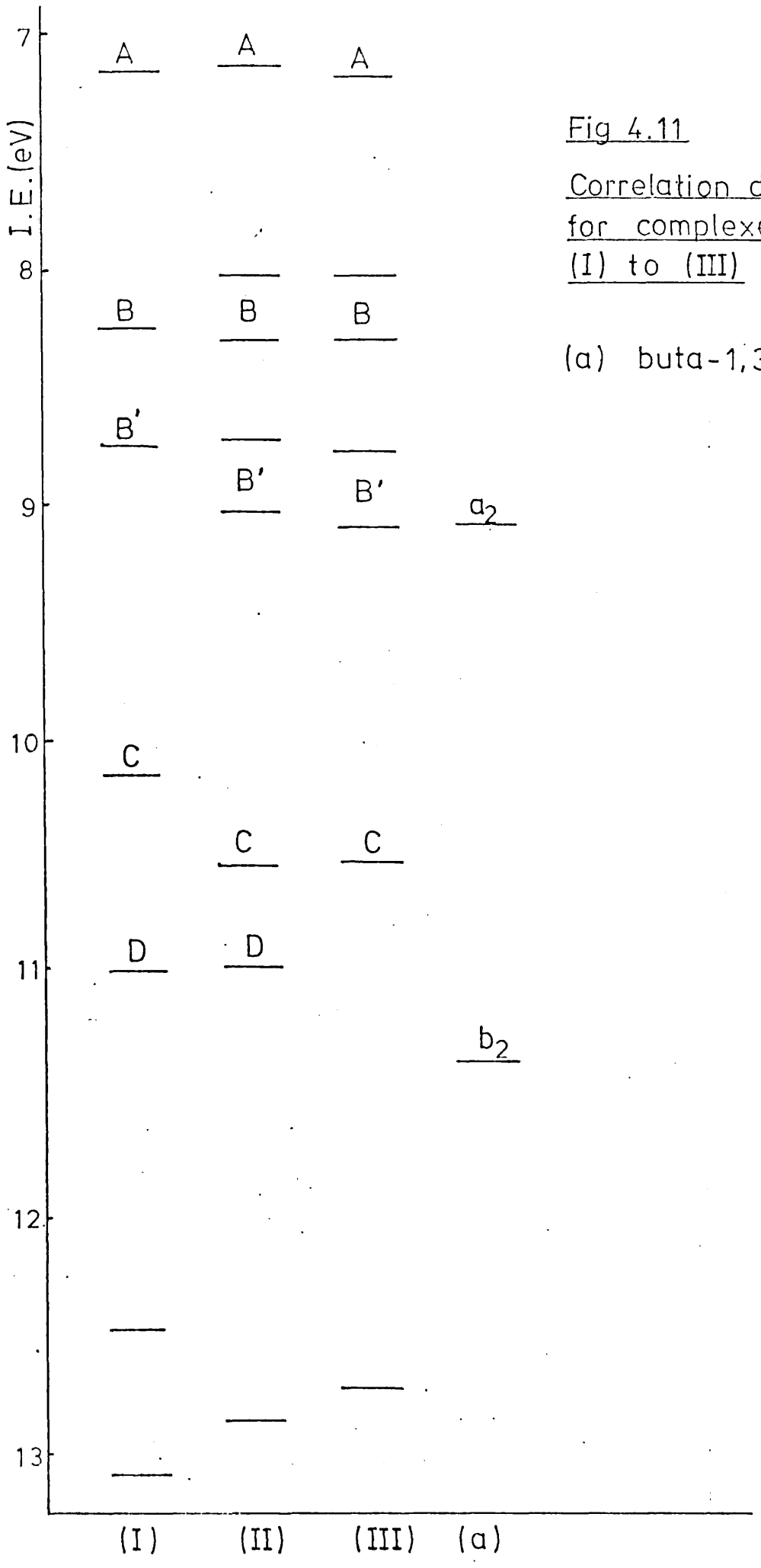

Fig 4.11

Correlation diagram for complexes (I) to (III)

(a) buta-1,3-diene

Table 4.2 cont.

	A	B	B'	C	D	E
(XI)	7.15	7.94, 8.24	8.65, 9.06	10.28	10.72	11.64, 12.59, 13.98
Relative) HeI	1.0	4.5		1.4	0.6	
Intensity) HeII	1.0	5.7		1.5		
(XII)	7.41	8.42	8.75	10.25	11.01	12.68, 13.74
Relative) HeI	1.00	4.9		1.5	0.8	24
Intensity) HeII	1.00	7.5		1.7	0.6	10

The PE spectra of complexes (VII), (X), (XI) and (XII) are all similar to those of complexes (I) to (III) as would be expected, and may be assigned in the same way. The ionisation energies for complex (VII) are almost identical to those for (I), however there is a clearly resolved band, e' to the low IE side of band E, which does not appear in the PE spectrum of (I). This is assigned to ionisation from the mainly ligand (cyclopentadienyl) orbital of σ symmetry.

The PE spectra of (X) and (XII) are very similar to that of (I), and that of (XI) to those of (II) and (III). In the spectrum of (XI), as for (II) and (III), four bands are resolved in the B/B' region. Relative intensity patterns are much the same as for (I) to (III), and band C, due to cyclopentadienyl e_1 ionisation, can be seen to possess some d character. As in the tricarbonyliron complexes, band D, corresponding to ionisation from the $b_2\pi$ mainly ligand level, remains relatively non-bonding.

Table 4.3 shows ionisation energy and relative intensity data for complexes (V), (Va), (VIII), (IX) and (I) and figure 4.12 is a correlation diagram showing the relative ionisation energies of the complexed dienes.

Comparison of the PE spectra of (IX) and (I) shows

Table 4.3 Ionisation energy data (eV) for (I), (IX), (V), (Va), (VIII)

Complex		A	B	B'	C	D	E	F
(I)		7.26	8.32	8.81	10.17	10.99	(13.05)	
(IX)		7.12	8.27	8.97	9.57	10.25	11.56	12.60,13.70
(V)		7.07	7.89,8.12	8.57,8.84	9.27	9.82	10.70(11.08)	12.27,12.99,13.53
(Va)		6.36	7.67	8.16	9.11		10.23	11.42
(VIII)		7.07	7.91	8.65,9.00	9.93	10.77(11.31)	12.29	13.90
Relative Intensity Data								
(I)	HeI	1.0	1.6	1.9	1.5	0.9	16	
	HeII	1.0	2.7	3.5	1.8	0.8	5.4	
(IX)	HeI	1.0	3.5		0.7	1.4	6.3	24
	HeII	1.0	6.2		1.2	1.8	3.1	13
(V)	HeI	1.0	1.3	1.8	0.5	1.3	1.9	18
	HeII	1.0	3.5	2.8	1.3	2.5	1.2	8
(Va)	HeI	1.0	3.5		2.6		33	
	HeII	1.0	5.8		3.3		24	
(VIII)	HeI	1.0	1.9	3.9	0.7	4.2	27	
	HeII	1.0	4.5	6.8	1.1	2.8	8	

Fig 4.12 Correlation diagram for dienes, ethylene and cyclooctatetraene

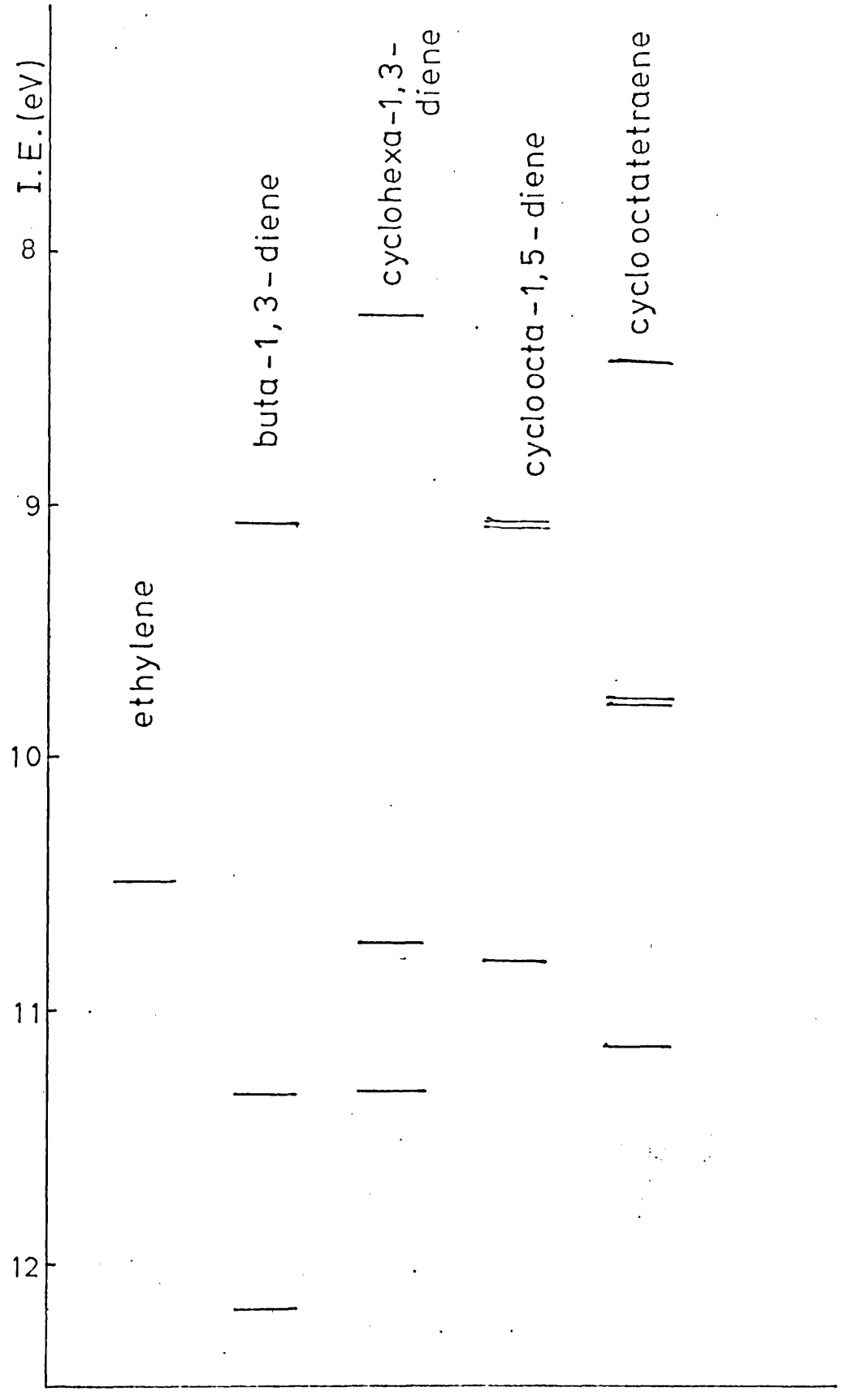

many similarities. Band A is similar for both complexes, and thus for complex (IX) is assigned to ionisation from a molecular orbital formed from interaction of the highest occupied ethylene π MO with a metal d orbital of appropriate symmetry (from the d_{xz}, d_{yz} set); however the orbital has mainly ligand character as shown by relative intensity measurements.

Bands B and B' are less well resolved than for complex (I), in fact, B' appears as a shoulder to the high IE side of B; its lower relative intensity suggests that ionisation from an ethylene π antibonding metal d bonding combination is responsible for this shoulder, the MO so formed having substantial ligand character. B and B' consist of four bands representing ionisation from four levels as in complex (I). The relative intensities A:B+B' are almost identical for the two complexes; thus a similar assignment is likely. The greater relative ligand character of the ethylene π antibonding - metal d MO is not unexpected since there is likely to be increased metal-ligand donation. This is due to the electron donating properties of the methyl groups on the cyclopentadienyl ring, increasing its donor properties compared to the unsubstituted ring. This will result in increased electron density at the metal centre making the CpM group more strongly electron donating.

Band C is of the correct relative intensity to represent ionisation from a mainly ligand orbital, as is band D, and it is proposed that C is due to ionisation from an ethylene bonding-metal antibonding combination, while D is assigned to ionisation from the mainly ligand pentamethyl-cyclopentadienyl e_1 level. It can be seen that band C has more metal d character relative to A (in (IX)) than the corresponding band D in the PE spectrum of complex (I). Using simple occupancy rules, and assuming that in the HeII spectrum the metal d and ligand p orbitals have approximately equal ionisation cross sections (see chapter 3), the calculated

relative intensities for the above assignment are 2:8:2:4. The experimentally observed ratio is 2:12:2:4, and thus the assignment is confirmed, allowing for the fact that 4d orbital ionisation cross sections are greater than 3d cross sections.

Band E is assigned to ionisation from the σ cyclopentadienyl level and the methyl groups on the cyclopentadienyl ring. The ionisation energies for complex (IX) and for (Va) which also contains a pentamethyl-substituted cyclopentadienyl ring, are generally much lower than for analogous complexes with unsubstituted cyclopentadienyl rings. Band E is fairly well resolved from region F which is due to ligand σ ionisation.

It is probable that in the gas phase free rotation of the ethylene units of complex (IX) about the metal ligand bond axis will occur, since the energy barrier to rotation is small. Since the PE experimental lifetime is short compared with the speed of rotation, it is likely that the conformations will give rise to overlapping bands; these are unlikely to be separately resolved and the PE spectrum will show one band.

The PE spectrum of complex (Va) is similar to that of (IX) as might be expected; however, in (Va), the two bonded ethylenic units are not free to rotate about the metal-ligand bond axis. The first ionisation energy of the free diene, cycloocta-1,5-diene is substantially lower than that of ethylene. Bands A, B and B' are assigned as for complex (IX); band C probably corresponds to C+D in complexes (I) and (IX) but with the two ligand levels too close in energy to be resolved separately in the PE spectrum. The intensity ratio C:A for (Va) is 2.6; the ratio C+D:A for (IX) is 2.1, and for (I) is 2.4. Thus the assignment of C in the PE spectrum of (Va) to ionisation from both a cyclooctadiene π level and the almost degenerate cyclopentadienyl π level, is probably correct. As for (IX), E is assigned to ionisation from the methyl groups of the substituted

cyclopentadienyl ring.

The PE spectrum of complex (V) is different in appearance to that of (Va). The relative intensities indicate that the same assignment as that of (Va) is valid, but the ionisation energies are very different. Band E is very well resolved and at low ionisation energy. It is a possibility that in complexes (Va) and (V), bands 'D' and E are due to ionisation from the e_1 cyclopentadienyl level which is no longer degenerate.

Bands B and B' are almost resolved into four bands; B' shows considerable metal character in contrast to the corresponding band in the PE spectrum of (Va). A possible reason for this (the comparative electron donating characteristics of the cyclopentadienyl and pentamethylcyclopentadienyl groups), was discussed earlier. Band C is assigned to the second mainly ligand π (cyclooctadiene) ionisation, and shows considerable metal character, which is not true of the corresponding bands (D) in (I) and (IX). It is difficult to judge whether band C in (Va) shows a similar effect, since bands C and D in this complex are not resolved. Band D in the PE spectrum of (V) is assigned to ionisation from the cyclopentadienyl $e_1\pi$ level, and band E either to the $e_1\pi$ cyclopentadienyl or a cyclopentadienyl σ level. Band E has a very much lower intensity relative to A than in the bis-ethylene complex (IX), but approximately the same as for (Va).

Complex (VIII) might be expected to show an extra band in the low ionisation energy region of the PE spectrum since there are two non-complexed double bonds in the cyclooctatetraene ring which should give rise to a doubly degenerate level corresponding to a high intensity band in the HeI PE spectrum. At first sight, band F appears to be high in intensity relative to F in complex (V), but in fact the PE spectra of (V) and (VIII) are very similar.

Bands A, B and B' are assigned in exactly the same way as for complex (V). Band C is probably due to a mainly ligand (cyclooctatetraene) π level, as for complex (V), and shows some metal d character. Bands must now be assigned to the cyclopentadienyl e_1 level and the two cyclooctatetraene π levels not involved in bonding to the metal, which are expected to be degenerate. There are three distinct bands that might be assigned to these ionisations, D, E and F, but the conclusions reached on the exact assignments are uncertain.

Figure 4.13 is a correlation diagram for the rhodium complexes discussed so far; (I), (V), (Va), (VII), (VIII) and (IX).

The cobalt complexes

Table 4.4 shows ionisation energy and relative intensity data for the three cobalt complexes, (IV), (IVa) and (VI). The photoelectron spectra of these complexes are surprisingly different to those of their rhodium analogues; in the introduction it was noted that chemical properties of these rhodium and cobalt analogues are markedly different.

The PE spectrum of complex (VI) does not resemble that of (VII), its rhodium analogue.

There is a shoulder to the low IE side of A labelled A"; A", A and A' are all assigned to ionisation from essentially metal d orbitals, from their relative intensities in the HeII PE spectrum. Apparently the bonding in complex (VI) shows substantial differences from that in complex (VII).

Band B' shows mainly ligand character and is therefore assigned to ionisation from the orbital formed from the highest occupied diene π orbital (corresponding

Fig 4:13 Correlation diagram for the rhodium complexes

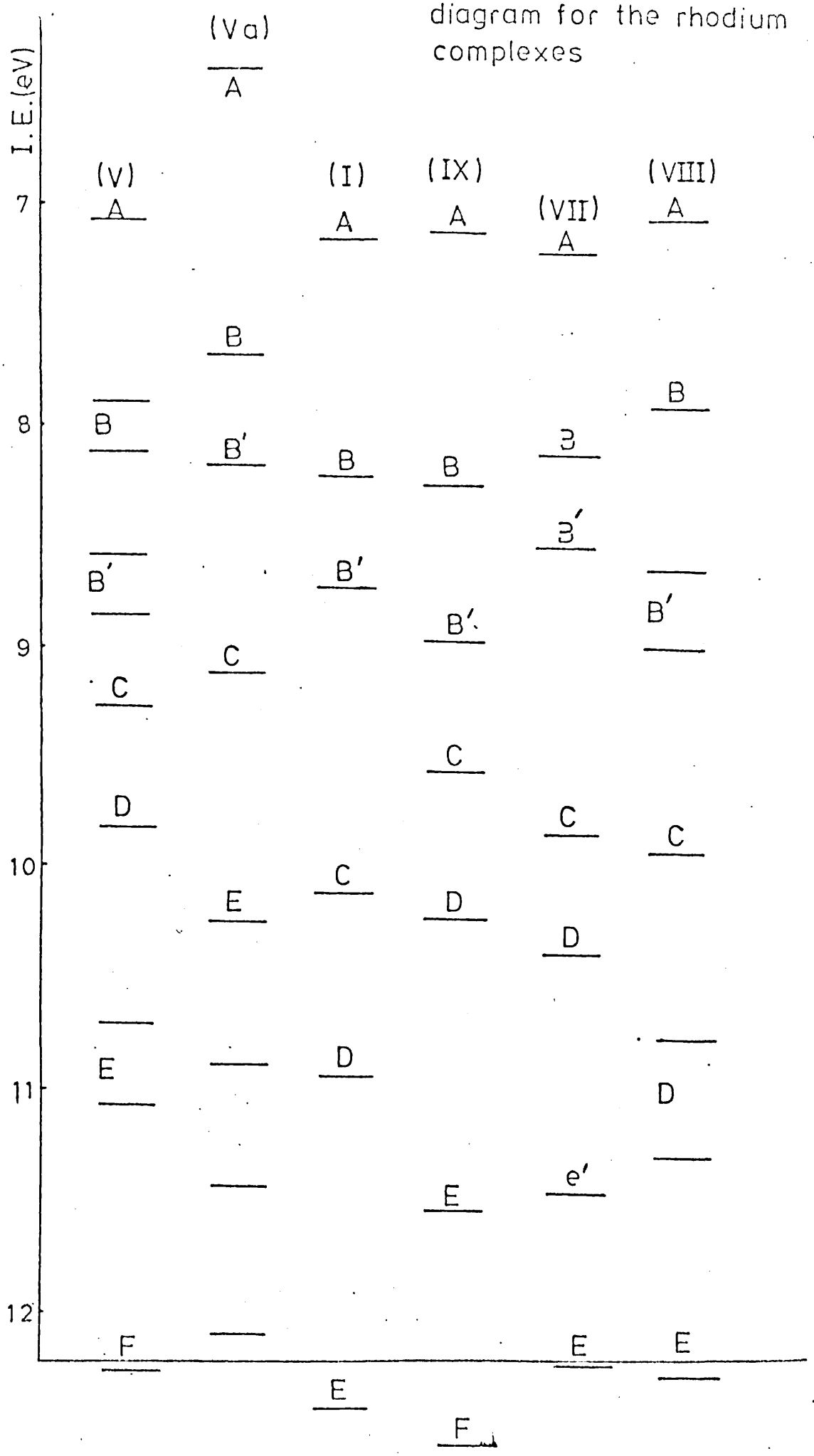

Table 4.4 Ionisation energy data (eV) for (IV), (IVa) and (VI)

Complex		A	A'	B'	B	C	D	E
(IV)		6.73	7.25	8.58	9.01	10.43,10.71	11.42	12.24,13.55
(IVa)		6.69	7.21	8.13	8.84		11.37	11.93,13.41
(VI)		6.92,7.43	7.97	8.47	9.27	10.43	11.21	12.28,13.51
Relative Intensity Data								
(IV)	HeI	1.0	0.9	0.9	2.0	1.3, 1.4	2.9	14
	HeII	1.0	1.3	0.6	1.7	1.4		6.8
(IVa)	HeI	1.0	1.0	0.9	1.8		33	
	HeII	1.0	1.1	0.8	1.2			
(VI)	HeI	1.0,2.2	1.6	2.5	3.3	2.6	2.7	56
	HeII	1.0,1.8	1.6	1.4	2.4	1.2	1.8	10

to $a_2\pi$ in buta-1,3-diene), and representing ligand to metal donation. Together with bands A", A and A', one would expect to find the band corresponding to ionisation from the ligand π antibonding-metal d combination and representing metal to ligand donation. Of these three bands, band A shows some ligand character. Band B appears to have essentially metal d character, and is assigned accordingly.

Band C is assigned to ionisation from a cyclopentadienyl π level, and D to ionisation from the lower π level of the diene.

The overall assignment points to great similarity between the bonding in this complex and the tricarbonyliron analogue. Figure 4.14 shows a qualitative MO diagram for complex (VI) constructed with the aid of the above assignment. Table 4.5 compares the IEs for free cyclohexa-1,3-diene with those for the complexed ligand in the three complexes; η^4-cyclohexa-1,3-dienetricarbonyliron, (VI) and (VII), assuming that the PE assignments are correct.

Table 4.5 Ionisation energy data (eV) for cyclohexa-1,3-diene, η^4-cyclohexa-1,3-dienetricarbonyliron (M), (VI) and (VII)

	cyclohexadiene	(M)	(VI)	(VII)
' a_2'π	8.25	9.33	8.47 (B')	7.21 (A)
' b_2'π	10.75	11.04	11.21 (D)	10.40 (D)

It can be seen from table 4.5 that in the iron and cobalt complexes, both diene π bonding levels are stabilised on complex formation, whereas for the rhodium complex, the opposite is true, the π levels being destabilised relative to those of the parent diene. Thus in complex (VII) there is evidence for substantial stabilisation of the diene lowest unoccupied π level, corresponding to an increase in

Figure 4.14 MO diagram for complex (VI)

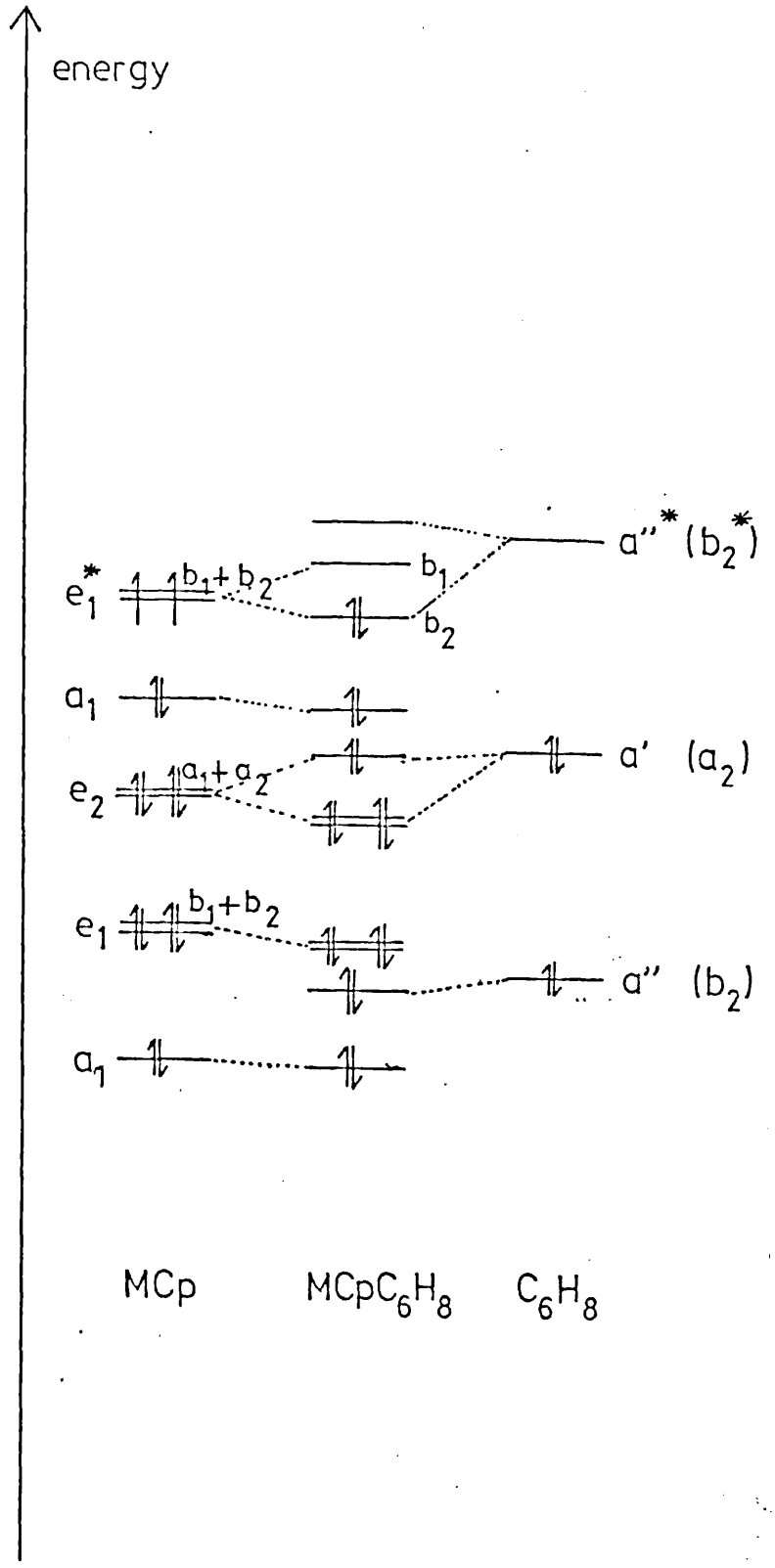

metal to diene ligand donation compared with complexes (V) and (VI), although even in these, the metal to diene ligand donation is thought to be the dominant interaction, resulting in the net negative charge on the diene ligand relative to the metal (see chapter 2).

The low IE regions A, A', B', B of PE spectra of (IV) and (IVa) are very similar to each other but very different in appearance to those of (VI) and of their rhodium analogues.

From relative intensity data, A, A' and B are assigned to ionisation from mainly metal d orbitals while B' shows mainly ligand character and is assigned to ionisation from an orbital representing ligand to metal electron donation, as for B' in the PE spectrum of complex (VI).

Band C in the PE spectrum of (IV) is assigned to ionisation from the almost degenerate cyclopentadienyl e_1 level, and D to ionisation of the lower π level of the diene. Bands C and D in the spectrum of (IVa) are not distinguishable from the ligand ionisations at E; this effect has been noted earlier in the PE spectra of the complexes with pentamethyl-substituted cyclopentadienyl groups, ((IX) and (Va)). Figure 4.15 shows a correlation diagram for the cobalt complexes.

Final conclusions

The assignments again imply that the bonding in complexes (IV) and (IVa) shows more similarity to that in the tricarbonyliron complexes than the rhodium analogues. The reversal of the lowest ionisation energy bands in the cobalt and rhodium analogues is interesting; in the case of the rhodium complexes, the band having lowest ionisation energy (which might be equated with the highest occupied molecular orbital in the neutral complex if Koopmans' theorem

Fig 4.15 Correlation diagram for complexes (IV), (IVa) and (VI)

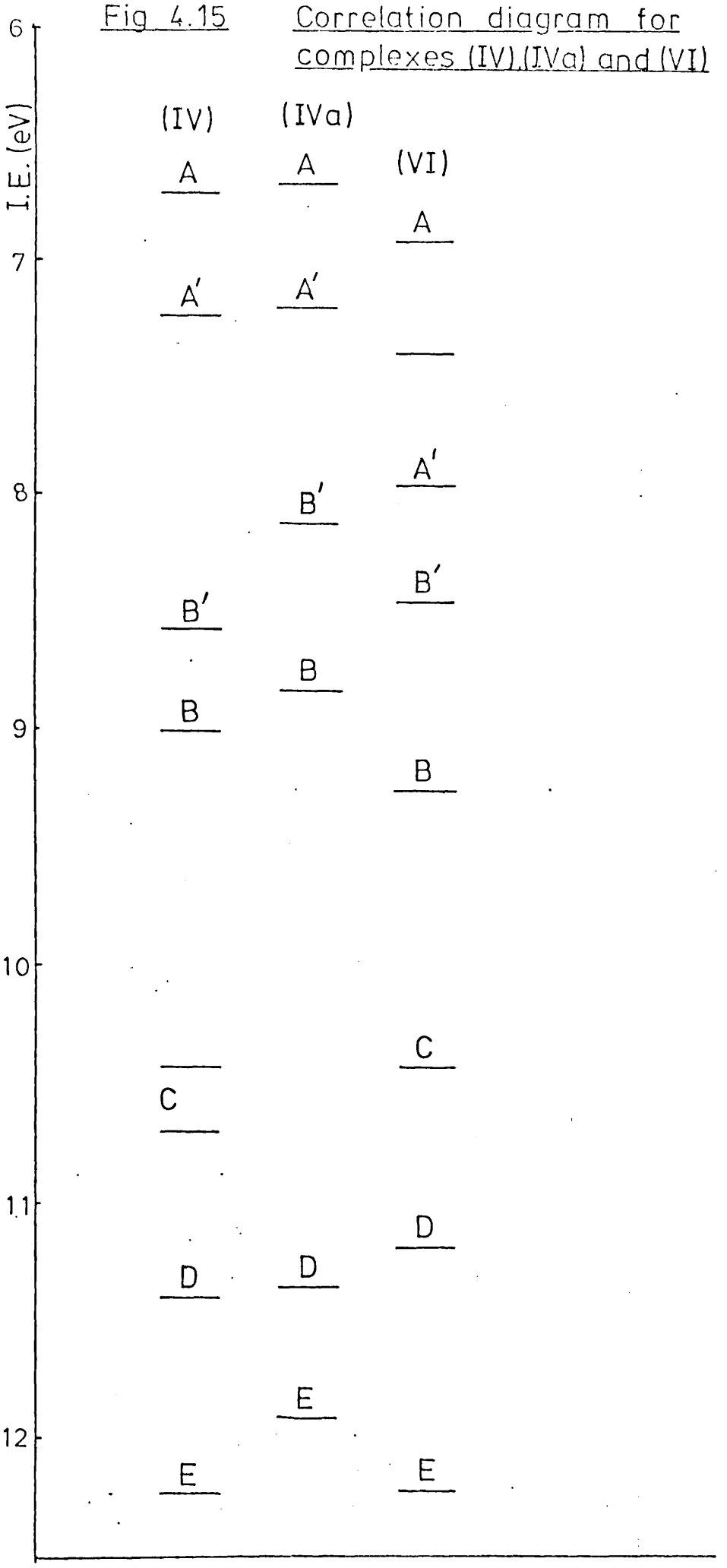

were observed) is always due to ionisation from an orbital of essentially ligand character, whereas for the cobalt complexes, the band of lowest ionisation energy is always due to metal d ionisation as would be expected from previous photoelectron work (chapters 2 and 3). This situation is not observed for the iron and ruthenium analogues studied. One would not expect the differences in the change in relaxation energies between the rhodium and cobalt analogues to be so great that there is a reversal of levels in the molecular ion of one complex relative to the other. It must be concluded that there are essential differences in the bonding of the two types of complex, which are concerned only with the way in which the metal is bonded to the diene (or ethylene) unit, since these changes are not observed with the two η^5-cyclopentadienyldicarbonyl complexes studied (chapter 5). This difference in bonding is not unexpected due to the noted differences in chemical properties of some of these rhodium/cobalt analogues, described in section 4.4. Figure 4.16 compares ionisation energies for some cobalt and rhodium analogues, and the uncomplexed dienes.

4.7 EXPERIMENTAL

The photoelectron spectra of complexes (I) to (XII) were obtained using the same instrumentation as in chapters 2 and 3 (see Appendix I). HeI and HeII spectra were obtained at least in duplicate for each complex, and calibration was carried out using xenon and nitrogen. The relative intensities of the bands in the spectra were measured and corrected as in chapter 3.

Most of the complexes described in this chapter were prepared and donated by the following:

a)	Dr. D. M. P. Mingos	I.C.L., Oxford (Va), (IX)
b)	Dr. P. Powell	(II), (III), (V), (Va)
c)	Dr. L. J. Russell	(IV), (VII), (VIII), (X)-(XII)
d)	Dr. R. Pardy	I.C.L., Oxford (IVa)

Fig 4.16 Ionisation energies for some cobalt and rhodium analogues

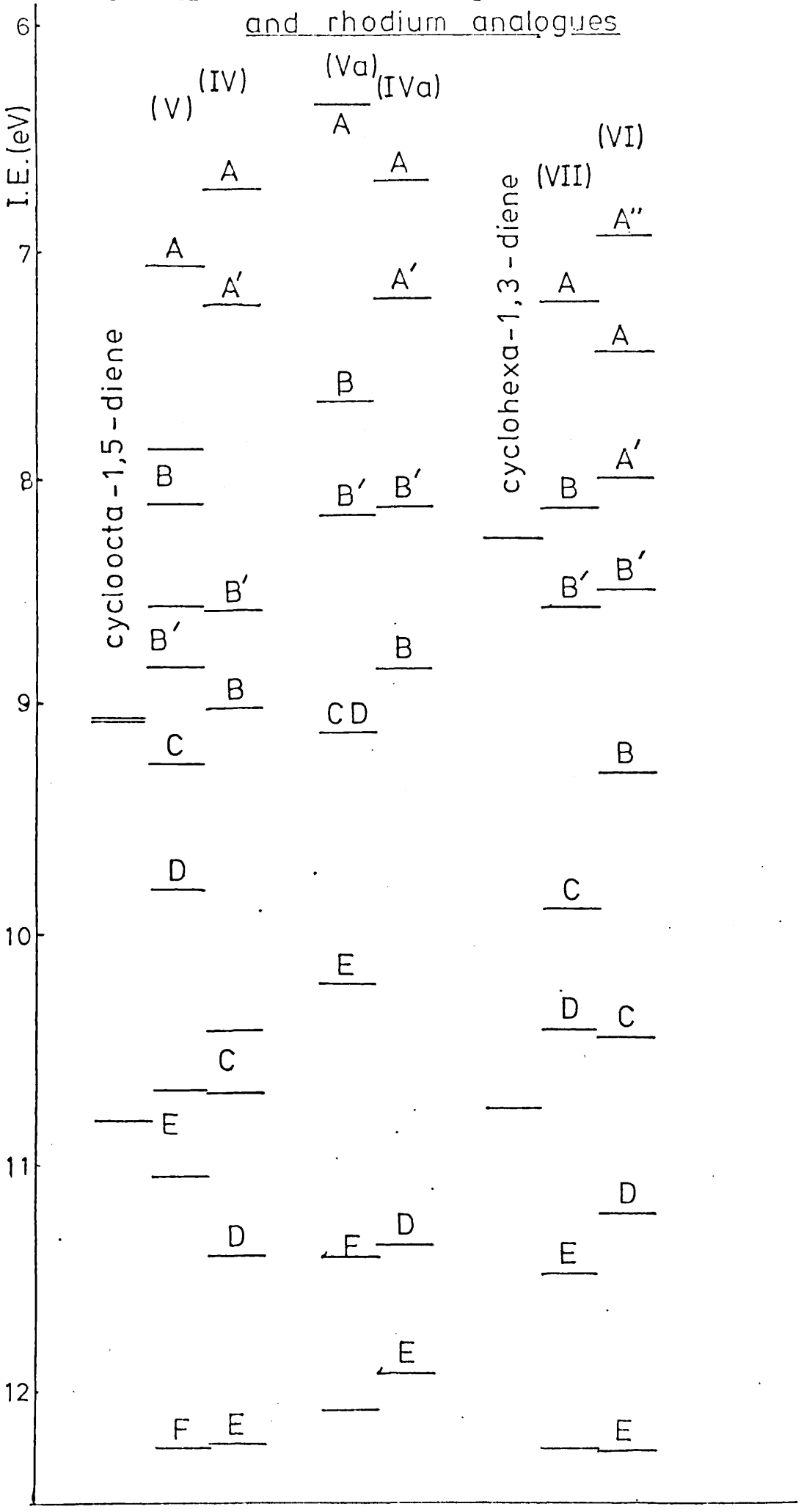

All complexes were purified by the author before the PE spectra were obtained. Preparative methods for those complexes prepared by the author are given, together with results of carbon and hydrogen analyses where these are available.

(i) (η^5-cyclopentadienyl)(η^4-butadiene) rhodium (I)

This was prepared from biscyclooctene-rhodium chloride dimer (350 mg) and liquid butadiene (a few cm^3). The resulting bisbutadiene-rhodium chloride was treated with thallium cyclopentadienide (269 mg) in dry diethylether at room temperature, in the dark. After stirring for about 30 min., the thallium chloride was filtered off, leaving a yellow solution; this was evaporated to give yellow crystals. The yield was approximately quantitative.

(ii) (η^4-cyclohexa-1,3-diene)(η^5-cyclopentadienyl)cobalt (VI)

This was prepared according the method described by King [243], with some modification. A mixture of η^5-cyclopentadienyldicarbonylcobalt (1 cm^3, 1.3 g) and ethylcyclohexane (5 cm^3) was refluxed for 12h at the boiling point of the solvent ($\sim$135°C) in a 50 cm^3 flask, under a nitrogen atmosphere. The entire reaction mixture was chromatographed on a 2 x 40 cm column of neutral alumina using pentane as eluent, again in a nitrogen atmosphere. The orange band was collected and the solvent evaporated, leaving an oil which was recrystallised from pentane at low temperature. The product was found to be liquid at slightly above room temperature and was sublimed under vacuum; it

condensed as a liquid on the water-cooled sublimation probe, and gradually solidified. The complex was difficult to characterise and obtain in pure form.

(iii) (η^4-cycloocta-1,5-diene)(η^5-cyclopentadienyl)cobalt (IV)

This was prepared according to King's method [243, 66] and the product was purified by sublimation at 50-70°C/0.1 mm. The orange crystals were found to be fairly air stable, but were stored in an atmosphere of nitrogen.

(Found: C, 67.46%; H, 7.58%; Calc: C, 67.24%; H, 7.38%)

(iv) (η^4-cycloocta-1,5-diene)(η^5-cyclopentadienyl)rhodium (V)

The yellow air stable complex (V) was purified by sublimation 90°C/0.1 mm.

(Found: C, 56.77%; H, 6.27%; Calc: C, 56.54%; H, 6.20%)

(v) (η^4-cycloocta-1,5-diene)(η^5-pentamethylcyclopentadienyl)rhodium (Va)

Sublimation at 90-110°C/0.1 mm gave yellow air stable crystals.

(Found: C, 65.80%; H, 8.32%; Calc: C, 62.43%; H, 7.86%)

A second sample of this complex was donated (a). The two samples gave identical PE spectra; the poor carbon/hydrogen analysis results of the first sample may have been due to traces of unremoved unreacted diene.

4.8 PHOTOELECTRON SPECTRA

1. (η^5-cyclopentadienyl)(η^4-buta-1,3-diene)rhodium (I)
2. (η^5-cyclopentadienyl)(η^4-buta-1,3-diene)iridium (II) HeI
3. (η^5-cyclopentadienyl)(η^4-buta-1,3-diene)iridium (II) HeII
4. (η^5-cyclopentadienyl)(η^4-2-methyl-buta-1,3-diene) iridium (III)
5. (η^4-cyclohexa-1,3-diene)(η^5-cyclopentadienyl) rhodium (VII)
6. (η^4-hepta-3,5-dien-2-one)(η^5-cyclopentadienyl)rhodium (X) HeI
7. (η^4-hepta-3,5-dien-2-one)(η^5-cyclopentadienyl)rhodium (X) HeII
8. (η^4-hexa-2,4-dien-1-al)(η^5-cyclopentadienyl)rhodium (XII) HeI
   (η^4-hepta-3,5-dien-2-one)(η^5-cyclopentadienyl)iridium (XI) HeI
9. (η^4-hexa-2,4-dien-1-al)(η^5-cyclopentadienyl)rhodium (XII) HeII
   (η^4-hepta-3,5-dien-2-one)(η^5-cyclopentadienyl)iridium (XI) HeII
10. (η^4-cycloocta-1,5-diene)(η^5-cyclopentadienyl)rhodium (V) HeI
    (η^4-cycloocta-1,5-diene)(η^5-cyclopentadienyl)rhodium (V) HeII
11. (η^4-cycloocta-1,5-diene)(η^5-pentamethylcyclopentadienyl) rhodium (Va)
12. (η^4-cycloocta-1,5-diene)(η^5-pentamethylcyclopenta-dienyl)rhodium (Va)
13. (η^4-cycloocta-1,3,5,7-tetraene)(η^5-cyclopentadienyl) rhodium (VIII)
14. (η^5-pentamethylcyclopentadienyl)(bis-ethylene)rhodium (IX)
15. (η^4-cyclohexa-1,3-diene)(η^5-cyclopentadienyl)cobalt (VI)
16. (η^4-cycloocta-1,5-diene)(η^5-cyclopentadienyl)cobalt (IV)
17. (η^4-cycloocta-1,5-diene)(η^5-tetramethylethylcyclopenta-dienyl)cobalt (IVa)

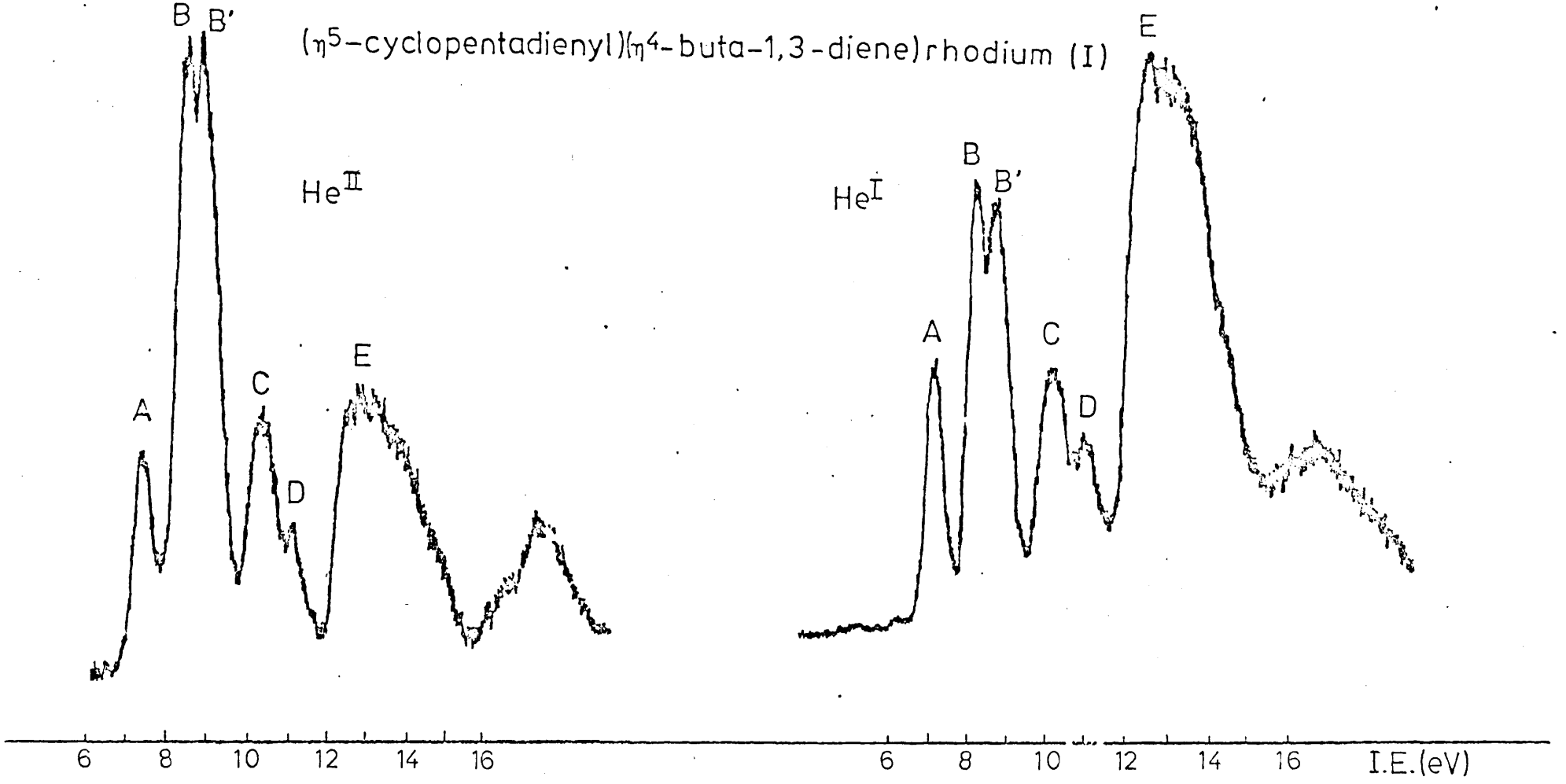
(η5-cyclopentadienyl)(η4-buta-1,3-diene)rhodium (I)
He II
He I
A
B
B'
C
D
E
6
8
10
12
14
16
I.E.(eV)

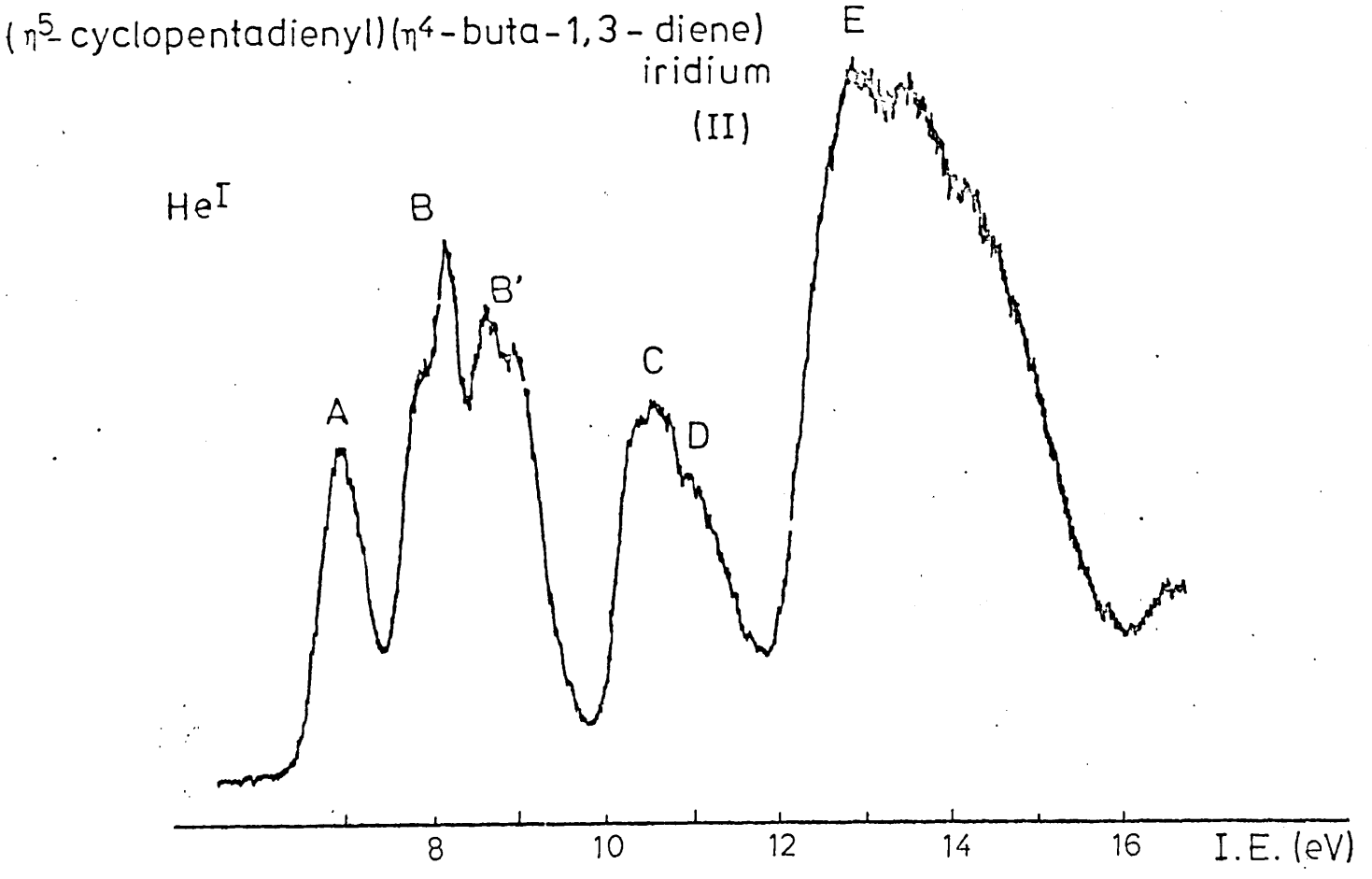
(η5-cyclopentadienyl)(η4-buta-1,3-diene)
iridium
(II)
HeI
A
B
B'
C
D
E
8
10
12
14
16
I.E. (eV)

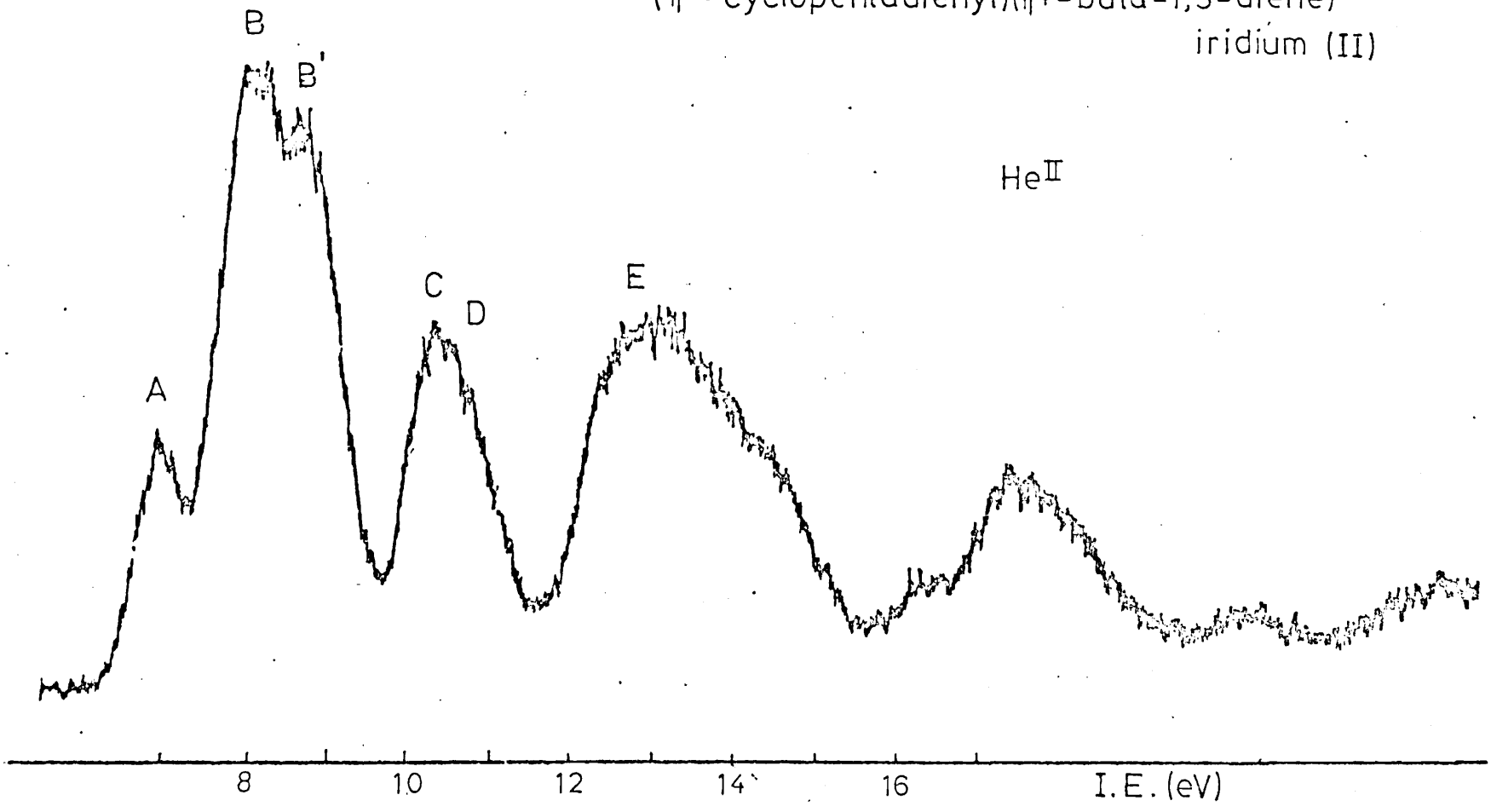
(η5-cyclopentadienyl)(η4-buta-1,3-diene)
iridium (II)
He II
A
B
B'
C
D
E
F
8
10
12
14
16
I.E. (eV)

(η^5-cyclopentadienyl)(η^4-2-methyl-buta-1,3-diene) iridium (III)

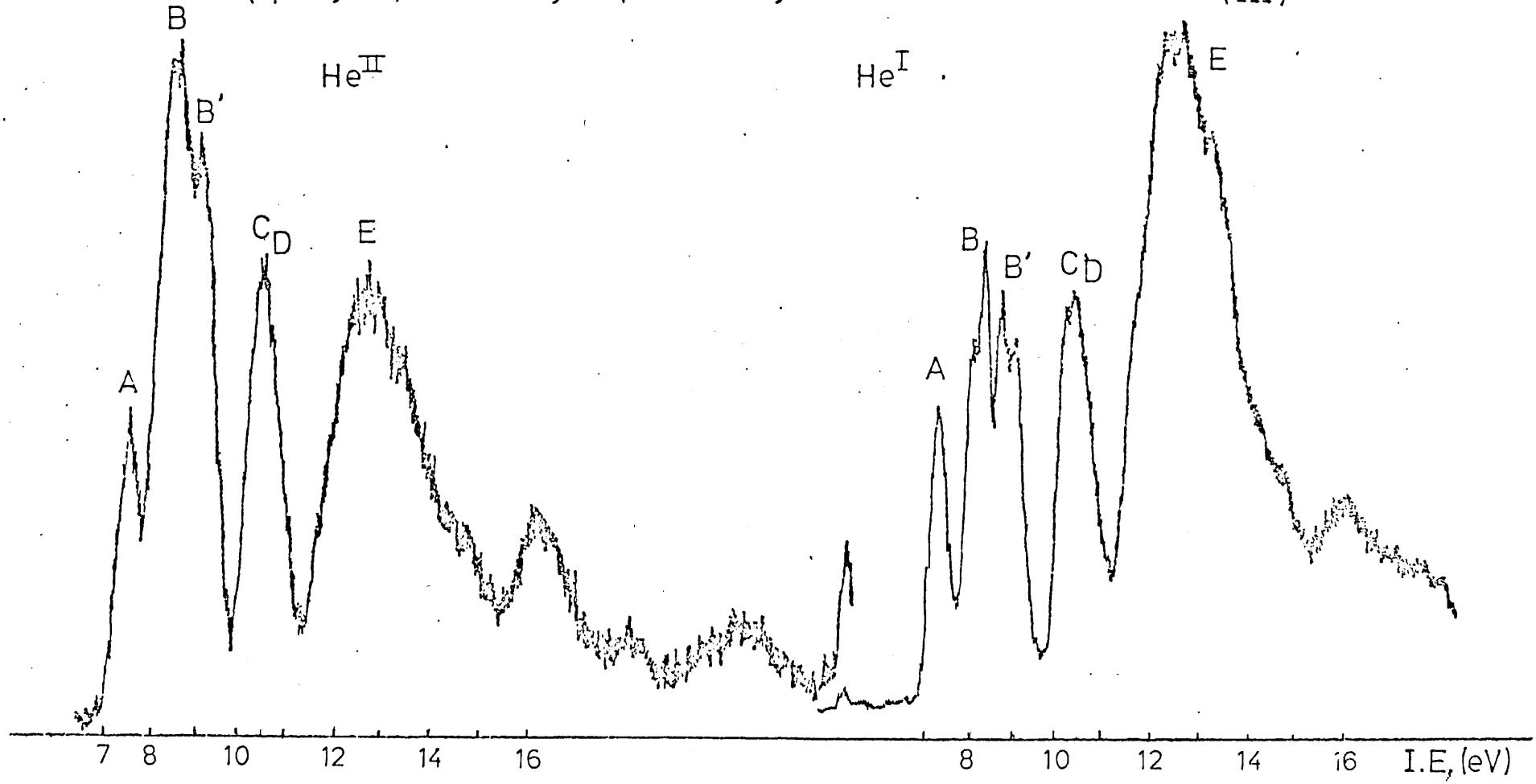

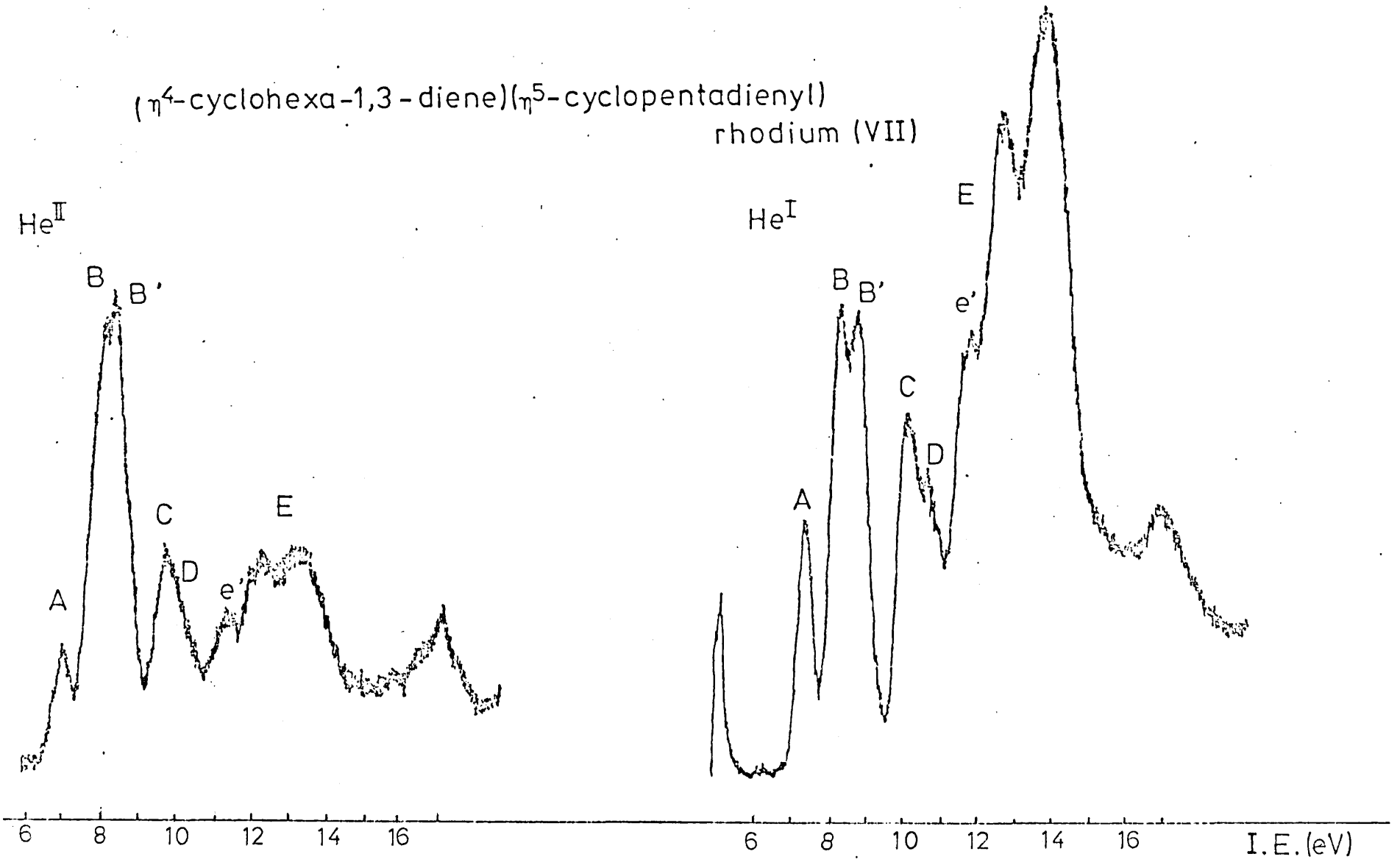
(η4-cyclohexa-1,3-diene)(η5-cyclopentadienyl)
rhodium (VII)
HeII
HeI
A
B
B'
C
D
e'
E
6
8
10
12
14
16
I.E.(eV)

(η^4-hepta-3,5-dien-2-one)(η^5-cyclopentadienyl) rhodium (X)

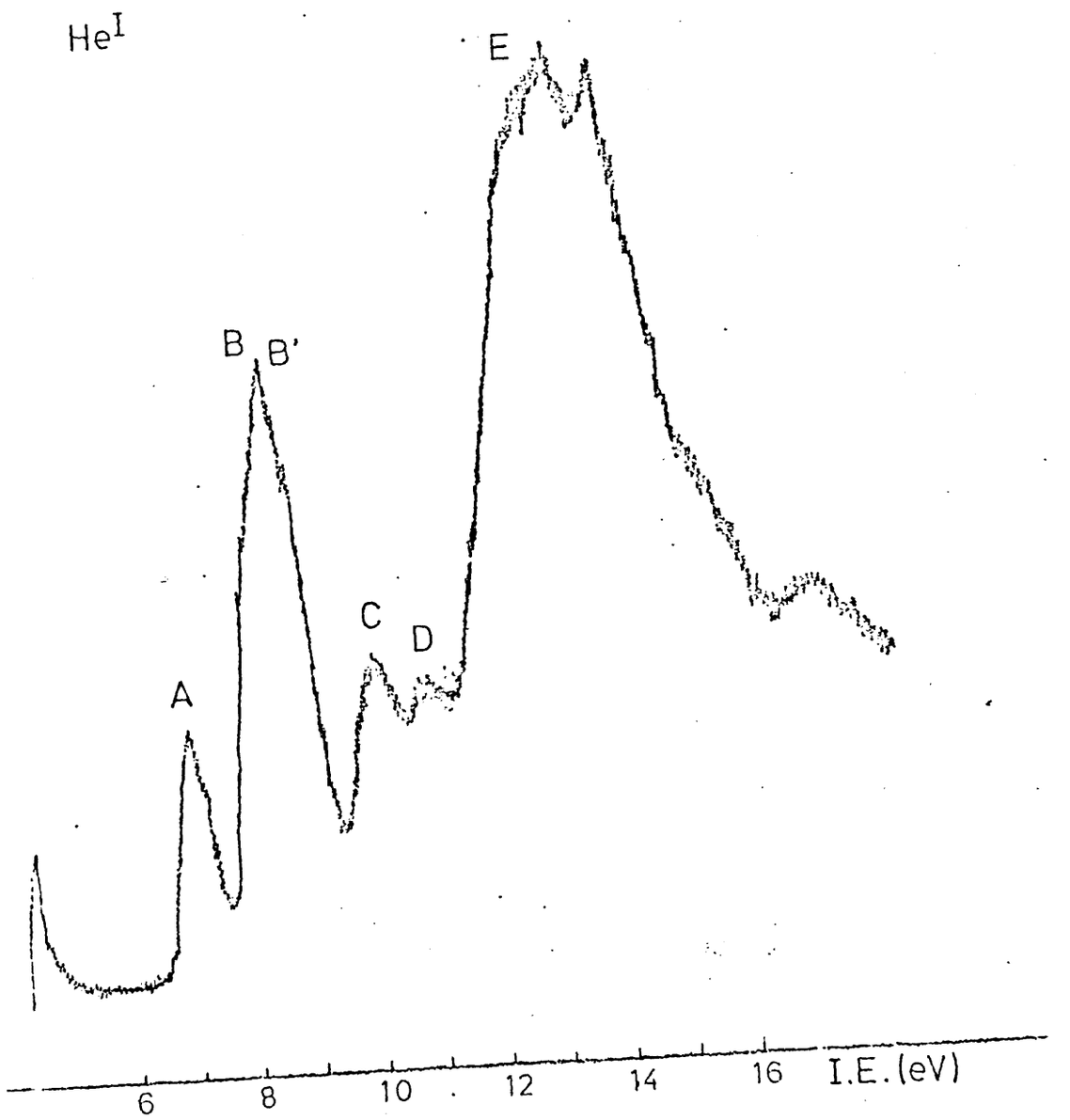

(η^4-hepta-3,5-dien-2-one)(η^5-cyclopentadienyl) rhodium (X)

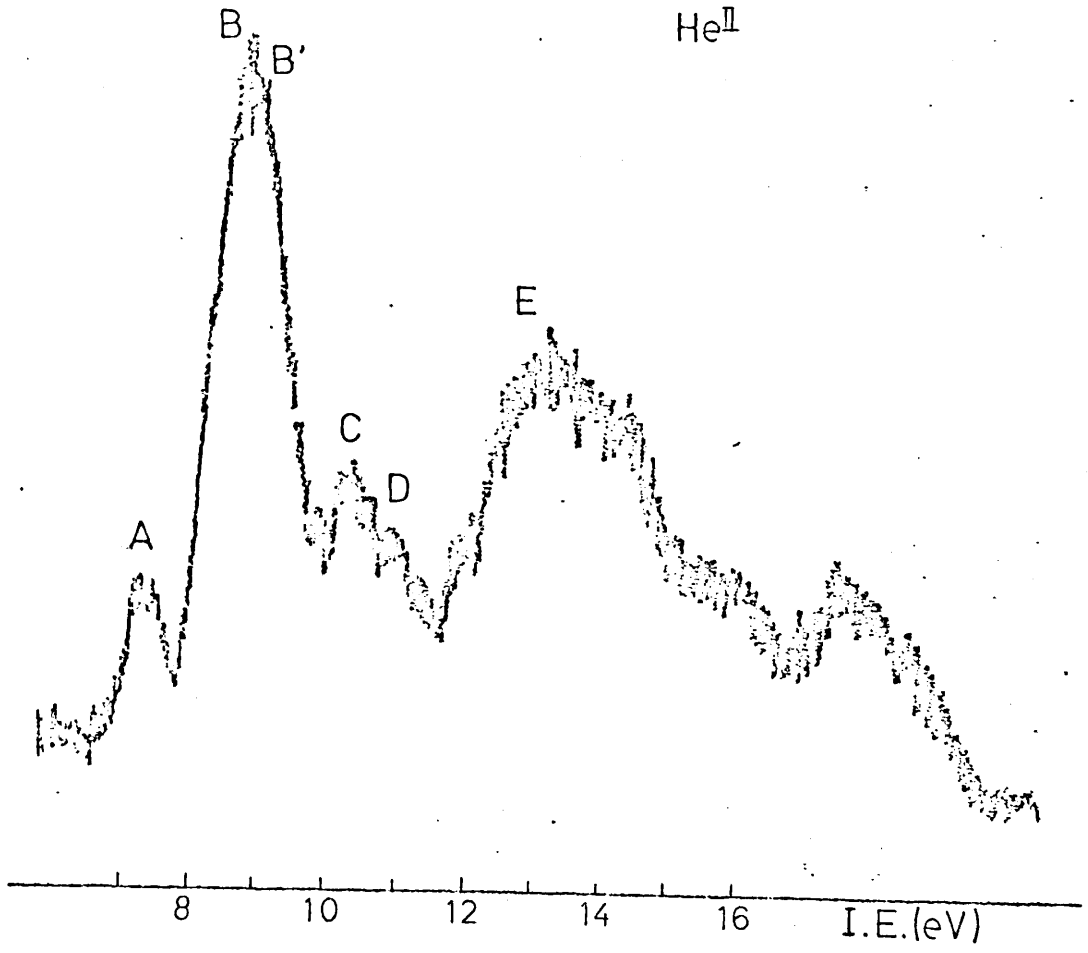

(η^4-hexa-2,4-dien-1-al)(η^5-cyclopentadienyl) rhodium (XII)

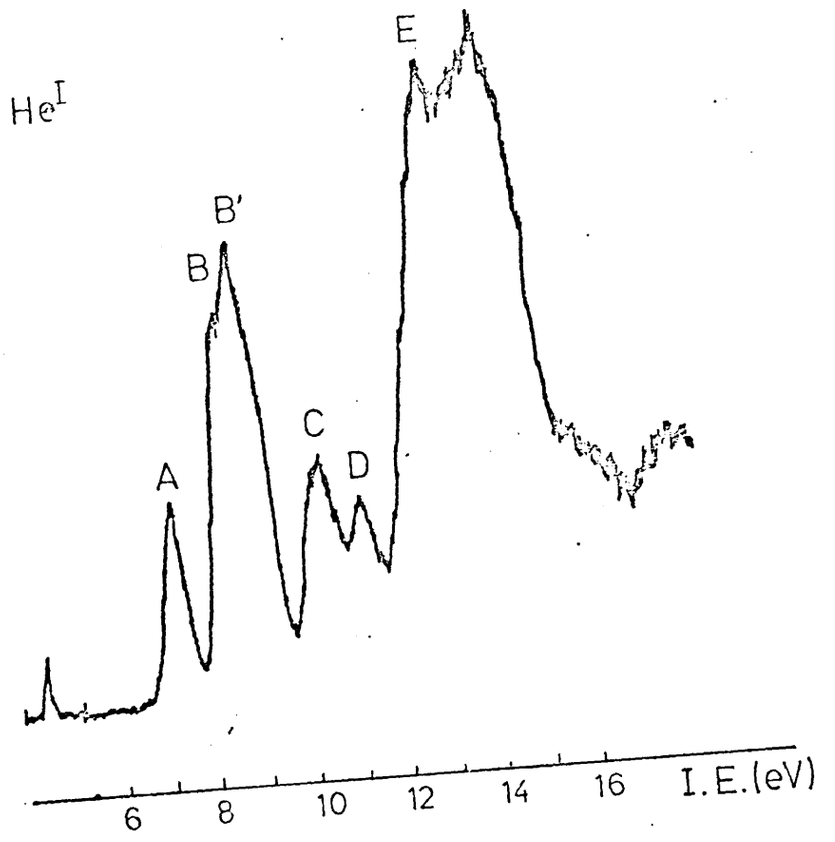

(η^4-hepta-3,5-dien-2-one)(η^5-cyclopentadienyl) iridium (XI)

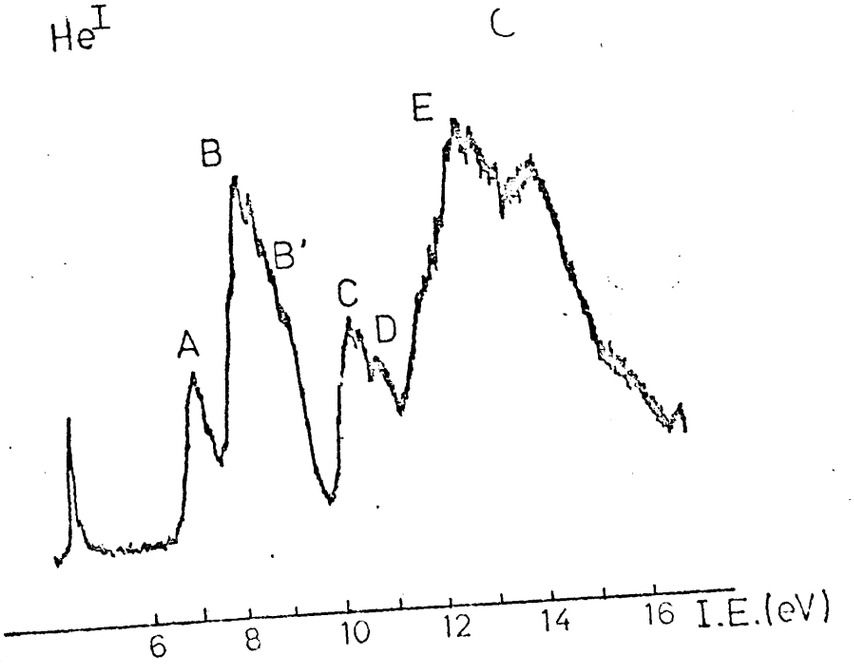

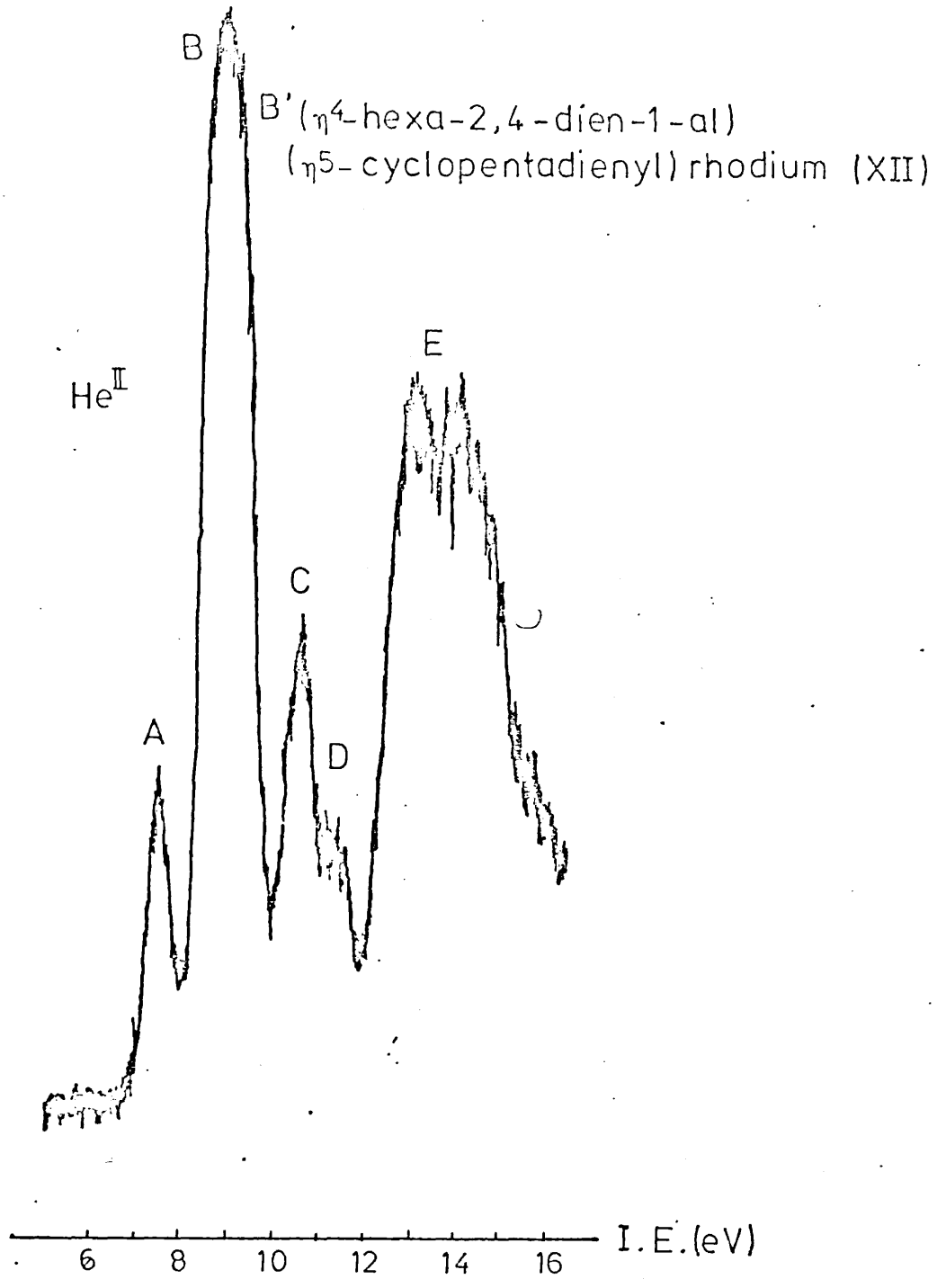

(η4-hepta-3,5-dien-2-one)(η5-cyclopentadienyl)
iridium (XI)

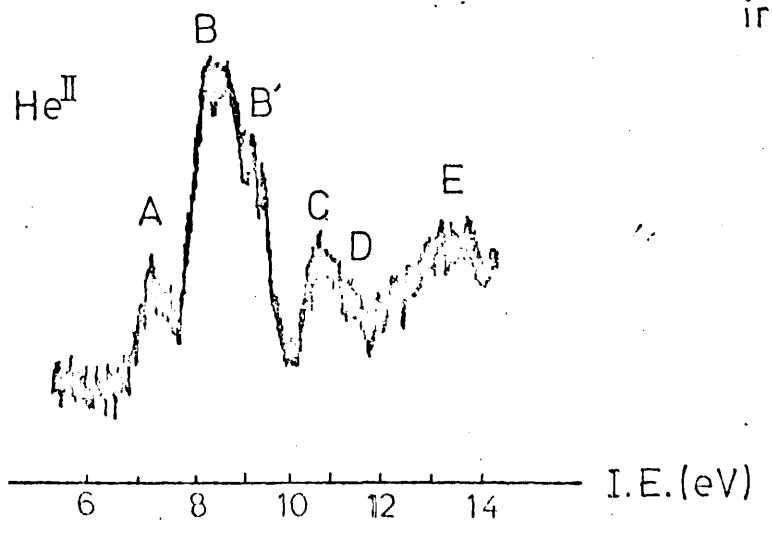

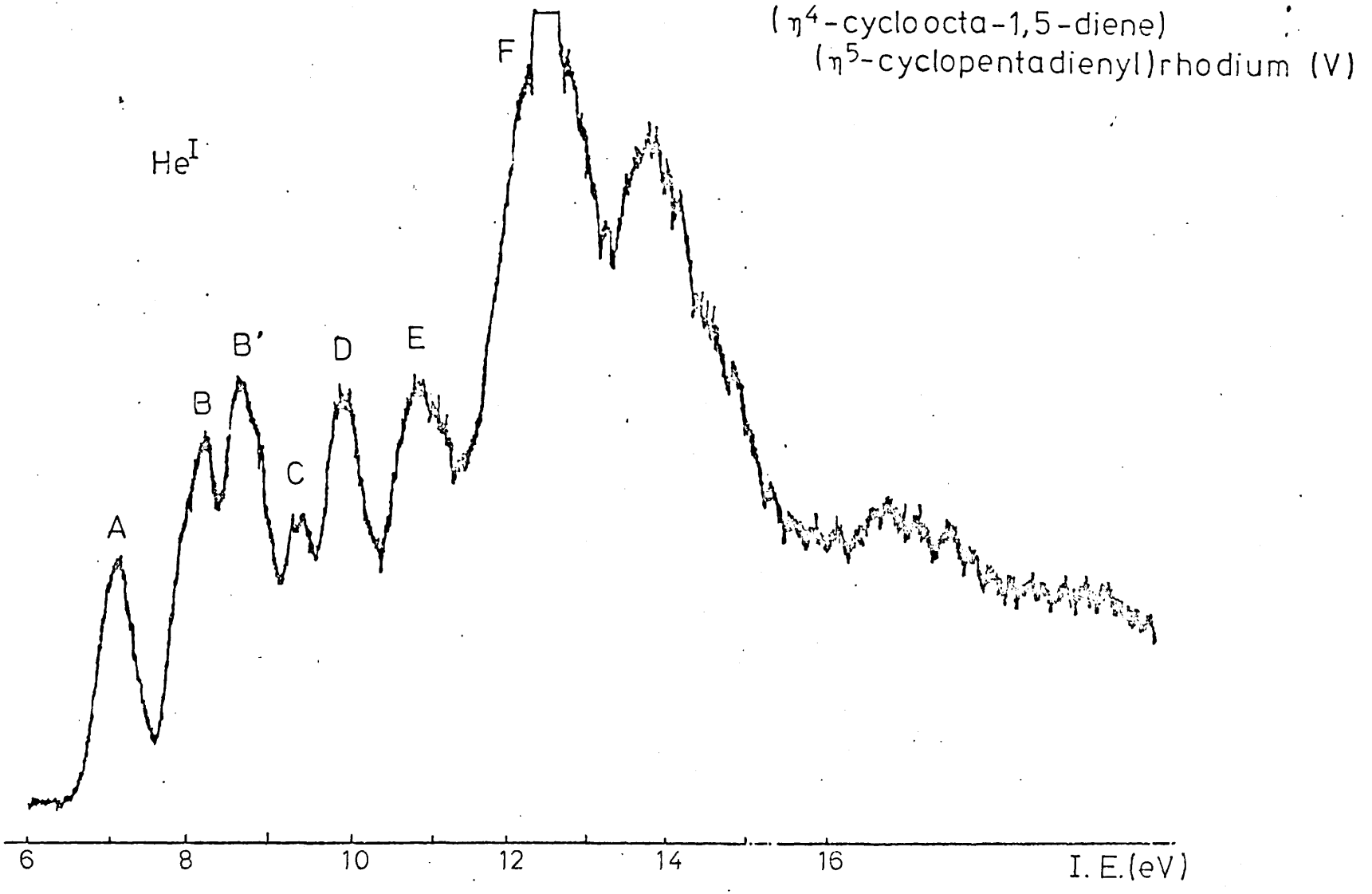
(η4-cycloocta-1,5-diene)
(η5-cyclopentadienyl)rhodium (V)
HeI
A
B
B'
C
D
E
F
6
8
10
12
14
16
I. E.(eV)

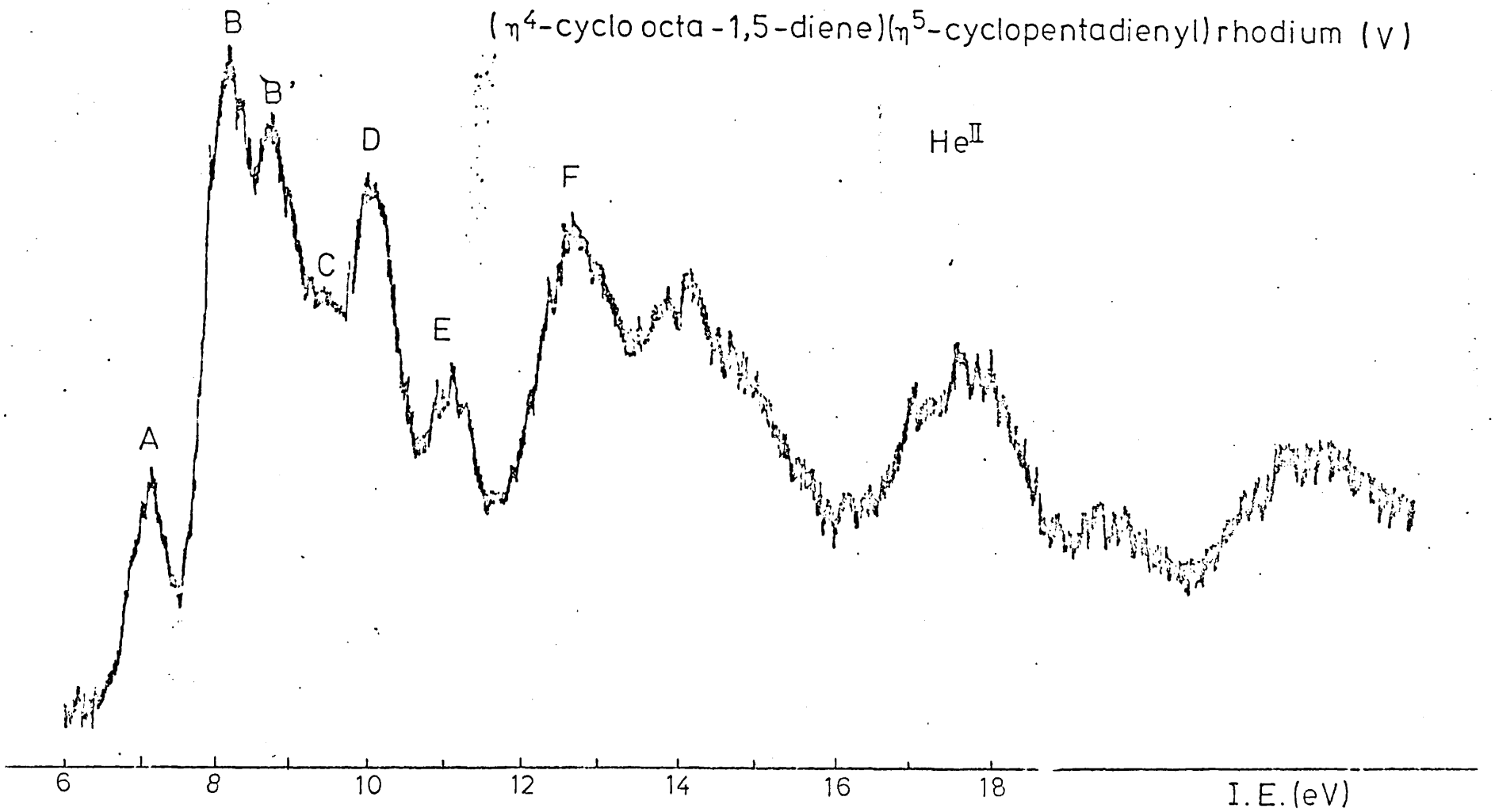
(η4-cyclo octa-1,5-diene)(η5-cyclopentadienyl) rhodium (V)
A
B
B'
C
D
E
F
HeII
6
8
10
12
14
16
18
I.E. (eV)

(η^4-cyclo octa-1,5-diene)(η^5-pentamethylcyclopentadienyl)rhodium (Va)

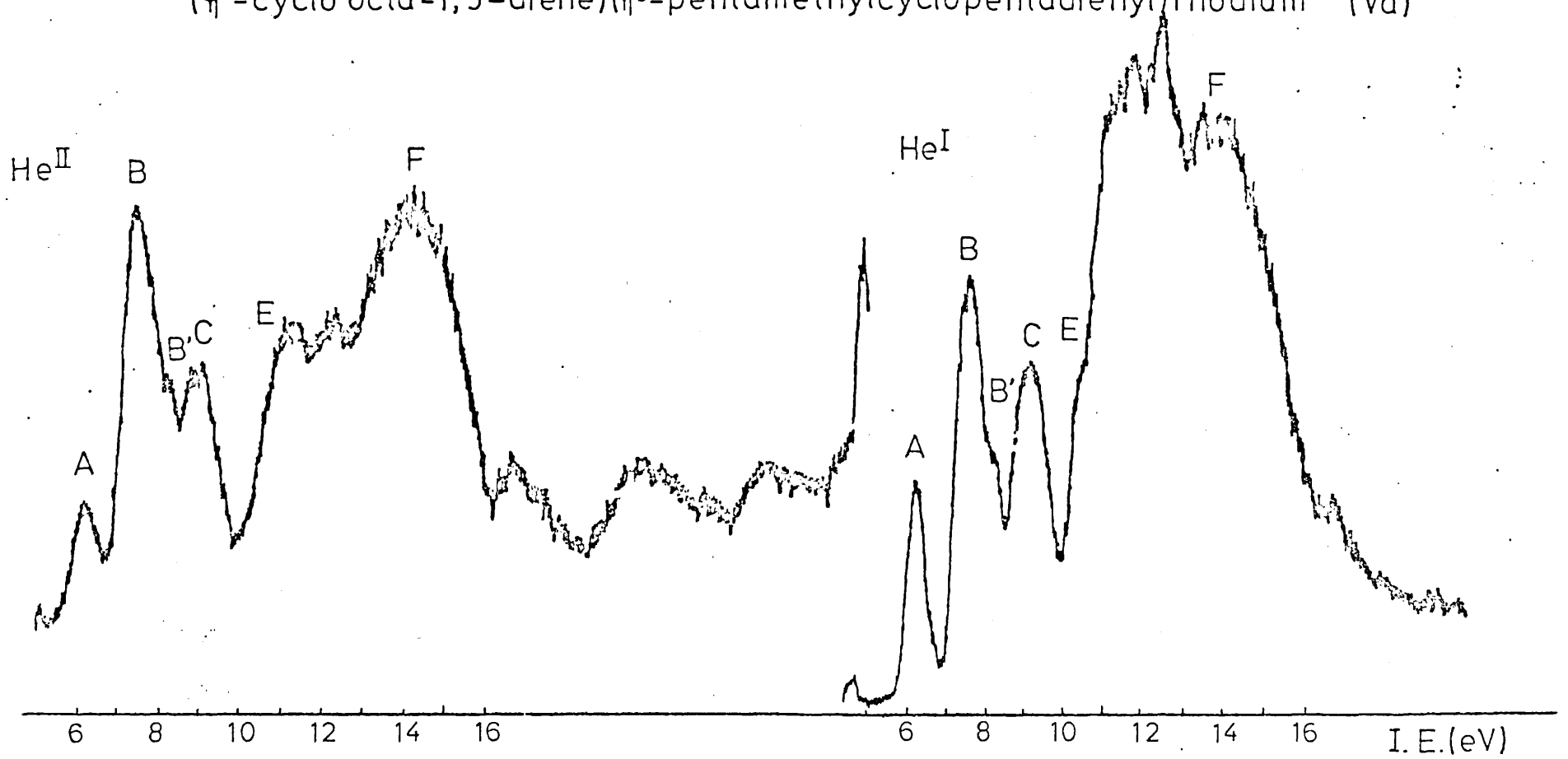

(η^4-cycloocta-1,5-diene)

(η^5-pentamethylcyclopentadienyl)

rhodium (Va)

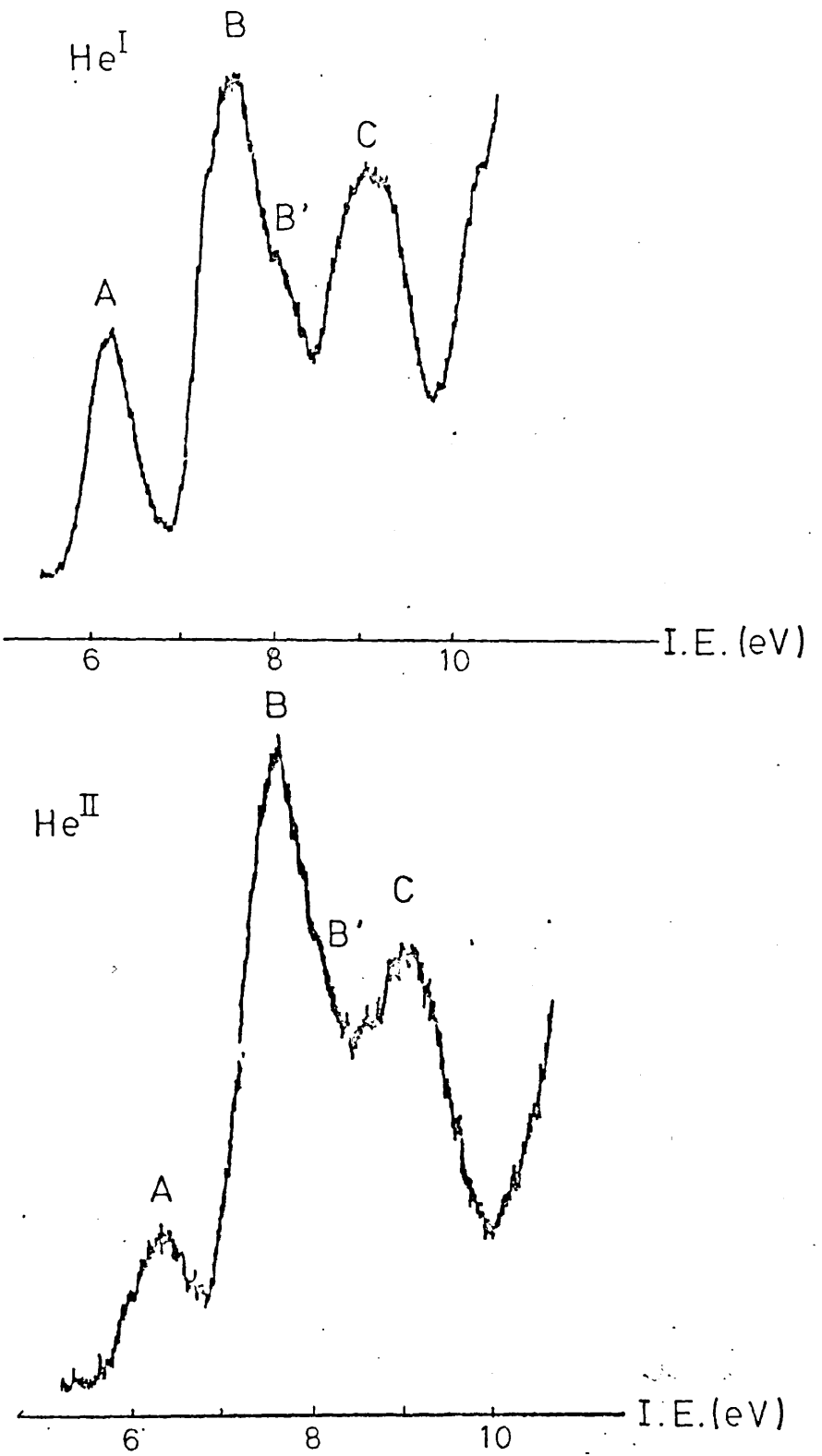

(η^4-cycloocta-1,3,5,7-tetraene)(η^5-cyclopentadienyl)rhodium (VIII)

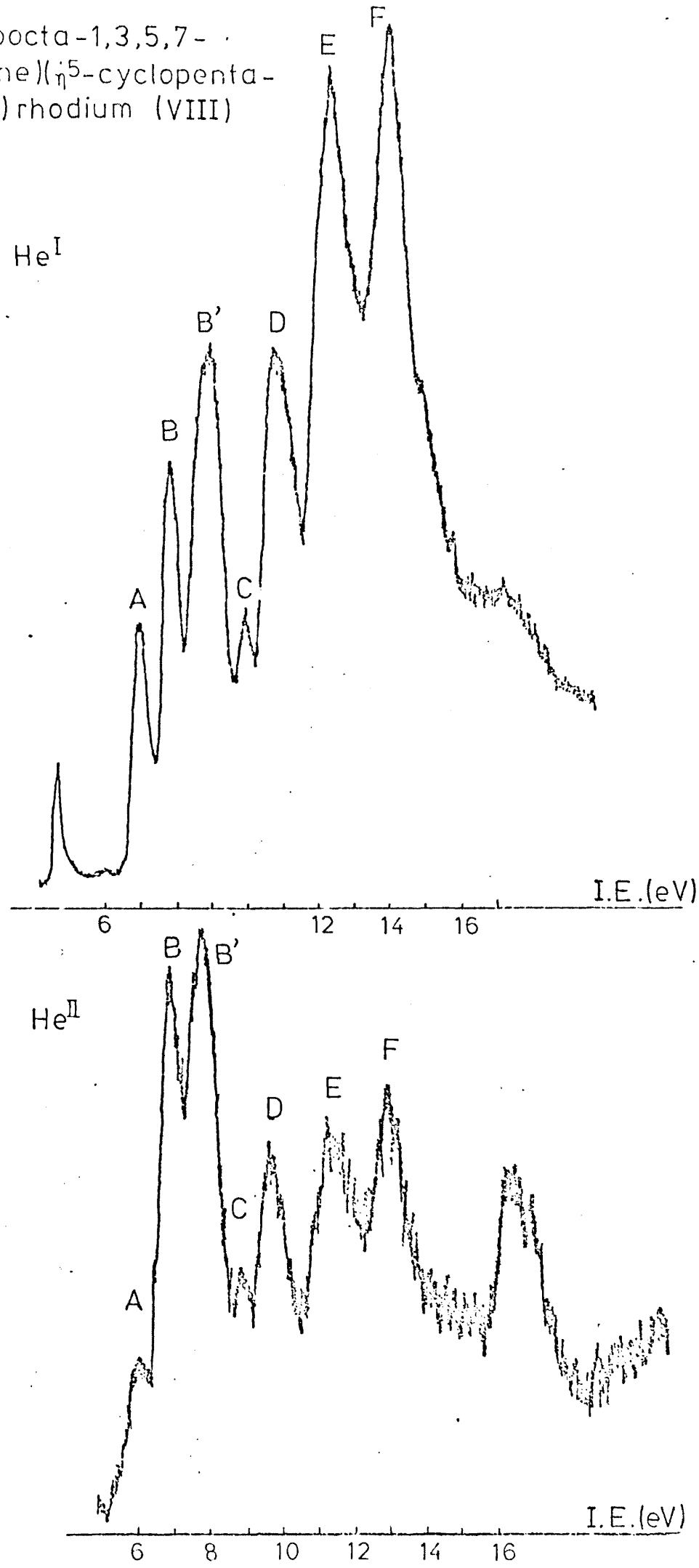

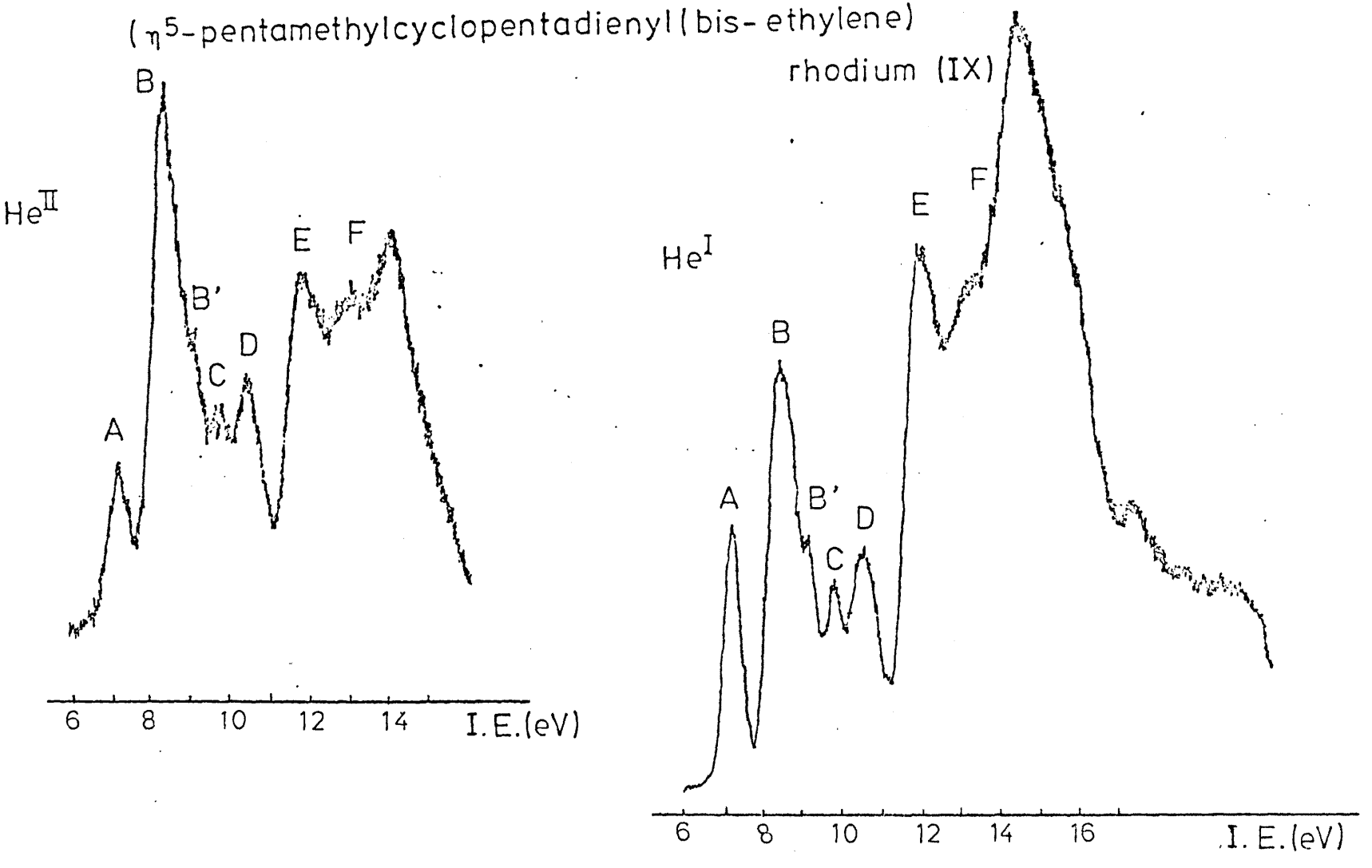
(η5-pentamethylcyclopentadienyl(bis-ethylene)
rhodium (IX)
HeII
HeI
A
B
B'
C
D
E
F
6
8
10
12
14
16
I.E.(eV)

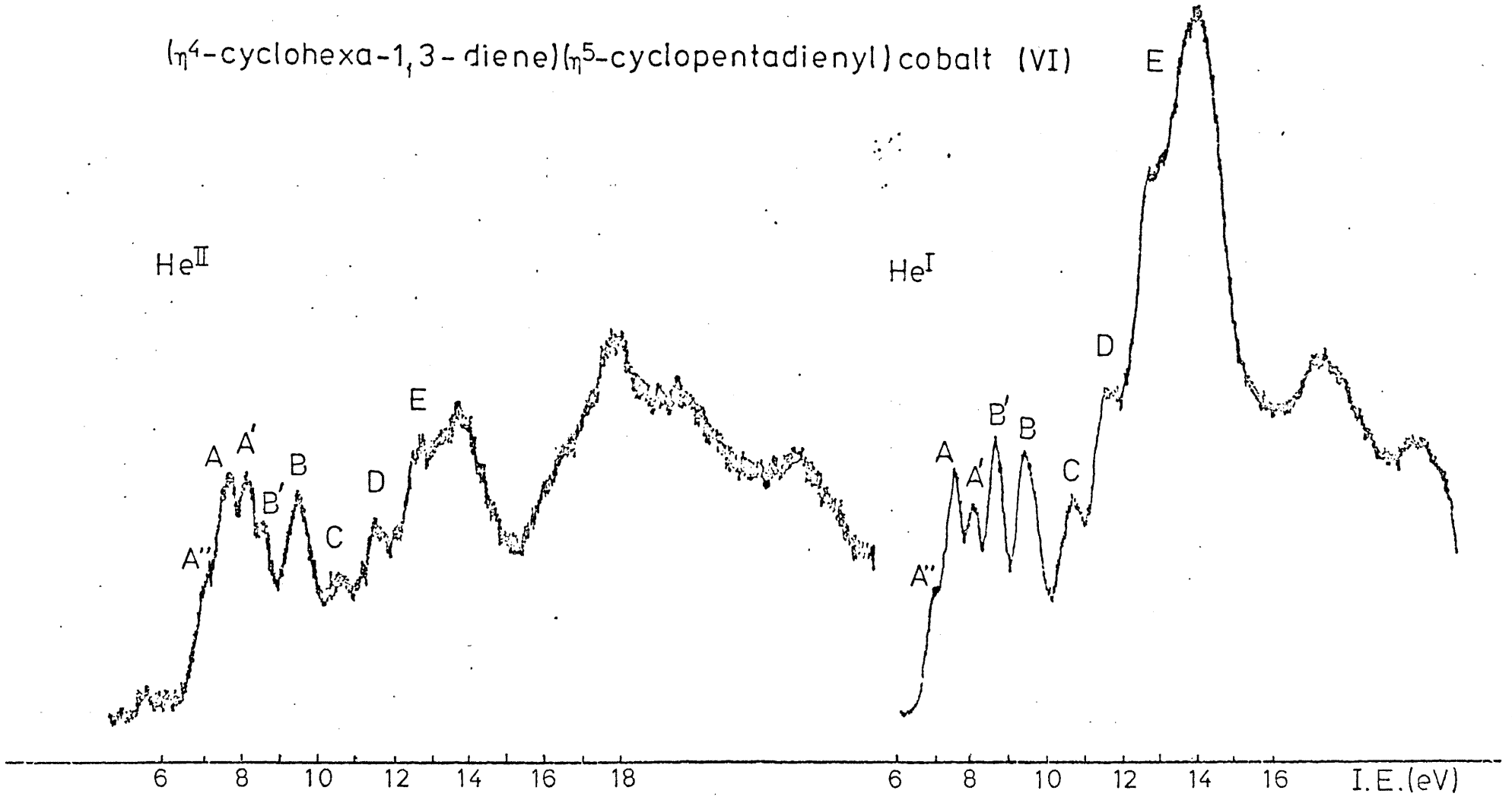
(η4-cyclohexa-1,3-diene)(η5-cyclopentadienyl)cobalt (VI)
HeII
HeI
A''
A
A'
B'
B
C
D
E
6
8
10
12
14
16
18
I.E.(eV)

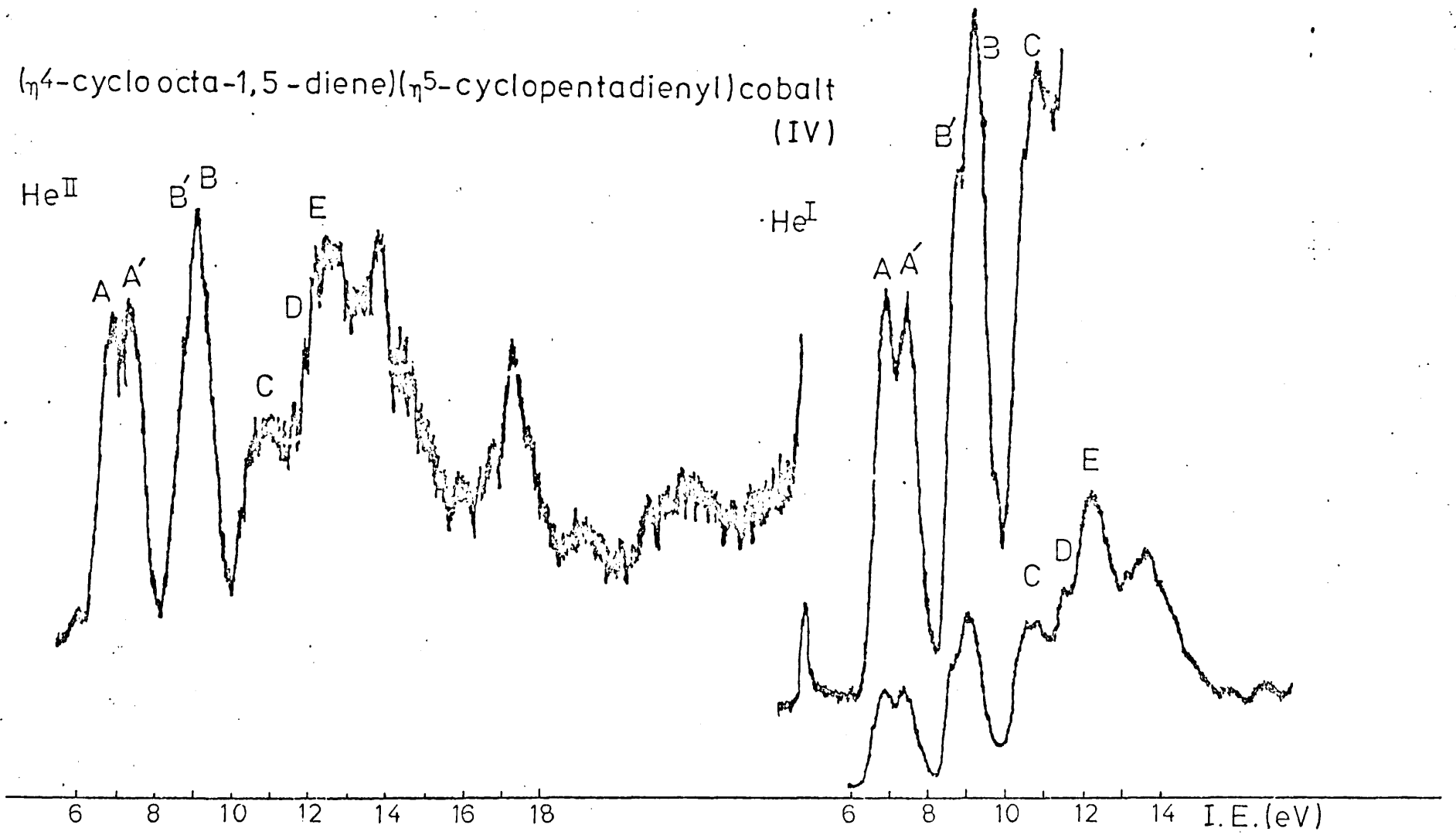
(η4-cycloocta-1,5-diene)(η5-cyclopentadienyl)cobalt
(IV)
HeII
HeI
A
A´
B´
B
C
D
E
6
8
10
12
14
16
18
I.E.(eV)

(η^4-cycloocta-1,5-diene)(η^5-tetramethylethyl-cyclopentadienyl)cobalt (IVa)

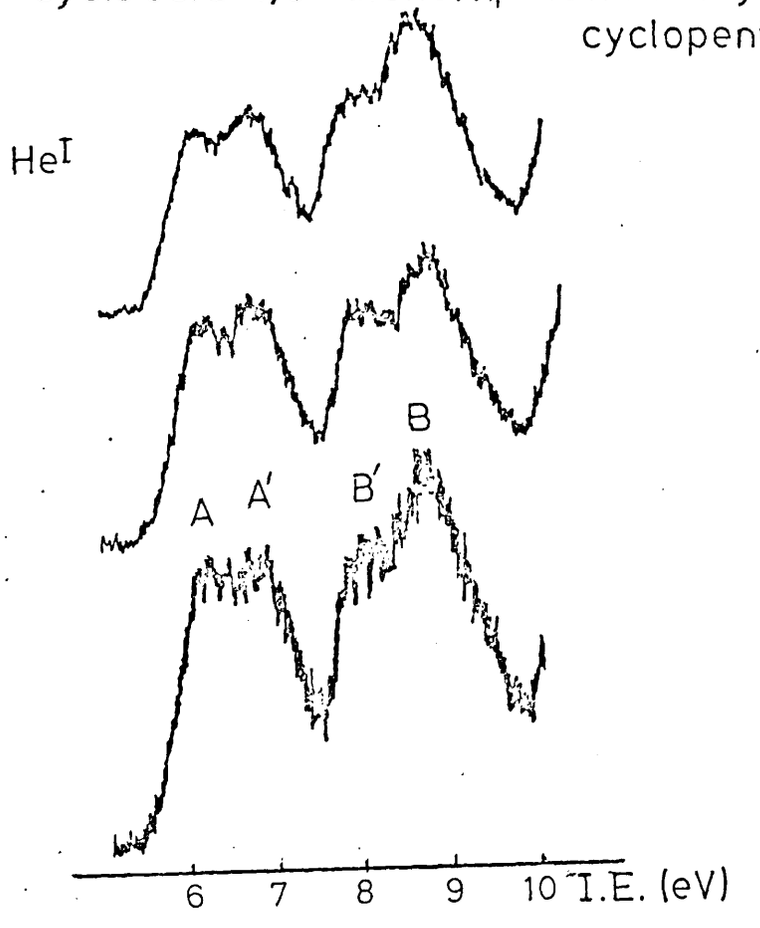

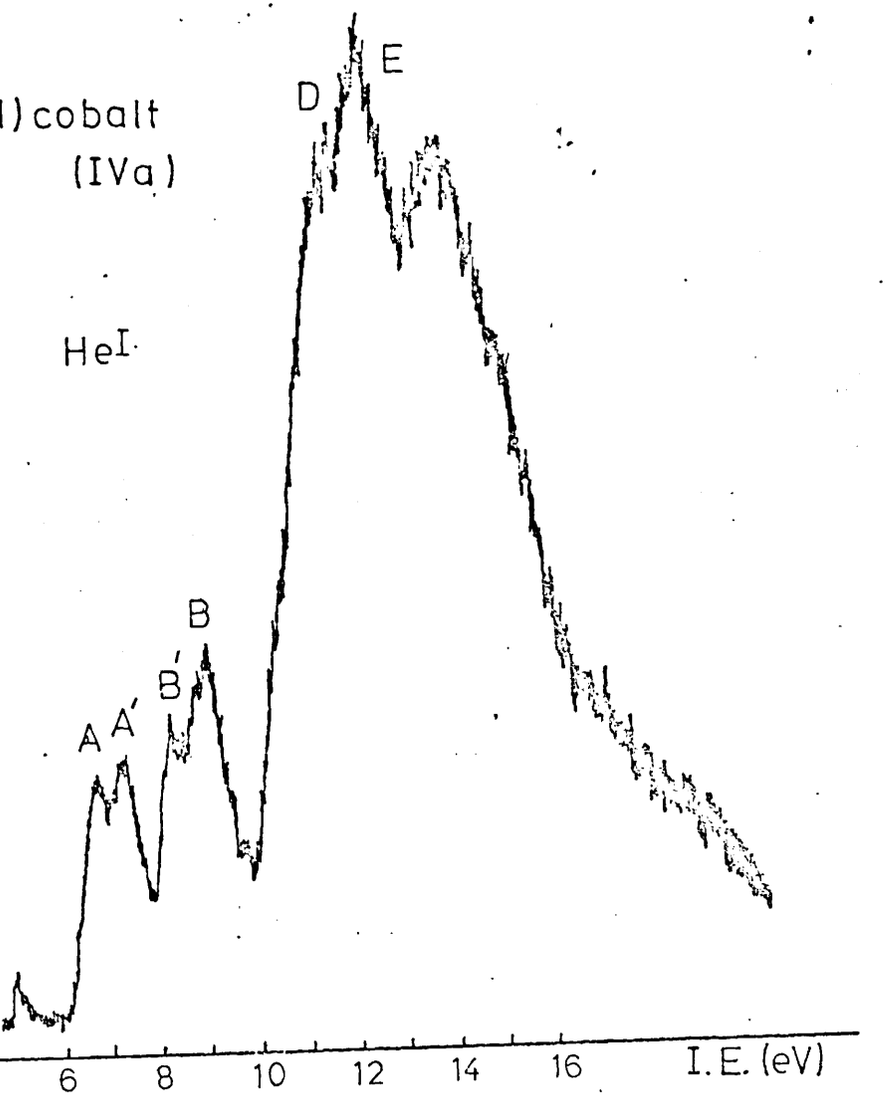

Chapter 5

Photoelectron spectra of η^5-cyclopentadienyldicarbonylcobalt and η^5-pentamethylcyclopentadienyldicarbonylrhodium

5.1 INTRODUCTION AND SUMMARY

The photoelectron spectra of η^5-cyclopentadienyldicarbonylcobalt (I) and η^5-pentamethylcyclopentadienyldicarbonylrhodium (II)(figure 5.1) are examined and related to the electronic structure as deduced in a semi-empirical way.

Figure 5.1 η^5-cyclopentadienyldicarbonylcobalt and η^5-pentamethylcyclopentadienyldicarbonylrhodium

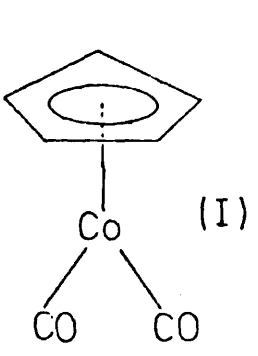

(I)

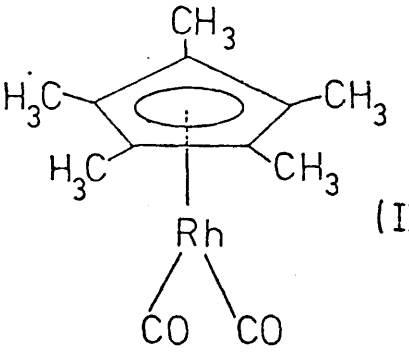

(II)

5.2 ELECTRONIC STRUCTURE

In the $CpM(CO)_2$ complexes, the $M(CO)_2$ group has C_{2v} symmetry; the carbonyl ligands will have an effect on the Cp ring to metal bond. In complexes $CpM(CO)_n$ where the $M(CO)_n$ local symmetry is C_{nv} and $n < 3$ (eg as in complexes (I) and (II) in contrast to η^5-cyclopentadienyltricarbonylmanganese, where n=3), the degeneracy of the d_{xz} and d_{yz} (e_1^*) mainly metal, and the mainly ligand e_1 π cyclopentadienyl molecular orbitals, will be lifted. These e_1 orbitals are the main orbitals involved in ring-metal bonding thus the cyclopentadienyl ring would be expected to undergo distortion. There is some evidence for a distortion from X-ray crystallographic study of similar complexes [267], although the small differences expected in carbon-carbon bond lengths may be within experimental error.

The cyclopentadienyl-metal system alone has C_{5v} symmetry and is discussed in detail by Hoffman et al [101].

Interaction of the metal and cyclopentadienyl levels is shown in figure 5.2a . A similar diagram is also given (figure 5.2b) for interaction between the metal and carbonyl groups under C_{2v} symmetry. The diagrams are qualitative only.

Figure 5.2

a) Interaction diagram for CpM

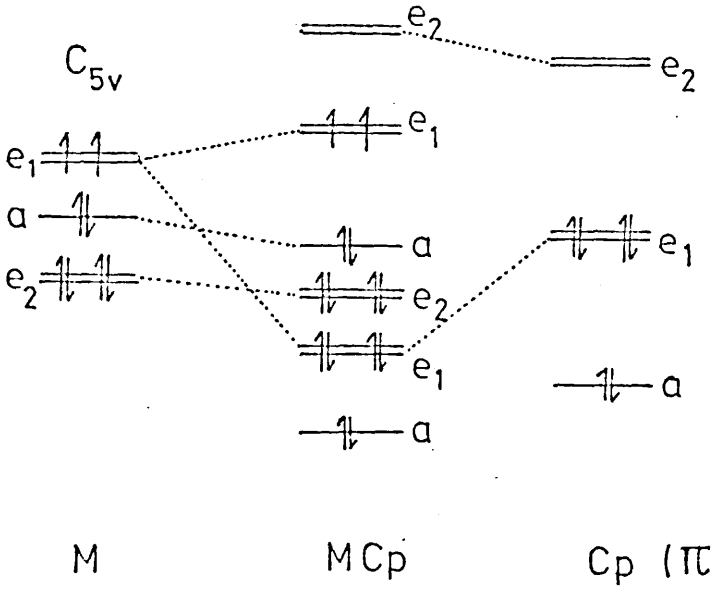

b) Interaction diagram for $M(CO)_2$

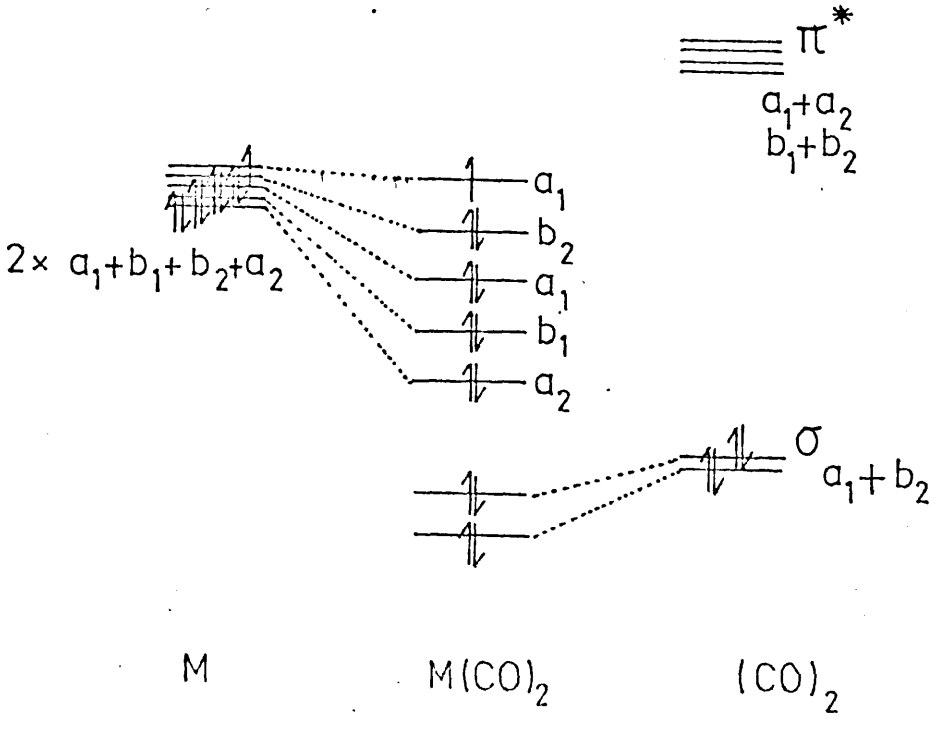

There are two possible methods for construction of a qualitative MO diagram for complexes (I) and (II); firstly, interaction of the CpM group with two carbonyl groups may be considered (figure 5.3), or secondly, the interaction between $M(CO)_2$ and the Cp group (figure 5.4). Axes assumed are as shown in figure 5.5 . If the η^5-cyclopentadienyl

Figure 5.5 Axes assumed for the construction of interaction diagrams

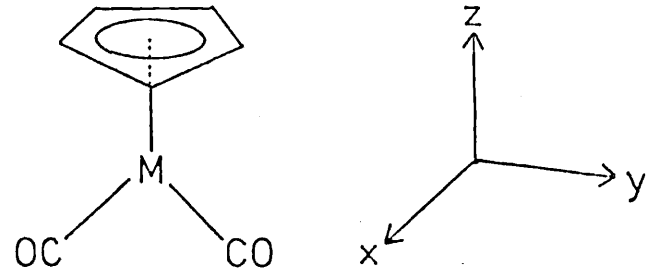

ring is taken as having a $C_{\infty v}$ rotational axis (free rotation of the ring may occur in the gas phase as for the metallocenes), the molecular symmetry is C_{2v}; the labels on the MO interaction diagrams refer to C_{2v} symmetry. Interaction may occur between the ring a_1+a_2 levels (derived from e_1) and the carbonyl antibonding π a_1+a_2 levels. One of the levels derived from the partly occupied metal 'e_1' d orbitals will be stabilised on complex formation by interaction with a CO π^* orbital; this corresponds to metal-carbonyl back donation. As a consequence the degeneracy of this level (metal e_1 d) is removed by population of a resulting b_1 or b_2 level, leading to ring distortion. It is not possible to say, from current data, which level will become populated; if it is the b_1 level, there will be a relative reduction in length of the C_1-C_2, C_1-C_5 and C_3-C_4 bonds, and if the b_2 level is populated, C_2-C_3 and C_4-C_5 will suffer a relative reduction in bond length.

In fact there is probably extensive interaction between the cyclopentadienyl e_1, metal d and carbonyl π antibonding orbitals, and the above localised picture of the bonding is rather inadequate. A detailed MO calculation

Figure 5.3 Molecular orbital diagram for $MCp(CO)_2$-

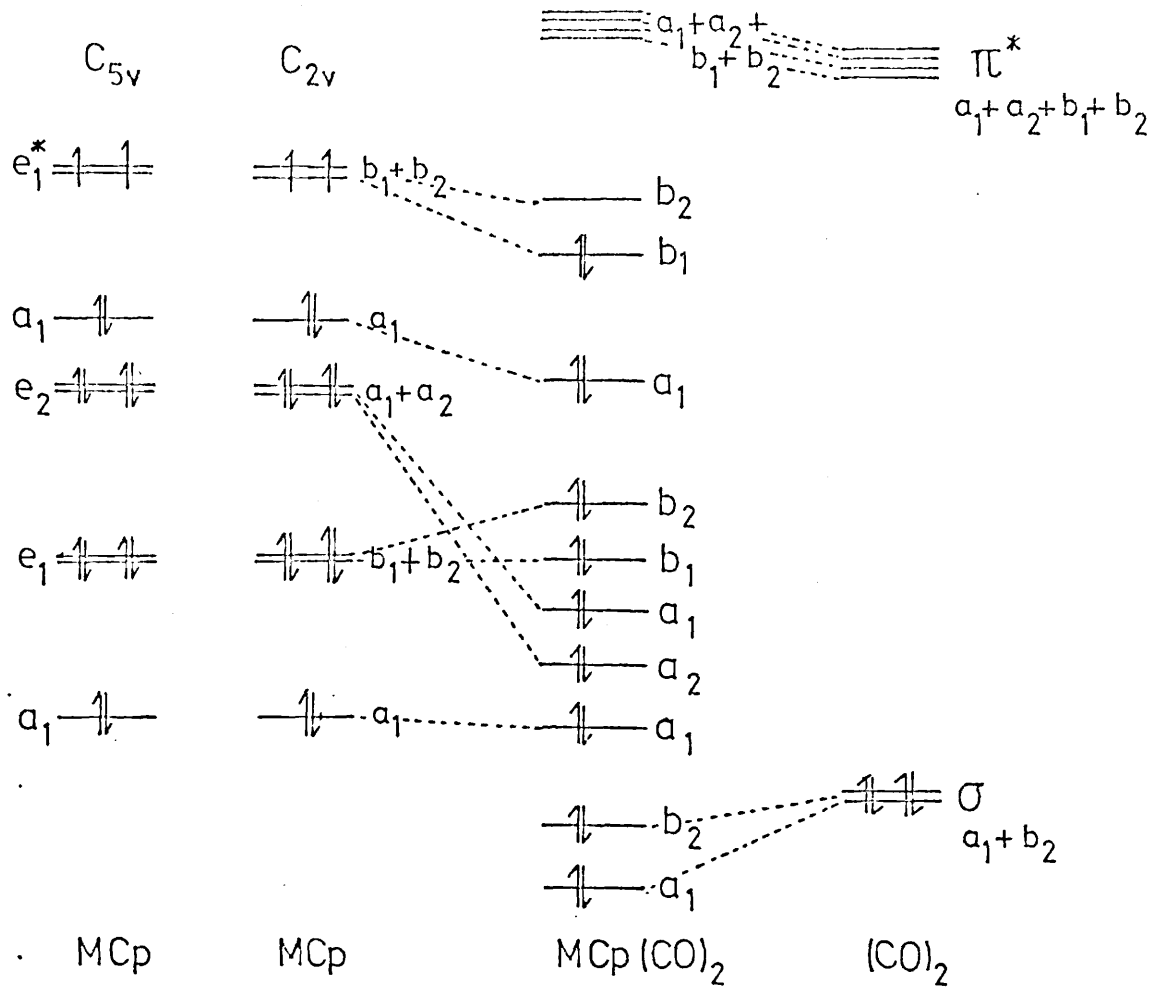

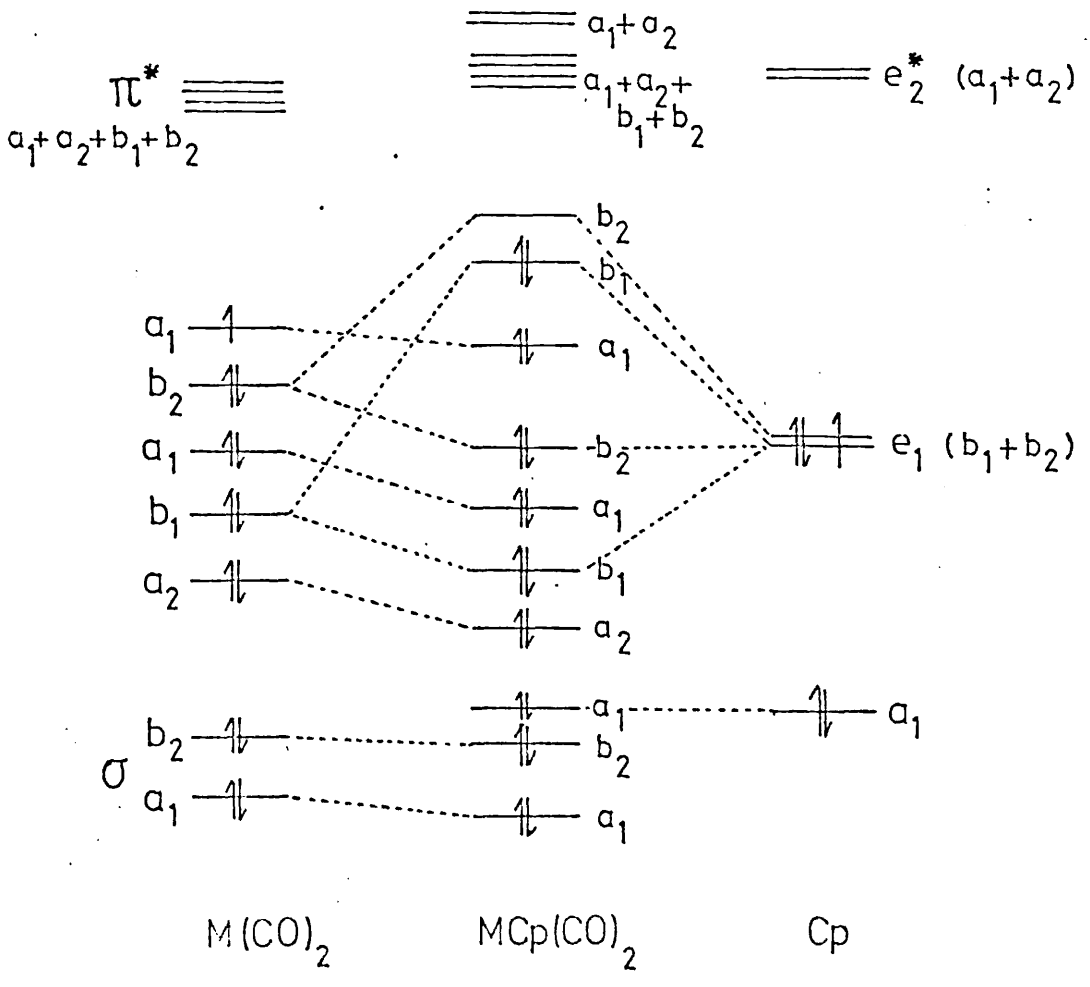

Figure 5.4 Molecular orbital diagram for $MCp(CO)_2$-

would be very useful.

5.3 PHOTOELECTRON SPECTRA: RESULTS AND DISCUSSION

Table 5.1 shows ionisation energy data for complexes (I) and (II) together with relative intensity measurements. Figure 5.6 is a correlation diagram showing the relative ionisation energies for the two complexes.

Table 5.1 Ionisation Energies (eV) for complexes (I) and (II)

Complex	A		B		C		D		
(I)	a	a'	b	b'	c	c'			
	7.51(s)	7.78	8.68	9.17	9.90	10.31	11.99(s)	13.54	
(II)	a	b	c	d		e	f	g	
	6.66	8.00	8.51	8.84		9.52	11.37	13.82,	16.70

Relative Intensities:

		A		B		C		D		
(I)	HeI	1.0		1.4		2.4		18.1		
	HeII	1.0		0.7		1.8		9.7		
		a	b		c+d		e	f	g	
(II)	HeI	1.0	0.8		2.9		2.5	7.2	~ 49	
	HeII	1.0	1.1		1.7		2.3	2.0	~ 11	

The PE spectra of (I) and (II) are obviously very different from those of similar complexes of the earlier transition metals, (eg $CpV(CO)_3$, $C_6H_6Cr(CO)_3$, and $CpMn(CO)_3$) in which the mainly ligand cyclopentadienyl π e_1 levels lie below the metal levels; this is certainly not the case for $CpCo(CO)_2$. This is probably due to the different symmetry and the increased contribution from the metal d* cyclopentadienyl π e_1 interaction, caused by the general lowering in energy of the metal levels across the transition series.

The PE spectrum of (I) shows three bands in the low IE region, A, B and C; on expansion these are seen each to consist of two peaks, labelled a, a'; b, b'; c, c'. The

Fig 5.6 Correlation diagram for complexes (I) and (II)

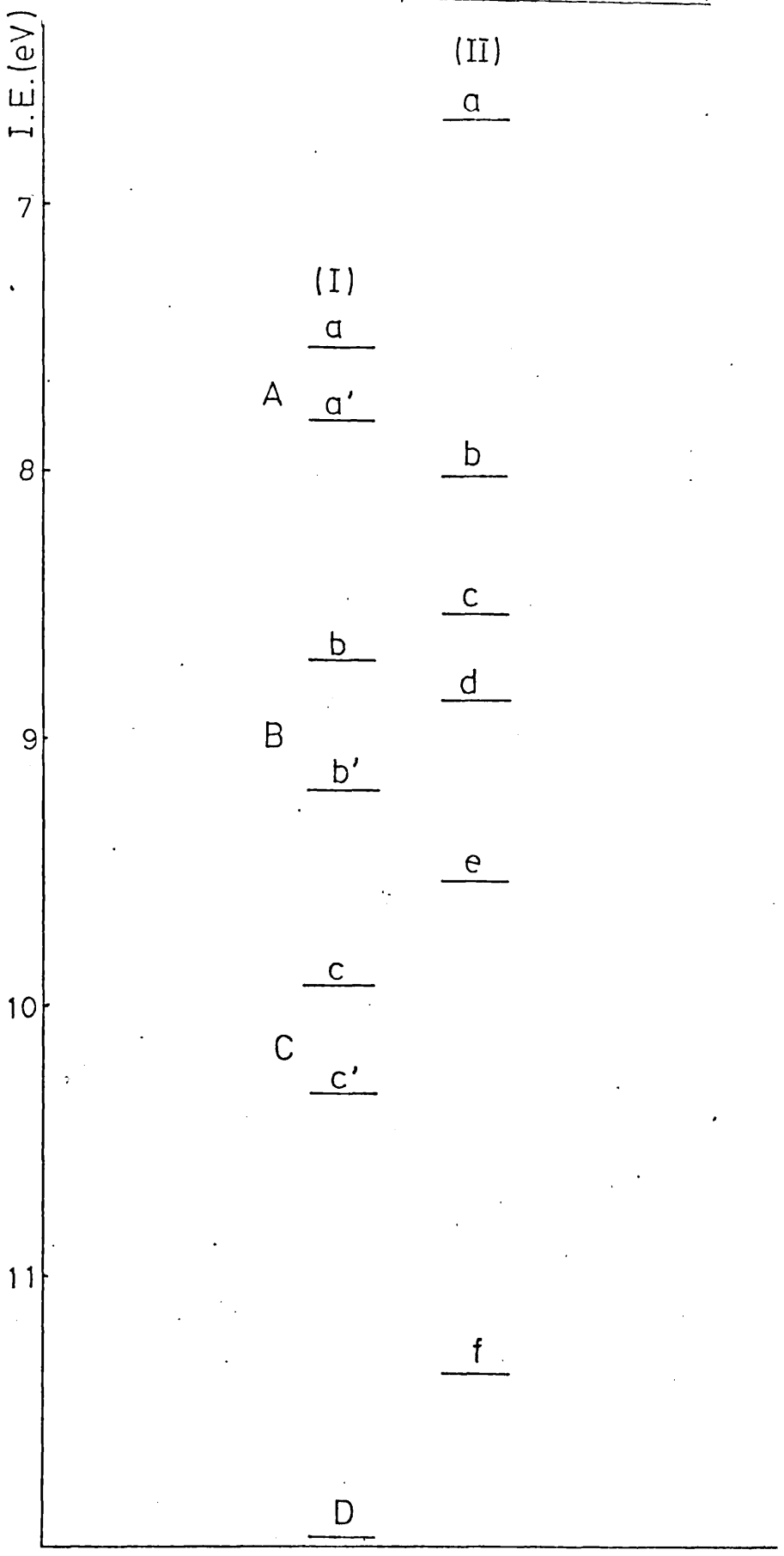

structure between C and D may be partly due to the HeI_β satellite of D, and is absent in the HeII spectrum. The baseline of the spectrum is difficult to determine; a great deal of decomposition of the complex is expected to occur within the spectrometer.

From relative intensity data in the HeII spectrum, clearly bands A and C are due to ionisation from essentially metal d orbitals, and band B to ionisation from orbitals of mainly ligand character. Thus region A is assigned to ionisation from the metal d 'e_1*' level which becomes the non-degenerate b_1+b_2 combination within the complex, and is expected to interact with the carbonyl π^* b_1+b_2 level. It is uncertain which of the b_1+b_2 levels is stabilised and populated; this should become clear with a knowledge of the cyclopentadienyl ring carbon-carbon bond distances. Ionisation from the essentially metal d a_1 level should also occur in region A. The very high HeII relative intensity of region A overall, is attributed to the high ionisation cross sections observed for e_1 metal d ionisation (chapter 3).

Band B is assigned to ionisation from the mainly ligand cyclopentadienyl orbitals, b_1+b_2 (derived from e_1); the bands b and b' are expected to show some metal character since some interaction with the b_1+b_2 (e_1) d metal levels is probable. Bands b and b' are not resolved in the HeII spectrum.

Region C (c and c') is assigned to ionisation from the metal a_1+a_2 (e_2) d orbitals which are likely to interact with the carbonyl π^* a_1+a_2 levels. Region D probably includes ionisation from the σ cyclopentadienyl level, and certainly includes ionisation from the carbonyl σ levels, as may be seen from HeII relative intensity data.

The PE spectrum of complex (II) is similar to that of (I); in general, the separation of the bands is better in

(II), indicating slight differences in metal-ligand interaction. The shifts to lower IE in the rhodium complex are largely due to the inductive effect of pentamethyl substitution of the cyclopentadienyl ring. Band f is probably due to ionisation from the methyl groups and is well separated from g, the region of ionisation from the carbonyl groups.

From the HeII relative intensity data, it appears that band b is due to ionisation from the mainly metal b_1 or b_2 (e_1) level, since it shows a large increase in relative intensity as noted for metal e_1 d ionisation in chapter 3. Band c is clearly due to ionisation from a mainly ligand (cyclopentadienyl) π b_1 or b_2 (e_1) level and does not show significant metal character. Band e is certainly due to ionisation from a mainly metal level, probably the $a_1+a_2(e_2)$ levels, as suggested by the HeII relative intensity. The remaining bands, a and d must be assigned to the other mainly metal a_1 level and the other mainly ligand π b_1 or b_2 level giving an assignment analogous to that of complex (I) with a reversal of the first two levels. However, both a and d show metal character compared to c. It is concluded that there is a more uneven interaction between the cyclopentadienyl ring b_1+b_2 (e_1) levels and the metal d b_1+b_2 (e_1) levels than in complex (I) resulting in an overall increase in ligand to metal donation (increased metal character in the mainly ligand π b_1 or b_2 level) in complex (II). This is not unexpected due to the increased inductive effect of the methyl groups on the cyclopentadienyl ligand, thus increasing the ligand to metal donation and resulting in increased population of the relevant d antibonding levels.

5.4 EXPERIMENTAL

Photoelectron spectra were obtained and calibrated as in chapter 4.

The complex (I), η^5-cyclopentadienyldicarbonyl-

cobalt was obtained from Fluorochem Ltd., and a sample of η^5-pentamethylcyclopentadienyldicarbonylrhodium was donated by Dr.D. M. P. Mingos of the Inorganic Chemistry Laboratory, Oxford and purified by the author.

5.5 PHOTOELECTRON SPECTRA

1. η^5-cyclopentadienyldicarbonylcobalt (I) HeI
2. η^5-cyclopentadienyldicarbonylcobalt (I) HeII
3. η^5-pentamethylcyclopentadienyldicarbonylrhodium (II) HeI
4. η^5-pentamethylcyclopentadienyldicarbonylrhodium (II) HeII

η^5- cyclopentadienyl dicarbonylcobalt (I)

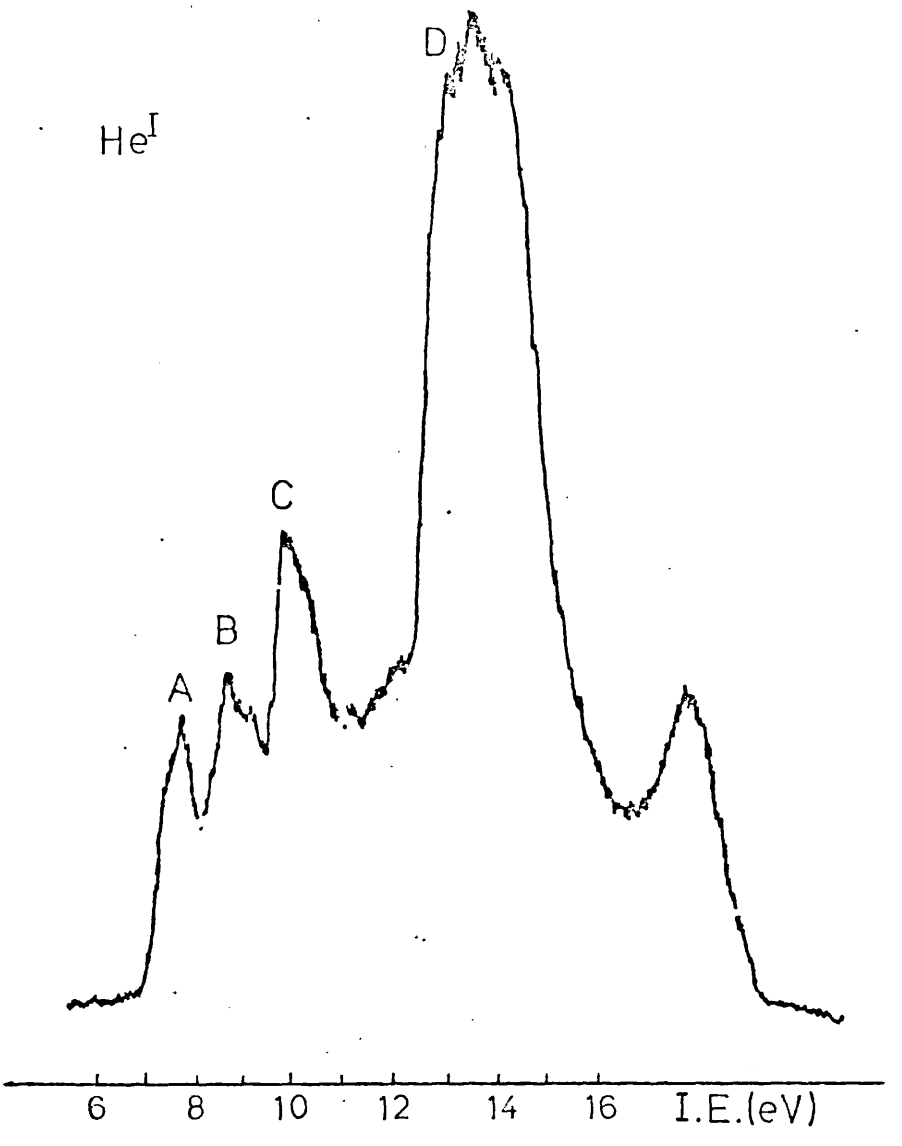

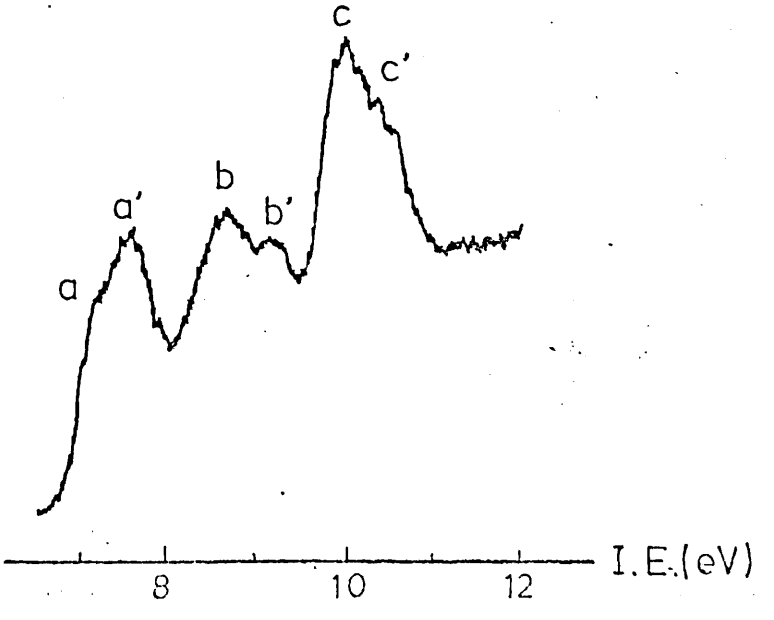

η^5- cyclopentadienyl dicarbonyl cobalt (I)

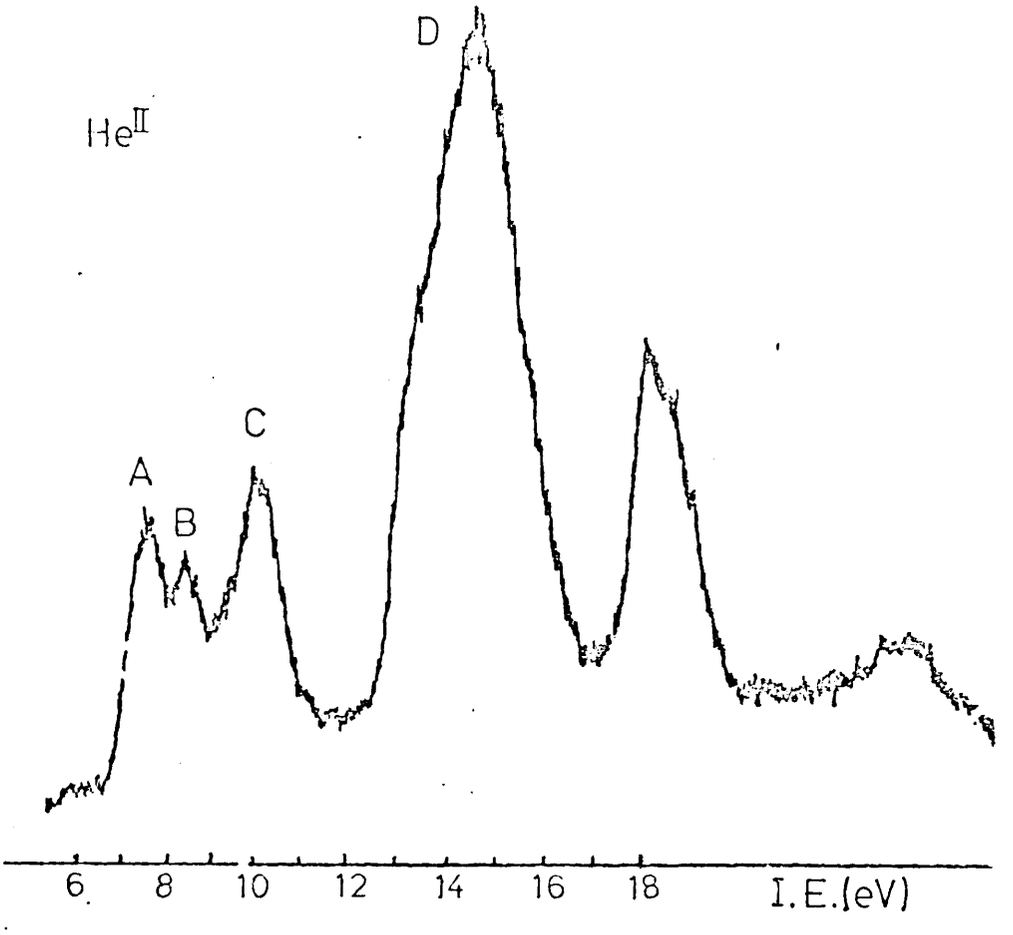

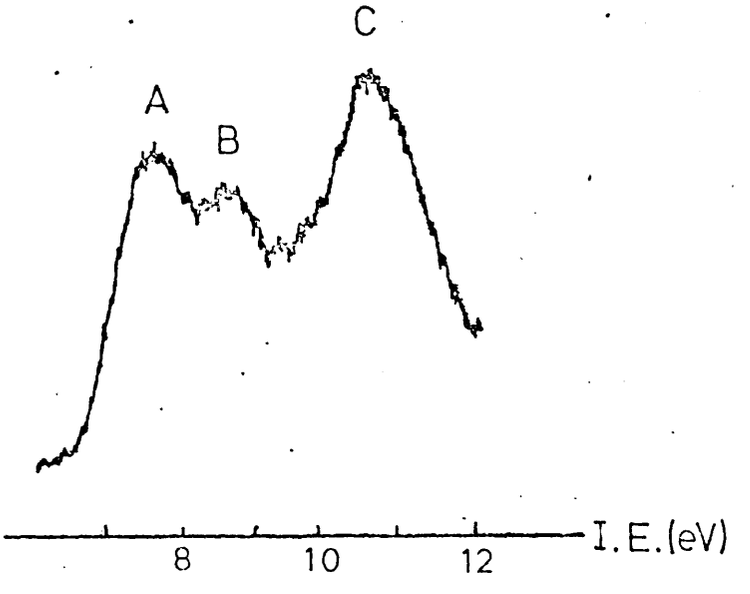

η^5-pentamethylcyclopentadienyl dicarbonyl rhodium (II)

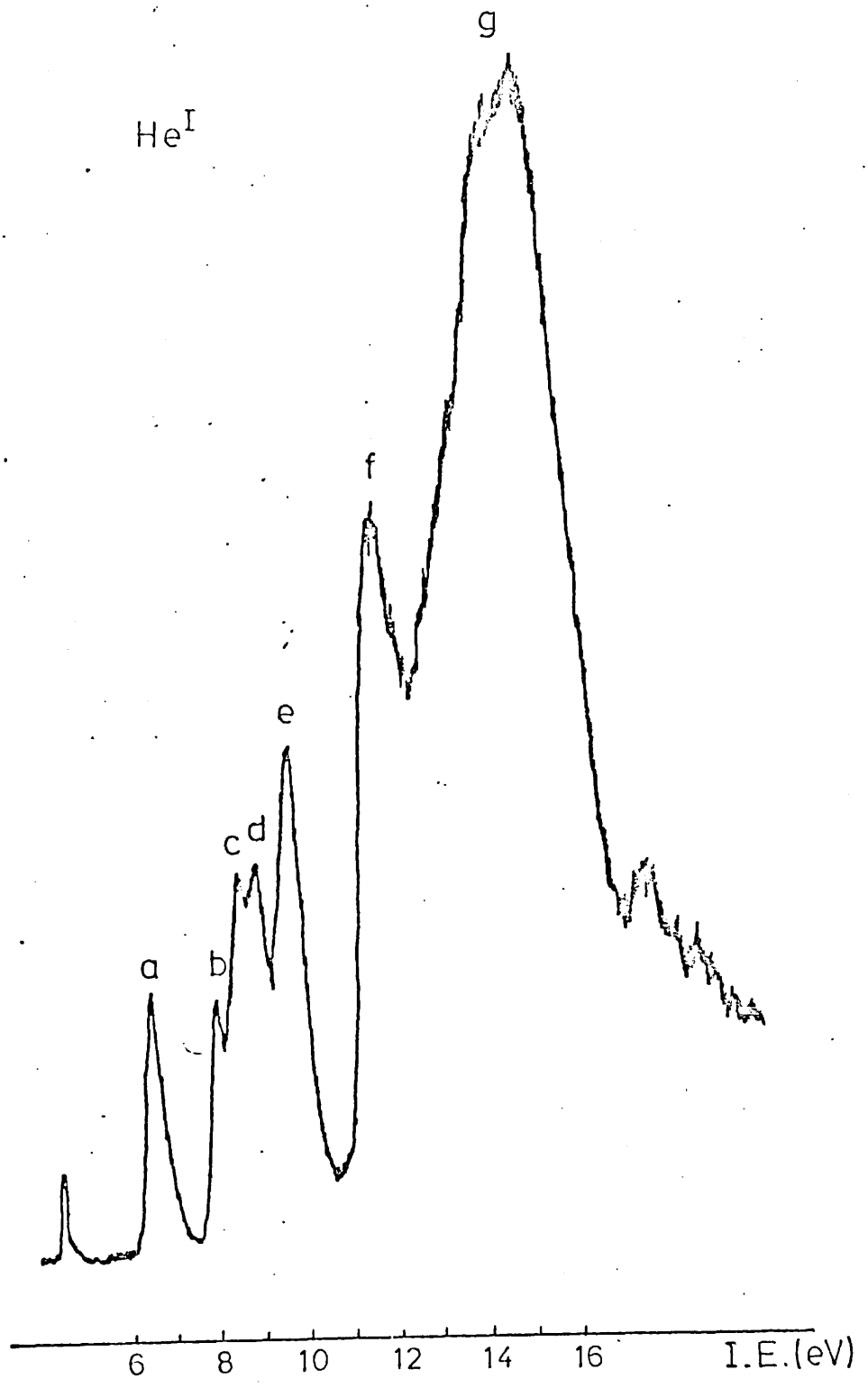

η^5-pentamethylcyclopentadienyl dicarbonyl rhodium (II)

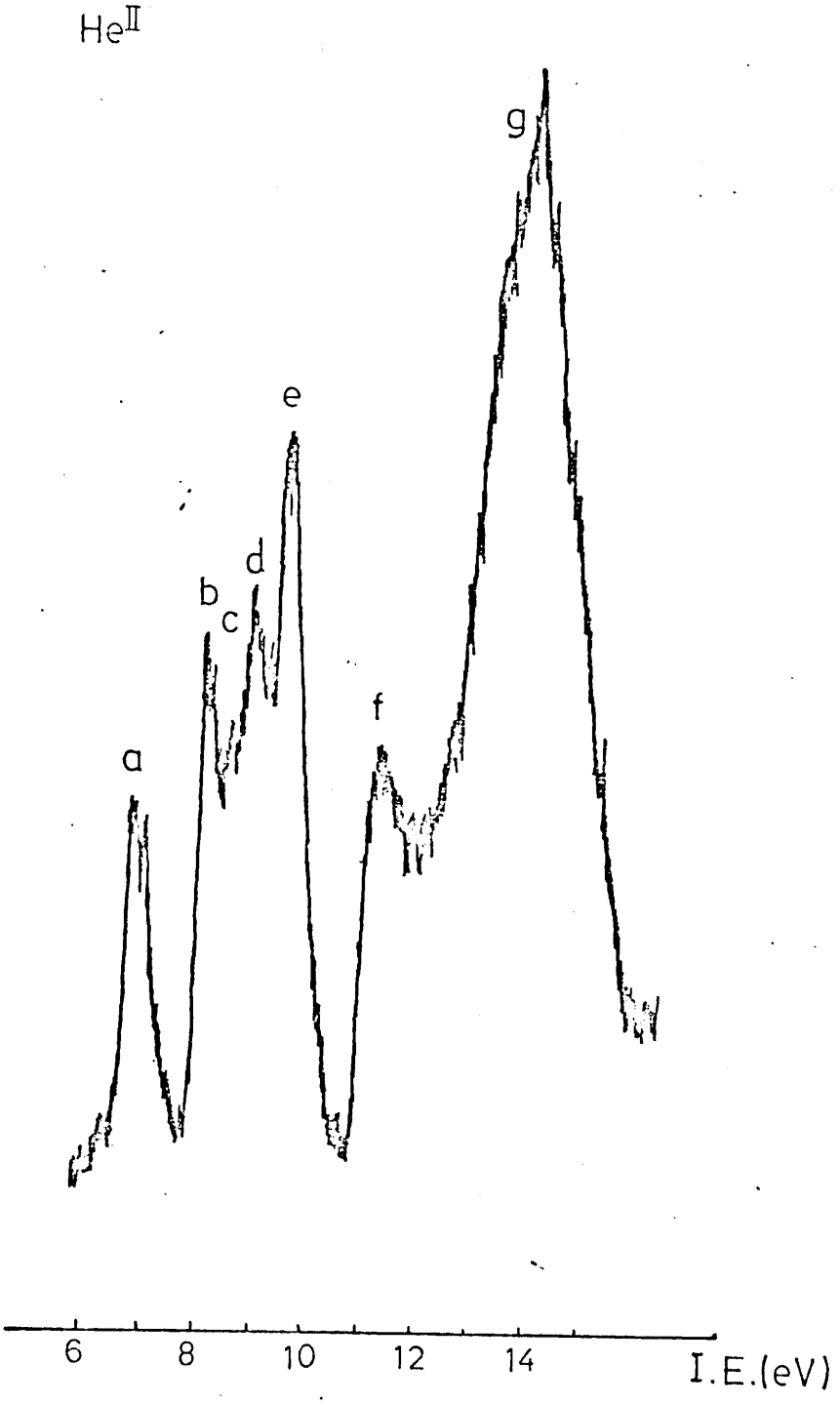

Appendix 1

Instrumentation

A1.1 THE PHOTOELECTRON SPECTROMETER

The photoelectron spectra of complexes described in chapter 2 were obtained using a Perkin Elmer model PS 16/18 spectrometer, developed from the work of Turner [6,45], and modified to take a heated sample probe in order to obtain PE spectra for relatively involatile materials.

The instrument was later modified so that HeII PE spectra could be obtained at temperatures up to 500°C, and the spectra of complexes described in chapters 3, 4 and 5, were recorded using this modification.

A block diagram of the spectrometer is given in figure A1.1.

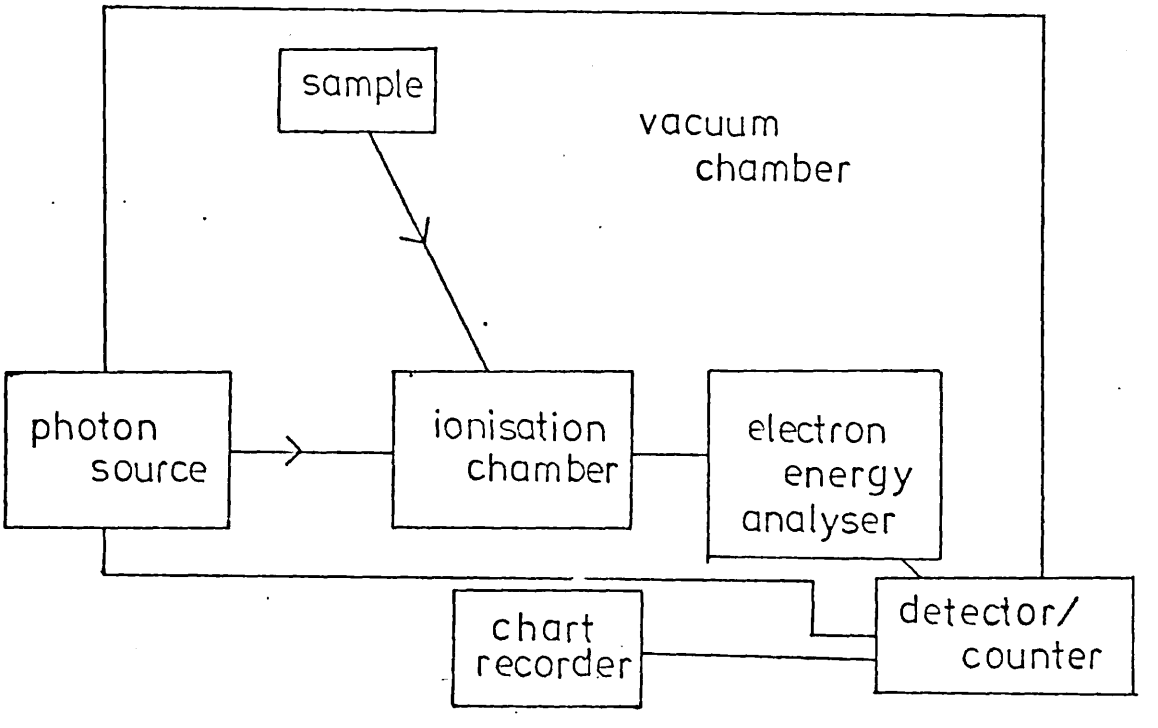

Figure A1.1 Schematic representation of a photoelectron spectrometer

A1.2 SIMPLE INLET SYSTEMS AND SAMPLE HEATING

The instrument is designed for vapour phase analysis; the pressure in the main chamber is approximately 10^{-6} torr (τ). Compounds having an adequate vapour pressure at room temperature, under the vacuum conditions of the instrument, are held in a vessel outside the vacuum chamber and are admitted to the ionisation chamber via a needle valve and probe.

For less volatile samples the instrument makes use of heat from the lamp (source) to vaporise the sample. Samples are acceptable for study using this instrument provided they are stable in vacuo at temperatures necessary to give them a vapour pressure between 10^{-1} and $10^{-2}\tau$. The PS 16/18 was designed to operate routinely up to 250°C; with the subsequent modification, temperatures up to 500°C are attainable.

The heated insert probe is shown in figure A1.2. Heat is conducted from the tip of the lamp to the glass sample tube through the copper tube holder, which includes within its construction the ionisation chamber, approximately 1 cm^3 by volume. By variation of the rate of flow of a coolant (air or water) through a heat exchanger surrounding the lamp tip, fine temperature control of the sample is possible. The temperature of the sample may also be roughly adjusted by variation of the lamp voltage. The glass sample tube is of 4 mm external diameter; typical sample consumption varies between 1 mg and 10 mg per hour, which should be sufficient for one spectrum.

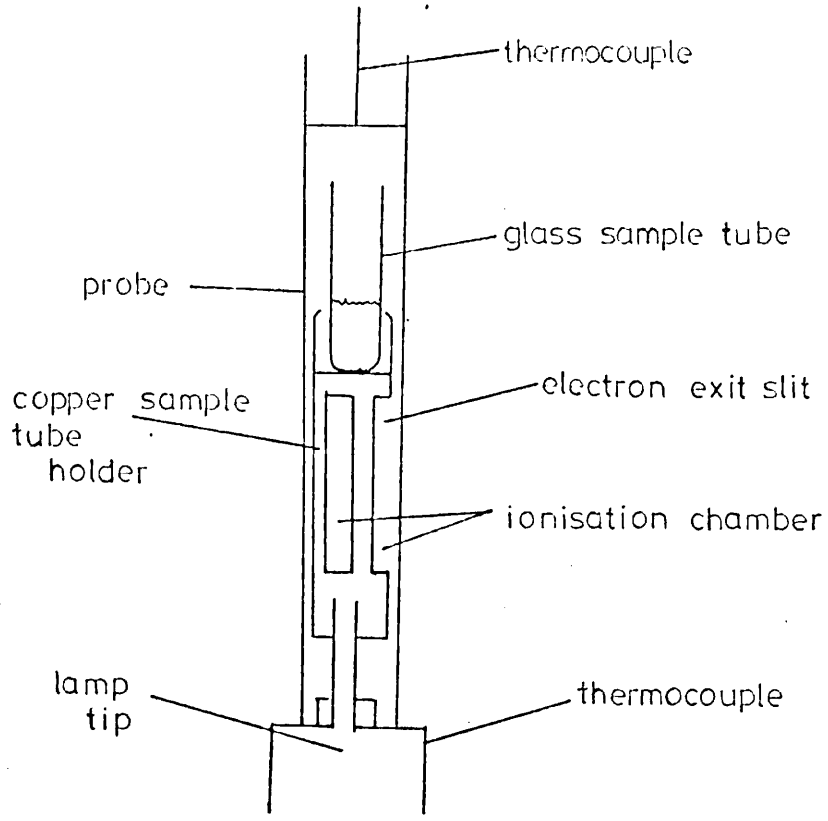

Figure A1.2 Heated sample inlet system

A1.3 PHOTON SOURCE

The photons produced in this system are generated from the direct current discharge through low pressure helium gas exciting the 584 Å HeI (21.22 eV) line. Using the modified instrumentation - a hollow cathode discharge lamp developed by H. J. Lempka (Helectros Developments Ltd.) - HeII 303.81 Å (40.81 eV) photons are produced in sufficient quantity for the HeII PE spectra of compounds to be obtained. In general a higher proportion of HeII photons may be obtained by use of lower pressures and greater power; this lamp operates with high currents (200-300 mA) and moderate voltages (0.3-1 kV) and discharges are successfully maintained under these conditions at an optimum pressure of 0.15τ, when the distribution of photon flux gives an estimated HeI_{α} : $HeII_{\alpha}$ ratio of approximately 2.5 : 1. Differential pumping of the helium gas takes place through a series of capillaries at the lamp tip.

Photons from the lamp are collimated by a steel

capillary tube terminating in a windowless capillary at the lamp tip, and pass into the ionisation chamber where they collide with the sample vapour. The HeII photons are unfiltered, thus it is not possible to explore ionisation processes in the ionisation energy region beyond 26 eV, partly because of overlap of the HeI and HeII spectra, and partly because of the large self absorption peak at 24.5 eV arising from ionisation of the helium gas by HeII photons.

The HeI and HeII photoelectron spectra of nitrogen obtained using the instrument described above, are shown in figures A1.3 and A1.4. Satellite peaks associated with higher energy HeI and HeII photons are visible. The HeII PE spectrum has no interference in the HeI region due to the fact that the sensitivity of this technique is an order of magnitude higher for HeI photons. However the $HeII_{\beta}$ satellite spectrum is significantly high in intensity - about 10% of the $HeII_{\alpha}$ spectrum - from which it is displaced by 7.56 eV to higher kinetic energy. This effect requires correction to be made where relative intensities of $HeII_{\alpha}$ PE spectra are compared, as in chapters 3 and 4.

A1.4 ANALYSER AND DETECTOR

The photoelectrons pass through the ionisation chamber exit slit (figure A1.2) into a 127° cylindrical electrostatic analyser [282] of rhodium plated copper, with constant resolving power ($E/\Delta E$). The sensitivity decreases linearly with decreasing electron kinetic energy, and so in any study making use of relative intensity measurements (chapters 3 and 4), a correction must be made for this effect.

The photoelectrons from the analyser pass through an exit slit of variable width, 0 to 4 thou; the width is adjusted to give a compromise between signal intensity and resolution. The photoelectrons then reach the electron multiplier detector, or channeltron. The electron count is

Figure A1.3 He I Photoelectron spectrum of nitrogen

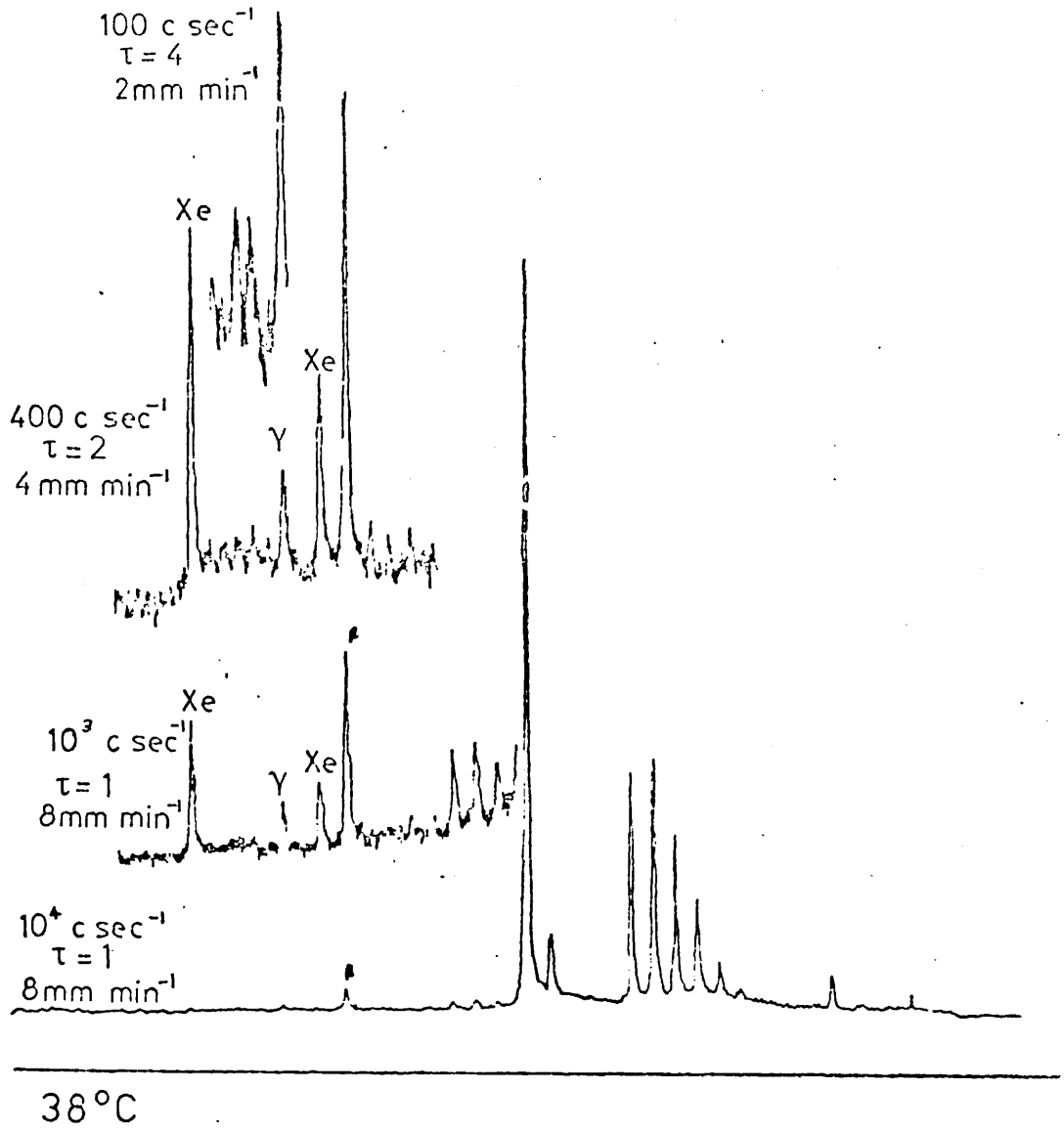

photon energies

		calculated difference	observed difference
He I_α	21·21 (eV)		
He I_β	23·09	1·87	1·87
He I_γ	23·74	2·52	2·53
He I_δ	24·05	2·83	2·96

Figure A1·4 He II Photoelectron spectrum of nitrogen showing α, β, γ, δ and ε satellites

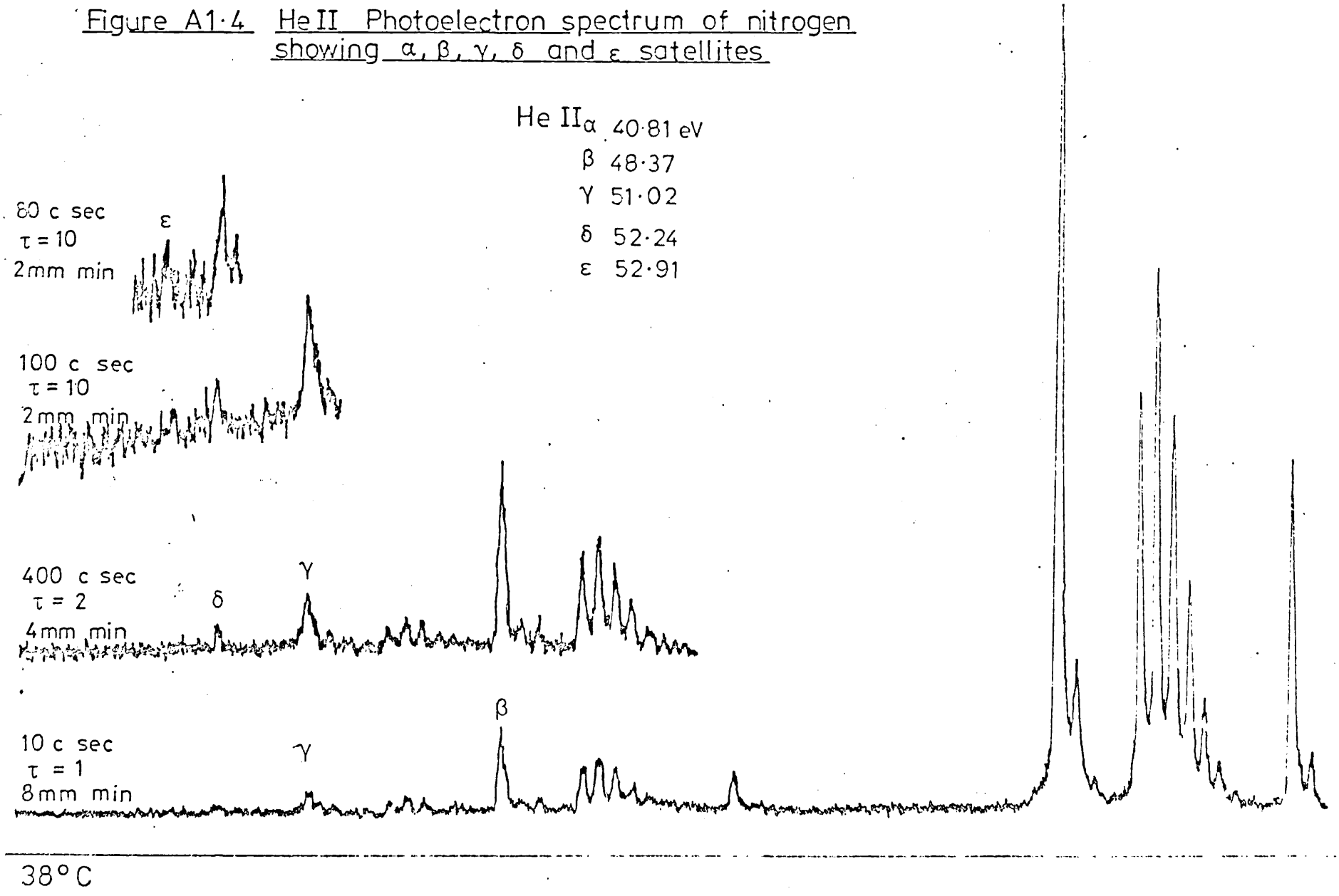

averaged over a period of time (time constant, τ) in order to enhance the signal to noise ratio. The time constant may be varied to one of several settings (0.4 to 20 s) depending on sensitivity and scan speed. The signal is plotted against electron kinetic energy by a chart recorder. The ordinate scale of electron flux is in counts s^{-1}, increasing upwards, and the abscissa scale of electron kinetic energy (in eV) increases from right to left; that is, ionisation energy increases from left to right. Figure A1.5 shows a diagram of the 127° cylindrical analyser and ionisation chamber .

All critical surfaces of the target chamber and analyser need to be as electrically uniform as possible, and clean. These surfaces are rhodium plated. The presence

Figure A1.5 Diagram showing analyser and ionisation chamber

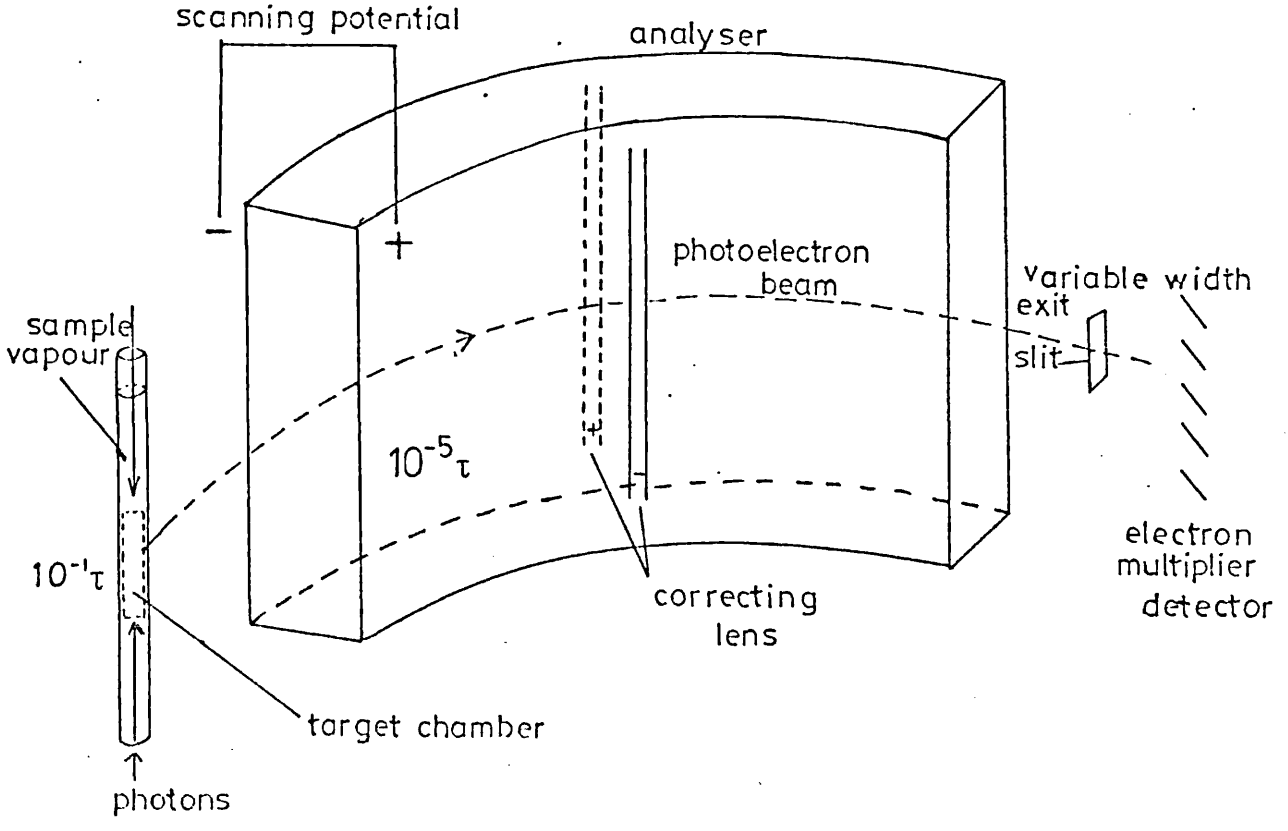

of unwanted magnetic and electromagnetic fields, to which low energy electrons are very sensitive, is eliminated by screening the analyser with a high permeability material, such as Mu-metal.

A1.5 CALIBRATION AND RESOLUTION

With the instrumentation described, 'internal' calibration of each spectrum may be carried out; this is necessary in high temperature work due to shifts caused by surface effects, such as metal deposition from the sample. A trace of the calibrant gas or mixture of gases may be metered into the ionisation chamber through a fine capillary during each run, giving direct calibration. However this will obviously have an effect on any relative intensity measurements.

Since the PE spectra described in chapters 3 to 5 were obtained at low temperatures, they were calibrated at the end of each run, when the calibration gas (either argon, xenon or nitrogen, or a mixture of these) was allowed into the ionisation chamber together with the sample vapour, and the main peaks recorded. Additional calibration (internal) is provided by the helium self-ionisation peak at 24.5 eV; this appears in many of the spectra given in chapters 3 to 5.

Using nitrogen calibration peaks at 15.57 and 16.69 eV, the resolution R, is defined in (A1)1, where P is

$$R = \frac{x}{y} \times P \qquad (A1)1$$

the spacing of the nitrogen doublet in meV, x is the width at half height of a nitrogen peak, and y the distance between the peak centres. Resolution for the complexes studied in chapters 2 to 5 was generally in the region of 40 meV although the optimum resolution claimed for this instrument (HeI) is 18 meV. In all the PE spectra presented here, a compromise

was made between signal intensity and resolution by varying the width of the analyser exit slit.

A1.6 EXPERIMENTAL RECORDING CONDITIONS

i) Chapter 2

compounds:

1. cyclohexa-1,3-diene
2. cyclohepta-1,3-diene
3. cycloocta-1,3-diene
4. cyclohepta-1,3,5-triene
5. cycloocta-1,3,5,7-tetraene

6. η^4-buta-1,3-dienetricarbonyliron (I)
7. η^4-cyclohexa-1,3-dienetricarbonyliron (II)
8. η^4-cyclohepta-1,3-dienetricarbonyliron (III)
9. η^4-cycloocta-1,3-dienetricarbonyliron (IV)

10. η^4-cyclohexa-1,3-dienetricarbonylruthenium (V)
11. η^4-cyclohepta-1,3-dienetricarbonylruthenium (VI)

12. η^4-cyclohepta-1,3,5-trienetricarbonyliron (VII)
13. η^4-cycloocta-1,3,5,7-tetraenetricarbonyliron (VIII)

14. η^4-hepta-3,5-dien-2-oltricarbonyliron (IX)
15. η^4-1-methylhexa-2,4-dien-1-oatetricarbonyliron (X)

16. HeII PE spectrum of (VIII)

COMPOUND	TIME CONSTANT	SCAN SPEED mm min^{-1}	COUNTS s^{-1}	INLET	TEMP °C
1	1	8	4×10^3	volatile	
2	1	8	4×10^3	"	
3	1	8	10^4	"	
4	2	4	10^3	"	
5	2	4	4×10^3	"	
6 (I)	10 (4)	1 (2)	100 (400)	"	
7 (II)	2	4	10^3	involatile	20
8 (III)	2	4	10^3	"	33
9 (IV)	1	8	10^4	"	40
10 (V)	1	8	10^4	volatile	
11 (VI)	1	8	4×10^3	"	
12 (VII)	2	4	10^3	involatile	20
13 (VIII)	2	4	4×10^3	"	40
14 (IX)	2	4	4×10^3	"	30
15 (X)	1	8	4×10^3	"	30
16 HeI	1	8	10^3	"	47
(VIII) HeII	10	1	100	"	"

ii) Chapter 3

compounds:

1. vanadocene (I)
2. chromocene (II)
3. manganocene (III)
4. 1,1'-dimethylmanganocene (IIIa)
5. ferrocene (IV)
6. cobaltocene (V)
7. nickelocene (VI)
8. ruthenocene (VII)
9. biscycloheptadienylruthenium (VIIa)

COMPOUND		TIME CONSTANT	SCAN SPEED mm min^{-1}	COUNTS s^{-1}	INLET	TEMP °C
(I)	(HeI)	2	4	4×10^3	involatile	55
	(HeII)	4	2	400	"	46
(II)	(HeI)	1	8	10^3	"	50
	(HeII)	4	2	100	"	54
	(HeII)	10	1	100	"	66
(III)	(HeI)	2	4	4×10^3	"	46
	(HeII)	10	2 (exp)*	400	"	63
(IIIa)	(HeI)	1	8	10^3	volatile	
	(HeI)	2	4 (exp)	10^3	"	
	(HeII)	4	2 (exp)	100	"	
(IV)	(HeI)	2	8 (exp)	10^3	involatile	28
	(HeII)	10	2 (exp)	100	"	30
(V)	(HeI)	1	8	4×10^3	"	40
	(HeII)	4	2	400	"	40
(VI)	(HeI)	1	8	4×10^3	"	50
	(HeII)	4	2	400	"	52
(VII)	(HeI)	2	4	10^3	"	63
	(HeI)	1	8 (exp)	10^3	"	73
	(HeII)	10	1	100	"	57
	(HeII)	10	2 (exp)	100	"	58
(VIIa)	(HeI)	1	8 (exp)	4×10^3	"	49
	(HeII)	4	2	400	"	59
	(HeII)	10	2 (exp)	400	"	55

*expanded scale (abscissa)

iii) Chapter 4

compounds:

1. (η^5-cyclopentadienyl)(η^4-buta-1,3-diene)rhodium (I)
2. (η^5-cyclopentadienyl)(η^4-buta-1,3-diene)iridium (II)
3. (η^5-cyclopentadienyl)(η^4-2-methyl-buta-1,3-diene) iridium (III)
4. (η^4-cycloocta-1,5-diene)(η^5-cyclopentadienyl) cobalt (IV)
5. (η^4-cycloocta-1,5-diene)(η^5-tetramethylethylcyclopentadienyl)cobalt (IVa)
6. (η^4-cycloocta-1,5-diene)(η^5-cyclopentadienyl) rhodium (V)
7. (η^4-cycloocta-1,5-diene)(η^5-pentamethylcyclopentadienyl)rhodium (Va)
8. (η^4-cyclohexa-1,3-diene)(η^5-cyclopentadienyl) cobalt (VI)
9. (η^4-cyclohexa-1,3-diene)(η^5-cyclopentadienyl) rhodium (VII)
10. (η^4-cycloocta-1,3,5,7-tetraene)(η^5-cyclopentadienyl) rhodium (VIII)
11. (η^5-pentamethylcyclopentadienyl)(bis-ethylene) rhodium (IX)
12. (η^4-hepta-3,5-dien-2-one)(η^5-cyclopentadienyl) rhodium (X)
13. (η^4-hepta-3,5-dien-2-one)(η^5-cyclopentadienyl) iridium (XI)
14. (η^4-hexa-2,4-dien-1-al)(η^5-cyclopentadienyl) rhodium (XII)

COMPOUND		TIME CONSTANT	SCAN SPEED mm min^{-1}	COUNTS s^{-1}	INLET	TEMP °C
1. (I)	(HeI)	1	8	4×10^3	involatile	45
	(HeII)	4	2	400	"	46
	(HeII)	10	2 (exp)	400	"	39
2. (II)	(HeI)	1	8	10^3	"	39
	(HeI)	2	8 (exp)	4×10^3	"	45
	(HeII)	4	2	400	"	43
	(HeII)	10	2 (exp)	400	"	44
3. (III)	(HeI)	1	8	4×10^3	"	41
	(HeII)	10	2 (exp)	400	"	40
	(HeII)	4	2	400	"	42
4. (IV)	(HeI)	1	8 (exp)	4×10^3	"	41
	(HeII)	4	2	100	"	38
5. (IVa)	(HeI)	2	4	10^3	"	52
	(HeII)	10	1	100	"	54
6. (V)	(HeI)	1	8 (exp)	4×10^3	"	57
	(HeII)	10	2 (exp)	100	"	51
7. (Va)	(HeI)	1	8	4×10^3	"	76
	(HeII)	2	8 (exp)	4×10^3	"	86
	(HeII)	10	1	400	"	80
8. (VI)	(HeI)	1	8 (exp)	4×10^3	"	41
	(HeII)	4	2	400	"	40
9. (VII)	(HeI)	1	8	4×10^3	"	56
	(HeI)	2	4	10^3	"	48
	(HeII)	4	2	400	"	52

	COMPOUND		TIME CONSTANT	SCAN SPEED mm min^{-1}	COUNTS s^{-1}	INLET	TEMP °C
10.	(VIII)	(HeI)	2	4	10^3	involatile	62
		(HeI)	2	4 (exp)	10^3	"	66
		(HeII)	4	2	100	"	69
		(HeII)	10	2 (exp)	100	"	72
11.	(IX)	(HeI)	1	8	4×10^3	"	76
		(HeII)	4	2	400	"	80
12.	(X)	(HeI)	1	8	4×10^3	"	76
		(HeII)	2	4	400	"	86
13.	(XI)	(HeI)	2	4	10^3	"	78
		(HeII)	4	2	100	"	81
14.	(XII)	(HeI)	2	4	10^3	"	84
		(HeII)	4	2	100	"	87

iv) Chapter 5

compounds:

1. η^5-cyclopentadienyldicarbonylcobalt (I)
2. η^5-pentamethylcyclopentadienyldicarbonylrhodium (II)

COMPLEX		TIME CONSTANT	SCAN SPEED mm min^{-1}	COUNTS s^{-1}	INLET	TEMP °C
1. (I)	(HeI)	1	8	4×10^3	volatile	
	(HeII)	4	2	10^3	"	
2. (II)	(HeI)	2	4	10^3	involatile	45
	(HeII)	4	2	100	"	52

REFERENCES

1. M. Robinson, W. F. Rawlinson, Phil. Mag., (1914), 28, 277.

2. M. de Broglie, C. r. Lebd. Seanc. Acad. Sci., Paris, (1921), 172, 274.

3. C. Nordling, E. Sokolowski, K. Siegbahn,
   a) Phys. Rev., (1957), 105, 1676.
   b) Arkiv. Physik, (1957), 12, 301.

4. S. Hagström, C. Nordling, K. Siegbahn, Phys. Lett., (1964), 9, 235.

5. L. Nemec, L. Chia, P. Delahay, J. Phys. Chem., (1975), 79, 2935.

6. D. W. Turner, M. I. Al-Joboury, J. Chem. Phys., (1962), 37, 3007.

7. D. C. Frost, C. A. McDowell, D. A. Vroom,
   a) Phys. Rev. Lett., (1965), 15, 512.
   b) J. Chem. Phys., (1967), 46, 4255.
   c) Proc. Roy. Soc. A, (1967), 296, 566.

8. a) W. C. Price, "Molecular Spectroscopy" ed. P. Hepple, Inst. of Petroleum, London, (1968).
   b) H. J. Lemka, T. R. Passmore, W. C. Price, Proc. Roy. Soc. A, (1968), 304, 53.

9. R. G. Egdell, A. F. Orchard, D. R. Lloyd, N. V. Richardson, J. Electr. Spectr. & Rel. Phen., (1977), 12, 415.

10. D. E. Eastman, Proceedings of the IV International Conference on vacuum ultra-violet radiation physics, ed. E. Koch, R. Haensel, C. Kunz, Pergamon Press, New York, N. Y., (1974).

11. J. B. West, G. V. Marr, Proc. Roy. Soc. A, (1976), 349, 397.

12. a) J. A. R. Samson, J. L. Gardner, Phys. Rev. Lett., (1974), 33, 671.
b) M.J. Lynch, A. B. Gardner, K. Codling, G. V. Marr, Phys. Lett. A., (1973), 43, 237.
c) R. G. Houlgate, J. B. West, K. Codling, G. V. Marr, J. Phys. B., (1974), 7, L470.
d) R. G. Houlgate, J. B West, K. Codling, G. V. Marr, J. Electr. Spectr. & Rel. Phen., (1976), 9, 205.

13. S. Süzer, P. R. Hilton, N. S. Hush, S. Nordholm, J. Electr. Spectr. & Rel. Phen., (1977), 12, 357.

14. G. M. Bancroft, T. K. Sham, D. E. Eastman, W. Gudat, J. Amer. Chem. Soc., (1977), 99, 1752.

15. J. H. D. Eland, "Photoelectron Spectroscopy", Butterworths, London, (1974).

16. D. R. Lloyd, J. Phys. E, scient. instrum., (1970), 3, 629.

17. T. Koopmans, Physica, (1934), 1, 104.

18. W. G. Richards, Int. J. Mass Spectr. & Ion Phys., (1969), 2, 419.

19. R. F. Fenske, Progr. in Inorg. Chem., (1976), 21, 179.

20. D. M. P. Mingos, Adv. in Organomet. Chem., (1977), 15, 1.

21. P. E. Cade, K. D. Sales, A. C. Wahl, J. Chem. Phys., (1966), 44, 1973.

22. L. S. Cederbaum, G. Hohlneicher, W. von Niessen, Mol. Phys., (1973), 26, 1405.

23. A. Hamnett, Part II thesis, Oxford, (1970).

24. C. C. J. Roothaan, Rev. Mod. Phys., (1951), 21, 69.

25. R. Walder, Dissertation, Oxford, (1975).

26. J. C. Slater, Phys. Rev., (1930), 36, 57.

27. M. F. Guest, M. B. Hall, I. H. Hillier, Mol. Phys., (1973), 25, 629.

28. L. S. Cederbaum, G. Hohlneicher, W. von Niessen, Chem. Phys. Lett., (1973), 18, 503.

29. J. A. Connor, L. M. R. Derrick, M. B. Hall, I. H. Hillier, M. F. Guest, D. R. Lloyd, Mol. Phys., (1974), 28, 1193.

30. J. A. Connor, I. H. Hillier, V. R. Saunders, M. H. Wood, M. Barber, Mol. Phys., (1972), 24, 497.

31. J. A. Connor, M. B. Hall, I. H. Hillier, W. N. E. Meredith, M. Barber, Q. Herd, J. Chem. Soc. Faraday II, (1973), 69, 1677.

32. B. R. Higginson, D. R. Lloyd, J. A. Connor, I. H. Hillier, J. Chem. Soc. Faraday II, (1974), 70, 1418.

33. M. F. Guest, I. H. Hillier, B. R. Higginson, D. R. Lloyd, Mol. Phys., (1975), 29, 113.

34. I. H. Hillier, R. M. Canadine, Discuss. Farad. Soc., (1969), 47, 27.

35. I. H. Hillier, M. F. Guest, B. R. Higginson, D. R. Lloyd, Mol. Phys., (1974), 27, 215.

36. I. H Hillier, V. R. Saunders,
    a) Mol. Phys., (1971), 22, 1025.
    b) Mol. Phys., (1972), 23, 449.

37. M. M. Rohmer, A. Veillard, Chem. Comm., (1973), 250.

38. J. Demuynck, A. Veillard, Theoret. Chim. Acta., (Berlin), (1973), 28, 241.

39. M. M. Coutière, J. Demuynck, A. Veillard, Theoret. Chim. Acta., (1972), 27, 281.

40. K. H. Johnson, Adv. Quantum Chem., (1973), 7, 143.

41. P. A. Cox, Structure and Bonding, (1975), 24, 59.

42. P. A. Cox, A. F. Orchard, Chem. Phys. Lett., (1970), 7, 273.

43. P. A. Cox, S. Evans, A. F. Orchard, Chem. Phys. Lett., (1972), 13, 386.

44. E. U. Condon, G. H. Shortley, "The Theory of Atomic Spectra", Cambridge University Press, Cambridge, (1935).

45. D. W. Turner, "Molecular Photoelectron Spectroscopy", Wiley, (1970).

46. J. A. R. Samson, R. B. Cairns, Phys. Rev., (1968), 173, 80.

47. F. Brogli, E. Heilbronner, Helv. Chim. Acta., (1971), 54, 1423.

48. H. Jahn, E. Teller, Proc. Roy. Soc., London, (1937), A161, 220.

49. G. Herzberg, "Electronic spectra and electronic structure of polyatomic molecules", Van Nostrand, Princeton, N. J., (1966).

50. M. D. Sturge, Solid State Physics, (1967), 20, 92.

51. M. O. Krause, Phys. Rev., (1969), 177, 151.

52. T. N. Chang, T. Isihara, Phys. Rev. Lett., (1971), 27, 838.

53. A. J. Blake, J. H. Carver, J. Quant. Spec. Rad. Transfer, (1972), 12, 59.

54. J. Cooper, R. N. Zare, Lectures in Theoretical Physics, Gordon and Breach, New York, (1969), 11C, 317.

55. T. A. Carlson, A. E. Jonas, J. Chem. Phys., (1971), 55, 4913.

56. A. J. Blake, Proc. Roy. Soc., London, (1971), A325, 555.

57. J. H. Carver, J. L. Gardner, J. Quant. Spec. Rad. Transfer, (1972), 12, 207.

58. A. J. Blake, J. H. Carver, J. Chem. Phys.. (1967), 47, 1038.

59. P. G. Burke, K. T. Taylor, J. Phys. B, (1975), 8, 2620.

60. C. D. Lin, Phys. Rev. A, (1974), 9, 171

61. H. Reihlen, A. Gruhl. G. von Hessling, O. Pfrengle, Ann. Chem., (1930), 482, 161.

62. W. Reppe, H. Vetter, Ann. Chem., (1953), 582, 133.

63. B. F. Hallam, P. L. Pauson, J. Chem. Soc., (1958), 642.

64. W. G. Dauben, M. E. Lorber, Org. Mass. Spectrometry, (1970), 3, 216.

65. R. B. King, T. A. Manuel, F. G. A. Stone, J. Inorg. & Nucl. Chem., (1961), 16, 233.

66. R. B. King, Organomet. Syntheses, (1965), 1.

67. B. F. G. Johnson, J. Lewis, P. McArdle, G. L. P. Randall, J. Chem. Soc. Dalton, (1972), 456.

68. B. A. Sosinsky, S. A. R. Knox, F. G. A. Stone, J. Chem. Soc. Dalton, (1975), 1633.

69. S. A. Miller, J. A. Tebboth, J. F. Tremaine, J. Chem. Soc., (1952), 632..

70. T. J. Kealy, P. L. Pauson, Nature, (1951), 168, 1039.

71. M. L. H. Green, L. Pratt, G. Wilkinson, J. Chem. Soc., (1959), 3753.

72. W. Haugen, M. Traetteberg, Sel. Topics in Struct. Chem., (1967), 113.

73. C. R. Brundle, M. Robin, J. Amer. Chem. Soc., (1970), 92, 5550.

74. C. Batich, O. Ermer, E. Heilbronner, J. R. Wiseman, Angew. Chem. (Int. ed.), (1973), 12, 312.

75. C. Batich, P. Bischof, E. Heilbronner, J. Electr. Spectr. & Rel. Phen., (1973), 1, 333.

76. P. Bischof, J. A. Hashmall, E. Heilbronner, V. Hornung, Helv. Chim. Acta, (1969), 52, 1745.

77. P. E. Haselbach, E. Heilbronner, G. Schroder, Helv. Chim. Acta, (1971), 54, 153.

78. P. Bischof, E. Heilbronner, Helv. Chim. Acta, (1970), 53, 1677.

79. A. Ansmann, B. Schrader, Angew. Chem. (Int. ed.), (1975), 14, 364.

80. G. Favini, F. Zuccarello, G. Buemi, J. Mol. Struct., (1969), 3, 385.

81. G. Dallinga, L. H. Toneman, J. Mol. Struct., (1967), 1, 11.

82. Z. Meić, M. Randić, Croat. Chem. Acta, (1968), 40, 43.

83. H. Oberhammer, S. H. Bauer, J. Amer. Chem. Soc., (1969), 91, 10.

84. S. S. Butcher, J. Chem. Phys., (1965), 42, 1830.

85. J. F. Chiang, S. H. Bauer, J. Amer. Chem. Soc., (1966), 88, 420.

86. K. Haugen, H Traetteberg, Acta Chem. Scand., (1972), 26, 3643.

87. P. Crews, Chem. Comm., (1971), 583.

88. a) P. Pesch, S. L. Freiss, J. Amer. Chem. Soc., (1950), 72, 5756.
b) K. Hafner, W. Kellensmann, Chem. Ber., (1962), 95, 2527.
c) E. A. Braude, Chem. Ind. (London), (1954), 1557.

89. M. Traetteberg, Acta Chem. Scand., (1970), 24, 2285.

90. O. Bastiansen, H. M. Seip, J. E. Boggs, Perspect. Struct. Chem., (1971), 4, 60.

91. M. Tractteberg, J. Amer. Chem. Soc., (1964), 86, 4265.

92. H. S. Kaufman, H. Mark, I. Fankuchen, Nature, (1948), 161, 165.

93. O. Bastiansen, L. Hedberg, K. Hedberg, J. Chem. Phys., (1957), 27, 1311.

94. O. S. Mills, G. Robinson, Acta Cryst., (1963), 16, 758.

95. F. A. Cotton, V. W. Day, B. F. Frenz, K. I. Hardcastle, J. M. Troup, J. Amer. Chem. Soc., (1973), 95, 4522.

96. S. M. Johnson, I. C. Paul, J. Chem. Soc. B, (1970), 1783.

97. V. A. Grieren, W. Hoppe, Acta Cryst., B, (1972), 28, 2766.

98. B. Dickens, W. Lipscomb, J. Chem. Phys., (1962), 37, 2084.

99. S. F. A. Kettle, Inorg. Chem., (1965), 4, 1661.

100. M. Elian, R. Hoffmann, Inorg. Chem., (1975), 14, 1058.

101. M. Elian, M. M. L. Chen, D. M. P. Mingos, R. Hoffmann, Inorg. Chem., (1976), 15, 1148.

102. M. L. H. Green, "Organometallic Compounds", Methuen, London, (1968), 2.

103. R. Pettit, G. Emerson, J. Mahler, J. Chem. Ed., (1963), 40, 175.

104. J. M. Landesberg, L. Katz., J. Organomet. Chem., (1971), 33, C15.

105. T. H. Whitesides, D. L. Lichtenberger, R. A. Budnik, Inorg. Chem., (1975), 14, 68.

106. D. M. P. Mingos, J. Chem. Soc. Dalton, (1977), 20.

107. C. A. Coulson, A. Golebiewski, Proc. Phys. Soc., (1961), 78, 1310.

108. G. I. Birnbaum, J. Amer. Chem. Soc., (1972), 94, 2455.

109 K. B. Birnbaum, Acta Cryst. B, (1972), 28, 161.

110. H. L. Retcofsky, E. N. Frankel, H. S. Gutowsky, J. Amer. Chem. Soc., (1966), 88, 2710.

111. H. G. Preston, J. C. Davis, J. Amer. Chem. Soc., (1966), 88 1585.

112. L. Kruczynski, J. Takats, J. Amer. Chem. Soc., (1974), 96, 932.

113. L. Kruczynski, J. Takats, Inorg. Chem., (1976), 15, 3140.

114. C. G. Kreiter, S. Struber, L. Wackerle, J. Organomet. Chem., (1974), 66, C49.

115. A. J Pearson, Aust. J. Chem., (1976), 29, 1679.

116. R. Bachmann, W. von Philipsborn, Org. Magn. Resonance, (1976), 8, 648.

117. R. Burton, M. L. H. Green, E. W. Abel, G. Wilkinson, Chem. Ind. (London), (1958), 1592.

118. R. Burton, L. Pratt, G. Wilkinson, J. Chem. Soc., (1961), 594.

119. T. A. Manuel, F. G. A. Stone, Proc. Chem. Soc., (1959), 90.

120. F. S. Mathews, W. N. Lipscomb,
a) J. Amer. Chem. Soc., (1958), 80, 4745;
b) J. Phys. Chem., (1959), 63, 845.

121. R. T. Bailey, E. R. Lippincott, D. Steele, J. Amer. Chem. Soc., (1965), 87, 5346.

122. F. L. Anet, J. Amer. Chem. Soc., (1967), 89, 2491.

123. C. E. Keller, B. A. Shoulders, R. Pettit, J. Amer. Chem. Soc., (1966), 88, 4760.

124. F. A. Cotton, A. Davison, J. W. Faller, J. Amer. Chem. Soc., (1966), 88, 4507.

125. F. A. Cotton, Acc. Chem. Res., (1968), 1, 257.

126. F. A. Cotton, R. Eiss, J. Amer. Chem. Soc., (1969), 91, 6593.

127. F. A. Cotton, A. Davison, T. Marks, A. Musco, J. Amer. Chem. Soc., (1969), 91, 6598.

128. F. A. Cotton, D. L. Hunter, J. Amer. Chem. Soc., (1976), 98, 1413.

129. A. J. Campbell, C. E. Cotrell, C. A. Fyfe, K. R. Jeffrey, Inorg. Chem., (1976), 15, 1321.

130. R. Pettit, G. F. Emerson, Adv. in Organomet. Chem., (1964), 1, 1.

131. J. E. Arnet, R. Pettit, J. Amer. Chem. Soc., (1961), 83, 2954.

132. R. Pettit, J. Amer. Chem. Soc., (1959), 81, 1266.

133. A. J. Deeming, S. S. Ullah, A. J. P. Domingos, B. F. G. Johnson, J. Lewis, J. Chem. Soc. Dalton, (1974), 2093.

134. S. Ruh, W. von Philipsborn, J. Organomet. Chem., (1977), 127, C59.

135. H. J. Dauben, D. J. Bertelli, J. Amer. Chem. Soc., (1961), 83, 497.

136. M. D. Rausch, G. N. Schrauzer, Chem. Ind., (1959), 957.

137. A. Nakamura, N. Hagihara, Bull. Chem. Soc. Japan, (1959), 32, 880.

138. E. B. Fleischer, A. L. Stone, R. B. K. Dewar, J. D. Wright, C. E. Keller, R. Pettit, J. Amer. Chem. Soc., (1966), 88, 3158.

139. T. A. Manuel, F. G. A. Stone, J. Amer. Chem. Soc., (1960), 82, 366.

140. G. F. Emerson, R. Pettit, L. Watts, J. Amer. Chem. Soc., (1965), 87, 131.

141. K. Ehrlich, G. F. Emerson, J. Amer. Chem. Soc., (1972), 94, 2464.

142. M. J. S. Dewar, S. D. Worley, J. Chem. Phys., (1969), 50, 654.

143. M. J. S. Dewar, S. D. Worley, J. Chem. Phys., (1969), 51, 1672.

144. S. D. Worley, Chem. Comm., (1970), 980.

145. M. I. Al-Joboury, D. W. Turner, J. Chem. Soc., (1964), 4434.

146. J. G. Aston, G. Szasz, H. W. Woolley, F. G. Brickwedde, J. Chem. Phys., (1946), 14, 67.

147. W. B. Smith, J. L. Massingill, J. Amer. Chem. Soc., (1961), 83, 4301.

148. D. J. Marais, N. Sheppard, B. P. Stoicheff, Tetrahedron, (1962), 17, 163.

149. W. C. Price, A. D. Walsh, Proc. Roy. Soc., A, (London), (1940), 174, 220.

150. M. J. S. Dewar, S. D. Worley, J. Chem. Phys., (1968), 49, 2454.

151. N. C. Baird, M. J. S. Dewar, Theor. Chim. Acta, (1967), 9, 1.

152. H. Kato, H. Konishi, H. Yamabe, T. Yonezawa, Bull. Chem. Soc . Japan,(1967), 40, 2761.

153. T. Kobayashi, J. Electron Spectr. & Rel. Phen., (1976), 9, 381.

154. J. H. D. Eland, Int. J. Mass Spectrom. & Ion Phys., (1968), 2, 471.

155. J. A. Connor, L. M. R. Derrick, I. H. Hillier, Mol. Phys., (1976), 31, 23.

156. J. C. Green, P. Powell, J. van Tilborg, J. Chem. Soc. Dalton, (1976), 1974.

157. W. J. Hehre, W. A. Latham, R. Ditchfield, M. D. Newton, J. A. Pople, 'Gaussian 70', Program 236, Quantum Chemistry Package Exchange, Indiana University (1971). Modified for U.L.C.C. CDC machine by P. D. Mallinson, D. Peters.

158. T. M. Sugden, A. D. Walsh, Trans. Faraday Soc., (1945), 41, 76.

159. N. Bodor, M. J. S. Dewar, S. D. Worley, J. Amer. Chem. Soc., (1970), 92, 19.

160. C. D. Batich, J. Amer. Chem. Soc., (1976), 98, 7585.

161. S. Evans, M. L. H. Green, B. Jewitt, A. F. Orchard, C. F. Pygall, J. Chem. Soc. Faraday II, (1972), 1847.

162. C. E. Moore, Nat. Bur. Stand. Circ. No. 467, (1949, 1952, 1958).

163. S. F. Kettle, R. Mason, J. Organomet. Chem., (1966), 5, 97.

164. A. J. Birch, J. Chem. Soc., (1944), 430.

165. J. P. Wibaut, F. A. Haak, Rec. des. Trav. Chim. des Pays Bas, (1948), 67, 85.

166. G. Wilkinson, M. Rosenblum, M. C. Whiting, R. B. Woodward, J. Amer. Chem. Soc., (1952), 74, 2125.

167. E. O. Fischer, W. Pfab, Z. Naturforsch, (1952), 76, 377.

168. J. M. Birmingham, Adv. in Organomet. Chem., (1964), 2, 365.

169. G. Wilkinson, F. A. Cotton, J. M. Birmingham, J. Inorg. & Nucl. Chem., (1956), 2, 95.

170. L. T. Reynolds, G. Wilkinson, J. Inorg. & Nucl. Chem., (1958), 9, 86.

171. G. Wilkinson, F. A. Cotton, Progr. in Inorg. Chem., (1959), 1, 1.

172. E. A. Siebold, L. E. Sutton, J. Chem. Phys., (1955), 23, 1967.

173. A. Almenningen, E. Gard, A. Haaland, J. Brunvoll, J. Organomet. Chem., (1976), 107, 273.

174. a) A. Haaland, J. Lusztyk, J. Brunvoll, K. B. Starowieyski, J. Organomet. Chem., (1975), 85, 279.
b) A. Haaland, J. Lusztyk, D. P. Novak, J. Brunvoll, K. B. Starowieyski, Chem. Comm., (1974), 54.

175. W. Bünder, Thesis, Universitat Hamburg, (1974).

176. A. Almenningen, E. Card, A. Haaland, J. Brunvoll, J. Organomet. Chem., (1975), 88, 181.

177. A. Almenningen, A. Haaland, T. Motzfeldt, Sel. Top. in Struct. Chem., (1967), 105, Univ. Oslo.

178. A. Almenningen, S. Samdal, A. Haaland,
a) Chem. Comm., (1977), 14.
b) J. Organomet. Chem., (1978), 149, 219.

179. J. D. Dunitz, L. E. Orgel, A. Rich, Acta Cryst., (1956), 9, 373.

180. A. Haaland, J. E. Nilsson, Acta Chem. Scand., (1968), 22, 2653.

181. R. K. Bohn, A. Haaland, J. Organomet. Chem., (1966), 5, 470.

182. P. A. Akishin, N. G. Rambidi, T. N. Bredikhina, Zhur. Struct. Khim., (1961), 2, 476.

183. G. L. Hardgrowe, D. H. Templeton, Acta Cryst., (1959), 12, 28.

184. F. Jellinek, Z. Naturforsch, (1959), 14b, 737.

185. A. K. Hedberg, L. Hedberg, K. Hedberg, J. Chem. Phys. (1975), 63, 1262.

186. I. A. Ronova, D. A. Bochvar, A. L. Chistjakov, Y. T. Struchkov, N. V. Alekseev, J. Organomet. Chem., (1969), 18, 337.

187. L. Hedberg, K. Hedberg, J. Chem. Phys., (1970), 53, 1228.

188. L. Asbrink, O. Edqvist, E. Lindholm, L. E. Selin, Chem. Phys. Lett., (1970), 5, 192.

189. L. Asbrink, E. Lindholm, O. Edqvist, Chem. Phys. Lett., (1970), 5, 609.

190. T. A. Carlson, C. P. Anderson, Chem. Phys. Lett., (1971), 10, 561.

191. E. M. Shustorovich, M. E. Dyatkina,
a) Dokl. Akad. Nauk. S.S.S.R., (1959), 128, 1234.
b) Zhur. Strukt. Khim., (1966), 7, 139.

192. J. P. Dahl, C. J. Ballhausen, Math. Fys. Meddr., (1961), 33, 5.

193. R. D. Fischer, Theoret. Chim. Acta, (Berlin), (1963), 1, 418.

194. J. H. Schachtschneider, R. Prins, P. Ros, Inorg. Chim. Acta, (1967), 1, 462.

195. M. F. Rettig, R. S. Drago, J. Amer. Chem. Soc., (1969), 91, 3432.

196. A. T. Armstrong, D. G. Carroll, S. P. McGlynn, J. Chem. Phys., (1967), 47, 1104.

197. A. Botrel, P. Dibout, R. Lissillour, Theoret. Chim. Acta, (1975), 37, 37.

198. N. Rosch, K. H. Johnson, Chem. Phys. Lett., (1974), 24, 179.

199. P. S. Bagus, U. I. Walgren, J. Almlof, J. Chem. Phys., (1976), 64, 2324.

200. D. W. Clack, Theoret. Chim. Acta, (1974), 35, 157.

201. J. W. Rabalais, L. O. Werme, T. Bergmark, L. Karlsson, M. Hussain, K. Siegbahn, J. Chem. Phys., (1972), 57, 1185.

202. Y. S. Sohn, D. N. Hendrickson, J. H. Smith, H. B. Gray, Chem. Phys. Lett., (1970), 6, 499.

203. Y. S. Sohn, D. N. Hendrickson, H. B. Gray, J. Amer. Chem. Soc., (1971), 93, 3603.

204. D. R. Armstrong, R. Fortune, P. G. Perkins, J. Organomet. Chem., (1976), 111, 197.

205. D. R. Armstrong, R. Fortune, P. G. Perkins, J. J. P. Stewart, J. Chem. Soc., Faraday II, (1972), 1839.

206. H. Leipfinger, Z. Naturforsch, (1958), 13B, 53.

207. R. Prins, J. D. W. van Voorst, J. Chem. Phys., (1968), 49, 4665.

208. R. Prins, P. Biloen, J. D. W. van Voorst, J. Chem. Phys., (1967), 46, 1216.

209 H. M. McConnell, W. W. Porterfield, R. E. Robertson, J. Chem. Phys., (1959), 30, 442.

210. D. W. Clack, M. Monshi, J. Organomet. Chem., (1976), 116, C41.

211. F. Englemann, Z. Naturforsch, (1953), 8B, 775.

212. H. P. Fritz, K. E. Schwarzhans, J. Organomet. Chem., (1964), 1, 208.

213. K. R. Gordon, K. D. Warren, J. Organomet. Chem., (1976), 117, C27.

214. S. E. Anderson, R. S. Drago, J. Amer. Chem. Soc., (1970), 92, 4244.

215. E. O Fischer, C. Joos, W. Meer, Z.Naturforsch, (1958), 13B, 456.

216. S. Evans, M. L. H. Green, B. Jewitt, G. H. King, A. F. Orchard, J. Chem. Soc. Faraday II, (1974), 356.

217. J. Voitlander, E. Schimitschek, Z. Elektrochem., (1957), 61, 941.

218. H. E. Switzer, R. Wang, M. F. Rettig, A. H. Maki, J. Amer. Chem. Soc., (1974), 96, 7669.

219. J. H. Ammeter, R. Bucher, N. Oswald, J. Amer. Chem. Soc., (1974), 96, 7833.

220. L. D. Dave, PhD. Thesis, London (1959).

221. K. D. Warren, Structure and Bonding, (1976), 27, 45.

222. E. O. Fischer, R. Jira, Z.Naturforsch, (1953), 8b, 217.

223. a) J. H. Ammeter, J. D. Swalen, J. Chem. Phys., (1972), 57, 678.
b) J. H. Ammeter, J. M. Brown, Chem. Phys. Lett., (1974), 27, 380.

224. K. D. Warren,
a) Inorg. Chem., (1974), 13, 1317.
b) Inorg. Chem., (1974), 13, 1243.

225. R. Prins, P. Biloen, J. D. W. van Voorst, Chem. Phys. Lett., (1967), 1, 54.

226. J. S. Griffith, The Theory of Transition Metal Ions, Cambridge University Press, London,(1961).

227. Y. S. Sohn, D. N. Hendrickson, H. D. Gray, J. Amer. Chem. Soc., (1970), 92, 3233.

228. S. Evans, J. C. Green, S. E. Jackson, B. Higginson, J. Chem. Soc. Dalton, (1974), 304.

229. S. Evans, J. C. Green, S. E. Jackson, J. Chem. Soc. Faraday II, (1972), 249.

230. H. O. van Oven, C. J. Groenenboom, H. J. de Liefde Meijer, J. Organomet. Chem., (1974), 81, 379.

231. H. O. van Oven, C. J. Groenenboom, H. J. de Liefde Meijer, J. Organomet. Chem., (1975), 97, 73.

232. M. Barber, J. A. Connor, L. M. R. Derrick, M. B. Hall, I. H. Hillier, J. Chem. Soc. Faraday II, (1973), 559.

233. D. T. Clark, D. B. Adams, Chem. Phys. Lett., (1971), 10, 121.

234. A. A. Bakke, W. L. Jolly, T. F. Schaaf, J. Electr. Spectr. & Rel. Phen., (1977), 11, 339.

235. D. T. Clark, D. B. Adams, Chem. Comm., (1971), 740.

236. S. Cradock, W. Duncan, J. Chem. Soc. Faraday II, (1978), 194.

237. J. A. R. Samson, Phil. Trans. A, (1970), 268, 141.

238. P. Pertici, G. Vitulli, L. Porri, Chem. Comm.,(1975), 846.

239. A. R. Pray, Inorganic Syntheses, (1957), 5, 153.

240. G. B. Heisig, B. Fawkes, R Hedin, Inorganic Syntheses, (1946), 2, 193.

241. J. Chatt, L. M. Venanzi, Nature, (1956), 177, 852.

242. J. Chatt, L. M. Venanzi, J. Chem. Soc., (1957), 4735.

243. R. B. King, P. M. Treichel, F. G. A. Stone, J. Amer. Chem. Soc., (1961), 83, 3593.

244. J. Lewis, A. W. Parkins, J. Chem. Soc. (A), (1967), 1151.

245 a) A. Nakamura, N. Hagihara, Bull. Chem. Soc. Japan, (1960), 33, 425.
b) H. P. Fritz, H. Keller, Z. Naturforsch, (1961), 16b, 348.

246. A. Davison, W. McFarlane, L. Pratt, G. Wilkinson, J. Chem. Soc., (1962), 4821.

247. R. Cramer, Inorg. Chem., (1962), 1, 722.

248. R. B. King, Inorg. Chem., (1963), 2, 528.

249. R. Cramer, J. Amer. Chem. Soc., (1964), 86, 217.

250. a) P. M. Maitlis, A. Efraty, M. L. Games, J. Organomet. Chem., (1964), 2, 284.
b) A. Efraty, P. M. Maitlis, Tetr. Lett., (1966), 34, 4025; J. Amer. Chem. Soc., (1967), 89, 3744.
c) R. G. Amiet, R. Pettit, J. Amer. Chem. Soc., (1968), 90, 1059.

251. R. L. Pruett, W. R. Myers,
a) U.S. Patent 3,159,659 (cl-260-429), Dec. 1, 1964.
b) U.S. Patent 3,201,484 (cl-260-666), Aug. 17, 1965.

252. H. Bönnemann, Angew. Chem., (Int. Ed.), (1973), 12, 964.

253. M. G. B. Drew, S. M. Nelson, M. Sloan, J. Chem. Soc. Dalton, (1973), 1484.

254. L. Oro, Inorg. Chim. Acta, (1977), 21, L6.

255. a) L. Porri, A. Lionetti, C. Allegra, A. Immerzi, Chem. Comm., (1965), 336.
b) L. Porri, A. Lionetti, J. Organomet. Chem., (1966), 6, 422.

256. J. W. Kang, P. M. Maitlis, J. Amer. Chem. Soc., (1968), 90, 3259.

257. K. Moseley, J. W. Kang, P. M. Maitlis, Chem. Comm., (1969), 1155.

258. K. Moseley, P. M. Maitlis, Chem. Comm., (1969), 1156.

259. S. M. Nelson, M. Sloan, M. G. B. Drew, J. Chem. Soc. Dalton, (1973), 2195.

260. A. K. Smith, P. M. Maitlis, J. Chem. Soc. Dalton, (1976), 1773.

261. B. F. G. Johnson, J. Lewis, D. J. Yarrow, J. Chem. Soc. Dalton, (1972), 2084.

262. a) M. R. Churchill, K. K. G. Lin, J. Amer. Chem. Soc., (1974), 96, 76.
b) M. R. Churchill, S. A. Bezman, Inorg. Chem., (1972), 11, 2243; Inorg. Chem., (1973), 12, 260, 531.
c) J. Mueller, W. Holzinger, H. Menig, Ger. Angew. Chem., (1976), 88, 768.

263. H. B. Lee, P. M. Maitlis, J. Chem. Soc. Dalton, (1975), 2316.

264. A. van der Ent, A. L. Onderdelinden, Inorganic Syntheses, (1973), 14, 92.

265. J. A. Ibers, R. G. Snyder, J. Amer. Chem. Soc., (1962), 84, 496.

266. L. F. Dahl, C. Martell, D. Wampler, J. Amer. Chem. Soc., (1962), 83, 1761.

267. M. G. B. Drew, S. M. Nelson, M. Sloan, J. Organomet. Chem., (1972), 39, C9.

268. D. P. Craig, A. Maccoll, R. S. Nyholm, L. E. Orgel, L. E. Sutton, J. Chem. Soc., (1954), 332.

269. J. Chatt, L. A. Duncanson, J. Chem. Soc., (1953), 2939.

270. M. J. S. Dewar, Bull. Soc. Chim. France, (1951), C71.

271. J. N. Dempsey, N. C. Baenziger, J. Amer. Chem. Soc., (1955), 77, 4984.

272. P. R. H. Alderman, P. G. Owston, J. M. Rowe, Acta Cryst., (1960), 13, 149.

273. J. A. Wunderlich, D. P. Melior,
a) Acta Cryst., (1954), 7, 130.
b) Acta Cryst., (1955), 8, 57.

274. G. B. Bokii, G. A. Kukina, Akad. Nauk. S.S.S.R. Kryst., (1957), 2, 400.

275. R. O. Fischer, R. D. Fischer, Z.Naturforsch, (1961), 16b, 556.

276. B. F. G. Johnson, J. Lewis, D. J. Yarrow, J. Chem. Soc. Dalton, (1974), 1054.

277. J. Evans, B. F. G. Johnson, J. Lewis, J. Chem. Soc. Dalton, (1977), 510.

278. R. B. King, A. Efraty, W. M. Douglas, J. Organomet. Chem., (1973), 56, 345.

279. R. Pardy, D. Phil. Thesis, Oxford (1977).

280. J. H. Richards, Abstr. 135th. Nat. Meeting, Amer. Chem. Soc., April, (1959), 86.

281. M. Rosenblum, J. O. Santer, W. G. Howells, J. Amer. Chem. Soc., (1963), 85, 1450.

282. D. W. Turner, Proc. Roy. Soc. A, (London), (1968), 307, 15.

He(I) Photoelectron Spectra of Tricarbonyl-iron and -ruthenium Complexes of Cyclic Dienes, and of Tricarbonylcycloheptatriene- and Tricarbonylcyclo-octatetraene-iron

By **Jennifer C. Green,*** Inorganic Chemistry Laboratory, South Parks Road, Oxford OX1 3QR
Paul Powell and **Jane van Tilborg**, The Bourne Laboratory, Royal Holloway College, Egham Hill, Egham TW20 OEX

Reprinted from

JOURNAL
OF
THE CHEMICAL SOCIETY

DALTON TRANSACTIONS

1976

He(I) Photoelectron Spectra of Tricarbonyl-iron and -ruthenium Complexes of Cyclic Dienes, and of Tricarbonylcycloheptatriene- and Tricarbonylcyclo-octatetraene-iron

By **Jennifer C. Green,*** Inorganic Chemistry Laboratory, South Parks Road, Oxford OX1 3QR
Paul Powell and **Jane van Tilborg**, The Bourne Laboratory, Royal Holloway College, Egham Hill, Egham TW20 0EX

The He(I) photoelectron spectra of the complexes [M·LM(CO)$_3$] [L = cyclohexa-1,3-diene and cyclohepta-1,3-diene (M = Fe or Ru); L = cyclo-octa-1,3-diene, cycloheptа-1,3,5-triene, and cyclo-octatetraene (M = Fe)] have been examined. The ionisation energies of the iron diene complexes show a regular variation with ring size, in contrast to those of the parent cyclic dienes.

THE photoelectron (p.e.) spectrum of butadienetricarbonyliron (1) has been reported previously.[1-3] The most recent paper[3] included both He(I) and He(II) spectra, which were assigned in the light of an *ab initio* SCF molecular-orbital calculation. The free ligands have also been studied.[4-6] The separation of the two bands of lowest ionisation energy in the spectra of the cyclic dienes has been correlated with the stereochemistry of the ring. We now report the spectra of complexes of the type [M(diene)(CO)$_3$] (M = Fe or Ru) and also of tricarbonylcycloheptatriene- and tricarbonylcyclo-octatetraene-iron.

EXPERIMENTAL

The complexes were prepared according to published methods.[7-12] The purity of the samples was confirmed by elemental analysis and by measurement of m.p., b.p., and i.r., ^{1}H n.m.r., and mass spectra, which agreed with reported values.[13,14]

The He(I) p.e. spectra were recorded on a Perkin-Elmer PS 16/18 instrument modified to take a heated insert. The spectra were calibrated using xenon and argon.

RESULTS AND DISCUSSION

Diene Complexes.—The spectra are summarised in the Table. Connor *et al.*[3] ascribed the first band (A) in the spectrum of butadienetricarbonyliron to the ionisation of electrons largely localised on the metal atom. The second peak (B) is assigned to an orbital which correlates with the higher filled π level of *cis*-butadiene ($1a_2$). The third band (C) arises through ionisation from a molecular orbital correlating with the lower filled π level ($1b_1$) of the free ligand. The bands (D) at higher ionisation energy (i.e.) are attributed to loss of electrons from σ levels of the diene, and from the carbonyl ligands.

The spectra of the tricarbonyl(diene)iron complexes [Fe(C$_6$H$_8$)(CO)$_3$] (2), [Fe(C$_7$H$_{10}$)(CO)$_3$] (3), and [Fe(C$_8$H$_{12}$)(CO)$_3$] (4) resemble that of the parent molecule, (1), and have been assigned similarly. In the former, however, band (B) was less well resolved from the metal '*a*' bands (A), and bands (C) occurred as shoulders on the low i.e. edge of the σ ionisations of the diene ligands. The i.e. values derived from bands (C) are therefore less well established than for the parent molecule.

Ionisation energies of the tricarbonyl complexes and the π levels of the free ligands

	Ionisation energy (eV)				
Compound	Band (A)		Band (B)	Band (C)	Band (D)
[Fe(C$_4$H$_6$)(CO)$_3$] (1)	8.16 (sh)	8.67	9.82	11.43	12.56
[Fe(C$_6$H$_8$)(CO)$_3$] (2)	7.98 (sh)	8.56	9.33	11.04	12.17
[Fe(C$_7$H$_{10}$)(CO)$_3$] (3)	7.78 (sh)	8.46	9.12	10.86	11.71
[Fe(C$_8$H$_{12}$)(CO)$_3$] (4)	7.45 (sh)	8.27	8.87	10.44	10.87
[Ru(C$_6$H$_8$)(CO)$_3$] (5)	8.01	8.91	9.39 (sh)	11.01	11.83
[Ru(C$_7$H$_{10}$)(CO)$_3$] (6)	7.96	8.94	9.40 (sh)	10.84	11.64
[Fe(C$_7$H$_8$)(CO)$_3$] (7)	7.76 (sh)	8.39	8.78	11.10	11.82
			10.23		
[Fe(C$_8$H$_8$)(CO)$_3$] (8)	7.84		8.74	11.63	
			10.61		
trans-Buta-1,3-diene [4]	9.08		11.34		
Cyclohexa-1,3-diene [5]	8.25		10.75		
Cycloheptа-1,3-diene [5]	8.31		10.63		
Cyclo-octa-1,3-diene [6]	8.68		10.00		
Cycloheptа-1,3,5-triene [5]	8.57		9.52	10.96	
Cyclo-octatetraene [6]	8.42		9.78	11.15	

For complexes (2)—(4) all bands show a decrease in i.e. with increase in ring size. This is not so, however, for the two π ionisations of the parent dienes.[5] Although the average of the first two i.e.s of the latter decreases with increase in ring size, the difference between them is irregular. The separation between these two bands has been correlated with the angle of twist between the conjugated double bonds. This correlation, however, does not agree well with a recent value of 0° twist in cycloheptadiene derived from i.r. spectroscopic data.[15]

[1] M. J. S. Dewar and S. D. Worley, *J. Chem. Phys.*, 1969, **50**, 654.
[2] S. D. Worley, *Chem. Comm.*, 1970, 980.
[3] J. A. Connor, L. M. R. Derrick, M. B. Hall, I. H. Hillier, M. F. Guest, B. R. Higginson, and D. R. Lloyd, *Mol. Phys.*, 1974, **28**, 1193.
[4] D. W. Turner, 'Molecular Photoelectron Spectroscopy,' Wiley, New York, 1970.
[5] C. Batich, P. Bischof, and E. Heilbronner, *J. Electron Spectroscopy*, 1973, **1**, 333.
[6] P. Bischof and E. Heilbronner, *Helv. Chim. Acta*, 1970, **53**, 1677.
[7] W. G. Dauben and M. E. Lorber, *Org. Mass Spectrometry*, 1970, **3**, 216.
[8] R. B. King, T. A. Manuel, and F. G. A. Stone, *J. Inorg. Nuclear Chem.*, 1961, **16**, 233.
[9] B. F. G. Johnson, J. Lewis, P. McArdle, and G. L. P. Randall, *J.C.S. Dalton*, 1972, 456.
[10] R. B. King, *Organometallic Synth.*, 1965, **1**, 126.
[11] B. F. G. Johnson, R. D. Johnson, P. L. Josty, J. Lewis, and J. G. Williams, *Nature*, 1967, **213**, 901.
[12] B. A. Sosinsky, S. A. R. Knox, and F. G. A. Stone, *J.C.S. Dalton*, 1975, 1633.
[13] R. Burton, L. Pratt, and G. Wilkinson, *J. Chem. Soc.*, 1961, 594.
[14] A. J. Deeming, A. J. P. Domingos, B. F. G. Johnson, J. Lewis, and S. S. Ullah, *J.C.S. Dalton*, 1974, 2093.
[15] B. Schrader and A. Ansmann, *Angew. Chem. Internat. Edn.*, 1975, **14**, 364.

It is interesting nonetheless that the separation between bands (B) and (C) in all the iron and ruthenium complexes is almost constant (1.7 ± 0.1 eV).* This is consistent with the suggestion that the dienes when complexed are constrained to assume an essentially *cis*-planar conformation in which the twist angle is close to 0°. If one assumes that free cycloheptadiene has this conformation, one can estimate the change of the π-ionisation energies on complexing by comparing the spectrum of cycloheptadiene itself with that of its tricarbonyliron complex. The '$1a_2$' i.e. is increased by 0.81 eV and the '$1b_2$' i.e. by 0.23 eV. If a similar change in i.e. occurs with other dienes we can predict the i.e.s for dienes in the *cis*-planar conformation. *cis*-Butadiene, for example, would be expected to show i.e.s of 9.01 and 11.20 eV. Worley [2] calculated values of 9.19 and 11.18 eV.

The spectra of the two ruthenium complexes [Ru(C_6H_8)$(CO)_3$] (5) and [Ru(C_7H_{10})$(CO)_3$] (6) resemble those of their iron analogues, and may be assigned similarly. The first band (A) lay to higher i.e., as do the metal orbital ionisations in [Ru(η-C_5H_5)$_2$] compared with [Fe(η-C_5H_5)$_2$].[16] Ionisation-energy data for both neutral and singly ionised atomic species similarly indicate an increase from Fe to Ru.[17] As a consequence of the shift in band (A), (B) was no longer so clearly resolved as in the spectra of the iron complexes, and appeared as a shoulder. It is interesting that the separation between bands (B) and (C) is still 1.7 ± 0.1 eV.

The intensity of the first group of bands (A) and (B) relative to (C) and (D) increases for both pairs of complexes from Fe to Ru. Similar increases in metal *d*-orbital cross section with principal quantum number have previously been noted, *e.g.* for [M(η-C_5H_5)$_2$] (M = Fe, Ru, and Os).[16]

Tricarbonylcycloheptatrieneiron.—Comparison between the spectra of [Fe(C_7H_{10})$(CO)_3$] (3) and [Fe(C_7H_8)$(CO)_3$] (7) shows that an additional band is present in the latter at 10.23 eV. To a first approximation the bonding in complex (7) can be considered as comprising a [Fe(diene)$(CO)_3$] system and a free >C=C< unit. We assign the band at 10.23 eV to ionisation from the π system of the uncomplexed double bond. Moreover the bands which correlate with the π molecular orbitals of the complexed *cis*-diene system have a greater separation (2.32 eV) than in the spectra of [Fe(diene)$(CO)_3$] (1.7 eV). This suggests that there is some interaction between the complexed diene system and the uncomplexed π bond.

Tricarbonylcyclo-octatetraeneiron.—The p.e. spectrum of the free ligand (C_8H_8, D_{2d} symmetry) has been discussed by Batich *et al.*[5] The first three ionisations correspond to loss of an electron from π orbitals of b_2, *e*, and a_1 symmetry respectively. In the crystal the ligand assumes a dihedral conformation,[18] and the molecule is fluxional in solution.[19]

If the bonding were composed of a [Fe(diene)$(CO)_3$] unit plus a free diene system, with little or no interaction between them, the spectrum would appear as the sum of the spectra of the two parts. On this basis, the first broad band with maxima at 7.84 and 8.74 eV

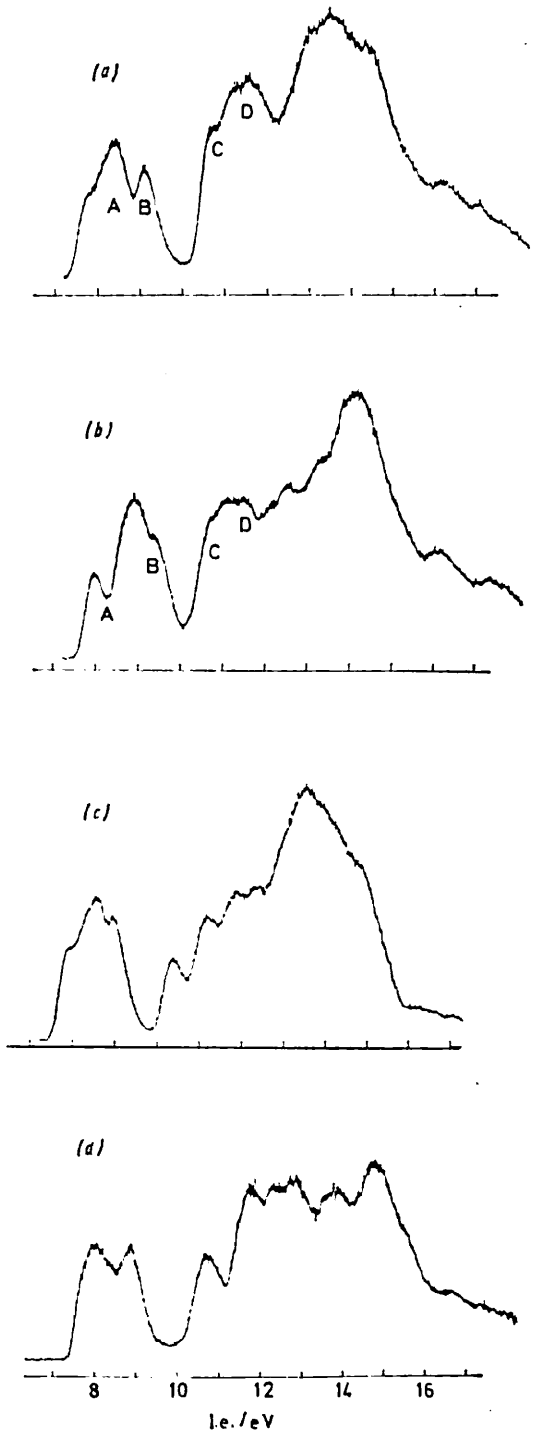

He(I) Photoelectron spectra of (*a*) [Fe(C_7H_{10})$(CO)_3$], (*b*) [Ru(C_7H_{10})$(CO)_3$], (*c*) [Fe(C_7H_8)$(CO)_3$], and (*d*) [Fe(C_8H_8)$(CO)_3$]

* 1 eV ≈ 1.60 × 10^{-19} J.

[16] S. Evans, M. L. H. Green, B. Jewitt, A. F. Orchard, and C. F. Pygall, *J.C.S. Faraday II*, 1972, 1847.

[17] C. E. Moore, Nat. Bur. Stand., Circ. No. 467, 1949, 1952, and 1958.

[18] B. Dickens and W. N. Lipscomb, *J. Chem. Phys.*, 1962, **37**, 2084.

[19] F. A. Cotton, A. Davison, T. J. Marks, and A. Mumo, *J. Amer. Chem. Soc.*, 1969, **91**, 6598.

(Figure) would correspond to bands (A) and (B) of the [Fe(diene)$(CO)_3$] unit together with the lower-energy π ionisation of the diene. The next band at 10.6 eV could be assigned to the higher π ionisation of the diene. This suggestion is supported by relative intensities. The ratio of the intensities of the first group of bands to the peak at 10.61 eV is *ca.* 6 : 1. The corresponding ratio in the spectrum of (7) is 4.8 : 1. The greater relative intensity of the first band in the spectrum of (8) is consistent with the inclusion of the '$1a_2$' 'free-diene' ionisation. It is likely, however, that there is significant interaction between the diene residue and the complexed diene unit. This is supported by the large ring angles (135°) in the unbound portion of the ring, and by SCF molecular-orbital calculations.[18]

We thank the S.R.C. for support and for the award of a maintenance grant (to J. v. T.), and Johnson, Matthey for a generous loan of ruthenium trichloride.

[6/563 *Received*, 24*th March*, 1976]